Electronic Supplementary Material (ESI) for Chemical Science.

Supporting information for the paper entitled,

Programmable Synthesis of Well-Defined, Glycosylated Iron(II) Supramolecular Assemblies with Multivalent Protein-Binding Capabilities

Jake H. Schwab[1], Jake B. Bailey[1], Milan Gembicky[1], and Julia M. Stauber[1*]

Affiliations:

[1]*Department of Chemistry and Biochemistry, University of California, San Diego, La Jolla, California, 92093, United States*

*Correspondence to: jstauber@ucsd.edu

S1. General considerations 5
S1.1. Materials 5
S1.2. Methods 5
S2. Synthetic procedures and characterization data for all compounds 6
S2.1. 4,4'-Diaminodiphenyl ether-2,2'-disulfonic acid 6
S2.2. Glycosylated ligand building blocks 7
S2.2.1. $(OAc)_4$-β-D-glucoseEtBr 7
S2.2.2. 5-($(OAc)_4$-β-D-glucoseEtO)-2-picolinaldehyde (subcomponent A) 9
S2.2.3. D-mannopyranose,1,2,3,4,6-pentaacetate (mixture of α and β anomers) 12
S2.2.4. $(OAc)_4$-α-D-mannoseEtBr 14
S2.2.5. 5-($(OAc)_4$-α-D-mannoseEtO)-2-picolinaldehyde (subcomponent B) 16
S2.2.6. $(OAc)_4$-β-D-galactoseEtBr 19
S2.2.7. 5-($(OAc)_4$-β-D-galactoseEtO)-2-picolinaldehyde (subcomponent C) 21
S2.2.8. $(OAc)_7$-β-D-maltoseEtBr 24
S2.2.9. 5-($(OAc)_7$-β-D-maltoseEtO)-2-picolinaldehyde (subcomponent D) 26
S2.3. Fe(II) Self-Assembly Complexes 29
S2.3.1. $[NMe_4]_4$[**1**-glc] 29
S2.3.2. $[Na]_4$[**1**-glc] 34
S2.3.3. $[K]_4$[**1**-glc] 35
S2.3.4. $[NMe_4]_2$[**2**-glc] 36
S2.3.5. [**3**-glc][SO_4] 41
S2.3.6. $[NMe_4]_4$[**1**-man] 46
S2.3.7. $[NMe_4]_2$[**2**-man] 50
S2.3.8. [**3**-man][SO_4] 54
S2.3.9. $[NMe_4]_4$[**1**-gal] 58
S2.3.10. $[NMe_4]_2$[**2**-gal] 62
S2.3.11. [**3**-gal][SO_4] 66
S2.3.12. $[NMe_4]_4$[**1**-mal] 70
S2.3.13. $[NMe_4]_2$[**2**-mal] 74
S2.3.14. [**3**-mal][SO_4] 78
S2.3.15. Unfunctionalized $[NMe_4]_4[Fe_4L_6]$ 82
S3. Solubility determination of $[NMe_4]_4$[1-glc] in H_2O 83
S4. Stability studies of glycosylated complexes to various conditions, buffers, and pH environments 85
S4.1. Water stability of $[NMe_4]_4$[**1**-glc] as analyzed by ^{1}H NMR spectroscopy 85

S4.2. Stability of $[NMe_4]_4$[**1**-glc] to solutions of various pH, common buffers, and biologically-relevant conditions as analyzed by UV-vis spectroscopy 86
S4.2.1. Carbonate buffer (10 mM), pH 10.0 86
S4.2.2. Tris buffer (10 mM), pH 9.0 86
S4.2.3. Tris buffer (10 mM), pH 7.4 87
S4.2.4. PBS buffer (10 mM), pH 7.4 87
S4.2.5. HEPES buffer (10 mM), pH 7.4 88
S4.2.6. Acetate buffer (10 mM), pH 5.0 88
S4.2.7. Acetate buffer (10 mM), pH 4.0 89
S4.2.8. Glutathione (2 mM) 89
S4.2.9. Fetal bovine serum cell culture media 90
S4.3. Stability of mannosylated complexes under ITC experimental conditions as assayed by UV-vis spectroscopy 91
S4.3.1. $[NMe_4]_4$[**1**-man] 91
S4.3.2. $[NMe_4]_2$[**2**-man] 92
S4.3.3. [**3**-man][SO_4] 92
S5. Turbidimetry Assay 93
S5.1. $[NMe_4]_4$[**1**-man] 93
S5.2. $[NMe_4]_2$[**2**-man] 94
S5.3. [**3**-man][SO_4] 94
S5.4. $[NMe_4]_4$[**1**-mal] 95
S5.5. $[NMe_4]_2$[**2**-mal] 95
S5.6. [**3**-mal][SO_4] 96
S6. ITC binding studies 97
S6.1. Binding of mannose-functionalized complexes to Con A dimer 98
S6.1.1. $[NMe_4]_4$[**1**-man] 98
S6.1.2. $[NMe_4]_2$[**2**-man] 99
S6.1.3. [**3**-man][SO_4] 100
S6.2. Binding of maltose-functionalized complexes to Con A dimer 101
S6.2.1. $[NMe_4]_4$[**1**-mal] 101
S6.2.2. $[NMe_4]_2$[**2**-mal] 102
S6.2.3. [**3**-mal][SO_4] 103
S6.3. Binding of $[NMe_4]_4$[**1**-glc] to Con A dimer 104
S6.4. Binding of $[NMe_4]_4$[**1**-gal] to Con A dimer 105
S6.5. Binding of unfunctionalized $[NMe_4]_4[Fe_4L_6]$ to Con A dimer – negative control 106

S6.6. Binding of methyl-α-D-mannose to Con A dimer.....107
S6.7. Binding of D-(+)-mannose to Con A dimer.....108
S7. X-Ray Crystallographic Details.....109
S8. References.....112

S1. General considerations

S1.1. Materials

Synthetic experiments performed under an inert atmosphere of N_2 were carried out using standard Schlenk techniques, and all other manipulations were performed under open atmosphere conditions in a fume hood. All reagents were purchased from ChemImpex, TCI, Fisher Scientific, AA Blocks, or Alfa Aesar, and used as received unless otherwise noted. Solvents (dichloromethane (DCM), acetone, isopropanol (^{i}PrOH), *N*,*N*-dimethylformamide (DMF), ethyl acetate (EtOAc), hexanes, pentane, and diethyl ether (Et_2O)) were used as received without further purification. Deuterated solvents ($CDCl_3$, DMSO-d_6, and D_2O) were obtained from Cambridge Isotope Laboratories and used as received. Concanavalin A was purchased from Thermo Scientific and stored at 4 °C. ITC buffers were prepared using Milli-Q water and solutions were filtered through a Corning® 0.22 μm pore sized filter prior to use.

S1.2. Methods

All NMR spectra were obtained on 300 MHz Bruker AVA or 400 MHz JEOL FT NMR spectrometers and ^{1}H and ^{13}C{^{1}H} NMR spectra were referenced to residual protio solvent signals. Mass spectrometry (MS) analysis was performed at the Molecular MS Facility at UC San Diego using an Agilent 6230 time-of-flight mass spectrometer (TOFMS) with a Jet Stream electrospray ionization (ESI) source. The Jet Stream ESI source was operated with the following parameters: VCap: 3500 V; fragmentor voltage: 165 V; drying gas temperature: 325 °C, sheath gas temperature: 325 °C, drying gas flow rate: 7.0 L/min; sheath gas flow rate: 10 L/min; nebulizer pressure: 40 psi. UV-vis measurements were conducted using an Agilent Cary 60 UV-vis spectrophotometer equipped with a Xenon flashlamp (80 Hz) light source. Flash chromatography was performed on a CombiFlash NexGen 300+ system using 24 g columns packed with 230-400 mesh grade 60 silica. UV-vis measurements were carried out using quartz cuvettes (1 cm or 0.1 cm path length) and conducted at 25 °C with solution samples at 50 μM concentration unless otherwise noted. ATR-IR spectra were collected on an Agilent Cary 630 FTIR spectrometer. ITC measurements were performed on an Affinity LV ITC (Waters/TA Instruments) instrument and experimental details are provided in Section S6. X-ray crystallographic methods are described in Section S7.

S2. Synthetic procedures and characterization data for all compounds

S2.1. 4,4’-Diaminodiphenyl ether-2,2’-disulfonic acid

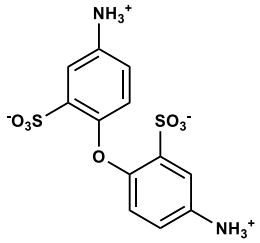

The preparation of 4,4′-diaminodiphenyl ether-2,2′-disulfonic acid was adapted from a procedure reported by Okamoto *et al*. and spectroscopic data of the isolated material match the literature report.[1]

A 50 mL round bottom flask was charged with a Teflon-coated stir bar and 4,4’-diaminodiphenyl ether (2.000 g, 9.988 mmol, 1.000 equiv). The flask was cooled to 0 °C, and then concentrated H_2SO_4 (1.7 mL) was slowly added to the mixture with vigorous stirring over the course of 5 min. To the stirring mixture was slowly added fuming sulfuric acid (SO_3 18-24%, 10.5 mL) at 0 °C, and the reaction was allowed to stir at 0 °C for 2 h. The reaction was then allowed to stir at 80 °C for an additional 2 h, at which point it was allowed to cool to ambient temperature and poured onto crushed ice (20 g). The resulting precipitate was isolated by filtration. The solids were then redissolved in aqueous NaOH (6 M, 10 mL), and the resulting pale-yellow solution was filtered. To the filtrate was added concentrated HCl (37%, 3 mL), resulting in the precipitation of colorless solids that were isolated by filtration, washed with H_2O (5 mL) and MeOH (5 mL) and then dried overnight in a vacuum oven at 70 °C to afford 4,4′-diaminodiphenyl ether-2,2′-disulfonic acid as a free-flowing colorless powder (80 wt% balance H_2O, yield: 3.400 g, 9.435 mmol, 94%). ^{1}H NMR (300 MHz, 25 °C, DMSO-d_6 spiked with Et_3N for dissolution of compound) δ: 7.00 (d, 2H, *J* = 2.8 Hz, benzidine-6,6’), 6.73 (d, 2H, *J* = 8.6 Hz, benzidine-4,4’), 6.38 (dd, 2H, *J* = 8.6, 2.8 Hz, benzidine-3,3’), 4.78 (s, 6H, N-*H*) ppm.

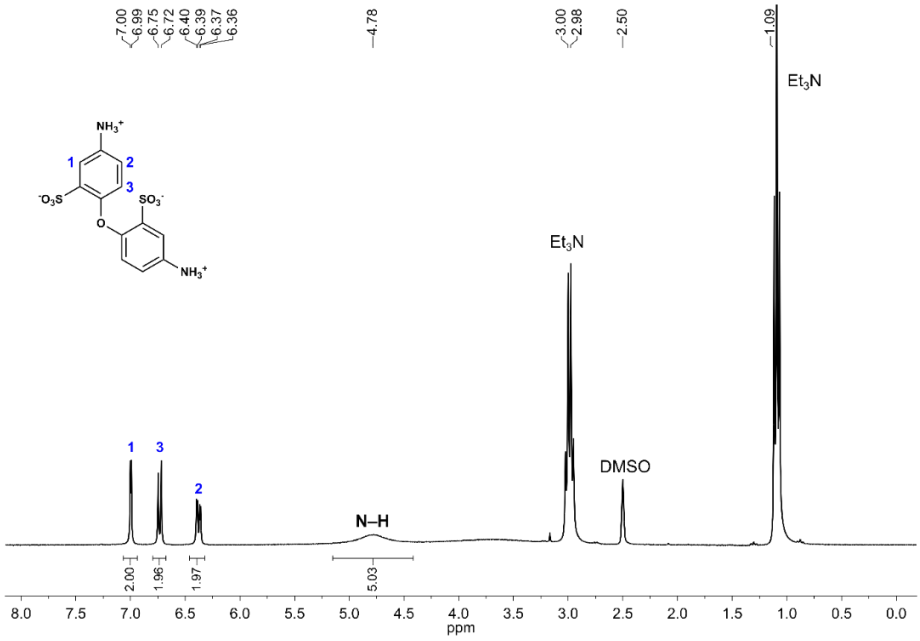

Figure S1. ^{1}H NMR spectrum of 4,4′-diaminodiphenyl ether-2,2′-disulfonic acid (DMSO-d_6 spiked with Et_3N, 300 MHz, 25 °C).

S2.2. Glycosylated ligand building blocks

S2.2.1. $(OAc)_4$-β-D-glucoseEtBr

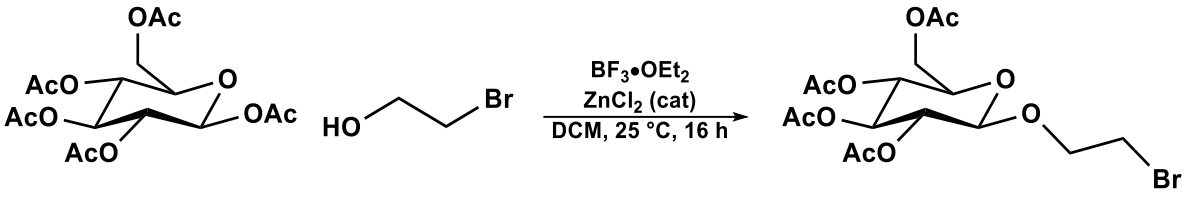

The preparation of $(OAc)_4$-β-D-glucoseEtBr was adapted from a similar procedure reported by Che *et al*.[2] and spectroscopic data match the literature report.[3]

A 250 mL two-neck flask was charged with $(OAc)_5$-β-D-glucose (5.000 g, 12.81 mmol, 1.000 equiv), $ZnCl_2$ (505 mg, 3.71 mmol, 0.290 equiv) and DCM (50 mL). To the flask was added 2-bromoethanol (1.4 mL, 19 mmol, 1.5 equiv), followed by $BF_3•Et_2O$ (5.4 mL, 44 mmol, 3.4 equiv) dropwise over the course of 10 min under an atmosphere of N_2. The pale-yellow reaction mixture was allowed to stir at ambient temperature for 16 h, at which point it was diluted with EtOAc (200 mL) and then washed with a saturated aqueous solution of NaCl (3 x 150 mL). The organic phase was dried over $MgSO_4$, and the solvent was evaporated under reduced pressure to yield a yellow oil, which was dissolved in a minimal amount of EtOAc (ca. 15 mL). The solution was layered with hexanes (ca. 30 mL) and then allowed to stand at ambient temperature overnight, resulting in the formation of colorless crystals. The crystals were isolated and dried under reduced pressure to yield pure $(OAc)_4$-β-D-glucoseEtBr as a colorless crystalline solid (yield: 3.584 g, 7.873 mmol, 61%). ^{1}H NMR (400 MHz, 25 °C, $CDCl_3$) δ: 5.20 (t, 1H, *J* = 9.7 Hz, glc-*H*-3), 5.07 (t, 1H, *J* = 9.7 Hz, glc-*H*-4), 5.00 (dd, 1H, *J* = 9.6, 8.0 Hz, glc-*H*-2), 4.56 (d, 1H, *J* = 8.0 Hz, glc-*H*-1), 4.24 (dd, 1H, *J* = 12.3, 4.8 Hz, glc-*H*-6_a), 4.15 (dd, 1H, OCH_{2a}CH_2Br), 4.11 (dd, 1H, glc-*H*-6_b), 3.80 (ddd, 1H, OCH_{2b3}CH_2Br), 3.69 (ddd, 1H, glc-*H*-5), 3.47–3.40 (m, 2H, CH_2Br), 2.07 (s, 3H, CH_3COO), 2.05 (s, 3H, CH_3COO), 2.01 (s, 3H, CH_3COO), 1.99 (s, 3H, CH_3COO) ppm. ^{13}C{^{1}H} NMR (100 MHz, 25 °C, $CDCl_3$) δ: 170.7 (CH$_3$*C*OO), 170.3 (CH$_3$*C*OO), 169.5 (CH$_3$*C*OO), 169.5 (CH$_3$*C*OO), 101.1 (glc-*C*-1), 72.7 (glc-*C*-3), 72.0 (glc-*C*-5), 71.1 (glc-*C*-2), 69.9 (O*C*H$_2$), 68.4 (glc-*C*-4), 61.9 (glc-*C*-6), 30.0 (*C*H$_2$Br), 20.9 (*C*H$_3$COO), 20.9 (*C*H$_3$COO), 20.7 (*C*H$_3$COO), 20.7 (*C*H$_3$COO) ppm.

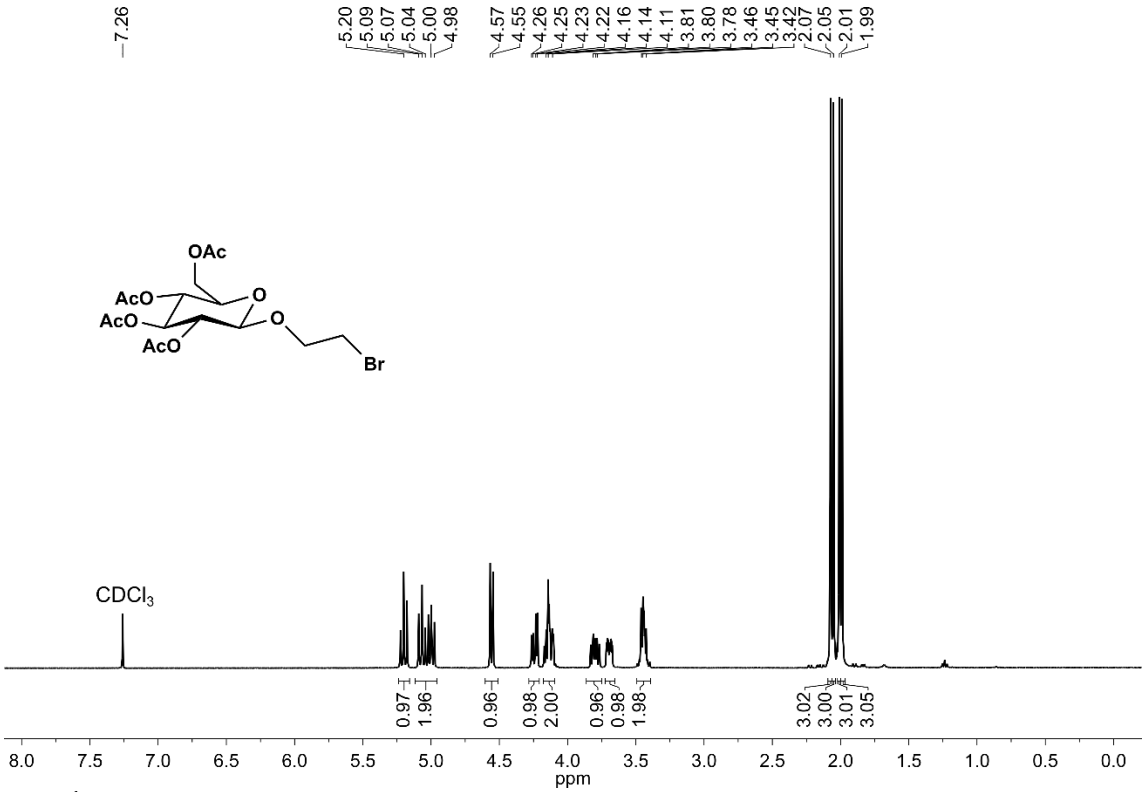

Figure S2. ^{1}H NMR spectrum of $(OAc)_4$-β-D-glucoseEtBr ($CDCl_3$, 400 MHz, 25 °C).

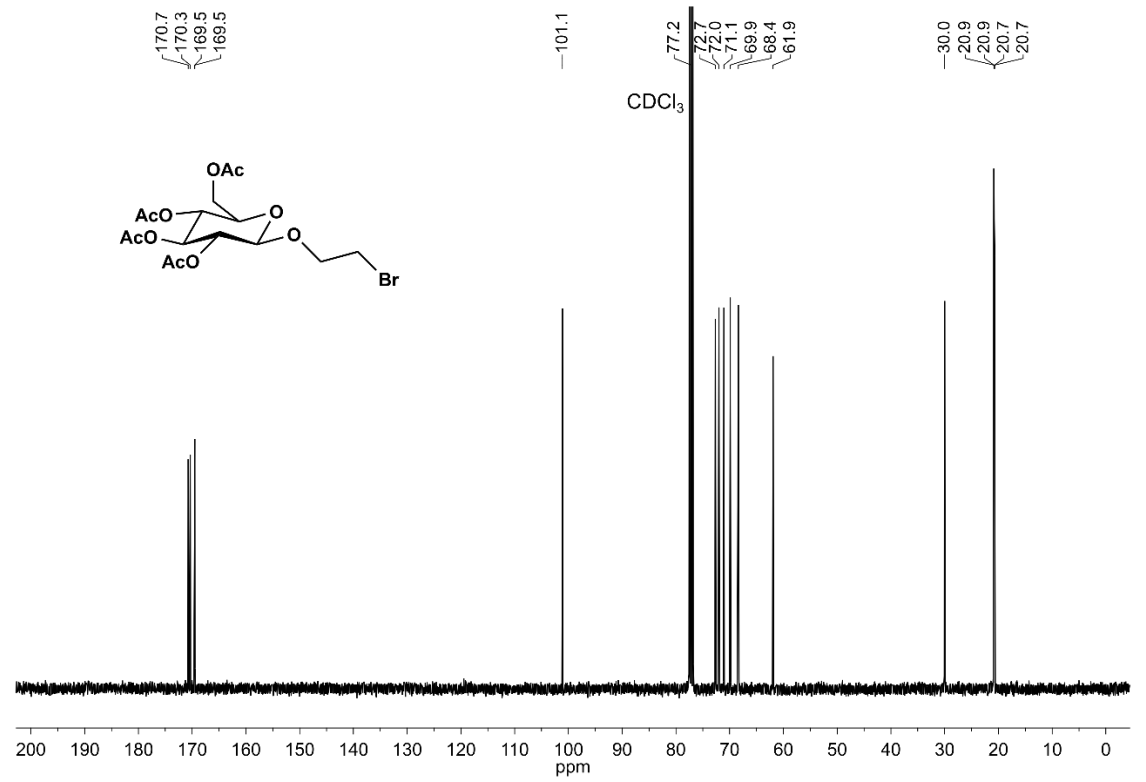

Figure S3. $^{13}C\{^{1}H\}$ NMR spectrum of $(OAc)_4$-β-D-glucoseEtBr ($CDCl_3$, 100 MHz, 25 °C).

S2.2.2. 5-((OAc)$_4$-β-D-glucoseEtO)-2-picolinaldehyde (subcomponent A)

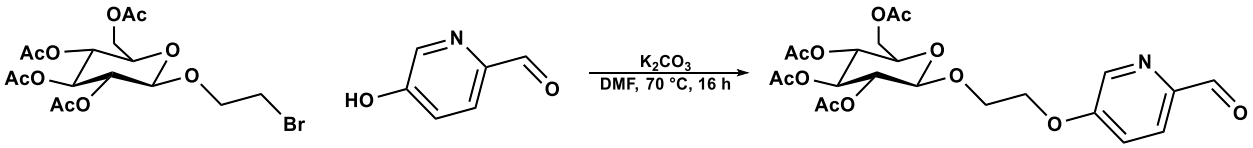

A 50 mL Schlenk flask was charged with (OAc)$_4$-β-D-glucoseEtBr (740 mg, 1.62 mmol, 1.00 equiv), K_2CO_3 (449 mg, 3.25 mmol, 2.00 equiv) and 5-hydroxypicolinaldehyde (200 mg, 1.62 mmol, 1.00 equiv). DMF (10 mL) was added to the flask, and the reaction mixture was allowed to stir at 70 °C for 16 h under an atmosphere of N_2, at which point it was allowed to cool to ambient temperature and diluted with EtOAc (200 mL). The solution was washed with a saturated aqueous solution of NaCl (3 x 150 mL), and the organic phase was dried over $MgSO_4$ and evaporated to dryness. The crude oil was purified by flash chromatography on silica gel (30-70% EtOAc/hexanes) to afford the pure product as a colorless solid (yield: 556 mg, 1.12 mmol, 69%). ^{1}H NMR (400 MHz, 25 °C, $CDCl_3$) δ: 9.95 (s, 1H, OC*H*), 8.40 (d, 1H, *J* = 2.7 Hz, py-*H*-6), 7.93 (d, 1H, *J* = 8.6 Hz, py-*H*-3), 7.29 (dd, 1H, *J* = 8.6, 2.7 Hz, py-*H*-4), 5.20 (t, 1H, *J* = 9.5 Hz, glc-*H*-3), 5.07 (t, 1H, *J* = 9.7 Hz, glc-*H*-4), 4.99 (dd, 1H, *J* = 9.7, 8.0 Hz, glc-*H*-2), 4.62 (d, 1H, *J* = 8.0 Hz, glc-*H*-1), 4.28–4.15 (m, 4H, glc-*H*-6$_b$, OC*H*$_{2b}$CH$_2$Opy, C*H*$_2$Opy signals overlapping), 4.13 (dd, 1H, *J* = 12.3, 2.4 Hz, glc-*H*-6$_a$), 3.95 (ddd, 1H, OC*H*$_{2a}$CH$_2$Opy), 3.71 (ddd, 1H, glc-*H*-5), 2.05 (s, 3H, C*H*$_3$COO), 2.00 (s, 3H, C*H*$_3$COO), 1.97 (s, 3H, C*H*$_3$COO), 1.92 (s, 3H, C*H*$_3$COO) ppm. ^{13}C{^{1}H} NMR (100 MHz, 25 °C, $CDCl_3$) δ: 192.0 (O*C*H), 170.7 (CH$_3$*C*OO), 170.3 (CH$_3$*C*OO), 169.5 (CH$_3$*C*OO), 169.3 (CH$_3$*C*OO), 158.2 (py-*C*-2), 146.6 (py-*C*-5), 138.9 (py-*C*-6), 123.5 (py-*C*-3), 120.7 (py-*C*-4), 101.0 (glc-*C*-1), 72.7 (glc-*C*-3), 72.1 (glc-*C*-5), 71.1 (glc-*C*-2), 68.3 (glc-*C*-4), 67.8 (O*C*H$_2$), 67.8 (O*C*H$_2$), 61.8 (glc-*C*-6), 20.8 (*C*H$_3$COO), 20.7 (*C*H$_3$COO), 20.6 (*C*H$_3$COO, two signals overlapping) ppm. ESI-MS(+): 498.1615 (calc'd, [M+H]$^+$ 498.1606 *m/z*). ATR-IR (ν): 2972, 2899, 2839, 1748 (HC=O), 1703 (C=O), 1577, 1372, 1319, 1211, 1126, 1036, 913, 846, 604 cm^{-1}.

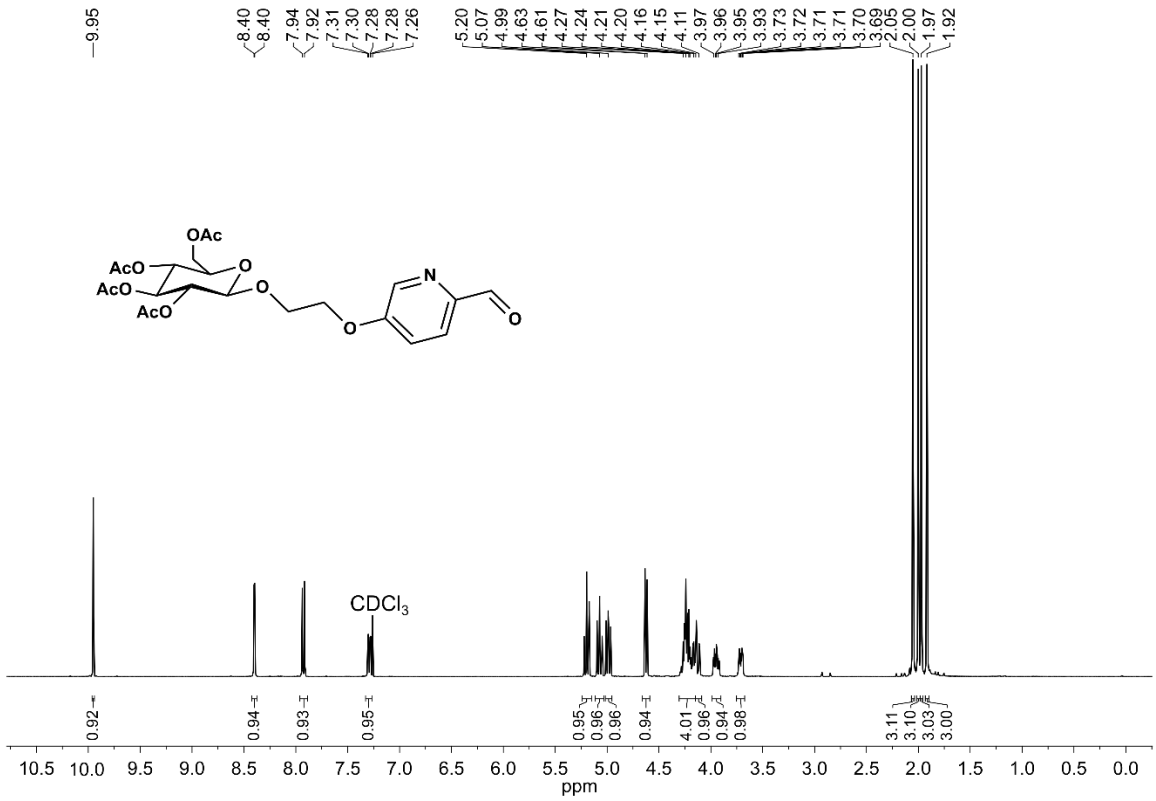

Figure S4. ^{1}H NMR spectrum of 5-((OAc)$_4$-β-D-glucoseEtO)-2-picolinaldehyde ($CDCl_3$, 400 MHz, 25 °C).

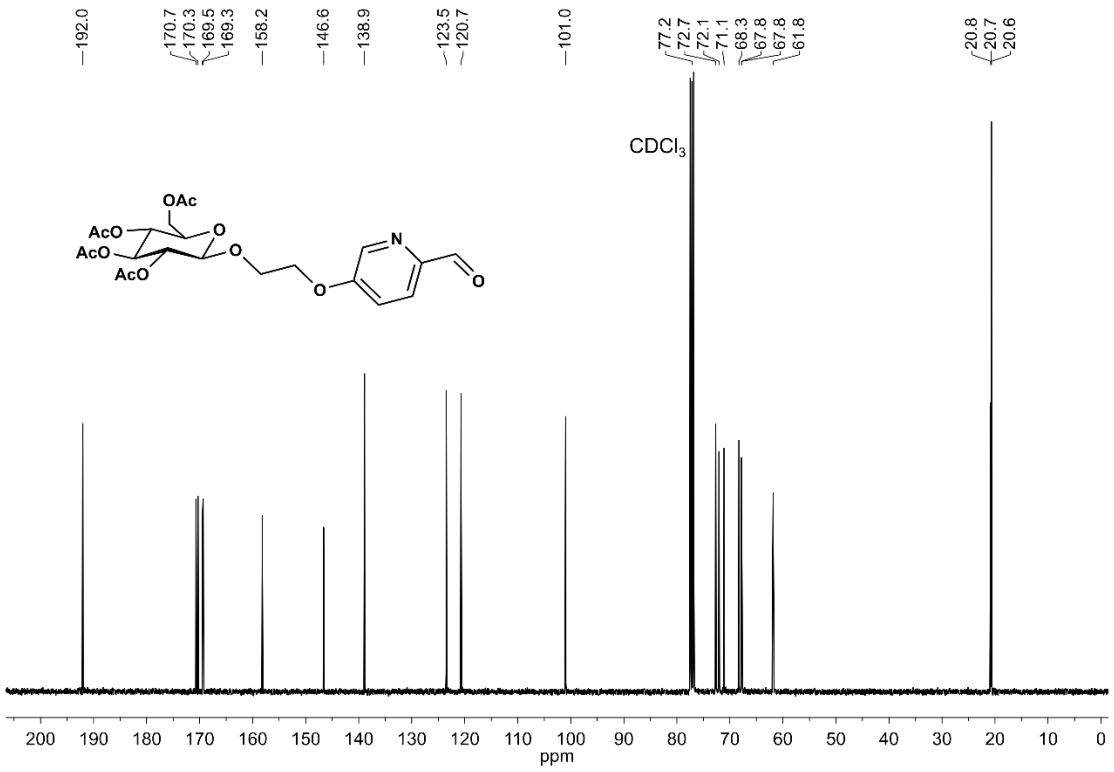

Figure S5. $^{13}C\{^{1}H\}$ NMR spectrum of 5-((OAc)$_4$-β-D-glucoseEtO)-2-picolinaldehyde ($CDCl_3$, 100 MHz, 25 °C).

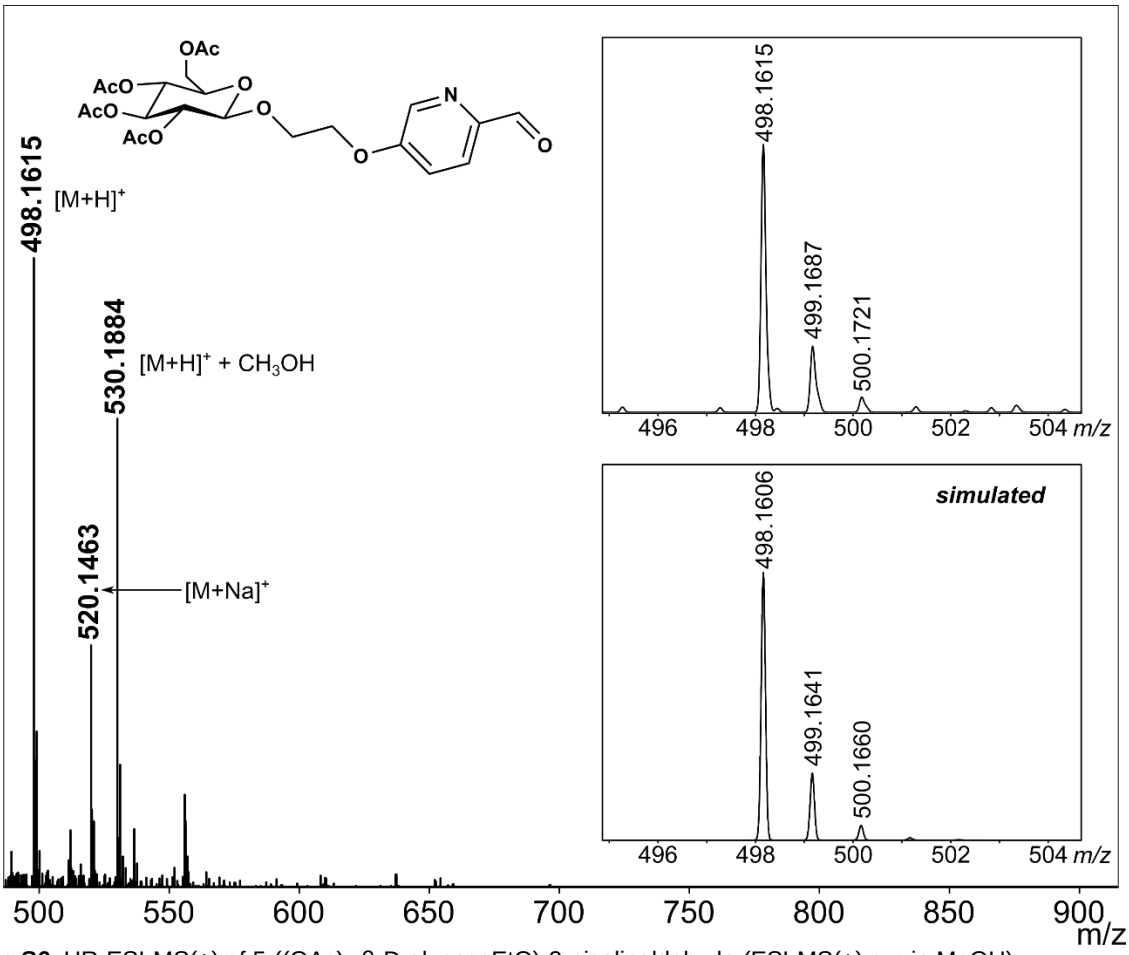

Figure S6. HR-ESI-MS(+) of 5-((OAc)$_4$-β-D-glucoseEtO)-2-picolinaldehyde (ESI-MS(+) run in MeOH).

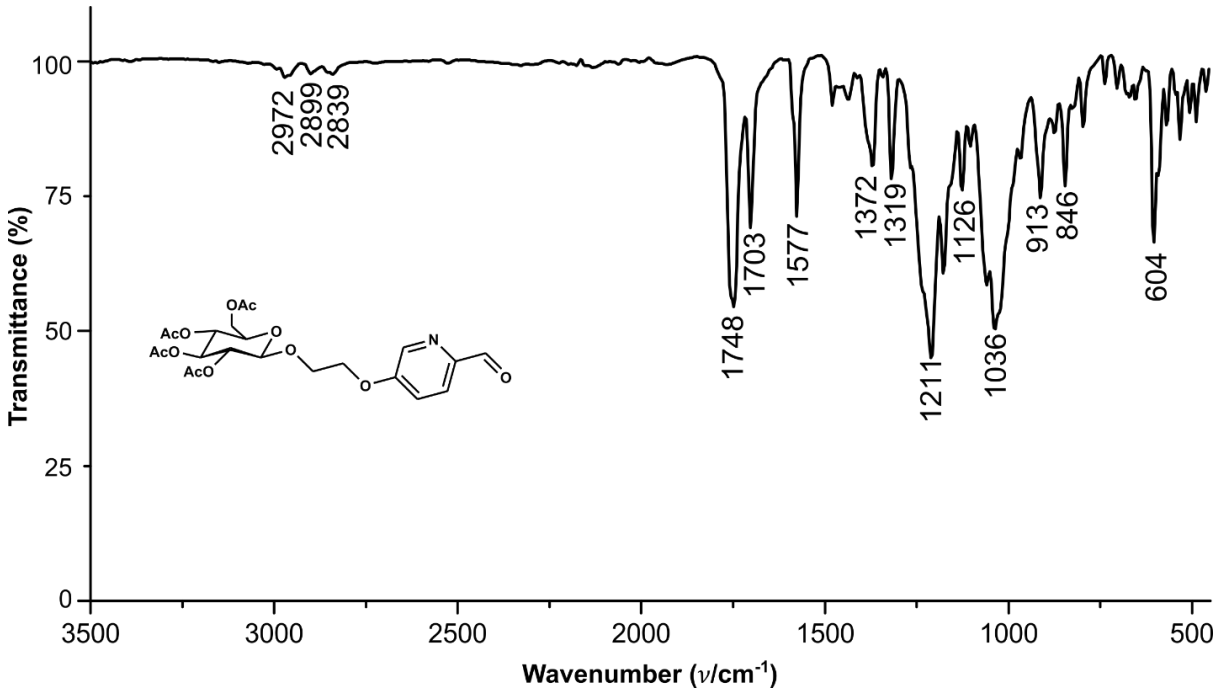

Figure S7. ATR-IR spectrum of 5-((OAc)$_4$-β-D-glucoseEtO)-2-picolinaldehyde.

S2.2.3. D-mannopyranose,1,2,3,4,6-pentaacetate (mixture of α and β anomers)

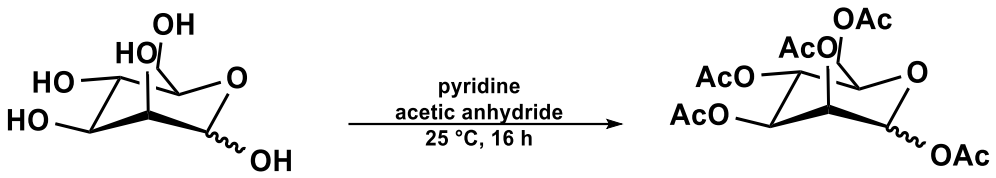

The preparation of D-mannopyranose,1,2,3,4,6-pentaacetate was adapted from a procedure reported by Seto *et al*.[4] and spectroscopic data match the literature reports.[5,6]

Pyridine (14 mL) was added to a solution of D-mannose (2.000 g, 11.10 mmol, 1.000 equiv) in acetic anhydride (6 mL) under an atmosphere of N_2. The reaction mixture was allowed to stir at ambient temperature for 16 h, at which point it was diluted with EtOAc (200 mL). The solution was then sequentially washed with HCl (1 M, 5 x 50 mL), a saturated aqueous solution of $NaHCO_3$ (10 x 100 mL), and a saturated aqueous solution of NaCl (150 mL). The organic phase was dried over $MgSO_4$ and evaporated to dryness to afford the product as a colorless viscous oil that was isolated as a mixture of anomers (α:β, 9:1) and used without further purification (yield 4.040 g, 10.36 mmol, 93%). ^{1}H NMR (400 MHz, 25 °C, $CDCl_3$) δ: 6.09 (d, 1H, *J* = 1.6 Hz, *H*-1), 5.36–5.34 (m, 2H, *H*-3, *H*-4 signals overlapping), 5.26 (m, 1H, *H*-2), 4.28 (dd, 1H, *J* = 12.4, 4.9 Hz, *H*-6_a), 4.11 (dd, 1H, *J* = 12.4, 2.9 Hz, *H*-6_b), 4.06–4.03 (m, 1H, *H*-5), 2.18 (s, 3H, C*H*$_3$COO), 2.17 (s, 3H, C*H*$_3$COO), 2.10 (s, 3H, C*H*$_3$COO), 2.05 (s, 3H, C*H*$_3$COO), 2.01 (s, 3H, C*H*$_3$COO) ppm. ^{13}C{^{1}H} NMR (100 MHz, 25 °C, $CDCl_3$) δ: 170.8 (CH$_3$*C*OO), 170.1 (CH$_3$*C*OO), 169.9 (CH$_3$*C*OO), 169.6 (CH$_3$*C*OO), 168.2 (CH$_3$*C*OO), 90.7 (*C*-1), 70.7 (*C*-5), 68.8 (*C*-3), 68.4 (*C*-2), 65.6 (*C*-4), 62.2 (*C*-6), 21.0 (*C*H$_3$COO), 20.9 (*C*H$_3$COO), 20.8 (*C*H$_3$COO), 20.8 (*C*H$_3$COO), 20.8 (*C*H$_3$COO) ppm. ^{1}H and ^{13}C NMR shifts are listed only for the α anomer.

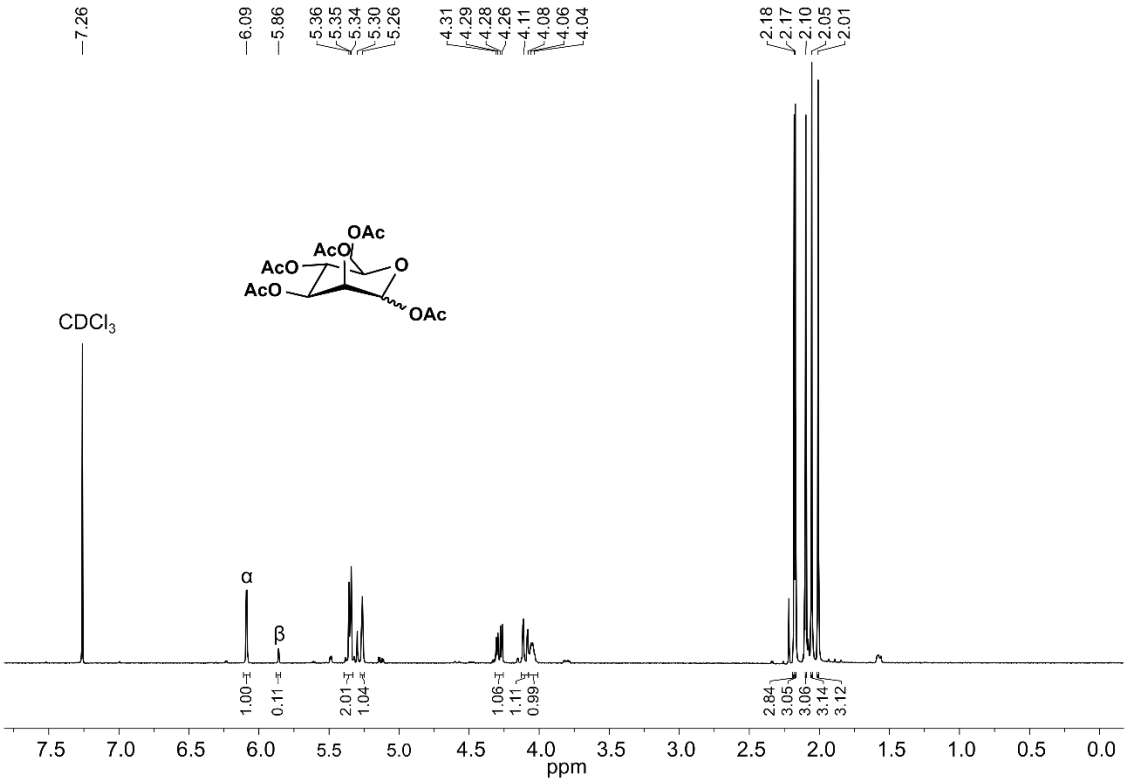

Figure S8. ^{1}H NMR spectrum of α/β-D-mannopyranose,1,2,3,4,6-pentaacetate ($CDCl_3$, 400 MHz, 25 °C).

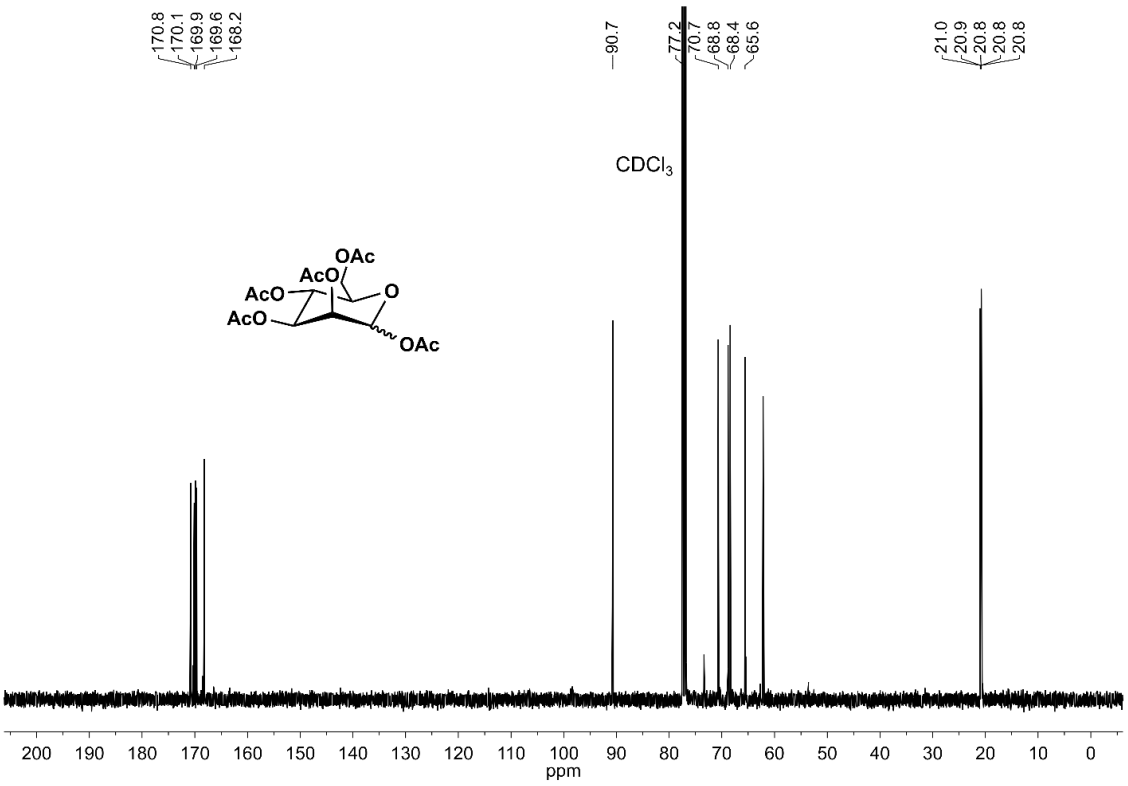

Figure S9. $^{13}C\{^{1}H\}$ NMR spectrum of α/β-D-mannopyranose,1,2,3,4,6-pentaacetate ($CDCl_3$, 100 MHz, 25 °C).

S2.2.4. $(OAc)_4$-α-D-mannoseEtBr

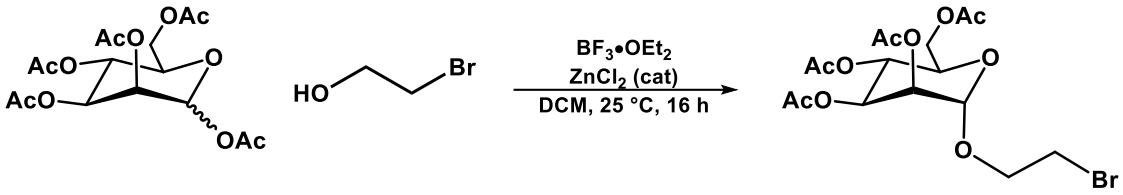

The preparation of $(OAc)_4$-α-D-mannoseEtBr was adapted from a similar procedure reported by Carell *et al*.[7] and spectroscopic data match the literature reports.[7,8]

A 250 mL two-neck flask was charged with D-mannopyranose,1,2,3,4,6-pentaacetate (mixture of α and β anomers) (4.500 g, 11.53 mmol, 1.000 equiv), $ZnCl_2$ (455 mg, 3.34 mmol, 0.290 equiv) and DCM (50 mL). To the flask was added 2-bromoethanol (1.2 mL, 17 mmol, 1.5 equiv), followed by BF_3•Et_2O (4.9 mL, 40 mmol, 3.4 equiv) dropwise over the course of 10 min under N_2. The pale-yellow reaction mixture was allowed to stir at ambient temperature for 16 h, at which point it was diluted with EtOAc (200 mL) and then washed with a saturated aqueous solution of NaCl (3 x 150 mL). The organic phase was dried over $MgSO_4$, and the filtrate was evaporated to dryness to yield a pale-yellow residue. The residue was suspended in Et_2O (15 mL), resulting in the precipitation of colorless solids. The solids were isolated by filtration and dried under reduced pressure to afford pure $(OAc)_4$-β-D-mannoseEtBr as a colorless solid. A second crop of pure product was obtained by evaporation of the filtrate to dryness and suspension of the resulting residue in Et_2O followed by filtration (yield: 2.309 g, 5.073 mmol, 44%). $(OAc)_4$-α-D-mannoseEtBr can also be purified through crystallization by layering pentane on top of a saturated Et_2O solution of the crude product and colorless crystals of the pure product are obtained at ambient temperature over the course of 48 h. ^{1}H NMR (400 MHz, 25 °C, $CDCl_3$) δ: 5.34 (dd, 1H, *J* = 9.9, 3.3 Hz, man-*H*-3), 5.32–5.25 (dd, 2H, man-*H*-2, man-*H*-4 signals overlapping), 4.87 (d, 1H, *J* = 1.6 Hz, man-*H*-1), 4.28 (dd, 1H, *J* = 12.6, 5.9 Hz, man-*H*-6_a), 4.16–4.11 (m, 2H, man-*H*-5, man-*H*-6_b signals overlapping), 3.99 (dt, 1H, *J* = 11.4, 5.9 Hz, OCH_{2a}), 3.88 (dt, 1H, *J* = 11.4, 5.9 Hz, OCH_{2b}), 3.52 (t, 1H, *J* = 5.9 Hz, CH_2Br), 2.16 (s, 3H, CH_3COO), 2.11 (s, 3H, CH_3COO), 2.05 (s, 3H, CH_3COO), 2.00 (s, 3H, CH_3COO) ppm. ^{13}C{^{1}H} NMR (100 MHz, 25 °C, $CDCl_3$) δ: 170.8 (CH_3*C*OO), 170.2 (CH_3*C*OO), 170.0 (CH_3*C*OO), 169.9 (CH_3*C*OO), 97.9 (man-*C*-1), 69.5 (man-*C*-2), 69.1 (man-*C*-3), 69.0 (man-*C*-5), 68.6 (O*C*H_2), 66.1 (man-*C*-4), 62.5 (man-*C*-6), 29.8 (*C*H_2Br), 21.0 (CH_3*C*OO), 20.9 (CH_3*C*OO), 20.8 (CH_3*C*OO), 20.8 (CH_3*C*OO) ppm.

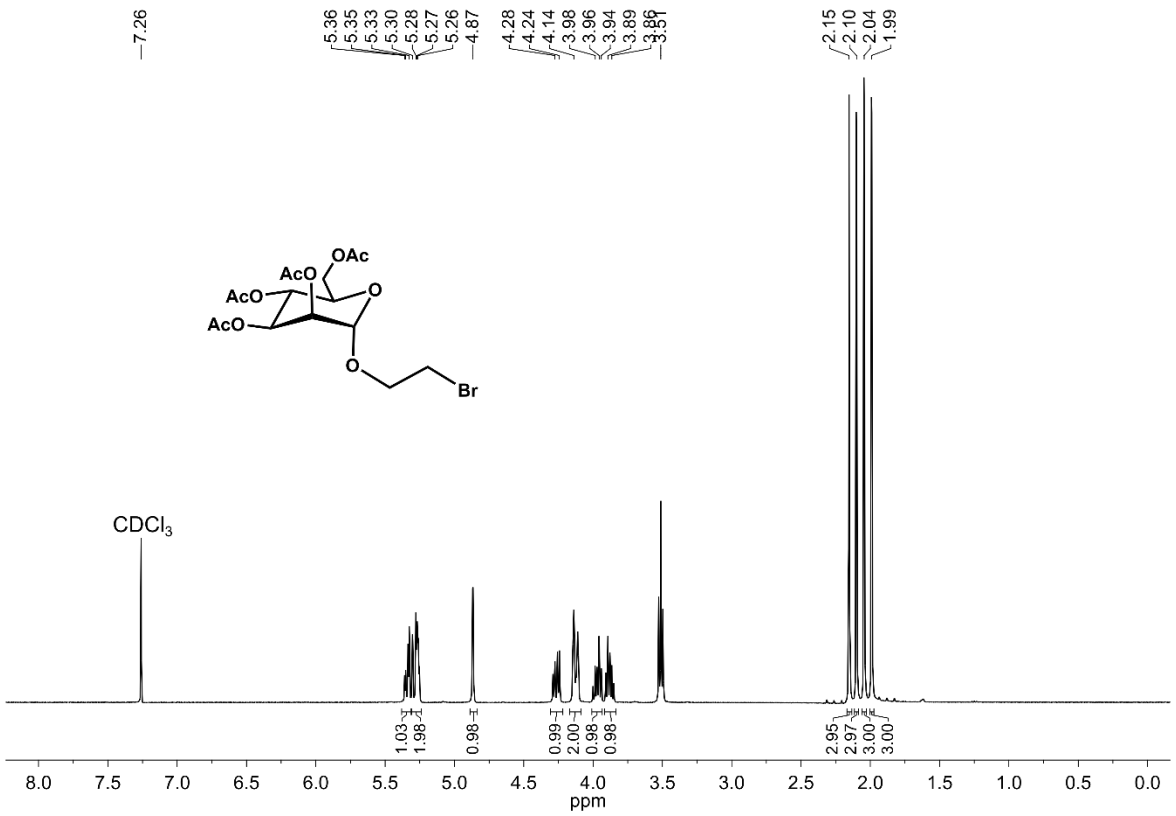

Figure S10. ^{1}H NMR spectrum of $(OAc)_4$-α-D-mannoseEtBr ($CDCl_3$, 400 MHz, 25 °C).

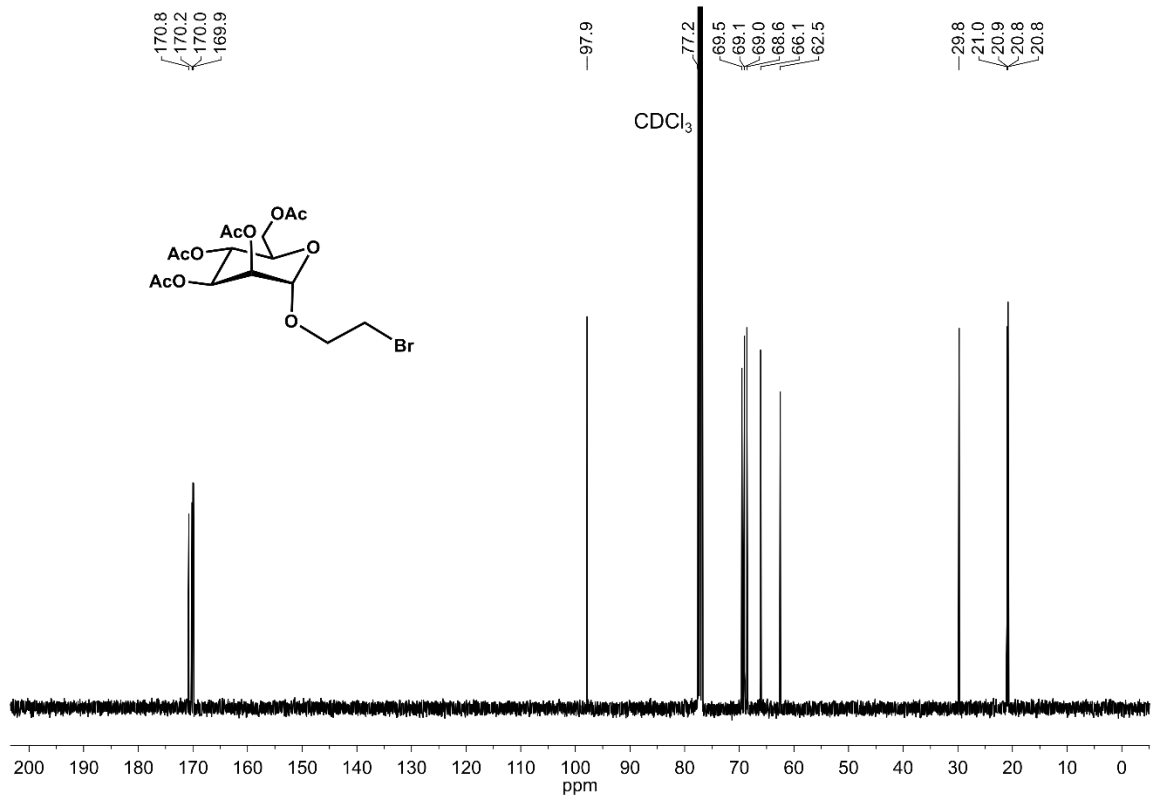

Figure S11. $^{13}C\{^{1}H\}$ NMR spectrum of $(OAc)_4$-α-D-mannoseEtBr ($CDCl_3$, 100 MHz, 25 °C).

S2.2.5. 5-((OAc)$_4$-α-D-mannoseEtO)-2-picolinaldehyde (subcomponent B)

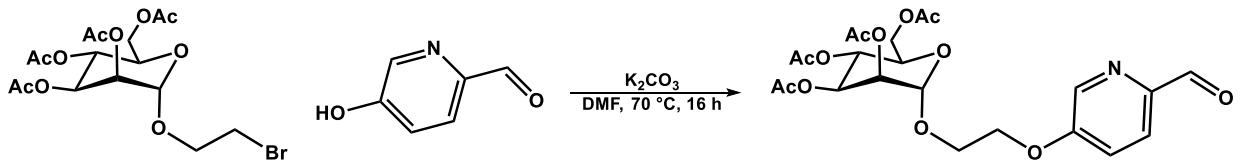

A 50 mL Schlenk flask was charged with (OAc)$_4$-α-D-mannoseEtBr (740 mg, 1.62 mmol, 1.00 equiv), K_2CO_3 (449 mg, 3.25 mmol, 2.00 equiv) and 5-hydroxypicolinaldehyde (200 mg, 1.62 mmol, 1.00 equiv). DMF (10 mL) was added to the flask, and the reaction mixture was allowed to stir at 70 °C for 16 h under an atmosphere of N_2, at which point it was allowed to cool to ambient temperature and diluted with EtOAc (200 mL). The solution was washed with a saturated aqueous solution of NaCl (3 x 150 mL), and the organic phase was dried over $MgSO_4$ and evaporated to dryness. The crude oil was purified by flash chromatography on silica gel (30-70% EtOAc/hexanes) to afford the pure product as a colorless oil (yield: 610 mg, 1.23 mmol, 76%). ^{1}H NMR (400 MHz, 25 °C, $CDCl_3$) δ: 9.93 (s, 1H, OC*H*), 8.40 (d, 1H, *J* = 2.6 Hz, py-*H*-6), 7.92 (d, 1H, *J* = 8.7 Hz, py-*H*-3), 7.25 (dd, 1H, *J* = 8.7, 2.8 Hz, py-*H*-4), 5.27–5.20 (m, 3H, man-*H*-3, man-*H*-2, man-*H*-4 signals overlapping), 4.89 (d, 1H, *J* = 1.6 Hz, man-*H*-1), 4.28–4.20 (m, 3H, man-*H*-6, man-*H*-5 signals overlapping), 4.08–4.01 (m, 2H, CH_2Opy), 4.00–3.97 (m, 1H,OCH_{2a}CH$_2$), 3.90–3.85 (m, 1H, OCH_{2b}CH$_2$), 2.11 (s, 3H, CH_3COO), 2.03 (s, 3H, CH_3COO), 1.98 (s, 3H, CH_3COO), 1.93 (s, 3H, CH_3COO) ppm. ^{13}C{^{1}H} NMR (100 MHz, 25 °C, $CDCl_3$) δ: 191.9 (O*C*H), 170.5 (CH$_3$*C*OO), 169.9 (CH$_3$*C*OO), 169.8 (CH$_3$*C*OO), 169.6 (CH$_3$*C*OO), 157.9 (py-*C*-2), 146.5 (py-*C*-5), 138.7 (py-*C*-6), 123.3 (py-*C*-3), 120.7 (py-*C*-4), 97.6 (man-*C*-1), 69.2 (man-*C*-2), 68.7 (man-*C*-3), 68.7 (man-*C*-5), 67.4 (man-*C*-4), 66.1 (O*C*H$_2$), 65.9 (O*C*H$_2$), 62.4 (man-*C*-6), 20.8 (CH$_3$*C*OO), 20.7 (CH$_3$*C*OO), 20.6 (CH$_3$*C*OO), 20.6 (CH$_3$*C*OO) ppm. ESI-MS(+): 498.1612 (calc'd, [M+H]$^+$ 498.1606 *m/z*). ATR-IR (v): 2949, 1741 (HC=O), 1707 (C=O), 1577, 1372, 1215, 1141, 1092, 1044, 980, 921, 846, 608 cm^{-1}.

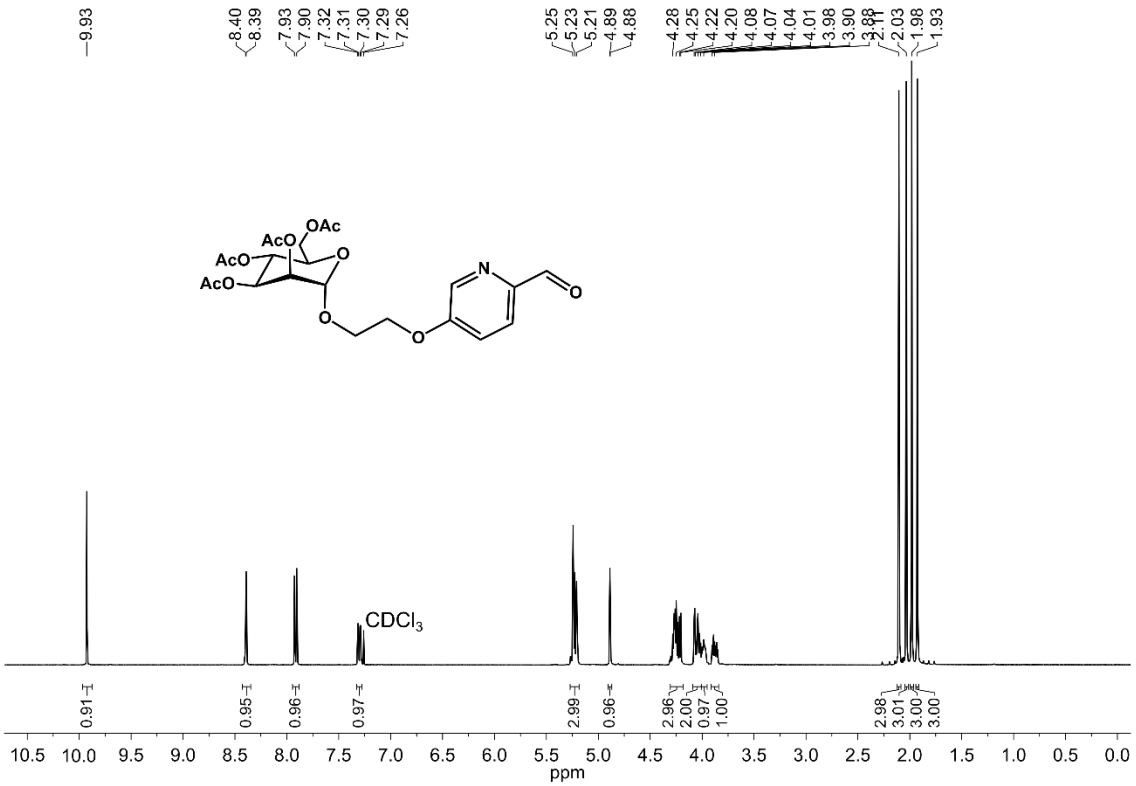

Figure S12. ^{1}H NMR spectrum of 5-((OAc)$_4$-α-D-mannoseEtO)-2-picolinaldehyde ($CDCl_3$, 400 MHz, 25 °C).

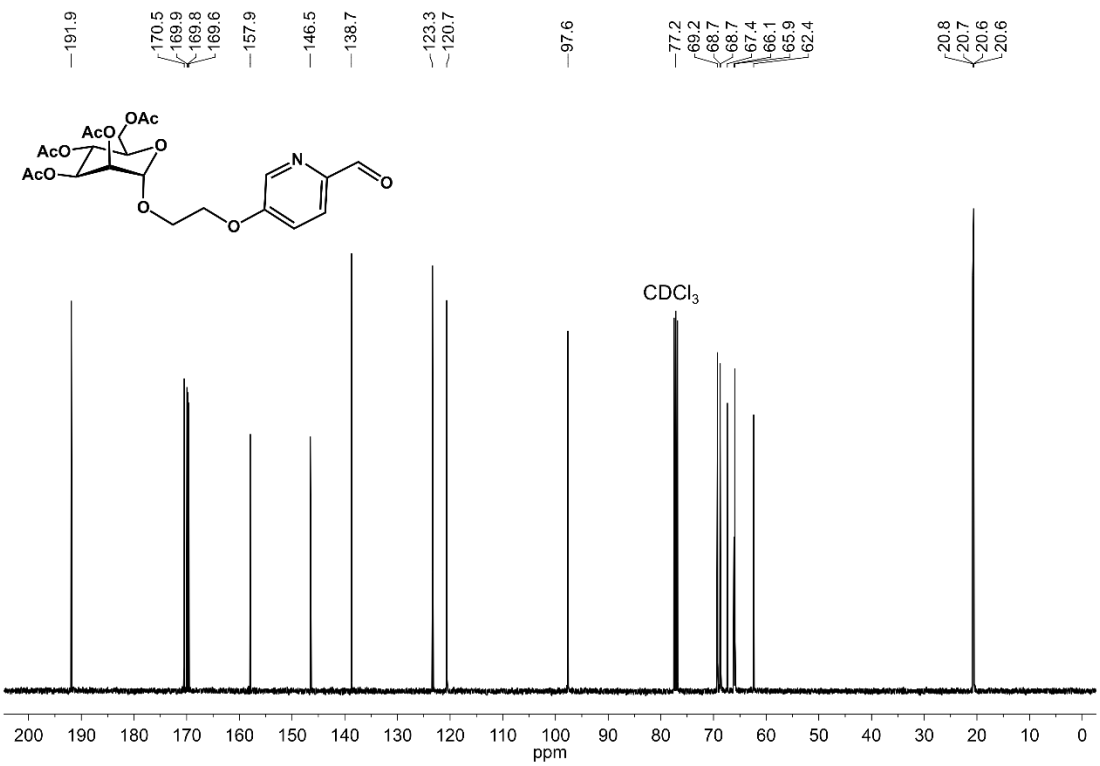

Figure S13. $^{13}C\{^{1}H\}$ NMR spectrum of 5-((OAc)$_4$-α-D-mannoseEtO)-2-picolinaldehyde ($CDCl_3$, 100 MHz, 25 °C).

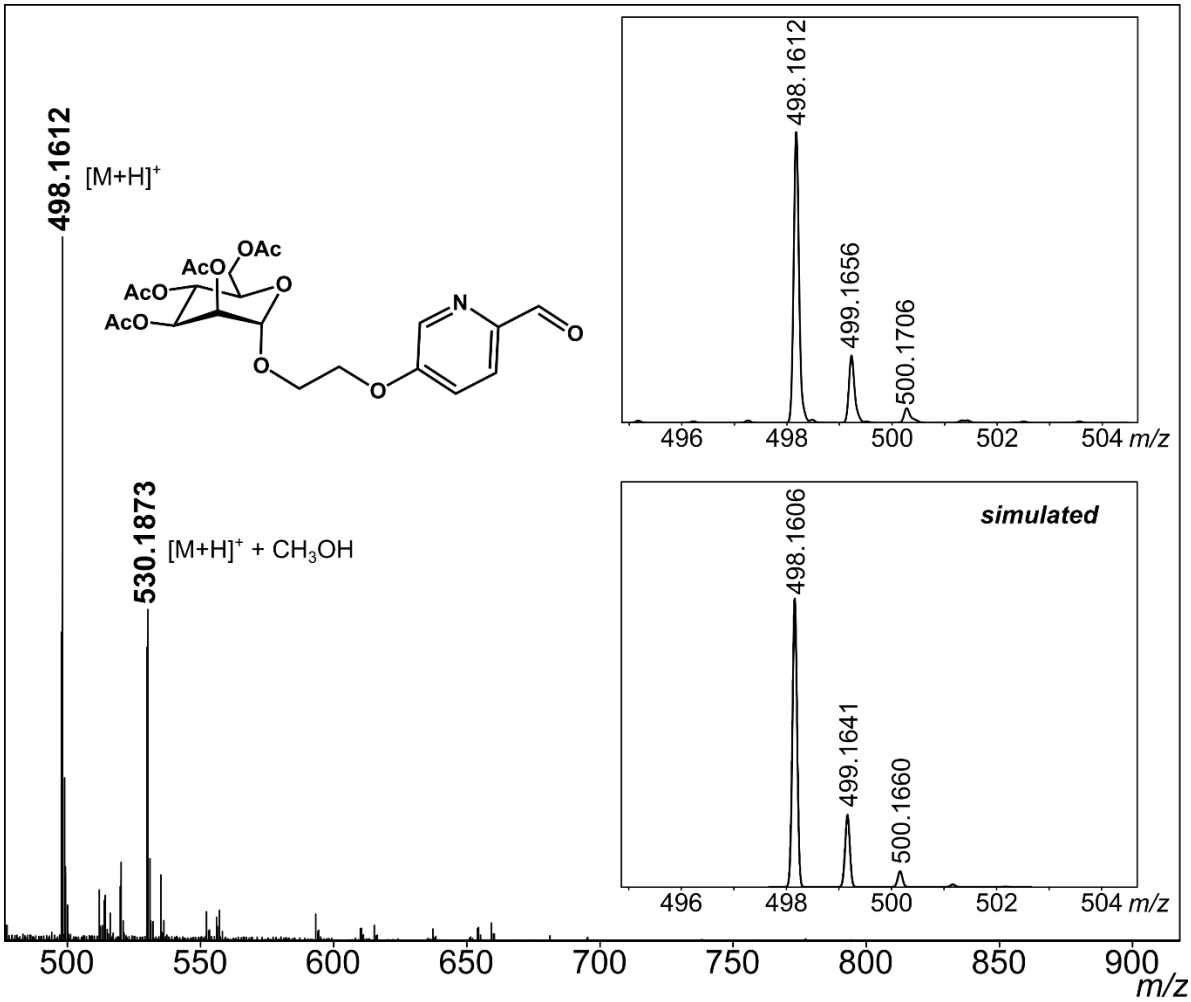

Figure S14. HR-ESI-MS(+) of 5-((OAc)$_4$-α-D-mannoseEtO)-2-picolinaldehyde (ESI-MS(+) run in MeOH).

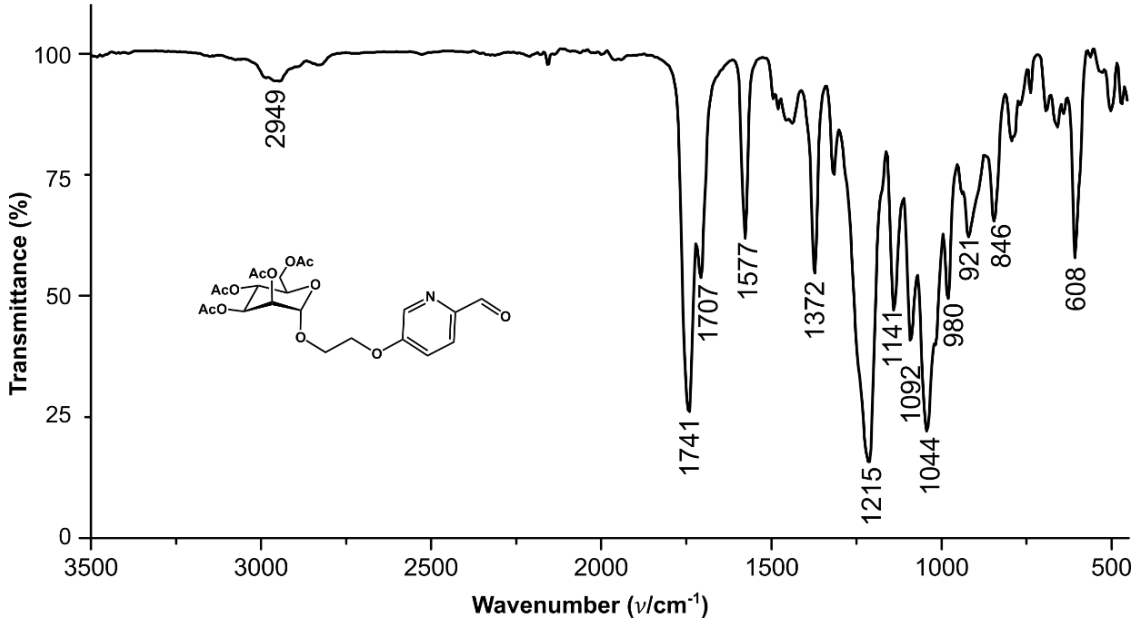

Figure S15. ATR-IR spectrum of 5-((OAc)$_4$-α-D-mannoseEtO)-2-picolinaldehyde.

S2.2.6. $(OAc)_4$-β-D-galactoseEtBr

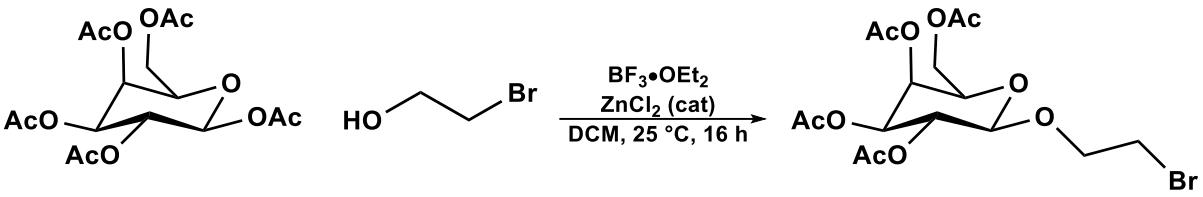

The preparation of $(OAc)_4$-β-D-galactoseEtBr was adapted from a procedure reported by Bradley *et al*.[9] and spectroscopic data match the literature reports.[10,11]

A 250 mL two-neck flask was charged with $(OAc)_5$-β-D-galactose (5.000 g, 12.81 mmol, 1.000 equiv), $ZnCl_2$ (505 mg, 3.71 mmol, 0.290 equiv) and DCM (50 mL). To the flask was added 2-bromoethanol (1.4 mL, 19 mmol, 1.5 equiv), followed by BF_3•Et_2O (5.4 mL, 44 mmol, 3.4 equiv) dropwise over the course of 10 min under N_2. The pale-yellow reaction mixture was allowed to stir at ambient temperature for 16 h, at which point it was diluted with EtOAc (200 mL) and then washed with a saturated aqueous solution of NaCl (3 x 150 mL). The organic phase was then dried over $MgSO_4$, and the resulting solution was evaporated to dryness to yield a crude yellow oil, which was dissolved in a minimal amount of EtOAc (ca. 15 mL). The solution was layered with pentane (ca. 30 mL) and then allowed to stand at ambient temperature overnight, resulting in the formation of colorless crystals. The crystals were isolated and dried under reduced pressure to yield pure $(OAc)_4$-β-D-galactoseEtBr (3.650 g, 8.021 mmol, 63%). ^{1}H NMR (400 MHz, 25 °C, $CDCl_3$) δ: 5.39 (dd, 1H, *J* = 3.4, 1.0 Hz, gal-*H*-4), 5.23 (dd, 1H, *J* = 10.5, 7.9 Hz, gal-*H*-2), 5.02 (dd, 1H, *J* = 10.5, 3.4 Hz, gal-*H*-3), 4.51 (d, 1H, *J* = 7.9 Hz, gal-*H*-1), 4.20–4.16 (m, 2H, OC$H_2$$CH_2$), 4.12–3.91 (m, 2H, gal-*H*-6), 3.84–3.78 (m, 1H, gal-*H*-5), 3.48–3.45 (m, 2H, CH_2Br), 2.15 (s, 3H, CH_3COO), 2.08 (s, 3H, CH_3COO), 2.05 (s, 3H, CH_3COO), 1.98 (s, 3H, CH_3COO) ppm. ^{13}C{^{1}H} NMR (100 MHz, 25 °C, $CDCl_3$) δ: 170.5 (CH_3*C*OO), 170.4 (CH_3*C*OO), 170.3 (CH_3*C*OO), 169.7 (CH_3*C*OO), 101.7 (gal-*C*-1), 70.9 (gal-*C*-5), 70.8 (gal-*C*-3), 69.9 (gal-*C*-2), 68.6 (gal-*C*-4), 67.1 (OCH_2), 61.4 (gal-*C*-6), 30.1 (*C*H_2Br), 21.0 (*C*H_3COO), 20.8 (*C*H_3COO), 20.8 (*C*H_3COO), 20.7 (*C*H_3COO) ppm.

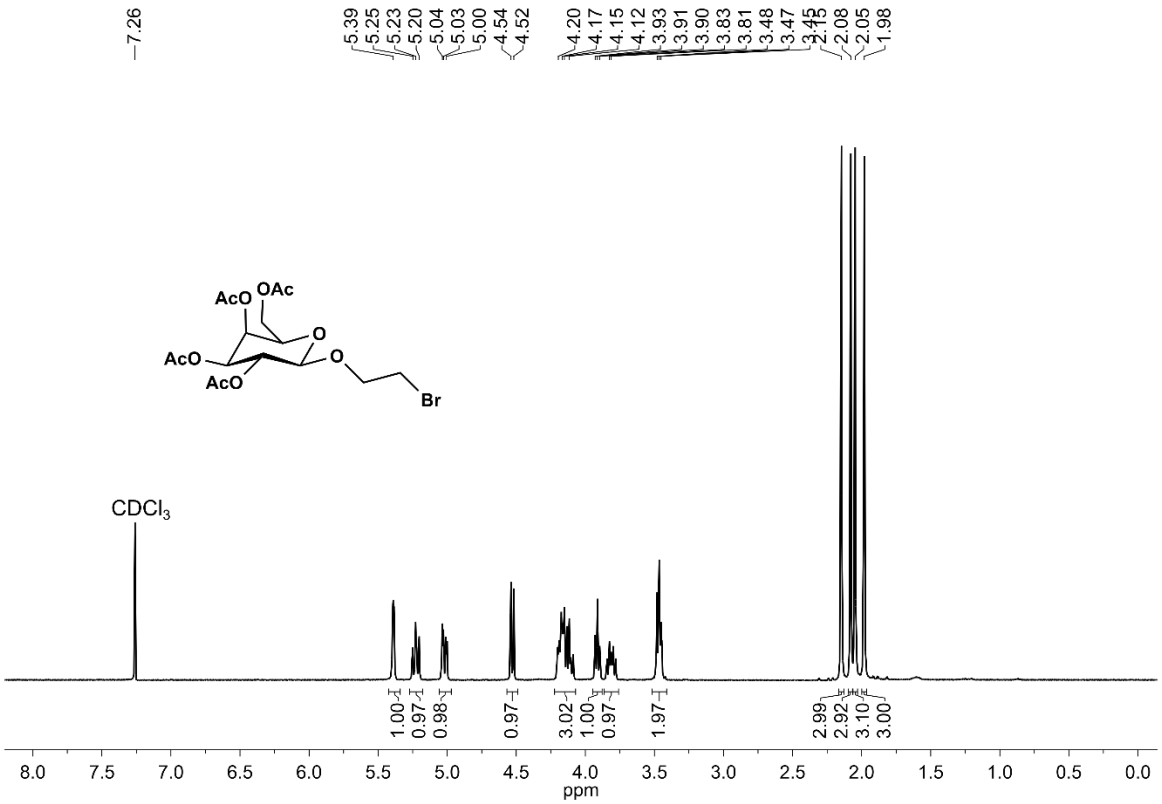

Figure S16. ^{1}H NMR spectrum of $(OAc)_4$-β-D-galactoseEtBr ($CDCl_3$, 400 MHz, 25 °C).

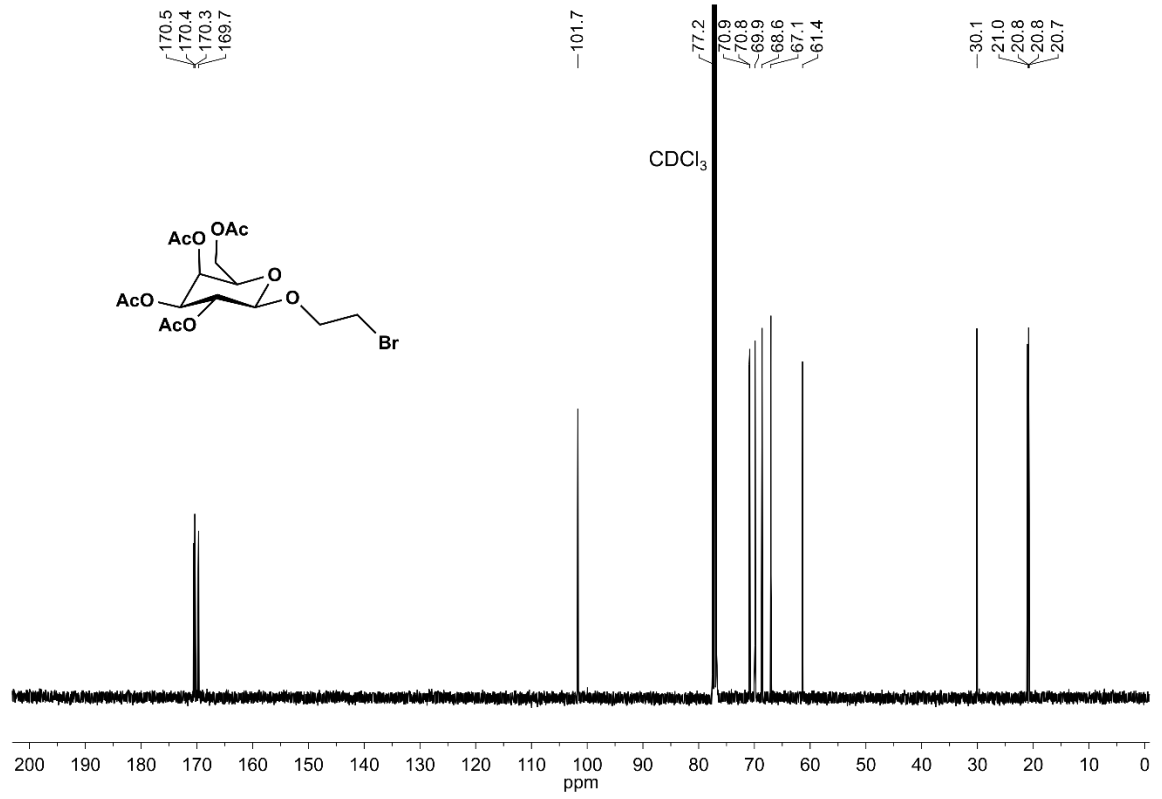

Figure S17. $^{13}C\{^{1}H\}$ NMR spectrum of $(OAc)_4$-β-D-galactoseEtBr ($CDCl_3$, 100 MHz, 25 °C).

S2.2.7. 5-((OAc)$_4$-β-D-galactoseEtO)-2-picolinaldehyde (subcomponent C)

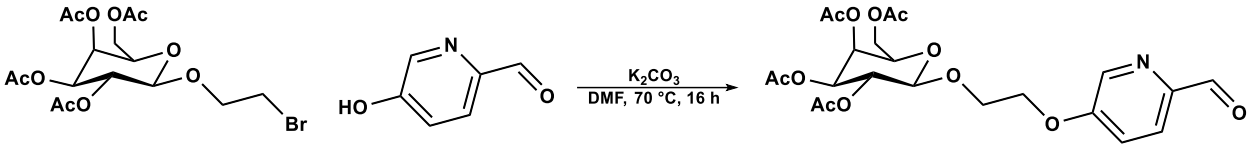

A 50 mL Schlenk flask was charged with (OAc)$_4$-β-D-galactoseEtBr (740 mg, 1.62 mmol, 1.00 equiv), K_2CO_3 (449 mg, 3.25 mmol, 2.00 equiv) and 5-hydroxypicolinaldehyde (200 mg, 1.62 mmol, 1.00 equiv). DMF (10 mL) was added to the flask, and the reaction mixture was allowed to stir at 70 °C for 16 h under an atmosphere of N_2, at which point it was allowed to cool to ambient temperature and diluted with EtOAc (200 mL). The solution was washed with a saturated aqueous solution of NaCl (3 x 150 mL), and the organic phase was dried over $MgSO_4$ and evaporated to dryness. The crude oil was purified by flash chromatography on silica gel (30-70% EtOAc/hexanes) to afford the pure product as a colorless oil (yield: 640 mg, 1.29 mmol, 79%). ^{1}H NMR (400 MHz, 25 °C, $CDCl_3$) δ: 9.88 (s, 1H, OC*H*), 8.34 (d, 1H, *J* = 2.6 Hz, py-*H*-6), 7.86 (d, 1H, *J* = 8.7 Hz, py-*H*-3), 7.25 (dd, 1H, *J* = 8.5, 2.4 Hz, py-*H*-4), 5.32 (d, 1H, *J* = 3.0 Hz, gal-*H*-4), 5.13 (dd, 1H, *J* = 10.4, 8.0 Hz, gal-*H*-2), 4.95 (dd, 1H, *J* = 10.5, 3.4 Hz, gal-*H*-3), 4.55 (d, 1H, *J* = 8.0 Hz, gal-*H*-1), 4.25–4.02 (m, 5H, CH_2Opy, gal-*H*-6, gal-*H*-5 signals overlapping), 3.93–3.87 (m, 2H, OCH_2CH$_2$), 2.06 (s, 3H, CH_3COO), 1.95 (s, 3H, CH_3COO), 1.89 (s, 3H, CH_3COO), 1.86 (s, 3H, CH_3COO) ppm. ^{13}C{^{1}H} NMR (100 MHz, 25 °C, $CDCl_3$) δ: 191.8 (O*C*H), 170.3 (CH$_3$*C*OO), 170.1 (CH$_3$*C*OO), 170.0 (CH$_3$*C*OO), 169.3 (CH$_3$*C*OO), 158.1 (py-*C*-2), 146.4 (py-*C*-5), 138.8 (py-*C*-6), 123.4 (py-*C*-3), 120.6 (py-*C*-4), 101.3 (gal-*C*-1), 70.8 (gal-*C*-5), 70.7 (gal-*C*-3), 68.5 (gal-*C*-2), 67.7 (O*C*H$_2$), 67.6 (O*C*H$_2$), 66.9 (gal-*C*-4), 61.2 (gal-*C*-6), 20.6 (*C*H$_3$COO), 20.6 (*C*H$_3$COO, two signals overlapping), 20.5 (*C*H$_3$COO) ppm. ESI-MS(+): 498.1608 (calc'd, [M+H]$^+$ 498.1606 *m/z*). ATR-IR (ν): 2961, 1748 (HC=O), 1707 (C=O), 1674 (C=O), 1577, 1372, 1215, 1044, 902, 736, 664, 608 cm^{-1}.

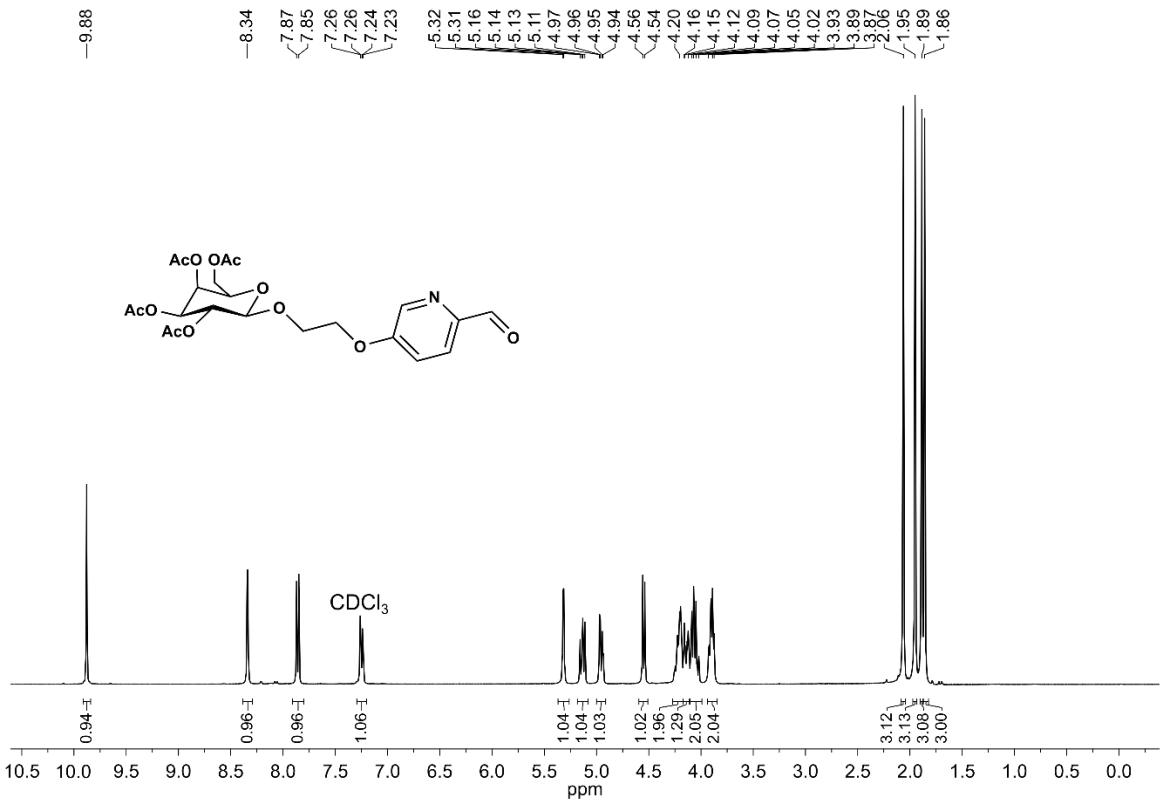

Figure S18. ^{1}H NMR spectrum of 5-((OAc)$_4$-β-D-galactoseEtO)-2-picolinaldehyde ($CDCl_3$, 400 MHz, 25 °C).

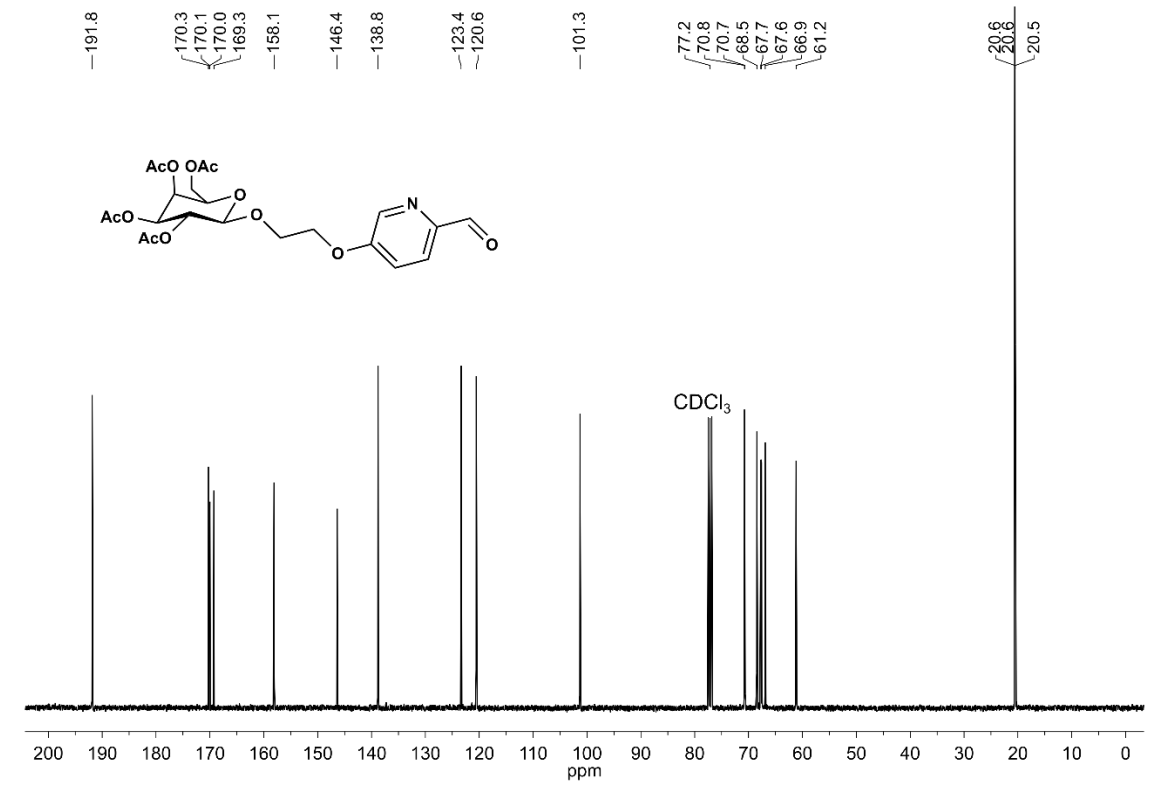

Figure S19. $^{13}C\{^{1}H\}$ NMR spectrum of 5-((OAc)$_4$-β-D-galactoseEtO)-2-picolinaldehyde ($CDCl_3$, 100 MHz, 25 °C).

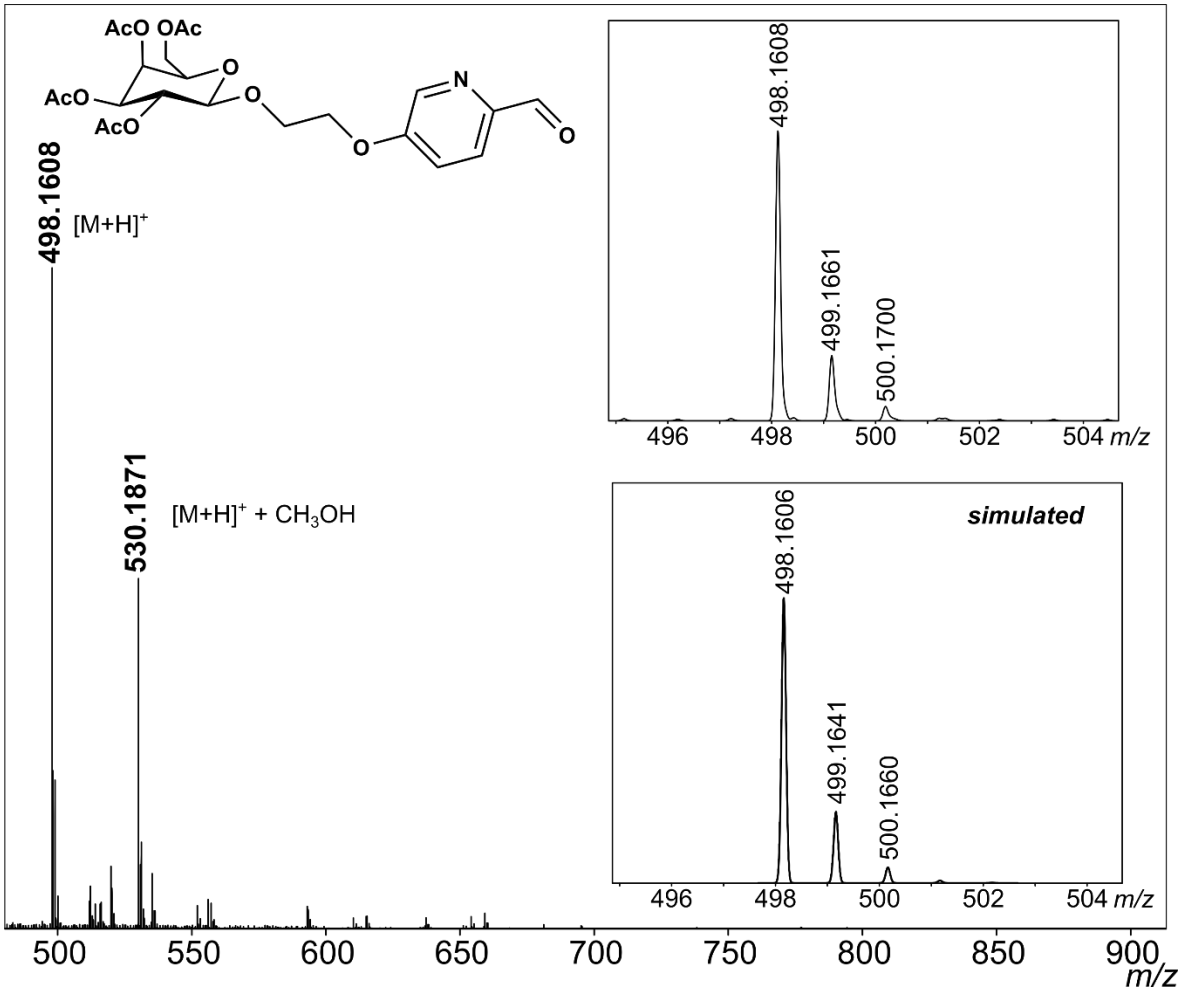

Figure S20. HR-ESI-MS(+) of 5-((OAc)$_4$-β-D-galactoseEtO)-2-picolinaldehyde (ESI-MS(+) run in MeOH).

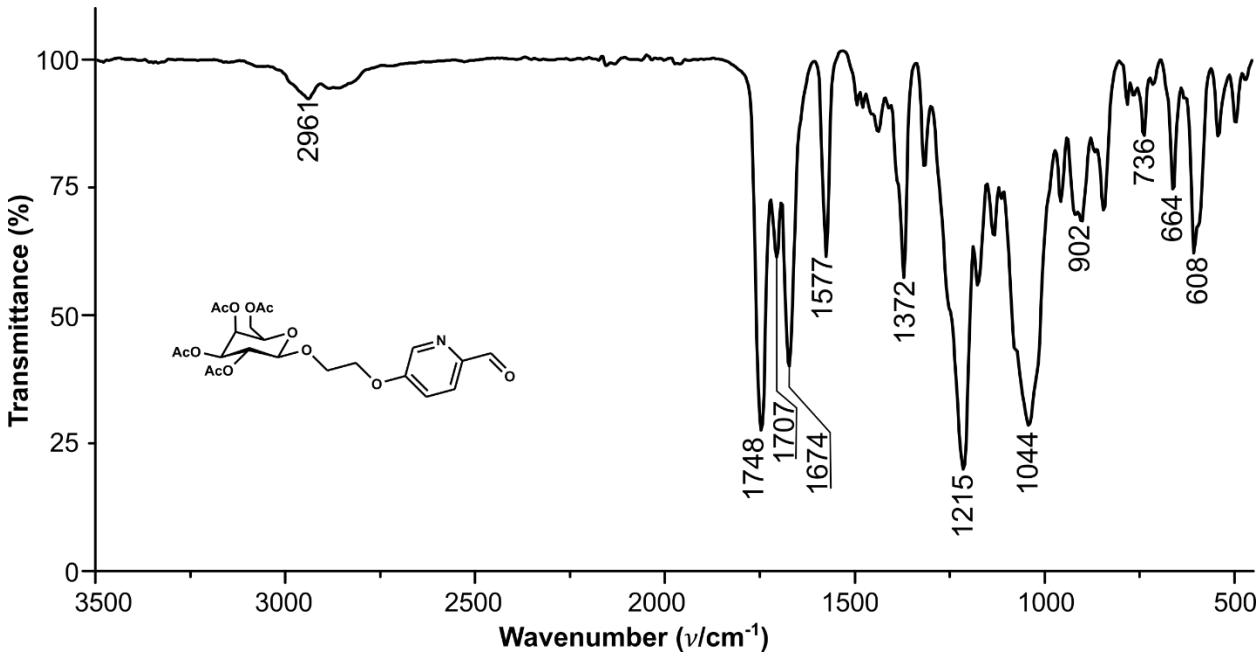

Figure S21. ATR-IR spectrum of 5-((OAc)$_4$-β-D-galactoseEtO)-2-picolinaldehyde.

S2.2.8. $(OAc)_7$-β-D-maltoseEtBr

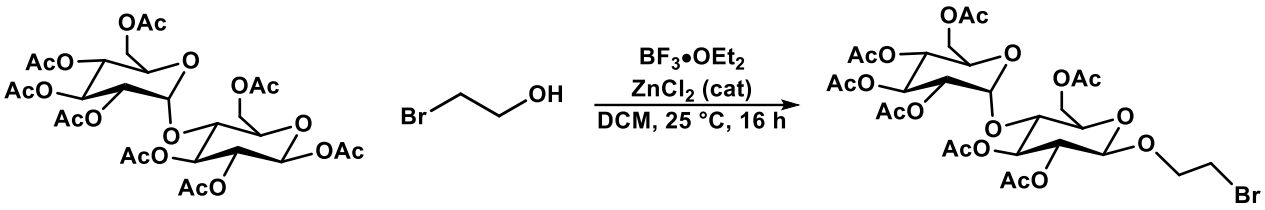

The preparation of $(OAc)_7$-β-D-maltoseEtBr was adapted from a similar procedure reported by Messersmith *et al*.[12] and spectroscopic data match the literature report.

A 100 mL two-neck flask was charged with $(OAc)_8$-β-D-maltose (2.000 g, 2.947 mmol, 1.000 equiv), $ZnCl_2$ (116 mg, 0.851 mmol, 0.290 equiv) and DCM (25 mL). To the flask was added 2-bromoethanol (0.31 mL, 4.4 mmol, 1.5 equiv), followed by BF_3•Et_2O (1.3 mL, 10 mmol, 3.4 equiv) dropwise over the course of 10 min under N_2. The pale-yellow reaction mixture was allowed to stir at ambient temperature for 16 h, at which point it was diluted with EtOAc (200 mL) and then washed with saturated aqueous solution of NaCl (3 x 150 mL). The organic phase was dried over $MgSO_4$, and the solution was evaporated to dryness to yield a residue, which was dissolved in Et_2O (15 mL). Pentane (25 mL) was layered on top of the solution, and the mixture was allowed to stand at ambient temperature overnight, resulting in the precipitation of colorless solids. The supernatant was removed, and the solids were dried under reduced pressure to afford $(OAc)_7$-β-D-maltoseEtBr as a colorless solid. The product was used without further purification (yield: 0.964 g, 1.297 mmol, 44%). ^{1}H NMR (400 MHz, 25 °C, $CDCl_3$) δ: 5.40 (d, 1H, *J* = 3.9 Hz, mal-*H*-1'), 5.34 (t, 1H, *J* = 10.5 Hz, mal-*H*-3'), 5.25 (t, 1H, *J* = 9.3 Hz, mal-*H*-3), 5.04 (t, 1H, *J* = 10.1 Hz, mal-*H*-4'), 4.85–4.83 (m, 2H, mal-*H*-2, mal-*H*-2' signals overlapping), 4.58 (d, 1H, *J* = 6.9 Hz, mal-*H*-1), 4.48 (dd, 1H, *J* = 12.1, 2.2 Hz, mal-*H*-6_a), 4.24 (dd, 1H, *J* = 12.5, 4.0 Hz, mal-*H*-$6'_a$), 4.21 (dd, 1H, *J* = 12.2, 4.0 Hz, mal-*H*-6_b), 4.11 (ddd, 1H, *J* = 11.4, 6.1, 5.2 Hz, OC*H*$_a$), 4.04–3.90 (m, 3H, mal-*H*-4, mal-*H*-$6'_b$, mal-*H*-5' signals overlapping), 3.80 (ddd, 1H, *J* = 11.4, 7.9, 6.4 Hz, OC*H*$_b$), 3.68 (m, 1H, mal-*H*-5), 3.45–3.41 (m, 2H, C*H*$_2$Br), 2.13 (s, 3H, C*H*$_3$COO), 2.09 (s, 3H, C*H*$_3$COO), 2.03 (s, 6H, C*H*$_3$COO, two signals overlapping), 2.01 (s, 3H, C*H*$_3$COO), 1.99 (s, 6H, C*H*$_3$COO, two signals overlapping) ppm. ^{13}C{^{1}H} NMR (100 MHz, 25 °C, $CDCl_3$) δ: 170.5 (CH_3*C*OO, two signals overlapping), 170.5 (CH_3*C*OO), 170.3 (CH_3*C*OO), 170.1 (CH_3*C*OO), 169.8 (CH_3*C*OO), 169.6 (CH_3*C*OO), 100.6 (mal-*C*-1), 95.6 (mal-*C*-1'), 75.3 (mal-*C*-3), 72.6 (mal-*C*-4), 72.4 (mal-*C*-5), 72.0 (mal-*C*-2), 70.1 (mal-*C*-2'), 70.0 (O*C*H$_2$), 69.4 (mal-*C*-3'), 68.6 (mal-*C*-5'), 68.1 (mal-*C*-4'), 62.8 (mal-*C*-6), 61.6 (mal-*C*-6'), 30.0 (*C*H$_2$Br), 21.0 (CH_3*C*OO), 21.0 (CH_3*C*OO), 20.8 (CH_3*C*OO), 20.8 (CH_3*C*OO), 20.7 (CH_3*C*OO), 20.7 (CH_3*C*OO), 20.7 (CH_3*C*OO) ppm.

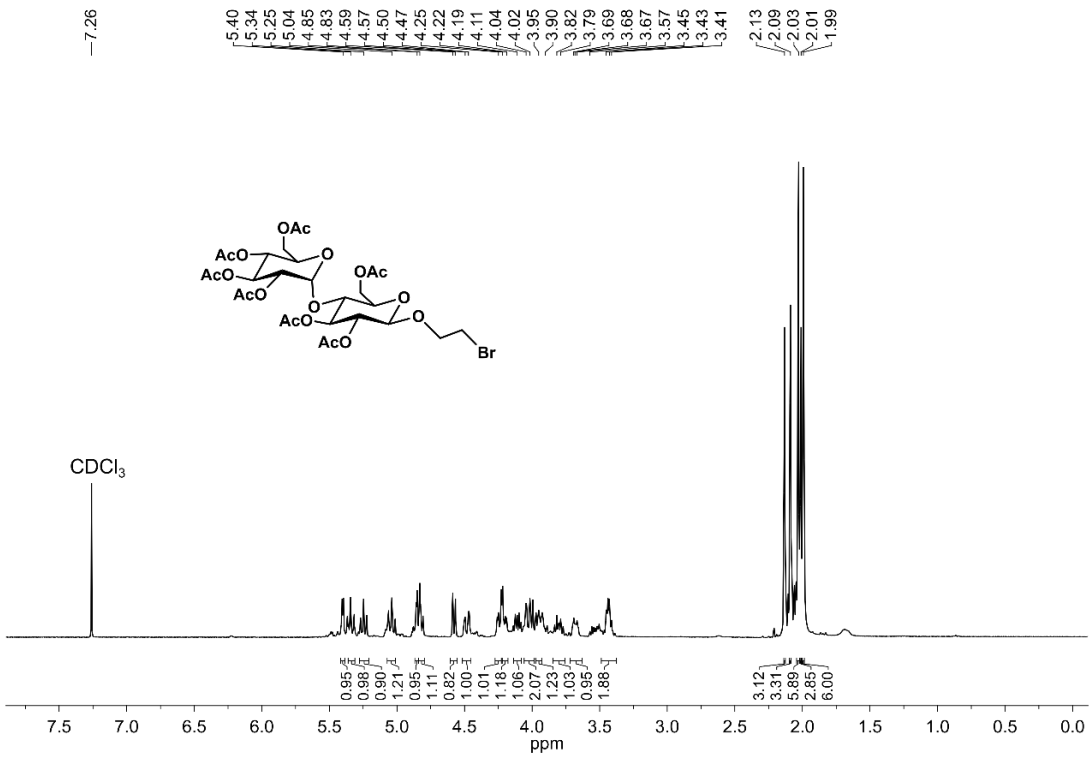

Figure S22. ^{1}H NMR spectrum of $(OAc)_7$-β-D-maltoseEtBr ($CDCl_3$, 400 MHz, 25 °C).

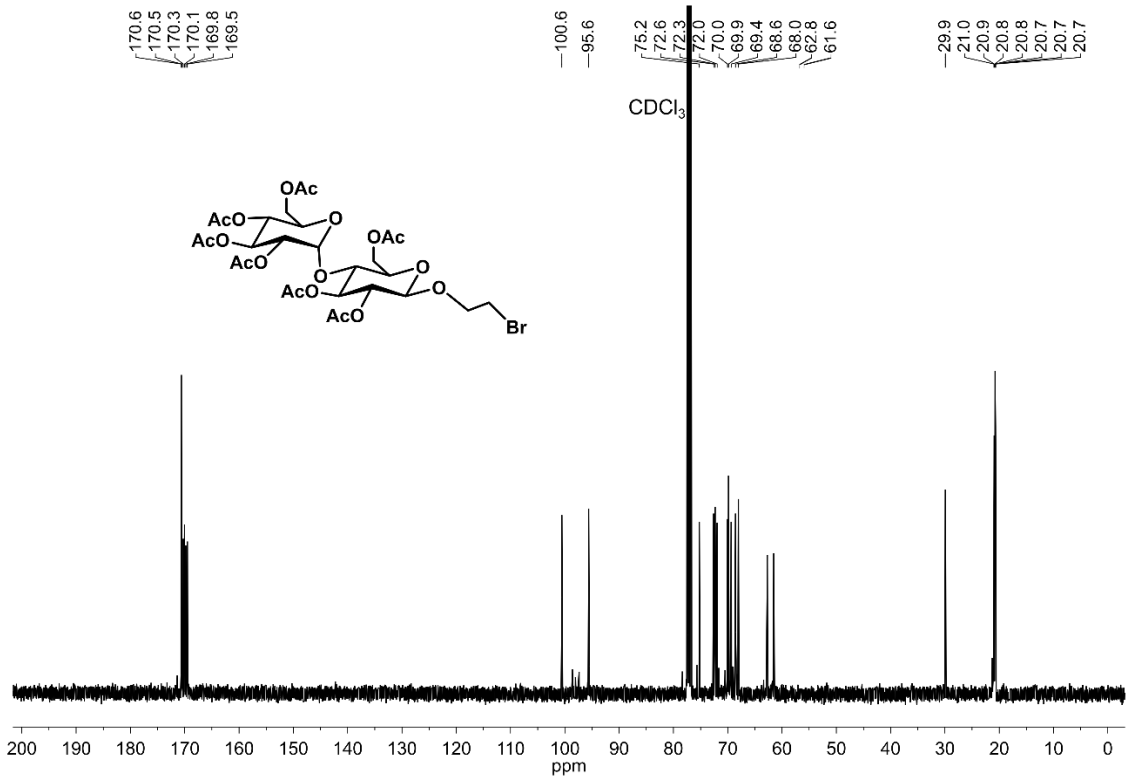

Figure 23. $^{13}C\{^{1}H\}$ NMR spectrum of $(OAc)_7$-β-D-maltoseEtBr ($CDCl_3$, 100 MHz, 25 °C).

S2.2.9. 5-((OAc)$_7$-β-D-maltoseEtO)-2-picolinaldehyde (subcomponent D)

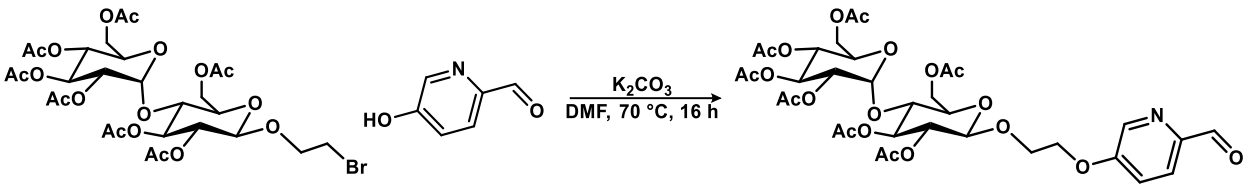

A 50 mL Schlenk flask was charged with (OAc)$_7$-β-D-maltoseEtBr (1.208 g, 1.625 mmol, 1.000 equiv), K_2CO_3 (449 mg, 3.25 mmol, 2.00 equiv) and 5-hydroxypicolinaldehyde (200 mg, 1.62 mmol, 1.00 equiv). DMF (10 mL) was added to the flask, and the reaction mixture was allowed to stir at 70 °C for 16 h under an atmosphere of N_2, at which point it was allowed to cool to ambient temperature and diluted with EtOAc (200 mL). The solution was washed with a saturated aqueous solution of NaCl (3 x 150 mL), and the organic phase was dried over $MgSO_4$ and evaporated to dryness. The crude oil was purified by flash chromatography on silica gel (30-70% EtOAc/hexanes) to afford the pure product as a colorless oily solid (yield: 900 mg, 1.15 mmol, 70%). ^{1}H NMR (400 MHz, 25 °C, $CDCl_3$) δ: 9.80 (s, 1H, OC*H*), 8.27 (d, 1H, *J* = 2.6 Hz, py-*H*-6), 7.78 (d, 1H, *J* = 8.7 Hz, py-*H*-3), 7.19 (dd, 1H, *J* = 8.7, 2.8 Hz, py-*H*-4), 5.25 (d, 1H, *J* = 3.9 Hz, mal-*H*-1'), 5.20 (t, 1H, *J* = 10.1 Hz, mal-*H*-3'), 5.12 (t, 1H, *J* = 9.1 Hz, mal-*H*-3), 4.89 (t, 1H, *J* = 9.9 Hz, mal-*H*-4'), 4.72–4.66 (m, 2H, mal-*H*-2, mal-*H*-2' signals overlapping), 4.54 (d, 1H, *J* = 7.9 Hz, mal-*H*-1), 4.38 (dd, 1H, *J* = 12.3, 2.5 Hz, mal-*H*-6$_a$), 4.13–4.04 (m, 4H, mal-*H*-6$_a$', mal-*H*-6$_b$, OC*H*$_{2a}$, mal-*H*-4 signals overlapping), 4.04–4.00 (m, 1H, mal-*H*-6$_b$'), 3.90 (dd, 1H, *J* = 10.3, 2.6 Hz, mal-*H*-5'), 3.88–3.80 (m, 3H, OC*H*$_{2b}$, mal-*H*-5, C*H*$_{2a}$Br signals overlapping), 3.59 (dt, 1H, *J* = 9.4, 3.4 Hz, C*H*$_{2b}$Br), 1.97 (s, 3H, C*H*$_3$COO), 1.93 (s, 3H, C*H*$_3$COO), 1.88 (s, 3H, C*H*$_3$COO), 1.86 (s, 3H, C*H*$_3$CO$_2$), 1.85 (s, 3H, C*H*$_3$COO), 1.84 (s, 3H, C*H*$_3$COO), 1.76 (s, 3H, C*H*$_3$COO) ppm. ^{13}C{^{1}H} NMR (100 MHz, 25 °C, $CDCl_3$) δ: 191.7 (O*C*H), 170.3 (CH$_3$*C*OO, two signals overlapping), 170.1 (CH$_3$*C*OO), 169.9 (CH$_3$*C*OO), 169.7 (CH$_3$*C*OO), 169.3 (CH$_3$*C*OO), 169.2 (CH$_3$*C*OO), 157.9 (py-*C*-2), 146.2 (py-*C*-5), 138.6 (py-*C*-6), 123.2 (py-*C*-3), 120.5 (py-*C*-4), 100.2 (mal-*C*-1), 95.3 (mal-*C*-1'), 74.9 (mal-*C*-3), 72.4 (mal-*C*-4), 72.1 (mal-*C*-5), 71.7 (mal-*C*-2), 69.8 (mal-*C*-2'), 69.0 (mal-*C*-3'), 68.3 (mal-*C*-5'), 67.8 (mal-*C*-4'), 67.6 (O*C*H$_2$CH$_2$), 67.6 (CH$_2$*C*H$_2$Opy), 62.3 (mal-*C*-6), 61.3 (mal-*C*-6'), 20.6 (CH$_3$*C*OO), 20.6 (CH$_3$*C*OO), 20.4 (CH$_3$*C*OO), 20.4 (CH$_3$*C*OO), 20.3 (CH$_3$*C*OO, two signals overlapping), 20.3 (CH$_3$*C*OO) ppm. ESI-MS(+): 786.2448 (calc'd, [M+H]$^+$ 786.2457) *m/z*. ATR-IR (v): 2962, 1744 (HC=O), 1707 (C=O), 1577, 1372, 1211, 1133, 1029, 902, 846, 608 cm^{-1}.

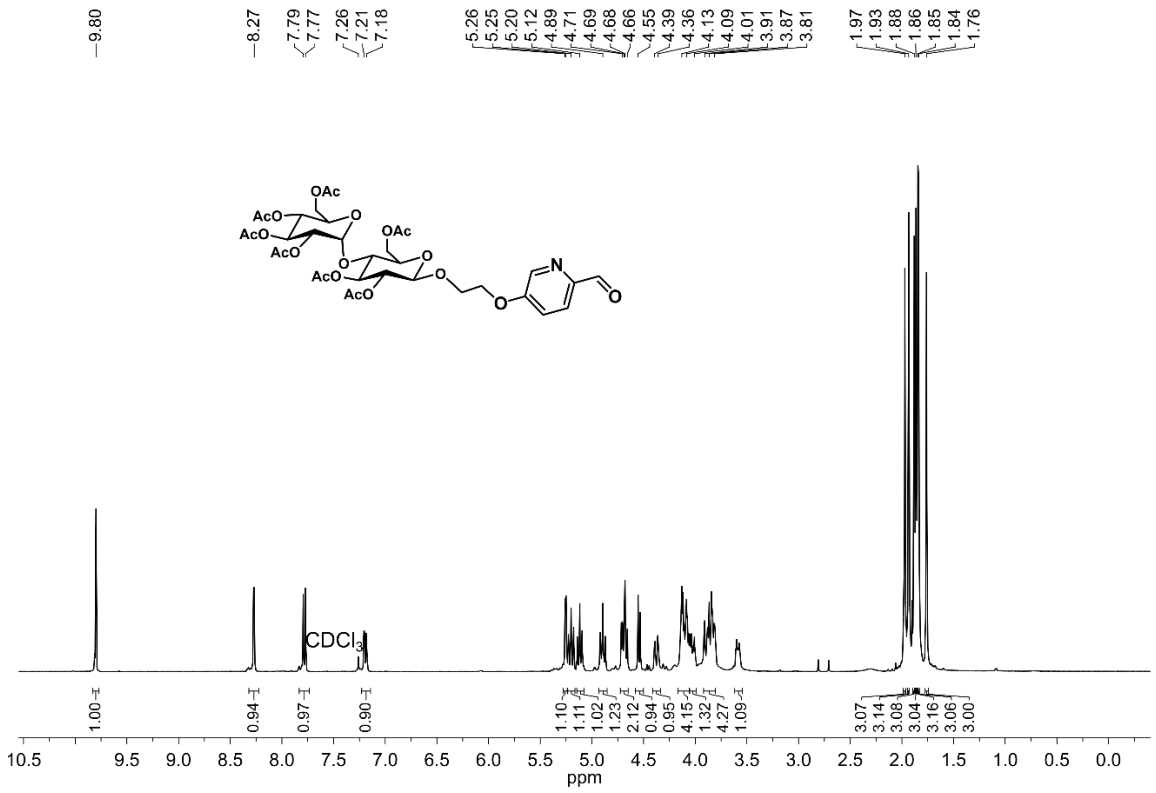

Figure S24. ^{1}H NMR spectrum of 5-((OAc)$_7$-β-D-maltoseEtO)-2-picolinaldehyde ($CDCl_3$, 400 MHz, 25 °C).

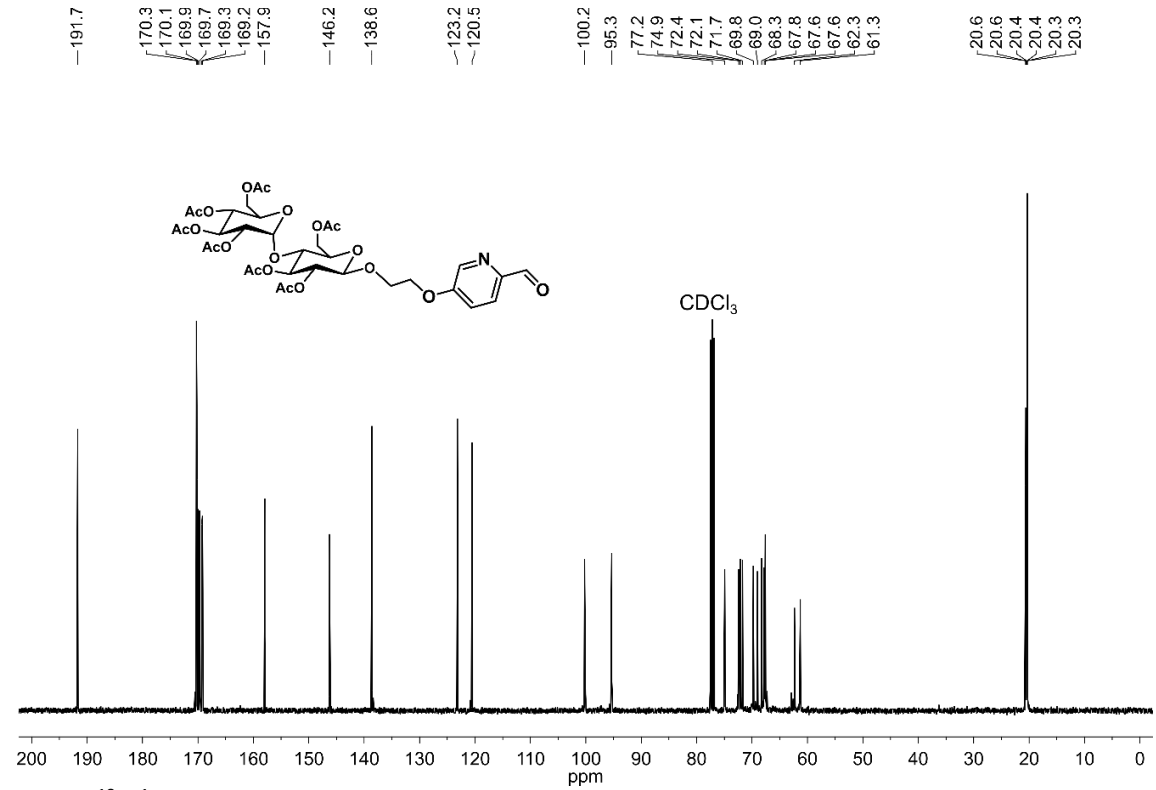

Figure S25. $^{13}C\{^{1}H\}$ NMR spectrum of 5-((OAc)$_7$-β-D-maltoseEtO)-2-picolinaldehyde ($CDCl_3$, 100 MHz, 25 °C).

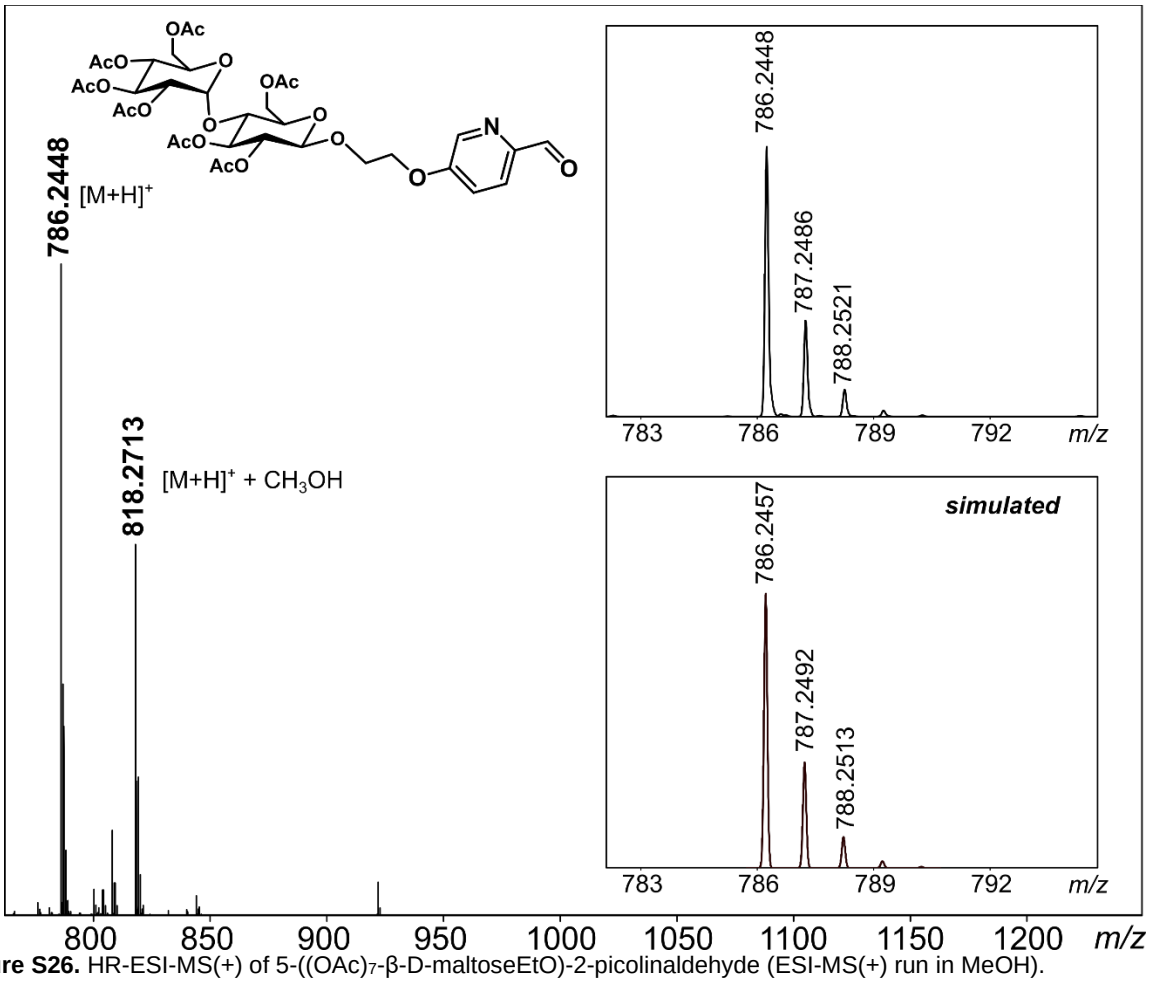

Figure S26. HR-ESI-MS(+) of 5-((OAc)$_7$-β-D-maltoseEtO)-2-picolinaldehyde (ESI-MS(+) run in MeOH).

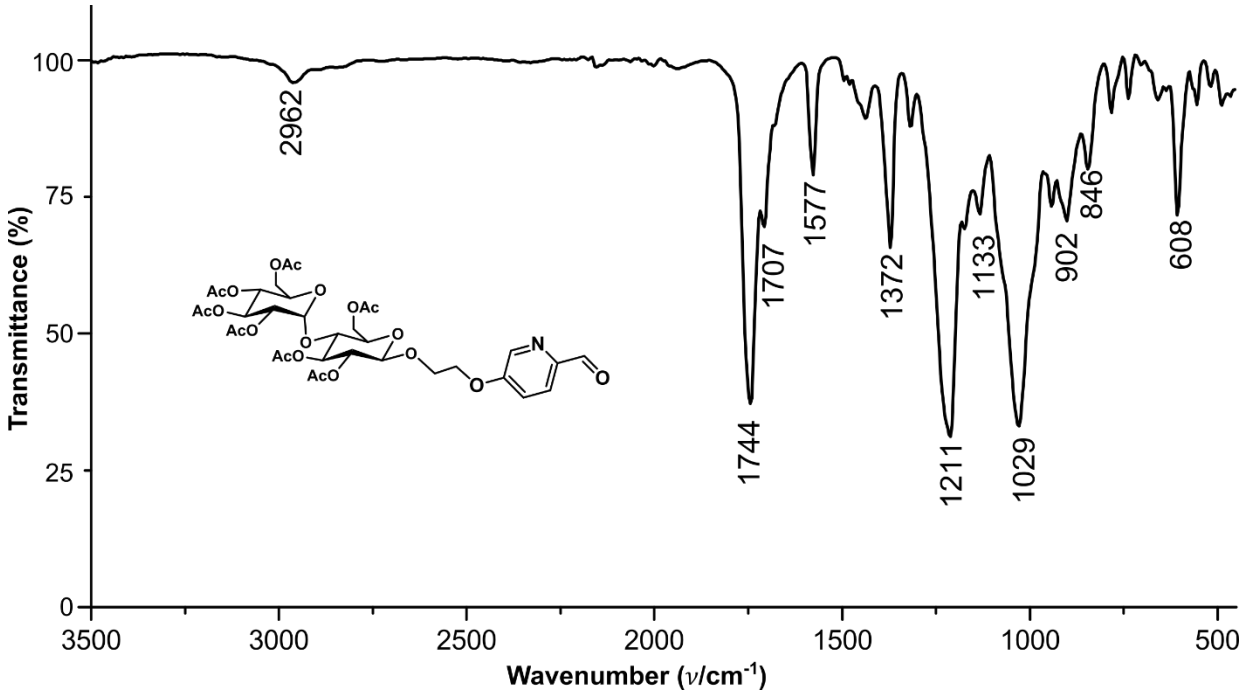

Figure S27. ATR-IR 5-((OAc)$_7$-β-D-maltoseEtO)-2-picolinaldehyde.

S2.3. Fe(II) Self-Assembly Complexes

S2.3.1. $[NMe_4]_4$[1-glc]

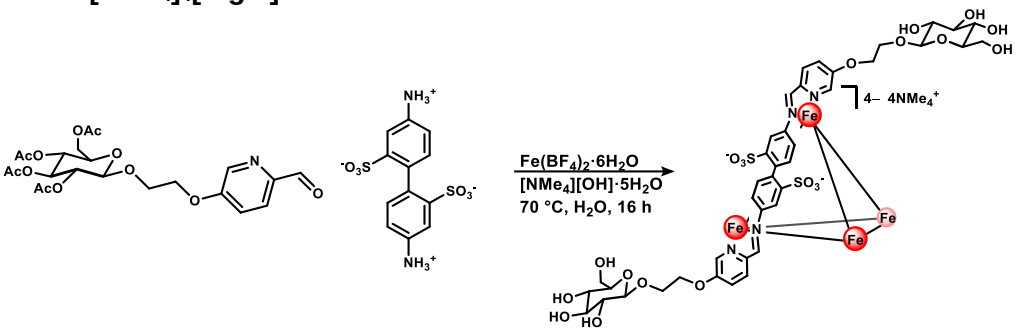

To an 8 mL reaction tube was added 5-((OAc)$_4$-β-D-glucoseEtO)-2-picolinaldehyde (68 mg, 0.14 mmol, 4.8 equiv) and [NMe$_4$][OH]•5H$_2$O (112 mg, 0.618 mmol, 22.0 equiv) as solids. Degassed H$_2$O (2 mL) was added, and the mixture was allowed to stir under an atmosphere of N$_2$ for 45 min at 70 °C, during which time it became homogeneous. To the solution was added 2,2'-benzidinedisulfonic acid (70 wt% balance H$_2$O, 14 mg, 0.028 mmol, 1.0 equiv) and Fe(BF$_4$)$_2$•6H$_2$O (15 mg, 0.044 mmol, 1.8 equiv) as solids, which resulted in an immediate color change to dark magenta. The reaction mixture was sparged with N$_2$ for 15 min and then allowed to stir at 70 °C for 16 h. The mixture was then allowed to cool to ambient temperature and the magenta solution was filtered through a piece of glass microfiber filter paper. To the filtrate was added ^{i}PrOH (20 mL), resulting in the precipitation of magenta solids. The suspension was centrifuged (1975 x g, 10 min), and the colorless supernatant was discarded. The resulting dark pink solids were suspended in Et$_2$O (5 mL), isolated by filtration, and dried under reduced pressure to afford the product as a dark magenta powder. The crude solids were dissolved in H$_2$O (4 mL) and filtered through a piece of glass microfiber filter paper into the sample reservoir of a Pall Microsep® (3K Omega membrane) centrifuge device. The device was centrifuged at 7500 x g for 75 min, at which point the filtrate in the collection tube was removed and fresh H$_2$O (4 mL) was added to the sample reservoir. The device was centrifuged again at 7500 x g for 75 min, and this process was repeated for a total of three centrifuge cycles. After the third cycle, the solution in the sample reservoir was removed and lyophilized overnight to afford the pure product, [NMe$_4$]$_4$[**1**-glc], as a magenta powder (yield: 15 mg, 2.4 μmol, 52% based on theoretical yield of 4.7 μmol with 2,2'-benzidinedisulfonic acid as the limiting reagent (4:12:6 ratio of Fe:py:benzidine)). ^{1}H NMR (400 MHz, 25 °C, D$_2$O) δ: 9.10 (s, 12H, *H*C=N), 8.59 (d, 12H, *J* = 7.0 Hz, py-*H*-3), 7.90 (d, 12H, *J* = 7.0 Hz, py-*H*-4), 7.17 (br s, 12H, py-*H*-6), 7.05 (br s, 12H, Ar-*H* 6,6'-benzidine), 6.44 (s, 12H, Ar-*H* 3,3'-benzidine), 5.77 (br s, 12H, Ar-*H* 5,5'-benzidine), 4.46 (t, 12H, *J* = 6.9 Hz, glc-*H*-1), 4.38 (br s, 24H, –C*H*$_2$–), 4.22–4.18 (m, 12H, glc-*H*$_{6a}$), 4.04–4.01 (m, 12H, glc-*H*$_{6b}$), 3.79 (t, 12H, *J* = 11.6 Hz, glc-*H*-3), 3.60 (dd, 12H, *J* = 12.2, 5.4 Hz, glc-*H*-5), 3.45–3.30 (m, 36H, glc-*H*-4, –C*H*$_2$– signals overlapping), 3.21 (t, 12H, *J* = 8.5 Hz, glc-*H*-2), 3.15 (s, 48H, N(C*H*$_3$)$_4$) ppm. ^{13}C{^{1}H} NMR (100 MHz, 25 °C, D$_2$O) δ: 174.2 (*C*=N), 159.3, 150.5, 150.2, 146.5, 142.9, 135.8, 133.0, 131.9, 122.0, 121.6, 121.0, 102.4, 76.0, 75.7, 73.0, 69.4, 68.4, 67.9, 60.7, 55.2 (N(*C*H$_3$)$_4$) ppm. ESI-MS(–) observed for [M]$^{4-}$: 1502.2307 (calc'd, 1502.2363) *m/z*. UV-vis [ε] (H$_2$O, 50 μM): λ$_{max}$ 505 [20,000 M^{-1}cm^{-1}], 545 [24,000 M^{-1}cm^{-1}] nm. ATR-IR (ν): 3365 (OH), 2884, 1558 (C=N), 1468, 1319, 1234, 1208, 1081, 1044, 626, 555 cm^{-1}.

***It is noted that balanced stoichiometry was not used in the optimized synthesis of $[NMe_4]_4$[**1**-glc]; however, the tetrahedral cage is the smallest (entropically-favored) self-assembled structure possible that is free of strain in which all iron(II) centers are six-coordinate and bound to an imine nitrogen (enthalpically-favored). Nitschke et al. have reported that a system employing similar components does not require balanced stoichiometry to be deterministic, and that varying amounts of each subcomponent still leads to the entropically and enthalpically-favored tetrahedral product,*[13] *which supports the correct formulation of our system despite the unbalanced stoichiometry used.*

Despite the reported ability for tetrahedral cages of similar size and shape to sequester small anions within their endohedral cavities,[14–16] *there was no indication of encapsulated BF_4^- within the [**1**-glc]$^{4-}$ cage core as indicated by the absence of any signal in the ^{19}F NMR spectrum of the purified product (Figure S30). The lack of any observable endo-BF_4^- anion can be rationalized by the fact that water-soluble cages bearing polar charged functional groups decorating their exterior have a tendency to sequester small nonpolar molecules from surrounding aqueous solution in their cores due to hydrophobic effects.*[17–23] *However, small hydrophilic anions such as BF_4^- have large free energies of hydration and are difficult to extract from water, and thus BF_4^- is typically sequestered within coordination cages in nonaqueous solvents and also with complimentarily charged cationic cages.*[24–26]

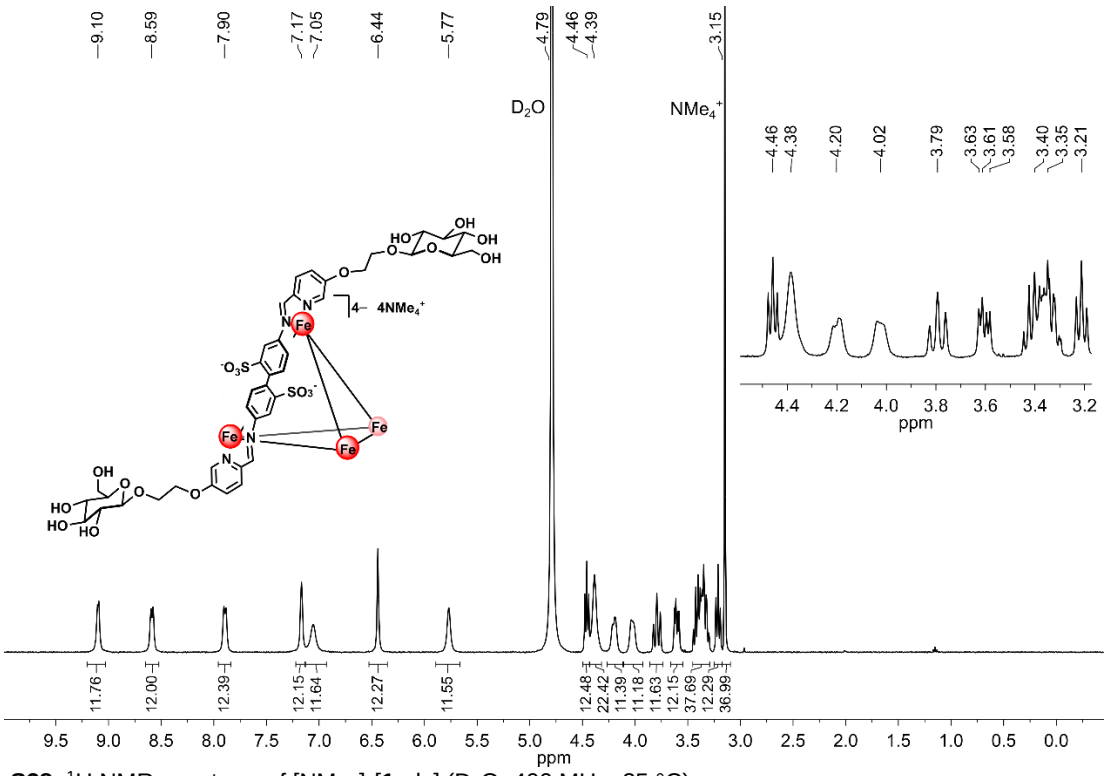

Figure S28. ^{1}H NMR spectrum of $[NMe_4]_4$[**1**-glc] (D_2O, 400 MHz, 25 °C).

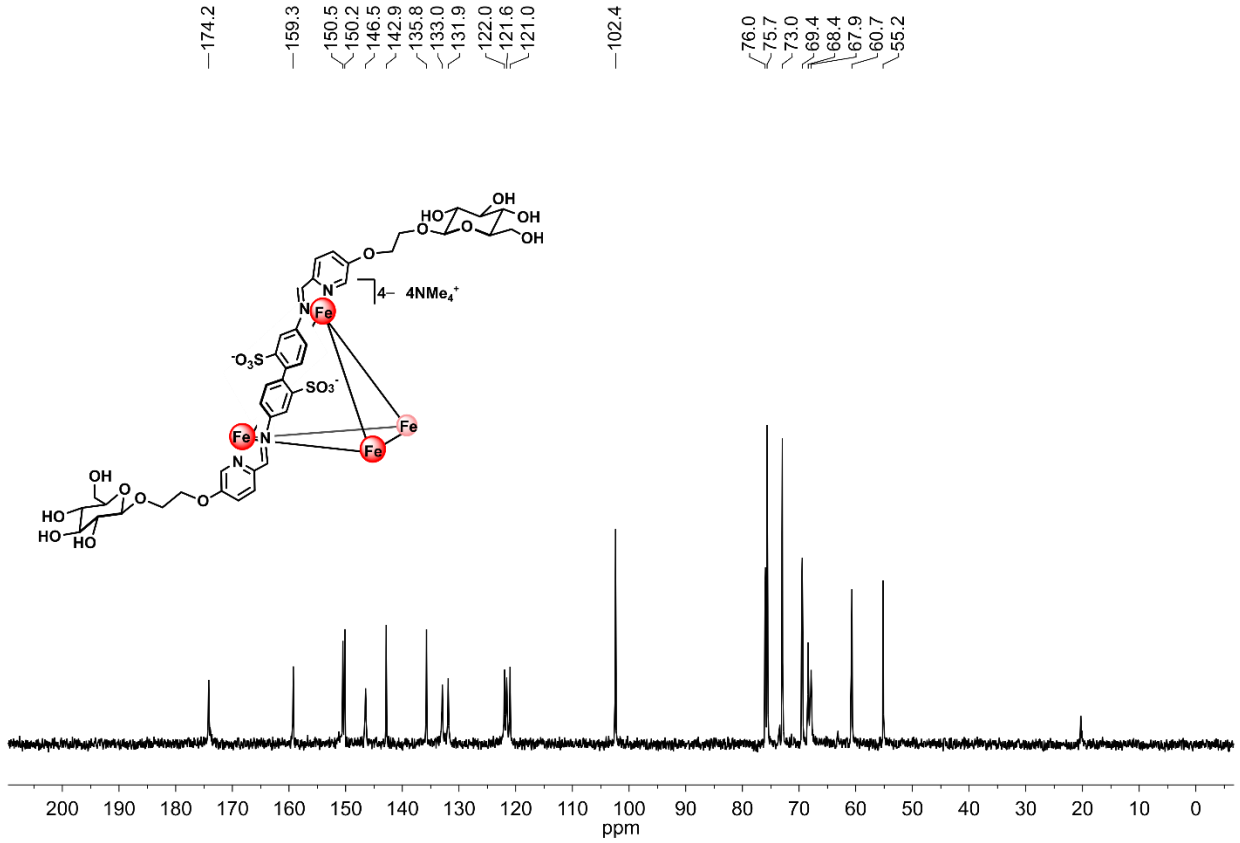

Figure S29. ^{13}C{^{1}H} NMR spectrum of $[NMe_4]_4$[**1**-glc] (D_2O, 100 MHz, 25 °C).

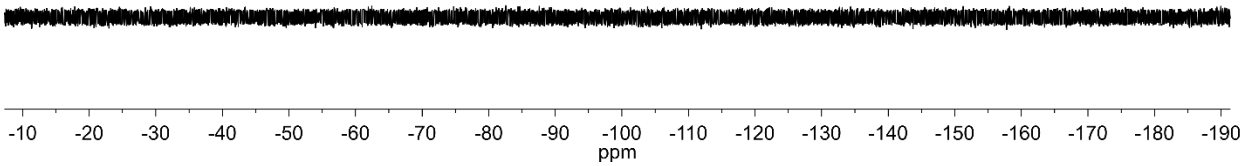

Figure S30. ^{19}F NMR spectrum of purified $[NMe_4]_4$[**1**-glc] indicating the absence of an *endo*-$[BF_4]^-$ ion (D_2O, 282 MHz, 25 °C).

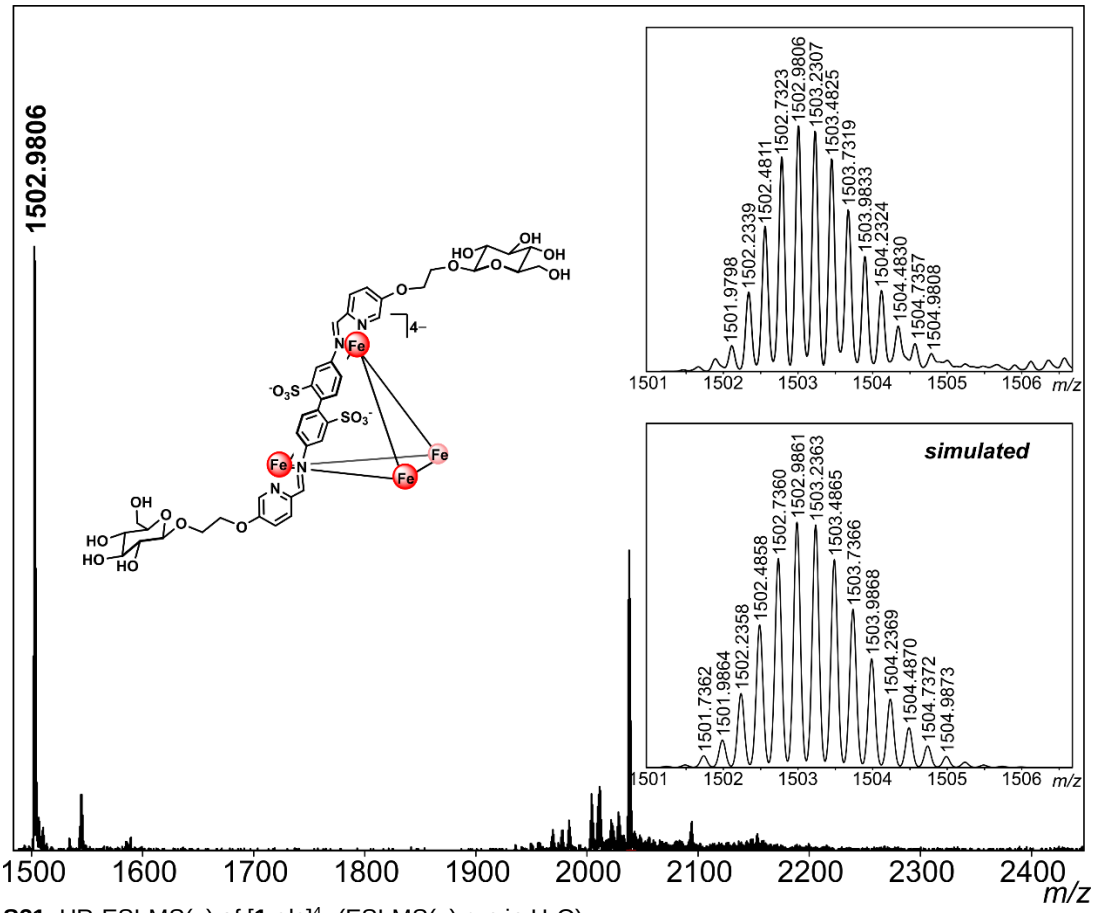

Figure S31. HR-ESI-MS(–) of [**1**-glc]$^{4-}$ (ESI-MS(–) run in H_2O).

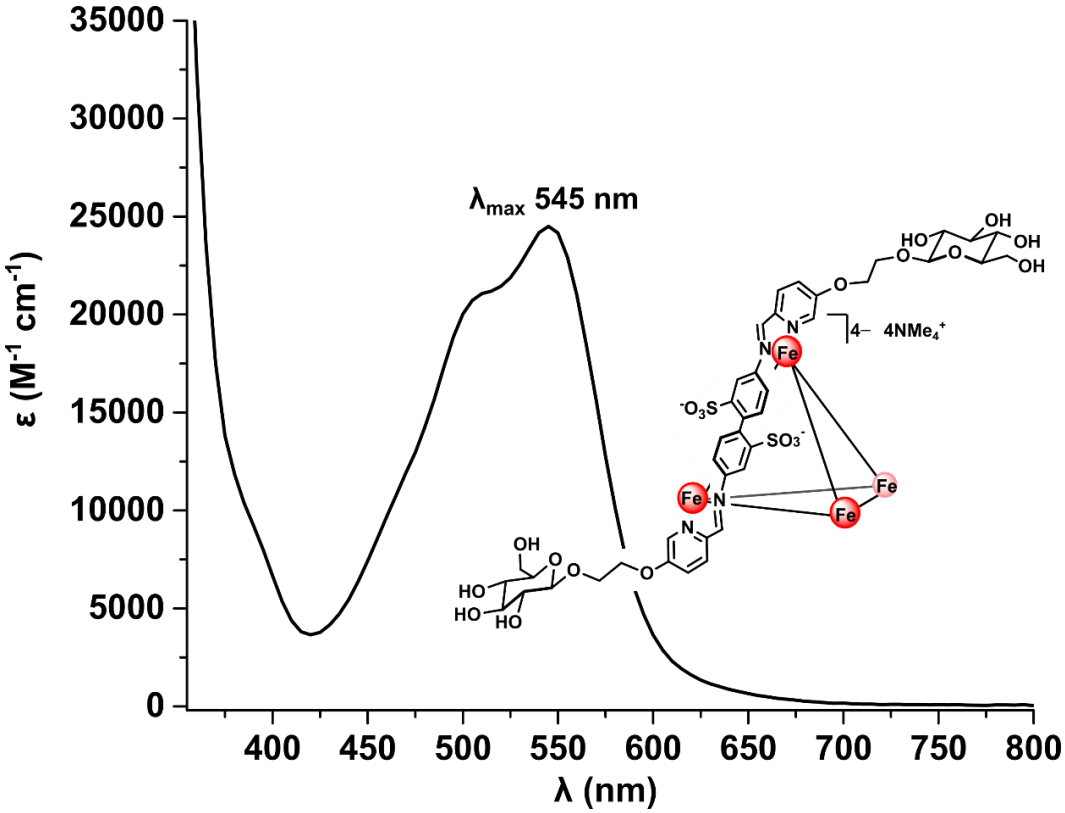

Figure S32. UV-vis spectrum of $[NMe_4]_4$[**1**-glc] (H_2O, 50 μM).

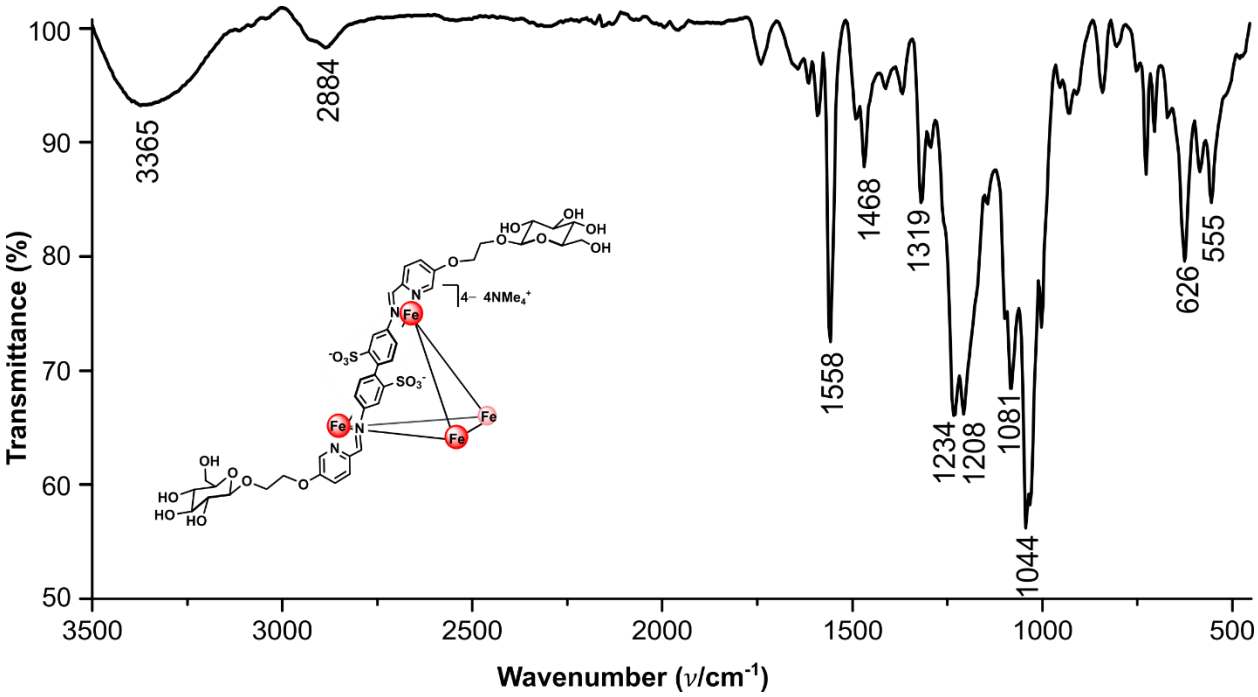

Figure S33. ATR-IR spectrum of $[NMe_4]_4$[**1**-glc].

S2.3.2. $[Na]_4$[1-glc]

To an 8 mL reaction tube was added 5-((OAc)$_4$-β-D-glucoseEtO)-2-picolinaldehyde (68 mg, 0.14 mmol, 4.8 equiv) and a degassed aqueous solution of NaOH (2.0 mL of 0.31 M solution, 0.63 mmol, 22 equiv). The mixture was allowed to stir under an atmosphere of N_2 for 45 min at 70 °C, during which time it became homogeneous. To the solution was added 2,2'-benzidinedisulfonic acid (70 wt% balance H_2O, 14 mg, 0.028 mmol, 1.0 equiv) and $Fe(BF_4)_2$•$6H_2O$ (15 mg, 0.044 mmol, 1.8 equiv) as solids, which resulted in an immediate color change to dark magenta. The reaction mixture was sparged with N_2 for 15 min and then allowed to stir at 70 °C for 16 h. The mixture was then allowed to cool to ambient temperature and the magenta solution was filtered through a piece of glass microfiber filter paper. To the filtrate was added ^{i}PrOH (20 mL), resulting in the precipitation of magenta solids. The suspension was centrifuged (1975 x g, 10 min), and the colorless supernatant was discarded. The resulting dark pink solids were suspended in Et_2O (5 mL), isolated by filtration, and dried under reduced pressure to afford the product as a dark magenta powder. The crude solids were dissolved in H_2O (4 mL) and filtered through a piece of glass microfiber filter paper into the sample reservoir of a Pall Microsep® (3K Omega membrane) centrifuge device. The device was centrifuged at 7500 x g for 75 min, at which point the filtrate in the collection tube was removed and fresh H_2O (4 mL) was added to the sample reservoir. The device was centrifuged again at 7500 x g for 75 min, and this process was repeated for a total of three centrifuge cycles. After the third cycle, the solution in the sample reservoir was removed and lyophilized overnight to afford the pure product, $[Na]_4$[**1**-glc], as a magenta powder (yield: 16 mg, 2.6 µmol, 56% based on theoretical yield of 4.7 µmol with 2,2'-benzidinedisulfonic acid as the limiting reagent (4:12:6 ratio of Fe:py:benzidine)). ^{1}H NMR (400 MHz, 25 °C, D_2O) δ: 9.09 (s, 12H, *H*C=N), 8.58 (d, 12H, *J* = 6.9 Hz, py-*H*-3), 7.90 (d, 12H, *J* = 6.9 Hz, py-*H*-4), 7.16 (br s, 12H, py-*H*-6), 7.06 (br s, 12H, Ar-*H* 6,6'-benzidine), 6.44 (s, 12H, Ar-*H* 3,3'-benzidine), 5.77 (br s, 12H, Ar-*H* 5,5'-benzidine), 4.46 (t, 12H, *J* = 6.9 Hz, glc-*H*-1), 4.39 (br s, 24H, –CH_2–), 4.19 (m, 12H, glc-H_{6a}), 4.03 (m, 12H, glc-H_{6b}), 3.80 (t, 12H, *J* = 12.2 Hz, glc-*H*-3), 3.60 (dd, 12H, *J* = 12.2, 5.4 Hz, glc-*H*-5), 3.43–3.34 (m, 36H, glc-*H*-4, –CH_2– signals overlapping), 3.21 (t, 12H, *J* = 8.5 Hz, glc-*H*-2) ppm.

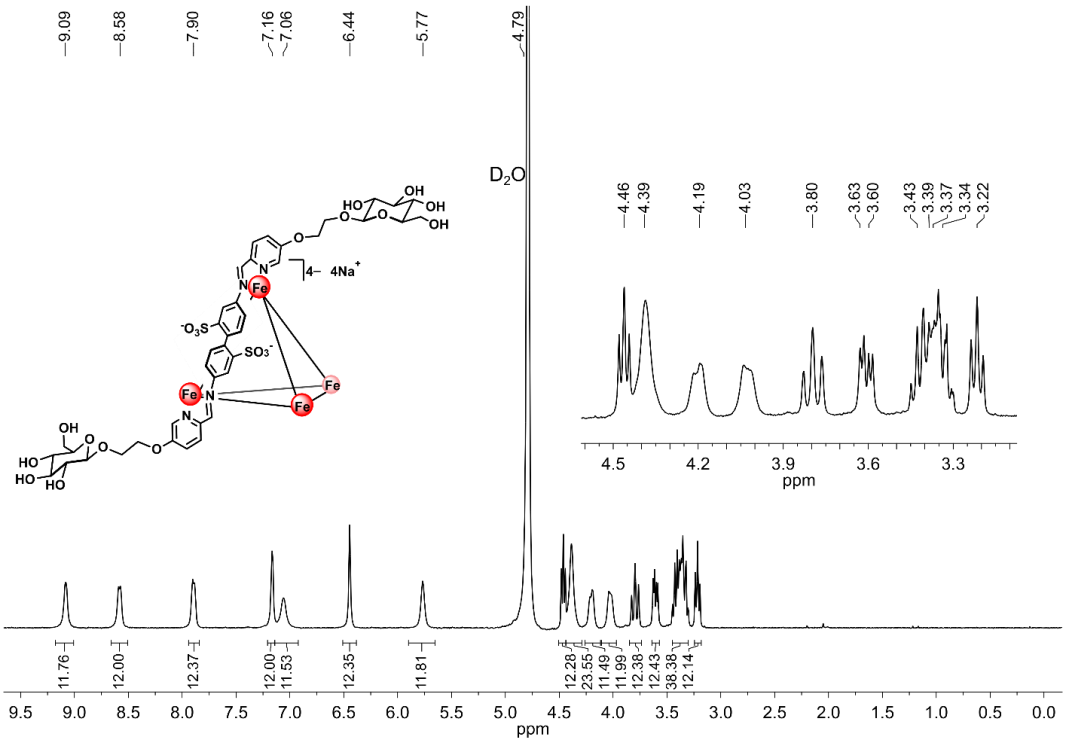

Figure S34. ^{1}H NMR spectrum of $[Na]_4$[**1**-glc] (D_2O, 400 MHz, 25 °C).

S2.3.3. [K]$_4$[1-glc]

To an 8 mL reaction tube was added 5-((OAc)$_4$-β-D-glucoseEtO)-2-picolinaldehyde (68 mg, 0.14 mmol, 4.8 equiv) and a degassed aqueous solution of KOH (2.0 mL of 0.31 M solution, 0.63 mmol, 22.4 equiv). The mixture was allowed to stir under an atmosphere of N_2 for 45 min at 70 °C, during which time it became homogeneous. To the solution was added 2,2'-benzidinedisulfonic acid (70 wt% balance H_2O, 14 mg, 0.028 mmol, 1.0 equiv) and $Fe(BF_4)_2$•$6H_2O$ (15 mg, 0.044 mmol, 1.8 equiv) as solids, which resulted in an immediate color change to dark magenta. The reaction mixture was sparged with N_2 for 15 min and then allowed to stir at 70 °C for 16 h. The mixture was then allowed to cool to ambient temperature and the magenta solution was filtered through a piece of glass microfiber filter paper. To the filtrate was added ^{i}PrOH (20 mL), resulting in the precipitation of magenta solids. The suspension was centrifuged (1975 x g, 10 min), and the colorless supernatant was discarded. The resulting dark pink solids were suspended in Et_2O (5 mL), isolated by filtration, and dried under reduced pressure to afford the product as a dark magenta powder. The crude solids were dissolved in H_2O (4 mL) and filtered through a piece of glass microfiber filter paper into the sample reservoir of a Pall Microsep® (3K Omega membrane) centrifuge device. The device was centrifuged at 7500 x g for 75 min, at which point the filtrate in the collection tube was removed and fresh H_2O (4 mL) was added to the sample reservoir. The device was centrifuged again at 7500 x g for 75 min, and this process was repeated for a total of three centrifuge cycles. After the third cycle, the magenta solution in the sample reservoir was removed and lyophilized overnight to afford the pure product, [K]$_4$[**1**-glc], as a magenta powder (yield: 19 mg, 2.6 μmol, 55% based on theoretical yield of 4.7 μmol with 2,2'-benzidinedisulfonic acid as the limiting reagent (4:12:6 ratio of Fe:py:benzidine)). ^{1}H NMR (400 MHz, 25 °C, D_2O) δ: 9.08 (s, 12H, *H*C=N), 8.57 (d, 12H, *J* = 7.6 Hz, py-*H*-3), 7.87 (d, 12H, *J* = 7.6 Hz, py-*H*-4), 7.13 (s, 12H, py-*H*-6), 7.02 (br s, 12H, Ar-*H* 6,6'-benzidine), 6.42 (s, 12H, Ar-*H* 3,3'-benzidine), 5.74 (br s, 12H, Ar-*H* 5,5'-benzidine), 4.43 (t, 12H, *J* = 7.3 Hz, glc-*H*-1), 4.36 (br s, 24H, –C*H*$_2$–), 4.17 (m, 12H, glc-*H*$_{6a}$), 3.99 (m, 12H, glc-*H*$_{6b}$), 3.76 (t, 12H, *J* = 12.7 Hz, glc-*H*-3), 3.58 (dd, 12H, *J* = 12.2, 5.4 Hz, glc-*H*-5), 3.39–3.29 (m, 36H, glc-*H*-4, –C*H*$_2$– signals overlapping), 3.18 (t, 12H, *J* = 8.4 Hz, glc-*H*-2) ppm.

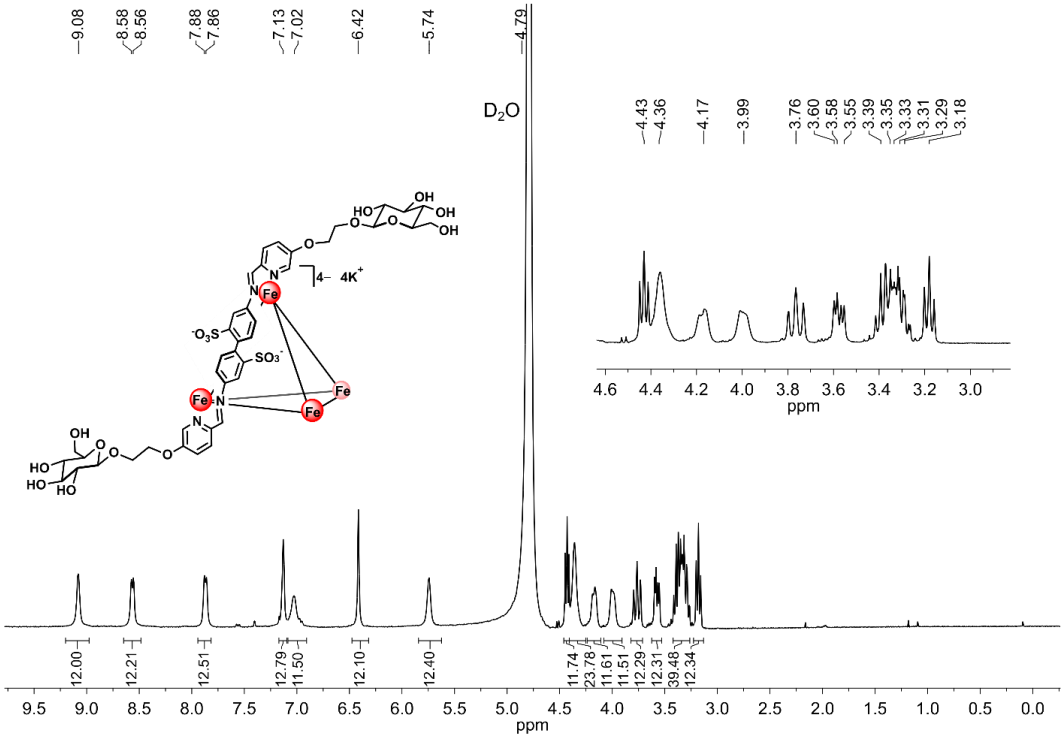

Figure S35. ^{1}H NMR spectrum of [K]$_4$[**1**-glc] (D_2O, 400 MHz, 25 °C).

S2.3.4. $[NMe_4]_2$[2-glc]

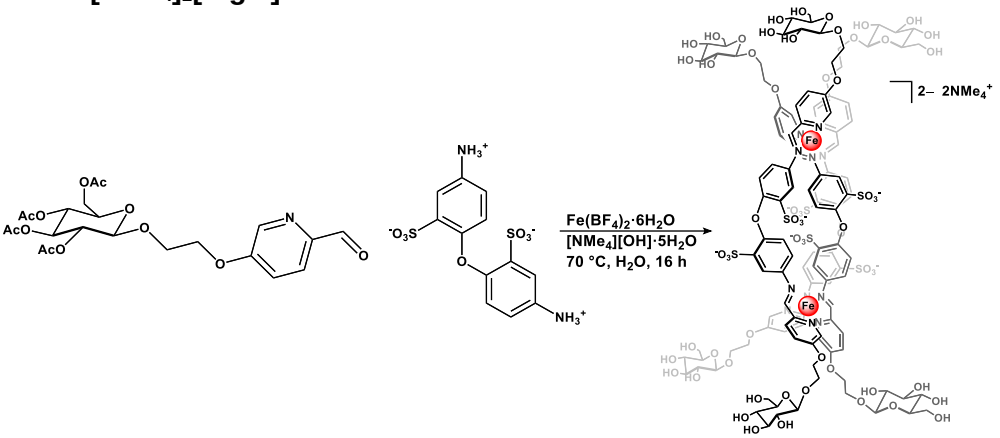

To an 8 mL reaction tube was added 5-((OAc)$_4$-β-D-glucoseEtO)-2-picolinaldehyde (60 mg, 0.12 mmol, 3.6 equiv), and $[NMe_4][OH]$•$5H_2O$ (111 mg, 0.612 mmol, 18.0 equiv) as solids. Degassed H_2O (2 mL) was added, and the mixture was stirred under a flow of N_2 at 70 °C for 45 min. To the tube was added 4,4′-diaminodiphenyl ether-2,2′-disulfonic acid (80 wt% balance H_2O, 15 mg, 0.033 mmol, 1.0 equiv), and $Fe(BF_4)_2$•$6H_2O$ (18 mg, 0.053 mmol, 1.6 equiv) as solids, which resulted in an immediate color change to dark pink. The reaction mixture was sparged with N_2 for 15 min, and the mixture was allowed to stir at 70 °C for 16 h. The reaction was then allowed to cool to ambient temperature and the magenta solution was filtered through a piece of glass microfiber filter paper. To the filtrate was added ^{i}PrOH (20 mL), resulting in the precipitation of magenta solids. The suspension was centrifuged (1975 x g, 10 min), and the colorless supernatant was discarded. The resulting solids were suspended in Et_2O (5 mL), isolated by filtration, and dried under reduced pressure to afford the product as a dark magenta powder. The crude solids were dissolved in H_2O (4 mL) and filtered through a piece of glass microfiber filter paper into the sample reservoir of a Pall Microsep® (1K Omega membrane) centrifuge device. The device was centrifuged at 7500 x g for 75 min, at which point the filtrate in the collection tube was removed and fresh H_2O (4 mL) was added to the sample reservoir. The device was centrifuged again at 7500 x g for 75 min, and this process was repeated for a total of three centrifuge cycles. After the third cycle, the solution in the sample reservoir was removed and lyophilized overnight to afford the pure product, $[NMe_4]_2$[**2**-glc], as a magenta powder (yield: 22 mg, 6.9 µmol, 62% based on theoretical yield of 11 µmol with 4,4′-diaminodiphenyl ether-2,2′-disulfonic acid as the limiting reagent (2:6:3 ratio of Fe:py:benzidine)). X-ray quality single crystals of $[NMe_4]_2$[**2**-glc] were grown by vapor diffusion of acetone into a saturated aqueous solution of the purified product over the course of 48 h, and crystallographic details are described in Section S7. ^{1}H NMR (400 MHz, 25 °C, D_2O) δ: 9.51, 9.48 (two singlets, 6H, *H*C=N, ΔΔ, ΛΛ, and ΔΛ configurations), 8.76, 8.75 (two doublets overlapping, 6H, *J* = 8.6 Hz, py-*H*-3, ΔΔ, ΛΛ, and ΔΛ configurations), 7.93 (d, 6H, *J* = 8.6 Hz, py-*H*-4), 7.58, 7.56 (two singlets, 6H, py-*H*-6, ΔΔ, ΛΛ, and ΔΛ configurations), 6.56 (d, 6H, *J* = 8.6 Hz, Ar-*H* 6,6'-benzidine), 6.41, 6.44 (two singlets, 6H, Ar-*H* 3,3'-benzidine, ΔΔ, ΛΛ, and ΔΛ configurations), 5.63 (d, 6H, *J* = 8.6 Hz, Ar-*H* 5,5'-benzidine), 4.49 (t, 6H, *J* = 6.8 Hz, glc-*H*-1), 4.42 (br s, 12H, –CH_2–), 4.23 (m, 6H, glc-H_{6a}), 4.04 (m, 6H, glc-H_{6b}), 3.81 (dd, 6H, *J* = 25.2, 11.1 Hz, glc-*H*-3), 3.63 (dt, 6H, *J* = 12.0, 5.8 Hz, glc-*H*-5), 3.47–3.31 (m, 18H, glc-*H*-4, –CH_2– signals overlapping), 3.23 (t, 12H, *J* = 8.6 Hz, glc-*H*-2), 3.14 (s, 24H, N(CH_3)$_4$) ppm. ^{13}C{^{1}H} NMR (100 MHz, 25 °C, D_2O) δ: 173.2 (*C*=N), 161.2, 155.1 (two signals overlapping), 149.5, 147.1, 134.7, 133.9, 126.0, 122.9, 122.7, 121.7, 102.4, 76.0, 75.7, 73.0, 69.4, 68.6, 67.9, 60.7, 55.2 (N(*C*H_3)$_4$) ppm. ESI-MS(–) observed for $[M]^{2-}$: 1526.7253 (calc'd, 1526.7282) *m/z*. UV-vis [ε] (H_2O, 50 µM): λ_{max} 505 [10,000 $M^{-1}cm^{-1}$], 545 [12,000 $M^{-1}cm^{-1}$] nm. ATR-IR (ν): 3361 (OH), 2930, 2873, 1592 (C=N), 1558 (C=N), 1472, 1319, 1245, 1204, 1085, 1025, 932, 850, 704, 630, 548 cm^{-1}.

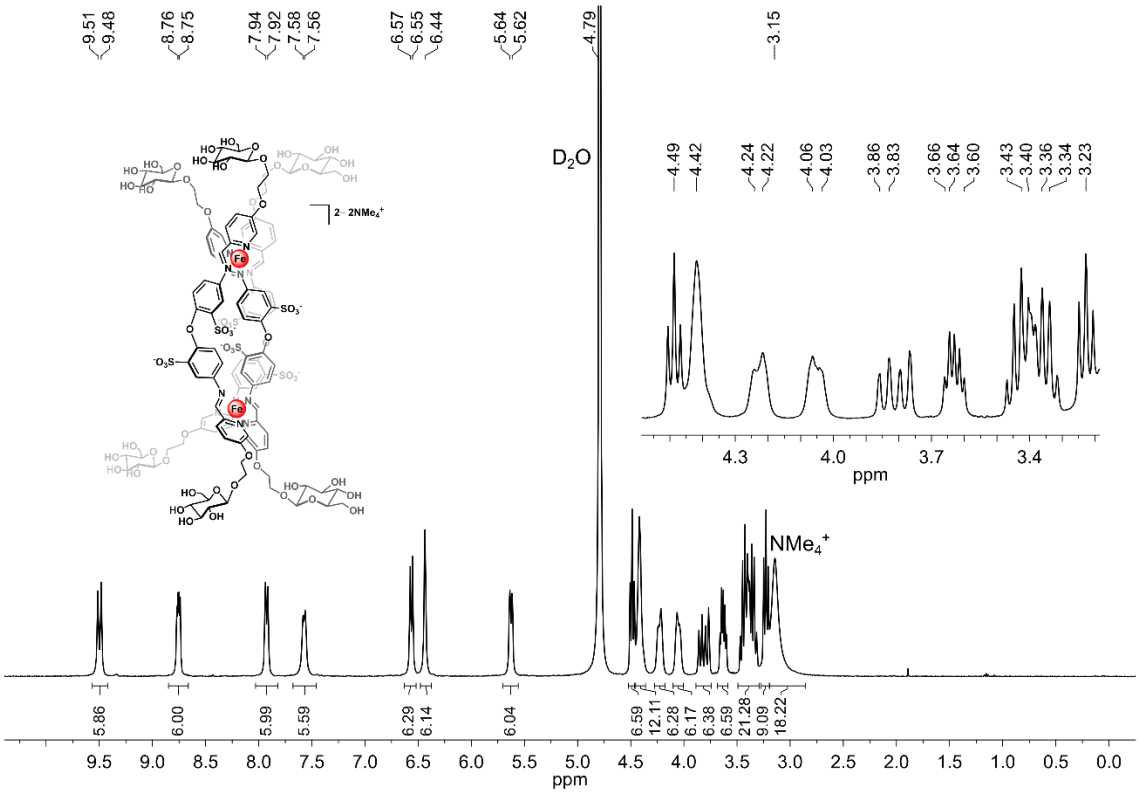

Figure S36. ^{1}H NMR spectrum of $[NMe_4]_2$[**2**-glc] (D_2O, 400 MHz, 25 °C).

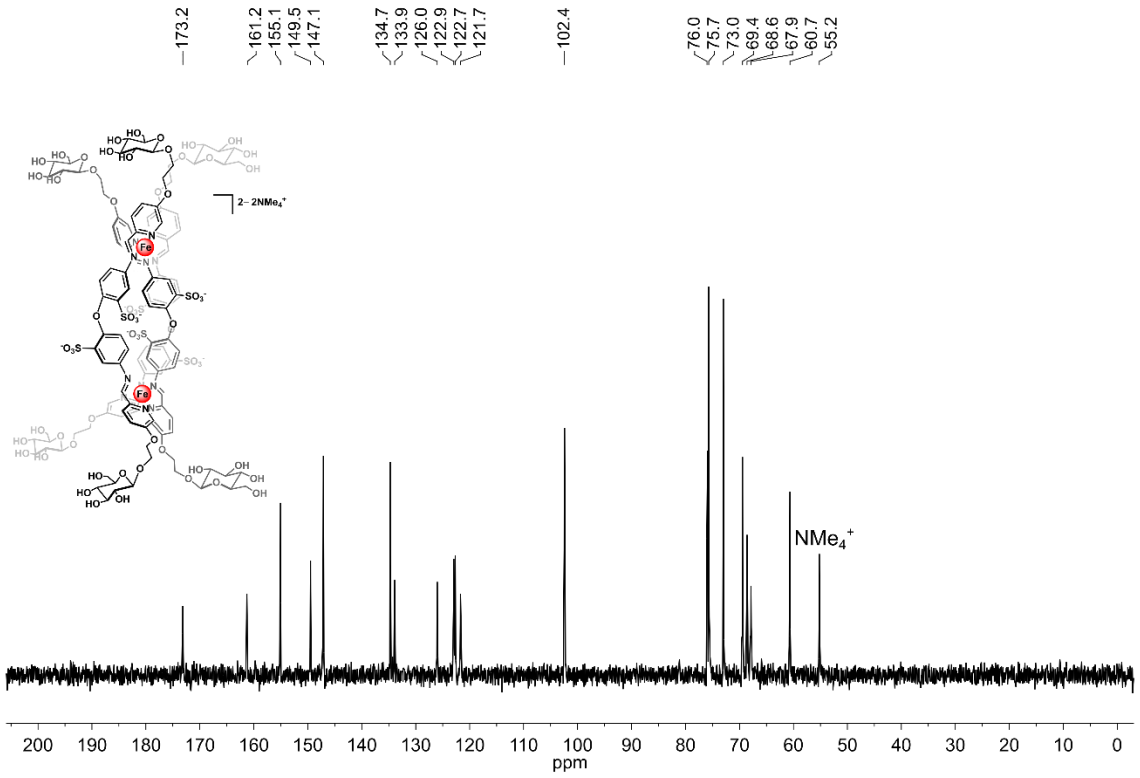

Figure S37. $^{13}C\{^{1}H\}$ NMR spectrum of $[NMe_4]_2$[**2**-glc] (D_2O, 100 MHz, 25 °C).

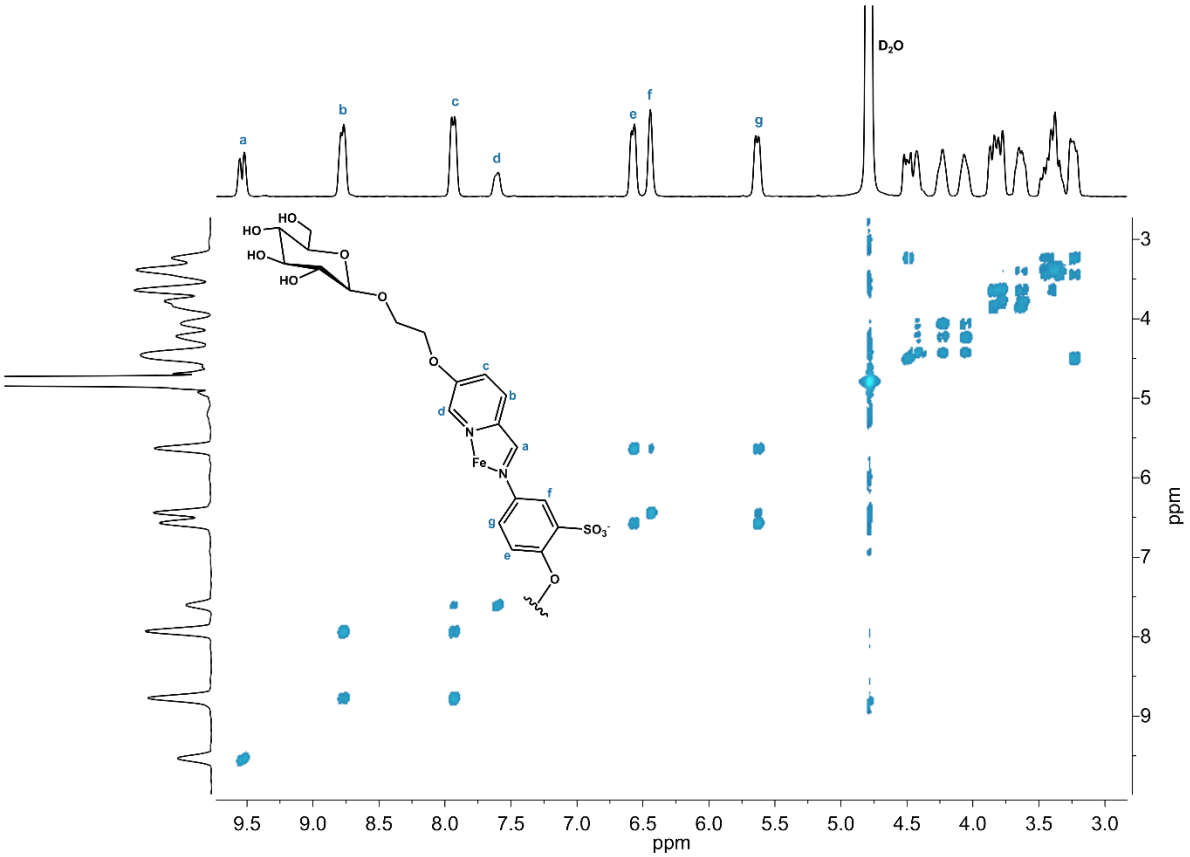

Figure S38. ^{1}H-^{1}H COSY NMR spectrum of $[NMe_4]_2$[**2**-glc] (D_2O, 400 MHz, 25 °C).

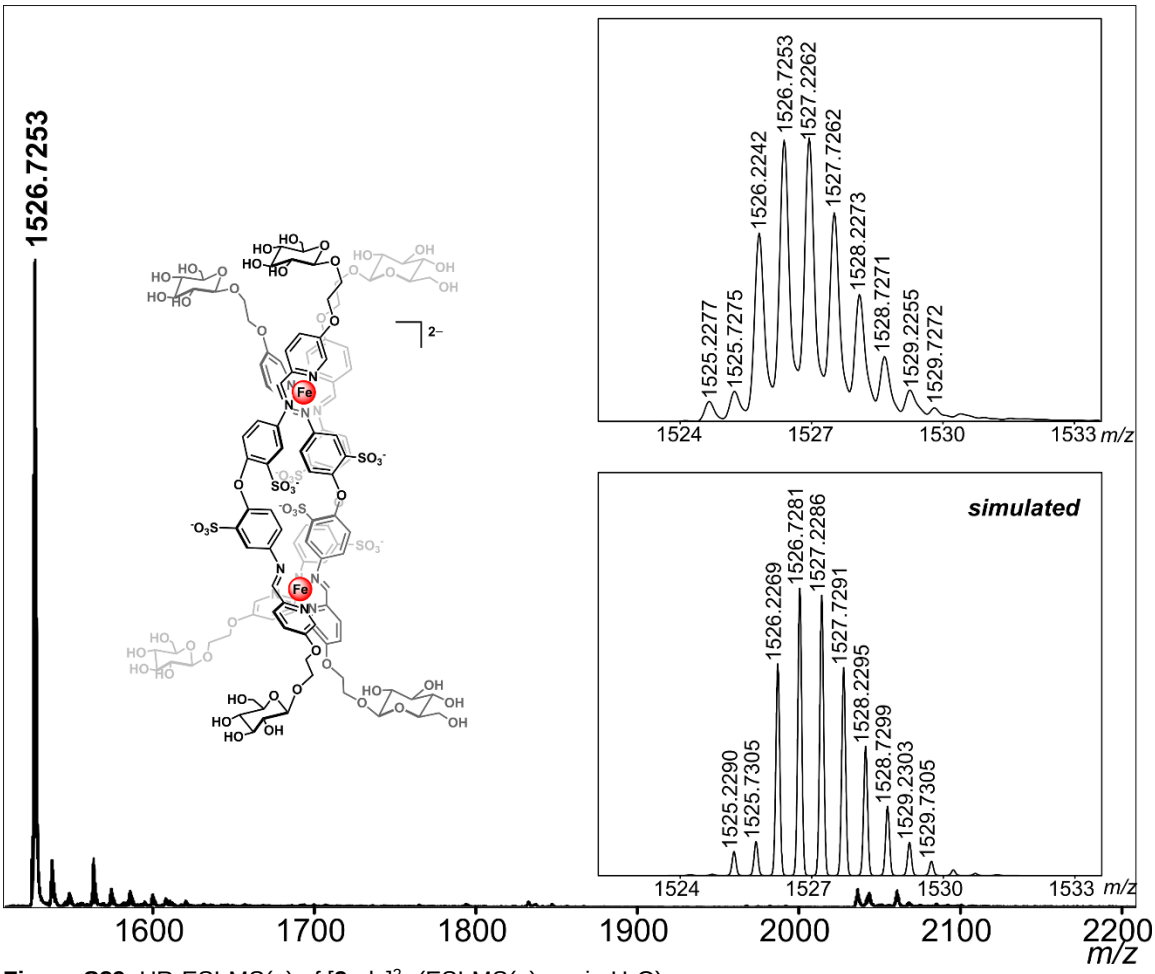

Figure S39. HR-ESI-MS(–) of [**2**-glc]$^{2-}$ (ESI-MS(–) run in H_2O).

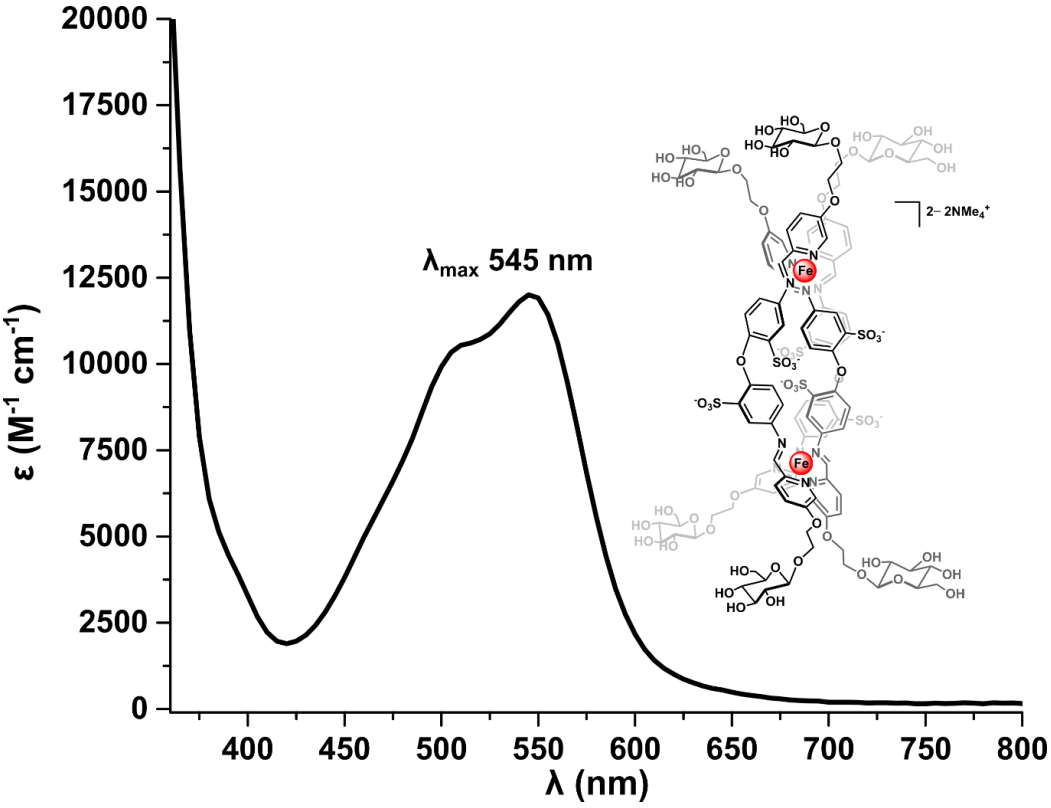

Figure S40. UV-vis spectrum of $[NMe_4]_2$[**2**-glc] (H_2O, 50 μM).

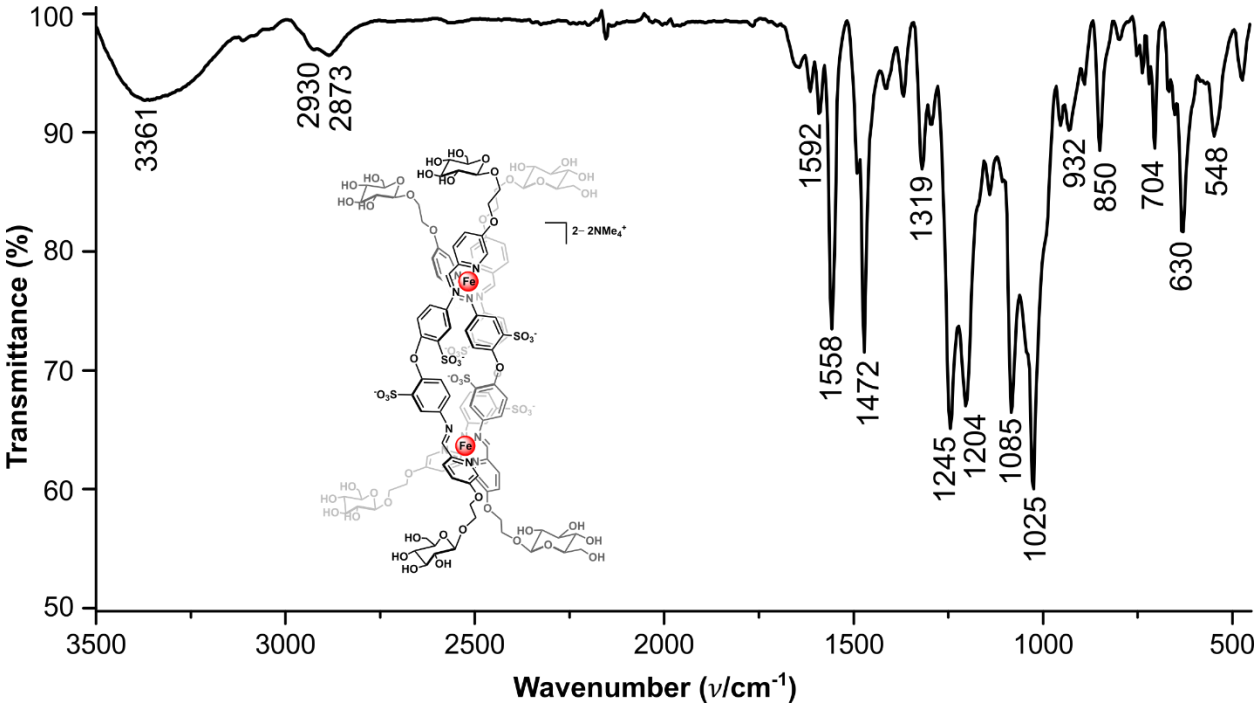

Figure S41. ATR-IR spectrum of $[NMe_4]_2$[**2**-glc].

S2.3.5. [3-glc][SO_4]

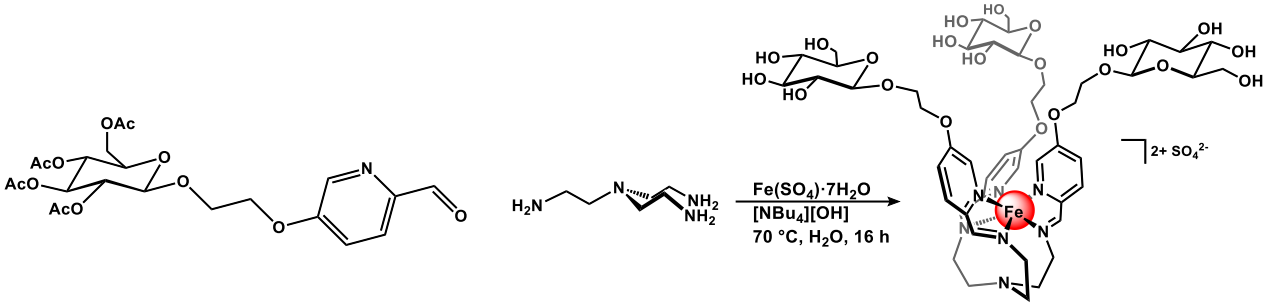

To an 8 mL reaction tube was added 5-((OAc)$_4$-β-D-glucoseEtO)-2-picolinaldehyde (51 mg, 0.10 mmol, 3.0 equiv), and [NBu$_4$][OH] (aq, 55%, 0.19 mL, 0.41 mmol, 12 equiv) followed by degassed H_2O (0.8 mL). The solution was allowed to stir under a flow of N_2 at 70 °C for 45 min, at which point tris(2-aminoethyl)amine (5 µL, 0.03 mmol, 1 equiv), and $Fe(SO_4)_2$•$7H_2O$ (9 mg, 0.03 mmol, 1 equiv) were added. The dark pink solution was then sparged with N_2 for 15 min. The reaction mixture was allowed to stir at 70 °C for 16 h, at which point the solution was allowed to cool to ambient temperature and filtered through a piece of glass microfiber filter paper. To the filtrate was added ^{i}PrOH (20 mL), resulting in the precipitation of magenta solids. The suspension was centrifuged (1975 x g, 10 min), and the pale pink supernatant was discarded. The resulting solids were suspended in Et_2O (5 mL), isolated by filtration, washed with ^{i}PrOH (2 mL) and Et_2O (2 mL) and dried under reduced pressure to afford the product as a dark magenta powder (yield: 35 mg, 0.028 mmol, 83%). ^{1}H NMR (400 MHz, 25 °C, D_2O) δ: 9.03 (s, 3H, *H*C=N), 8.19 (d, 3H, *J* = 8.7 Hz, py-*H*-3), 7.69 (d, 3H, *J* = 8.7 Hz, py-*H*-4), 6.77 (s, 3H, py-*H*-6), 4.46 (dd, 3H, *J* = 8.0, 3.0 Hz, glc-*H*-1), 4.24 (m, 6H, –C*H*$_2$–), 4.15 (m, 3H, glc-*H*$_{6a}$), 3.96 (m, 6H, glc-*H*$_{6b}$), 3.81 (dd, 3H, *J* = 12.3, 1.9, Hz, glc-*H*-3), 3.63 (dd, 3H, *J* = 12.3, 5.4 Hz, glc-*H*-5), 3.53 (d, 3H, *J* = 10.7 Hz, tren –C*H*$_2$–), 3.46–3.30 (m, 12H, glc-*H*-4, –C*H*$_2$–, tren–C*H*$_2$– signals overlapping), 3.21 (dd, 3H, *J* = 9.0, 8.3 Hz, glc-*H*-2), 3.17 (m, 3H, tren-C*H*$_2$), 3.04 (m, 3H, tren-C*H*$_2$) ppm.^{13}C{^{1}H} NMR (100 MHz, 25 °C, D_2O) δ: 169.7 (*C*=N), 157.8, 150.5, 144.0, 129.1, 121.0, 102.3, 76.0, 75.7, 73.0, 69.5, 68.1, 67.9, 60.7, 58.3, 53.6 ppm. ESI-MS(+) observed for [M]$^{2+}$: 567.6938 (calc'd, 567.6944) *m/z*. UV-vis [ε] (H_2O, 50 µM): λ_{max} 375 [5,800 $M^{-1}cm^{-1}$], 495 [6,000 $M^{-1}cm^{-1}$], 540 [7,900 $M^{-1}cm^{-1}$] nm. ATR-IR (ν): 3253 (OH), 2873, 2873, 1562 (C=N), 1558 (C=N), 1465, 1312, 1234, 1029, 611 cm^{-1}.

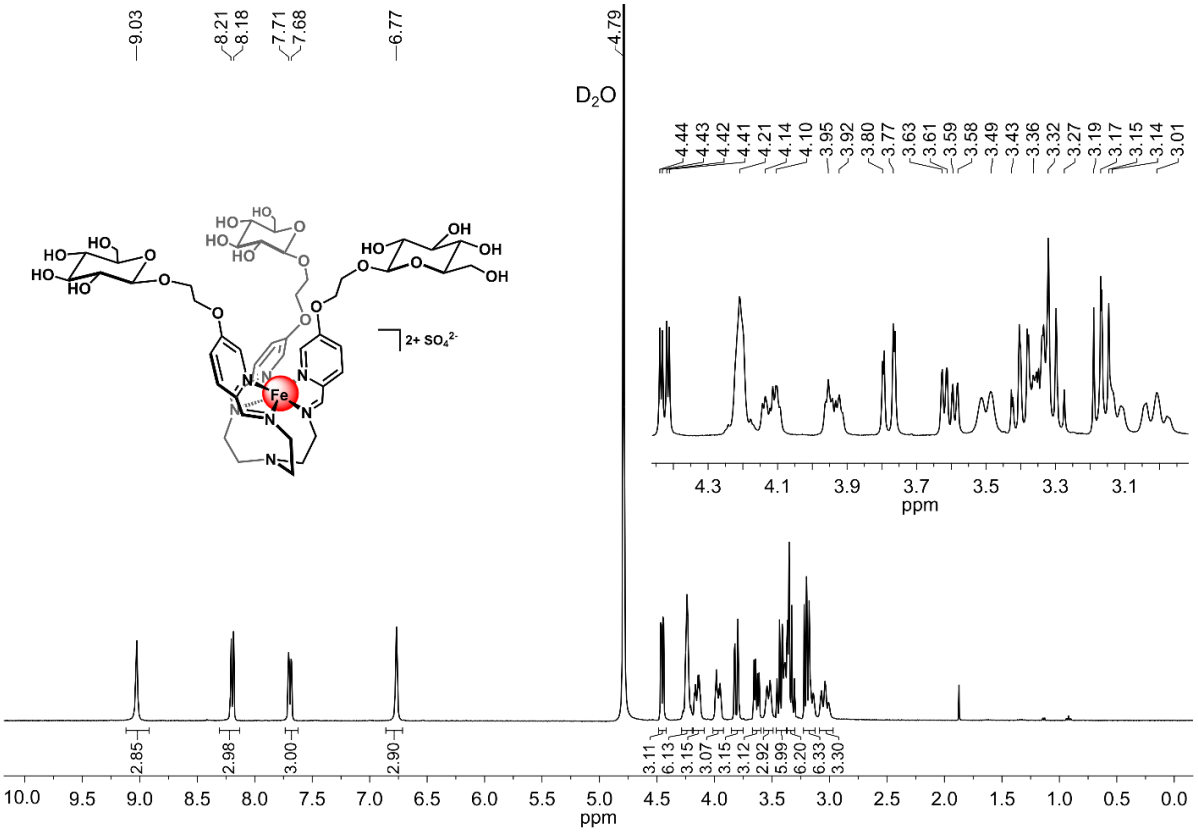

Figure S42. ^{1}H NMR spectrum of [**3**-glc][SO_4] (D_2O, 400 MHz, 25 °C).

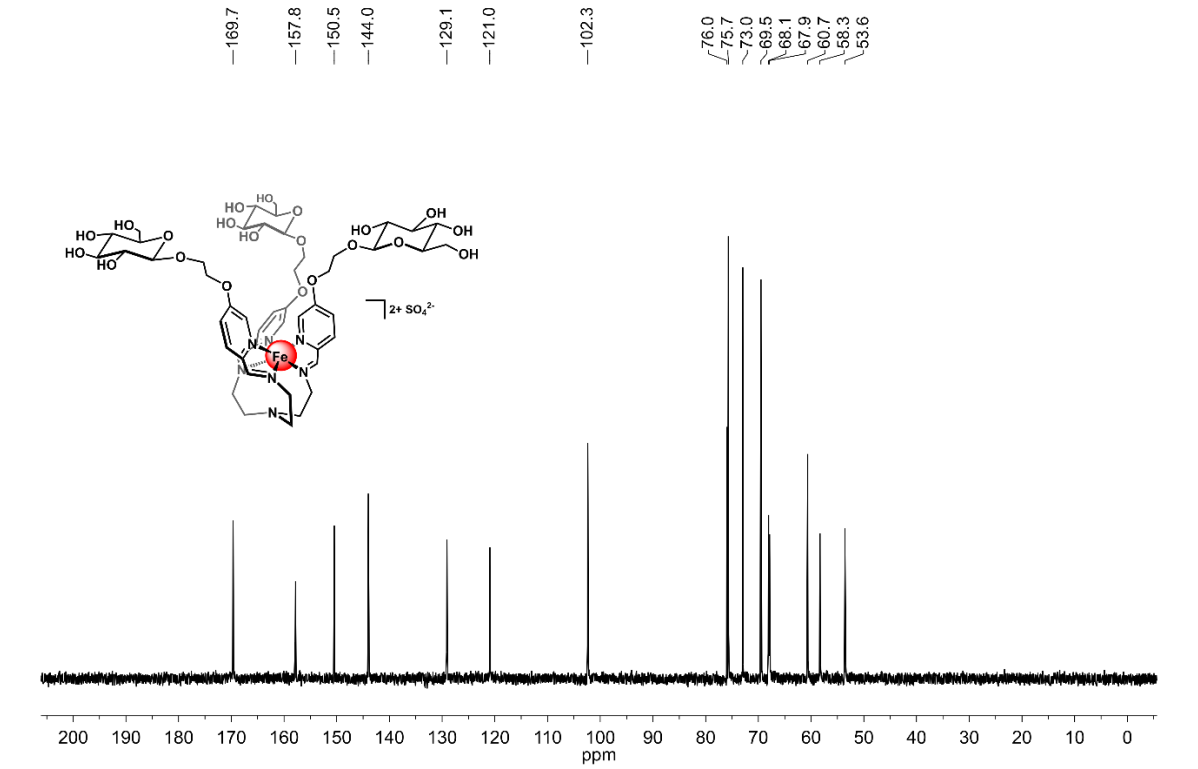

Figure S43. $^{13}C\{^{1}H\}$ NMR spectrum of [**3**-glc][SO_4] (D_2O, 100 MHz, 25 °C).

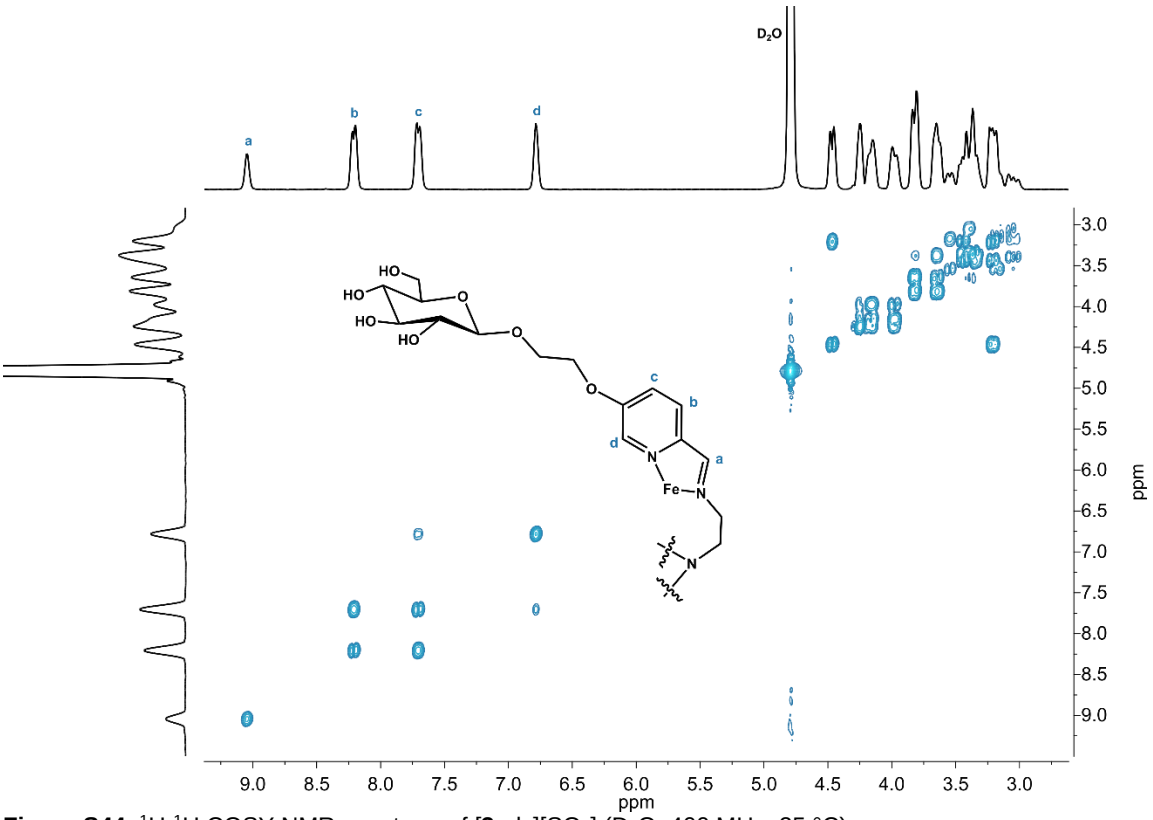

Figure S44. ^{1}H-^{1}H COSY NMR spectrum of [**3**-glc][SO_4] (D_2O, 400 MHz, 25 °C).

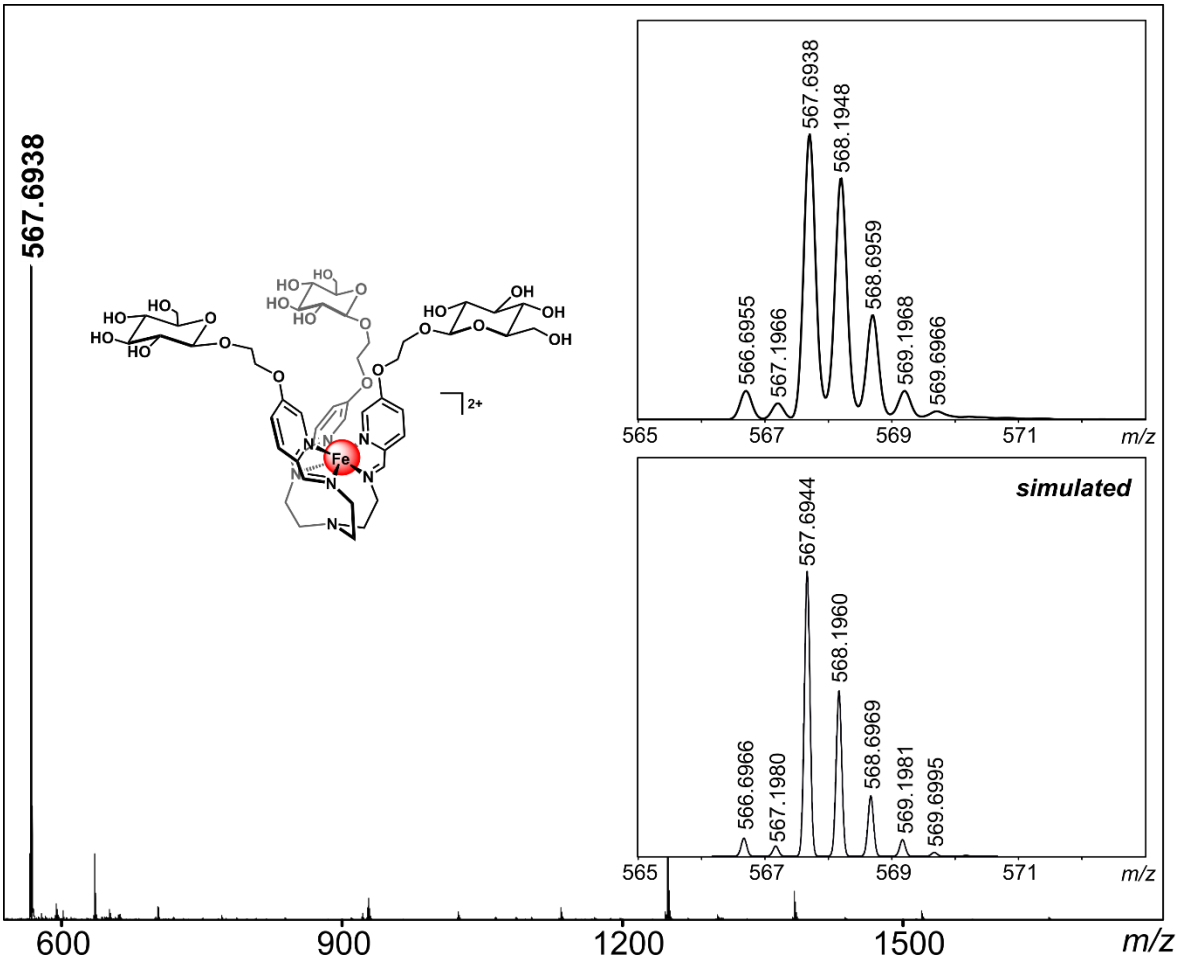

Figure S45. HR-ESI-MS(+) of [**3**-glc]$^{2+}$ (ESI-MS(+) run in H_2O).

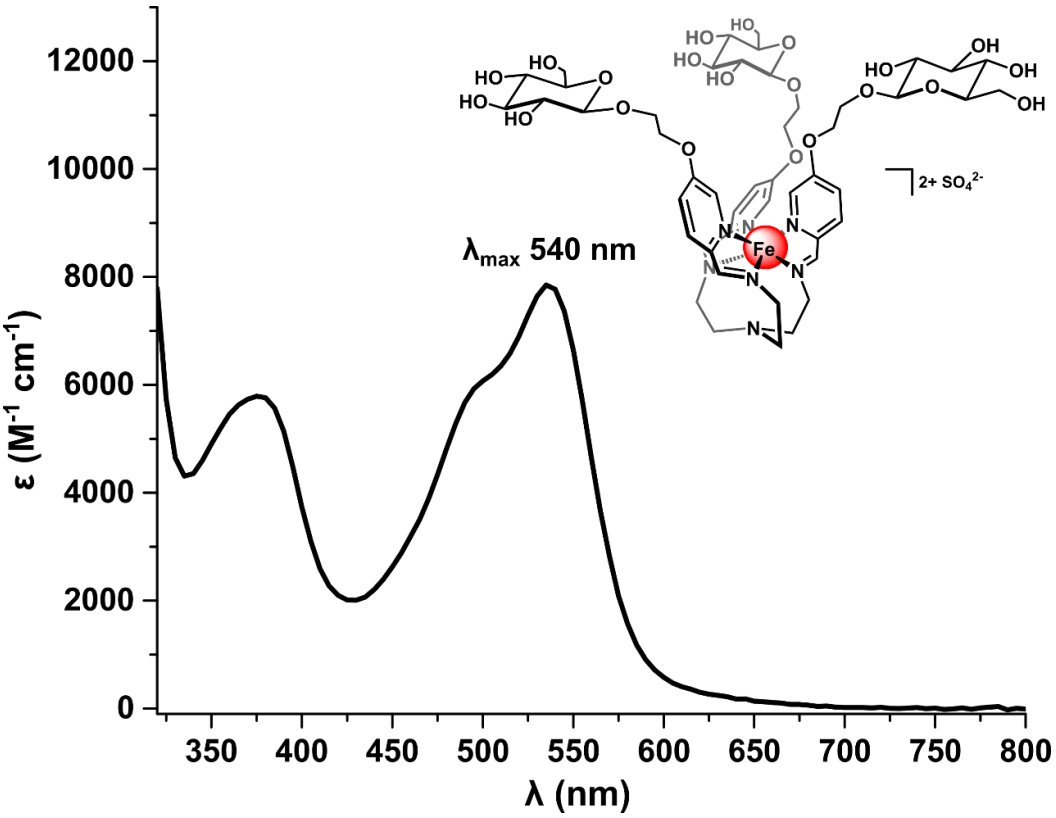

Figure S46. UV-vis spectrum of [**3**-glc][SO_4] (H_2O, 50 μM).

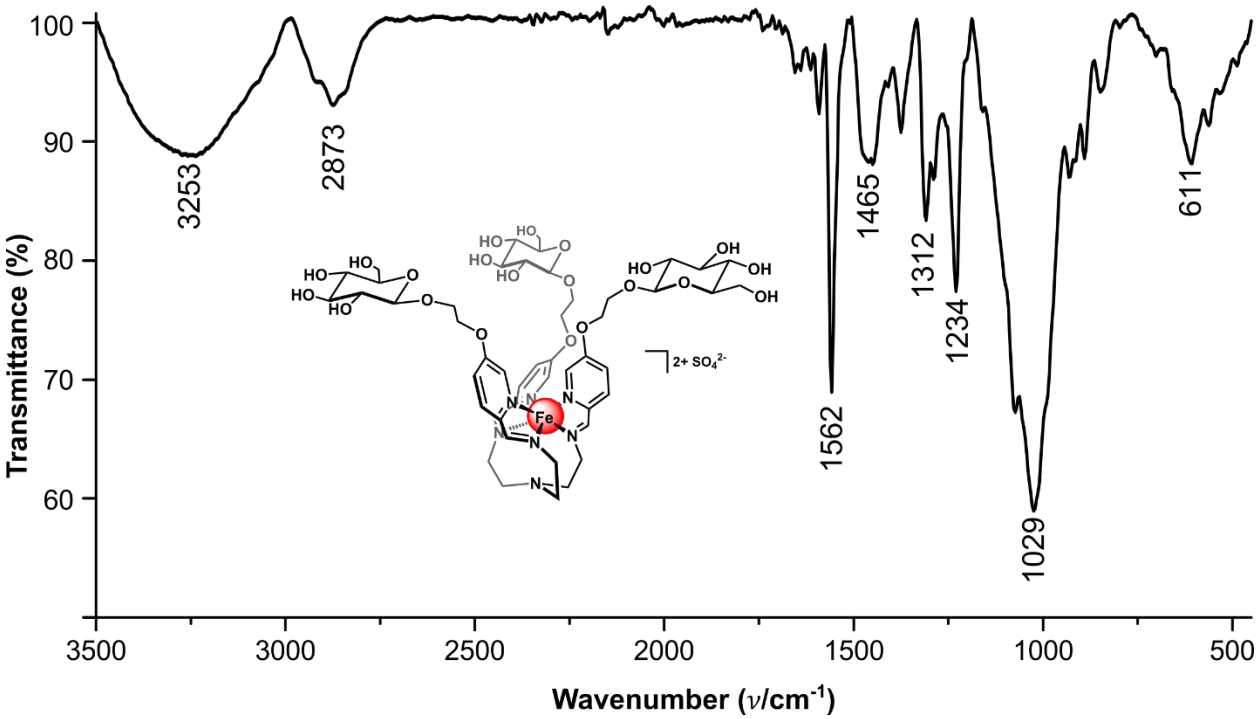

Figure S47. ATR-IR spectrum of [**3**-glc][SO_4].

S2.3.6. [NMe_4]$_4$[1-man]

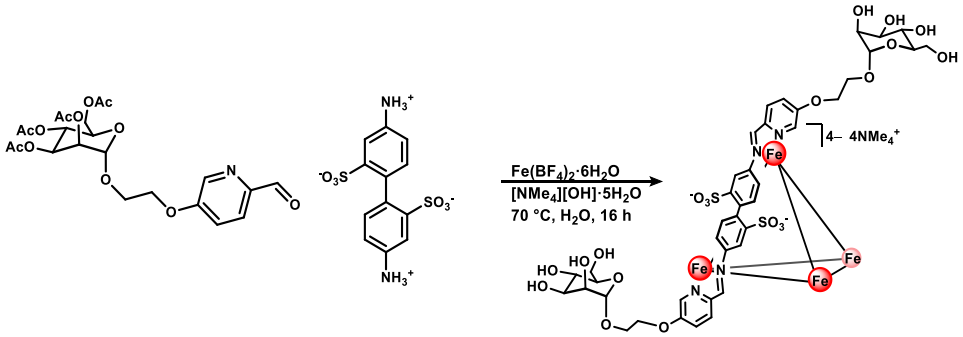

To an 8 mL reaction tube was added 5-((OAc)$_4$-α-D-mannoseEtO)-2-picolinaldehyde (68 mg, 0.14 mmol, 4.8 equiv) and [NMe_4][OH]•5H_2O (112 mg, 0.618 mmol, 22.0 equiv) as solids. Degassed H_2O (2 mL) was added, and the mixture was allowed to stir under an atmosphere of N_2 for 45 min at 70 °C, during which time it became homogeneous. To the solution was added 2,2'-benzidinedisulfonic acid (70 wt% balance H_2O, 14 mg, 0.028 mmol, 1.0 equiv) and Fe(BF_4)$_2$•6H_2O (15 mg, 0.044 mmol, 1.8 equiv) as solids, which resulted in an immediate color change to dark magenta. The reaction mixture was sparged with N_2 for 15 min and then allowed to stir at 70 °C for 16 h. The mixture was then allowed to cool to ambient temperature and the magenta solution was filtered through a piece of glass microfiber filter paper. To the filtrate was added ^{i}PrOH (20 mL), resulting in the precipitation of magenta solids. The suspension was centrifuged (1975 x g, 10 min), and the colorless supernatant was discarded. The resulting dark pink solids were suspended in Et_2O (5 mL), isolated by filtration, and dried under reduced pressure to afford the product as a dark magenta powder. The crude solids were dissolved in H_2O (4 mL) and filtered through a piece of glass microfiber filter paper into the sample reservoir of a Pall Microsep® (3K Omega membrane) centrifuge device. The device was centrifuged at 7500 x g for 75 min, at which point the filtrate in the collection tube was removed and fresh H_2O (4 mL) was added to the sample reservoir. The device was centrifuged again at 7500 x g for 75 min, and this process was repeated for a total of three centrifuge cycles. After the third cycle, the solution in the sample reservoir was removed and lyophilized overnight to afford the pure product, [NMe_4]$_4$[**1**-man], as a magenta powder (yield: 18 mg, 2.9 μmol, 61% based on theoretical yield of 4.7 μmol with 2,2'-benzidinedisulfonic acid as the limiting reagent (4:12:6 ratio of Fe:py:benzidine)). ^{1}H NMR (400 MHz, 25 °C, D_2O) δ: 9.11 (s, 12H, *H*C=N), 8.61 (d, 12H, *J* = 7.5 Hz, py-*H*-3), 7.90 (d, 12H, *J* = 7.5 Hz, py-*H*-4), 7.19 (s, 12H, py-*H*-6), 7.05 (br s, 12H, Ar-*H* 6,6'-benzidine), 6.40 (s, 12H, Ar-*H* 3,3'-benzidine), 5.75 (br s, 12H, Ar-*H* 5,5'-benzidine), 4.86 (s, 12H, man-*H*-1), 4.38 (s, 24H, –CH_2–), 4.02 (m, 12H, man-*H*-6$_a$), 3.90 (m, 12H, man-*H*-6$_b$), 3.87 (m, 12H, man-*H*-2), 3.74 (m, 12H, man-*H*-3), 3.67–3.6.4 (m, 12H, man-*H*-4), 3.55–3.47 (m, 36H, man-*H*-5, –CH_2– signals overlapping) ppm. ^{13}C{^{1}H} NMR (100 MHz, 25 °C, D_2O) δ: 174.1 (*C*=N), 159.3, 150.6, 150.1, 146.4, 142.7, 135.8, 133.0, 131.9, 122.0, 121.7, 120.9, 100.0, 72.7, 70.4, 69.8, 68.4, 66.5, 65.4, 60.8, 55.2 (N(*C*H$_3$)$_4$) ppm. ESI-MS(–) observed for [M]$^{4–}$: 1502.2395 (calc'd, 1502.2363) *m/z*. UV-vis [ε] (H_2O, 50 μM): λ_{max} 505 [22,000 $M^{-1}cm^{-1}$], 545 [26,000 $M^{-1}cm^{-1}$] nm. ATR-IR (ν): 3337 (OH), 2932, 1558 (C=N), 1469, 1316, 1234, 1208, 1141, 1044, 626, 555 cm^{-1}.

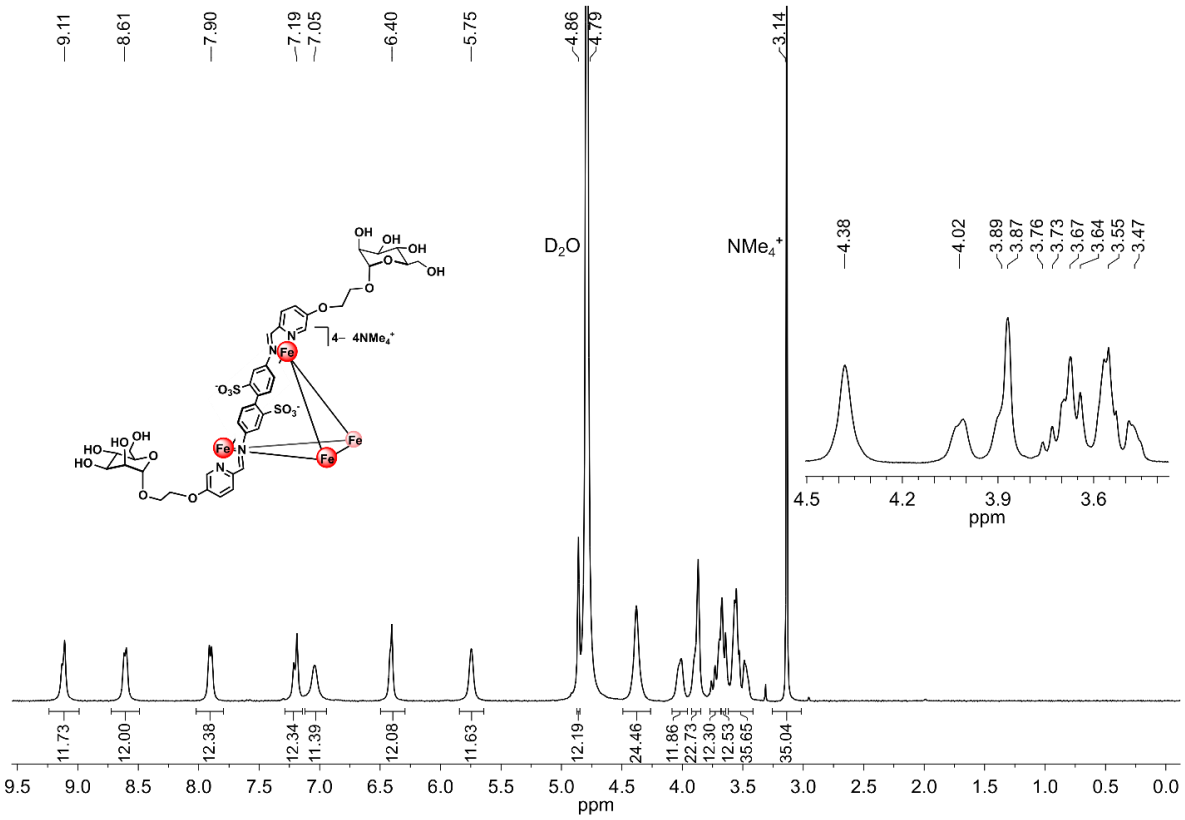

Figure S48. ^{1}H NMR spectrum of $[NMe_4]_4$[**1**-man] (D_2O, 400 MHz, 25 °C).

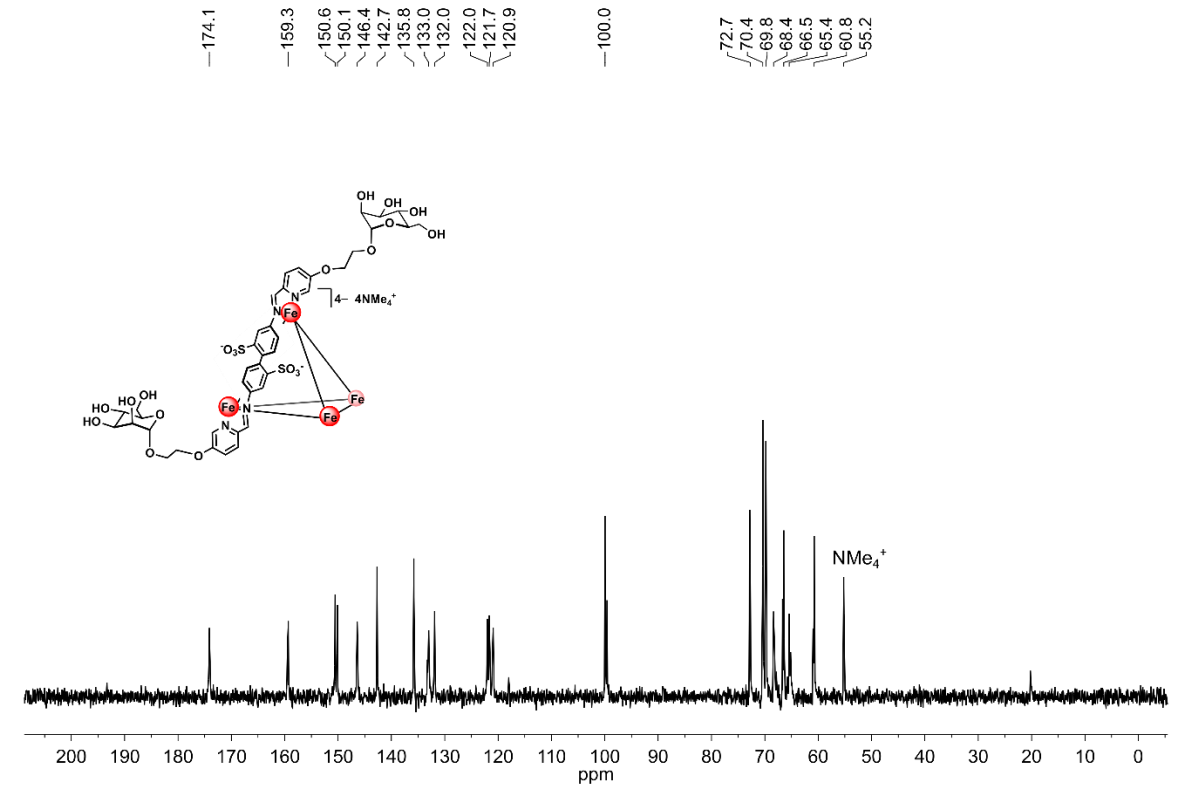

Figure S49. ^{13}C{^{1}H} NMR spectrum of $[NMe_4]_4$[**1**-man] (D_2O, 100 MHz, 25 °C).

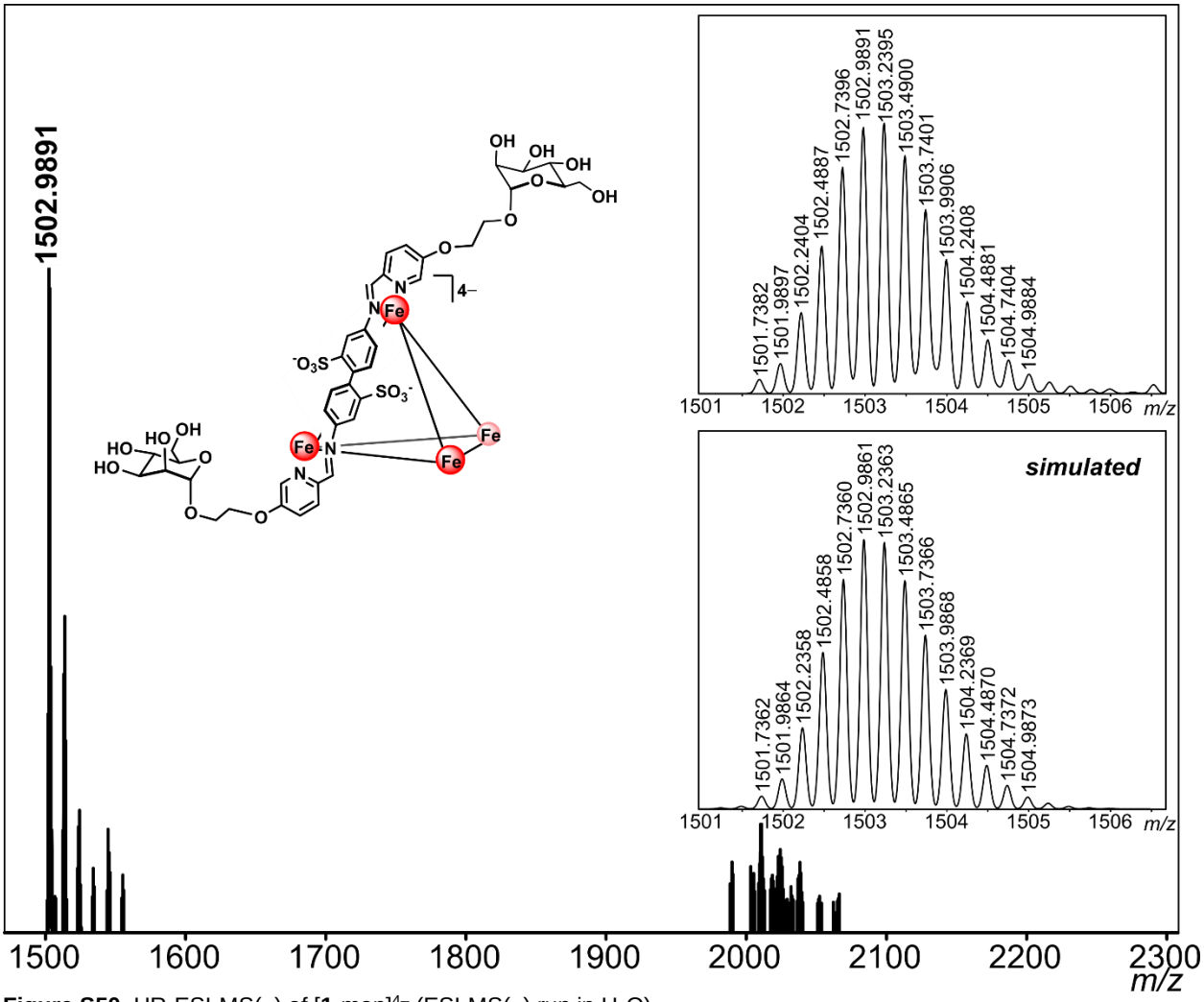

Figure S50. HR-ESI-MS(–) of [**1**-man]$^{4-}$ (ESI-MS(–) run in H_2O).

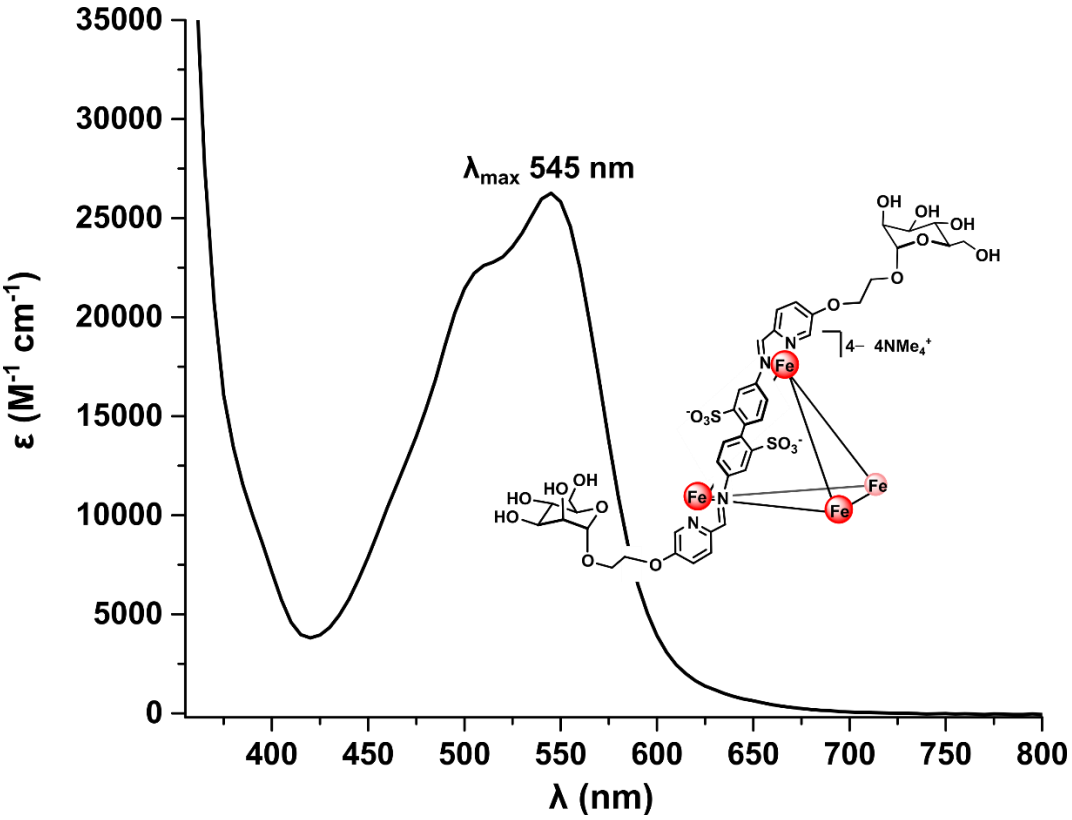

Figure S51. UV-vis spectrum of $[NMe_4]_4$[**1**-man] (H_2O, 50 μM).

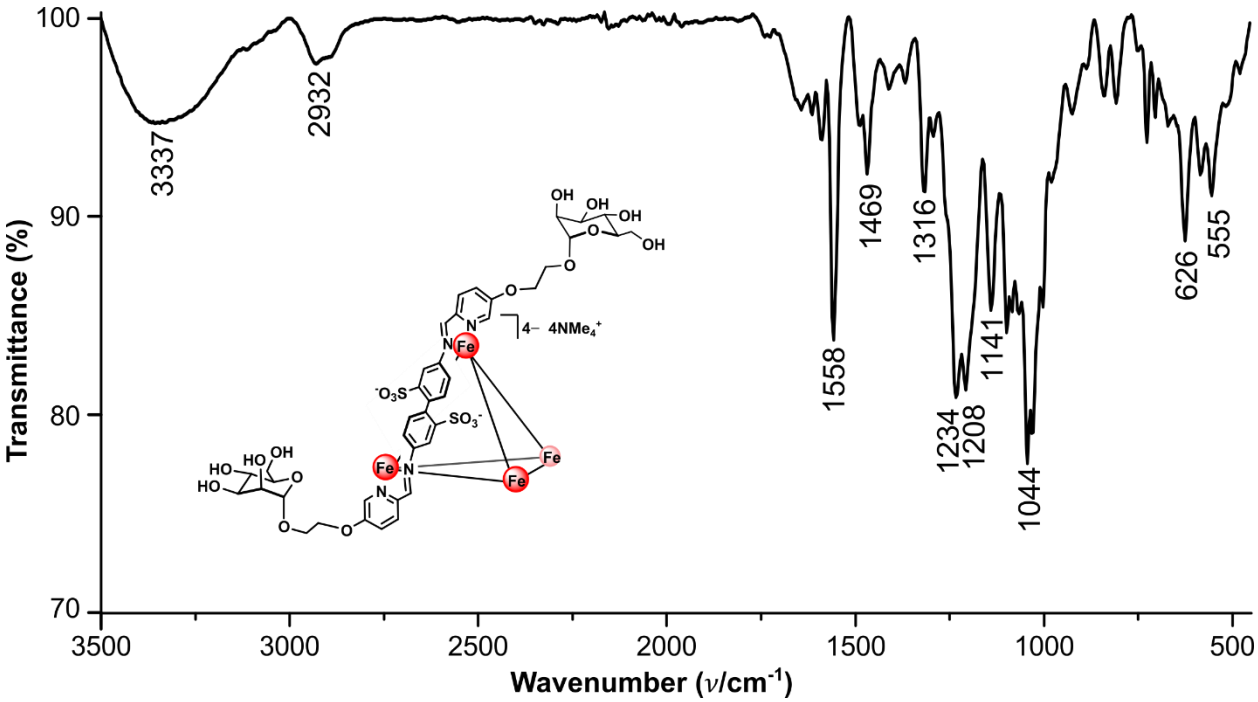

Figure S52. ATR-IR spectrum of $[NMe_4]_4$[**1**-man].

S2.3.7. $[NMe_4]_2$[2-man]

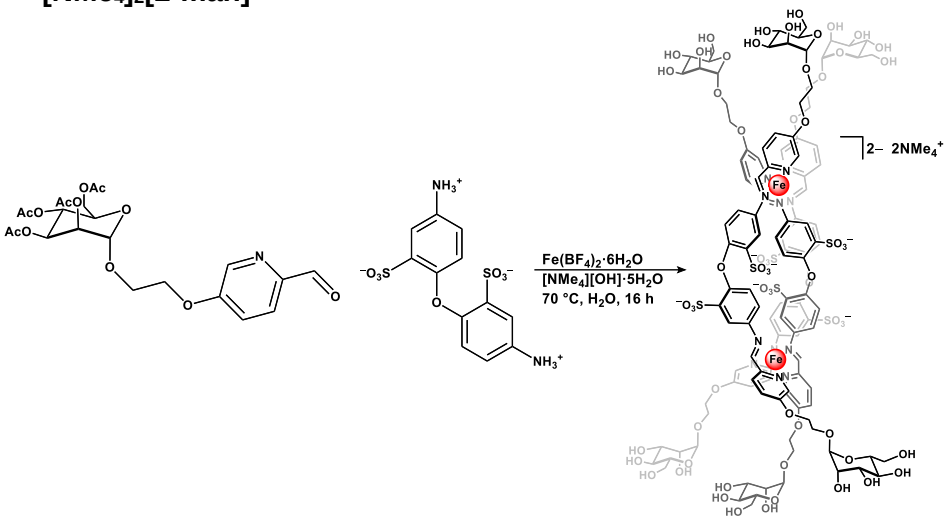

To an 8 mL reaction tube was added 5-((OAc)$_4$-α-D-mannoseEtO)-2-picolinaldehyde (60 mg, 0.12 mmol, 3.6 equiv), and [NMe$_4$][OH]•5H$_2$O (111 mg, 0.612 mmol, 18.0 equiv) as solids. Degassed H$_2$O (2 mL) was added, and the mixture was stirred under a flow of N$_2$ at 70 °C for 45 min. To the tube was added 4,4′-diaminodiphenyl ether-2,2′-disulfonic acid (80 wt% balance H$_2$O, 15 mg, 0.033 mmol, 1.0 equiv), and Fe(BF$_4$)$_2$•6H$_2$O (18 mg, 0.053 mmol, 1.6 equiv) as solids, which resulted in an immediate color change to dark pink. The reaction mixture was sparged with N$_2$ for 15 min, and then the mixture was allowed to stir at 70 °C for 16 h. The reaction was then allowed to cool to ambient temperature and the magenta solution was filtered through a piece of glass microfiber filter paper. To the filtrate was added ^{i}PrOH (20 mL), resulting in the precipitation of magenta solids. The suspension was centrifuged (1975 x g, 10 min), and the colorless supernatant was discarded. The resulting solids were suspended in Et$_2$O (5 mL), isolated by filtration, and dried under reduced pressure to afford the product as a dark magenta powder. The crude solids were dissolved in H$_2$O (4 mL) and filtered through a piece of glass microfiber filter paper into the sample reservoir of a Pall Microsep® (1K Omega membrane) centrifuge device. The device was centrifuged at 7500 x g for 75 min, at which point the filtrate in the collection tube was removed and fresh H$_2$O (4 mL) was added to the sample reservoir. The device was centrifuged again at 7500 x g for 75 min, and this process was repeated for a total of three centrifuge cycles. After the third cycle, the solution in the sample reservoir was removed and lyophilized overnight to afford the pure product, $[NMe_4]_2$[**2**-man], as a magenta powder (yield: 19 mg, 5.9 μmol, 54% based on theoretical yield of 11 μmol with 4,4′-diaminodiphenyl ether-2,2′-disulfonic acid as the limiting reagent (2:6:3 ratio of Fe:py:benzidine)). ^{1}H NMR (400 MHz, 25 °C, D$_2$O) δ: 9.70, 9.61 (two singlets, 6H, *H*C=N, ΔΔ, ΛΛ, and ΔΛ configurations), 8.82 (two doublets overlapping, 6H, py-*H*-3, ΔΔ, ΛΛ, and ΔΛ configurations), 7.94 (d, 6H, *J* = 8.3 Hz, py-*H*-4), 7.77, 7.67 (s, 6H, py-*H*-6, ΔΔ, ΛΛ, and ΔΛ configurations), 6.57 (d, 6H, *J* = 8.7 Hz, Ar-*H* 6,6'-benzidine), 6.41, 6.40 (s, 6H, Ar-*H* 3,3'-benzidine, ΔΔ, ΛΛ, and ΔΛ configurations), 5.60 (br s, 6H, Ar-*H* 5,5'-benzidine), 4.89 (s, 6H, man-*H*-1), 4.42 (s, 12H, –C*H*$_2$–), 4.06 (m, 6H, man-*H*-6$_a$), 3.93 (m, 6H, man-*H*-6$_b$), 3.90 (m, 6H, man-*H*-2), 3.79–3.72 (m, 6H, man-*H*-3), 3.70 (m, 6H, man-*H*-4), 3.63–3.51 (m, 18H, man-*H*-5, –C*H*$_2$– signals overlapping) ppm. ^{13}C{^{1}H} NMR (100 MHz, 25 °C, D$_2$O) δ: 172.8 (*C*=N), 162.2, 161.7, 154.9, 149.3, 147.1, 134.7, 134.2, 126.3, 122.9, 121.7, 99.6, 72.8, 70.5, 69.8, 68.6, 66.7, 65.2, 61.0, 55.3 (N(*C*H$_3$)$_4$) ppm. ESI-MS(–) observed for $[M]^{2-}$: 1526.7267 (calc'd, 1526.7282) *m/z*. UV-vis [ε] (H$_2$O, 50 μM): λ$_{max}$ 505 [10,000 M^{-1}cm^{-1}], 545 [12,000 M^{-1}cm^{-1}] nm. ATR-IR (ν): 3369 (OH), 2930, 2887, 1592 (C=N), 1558 (C=N), 1472, 1319, 1245, 1204, 1141, 1085, 1025, 850, 704, 634, 548 cm^{-1}.

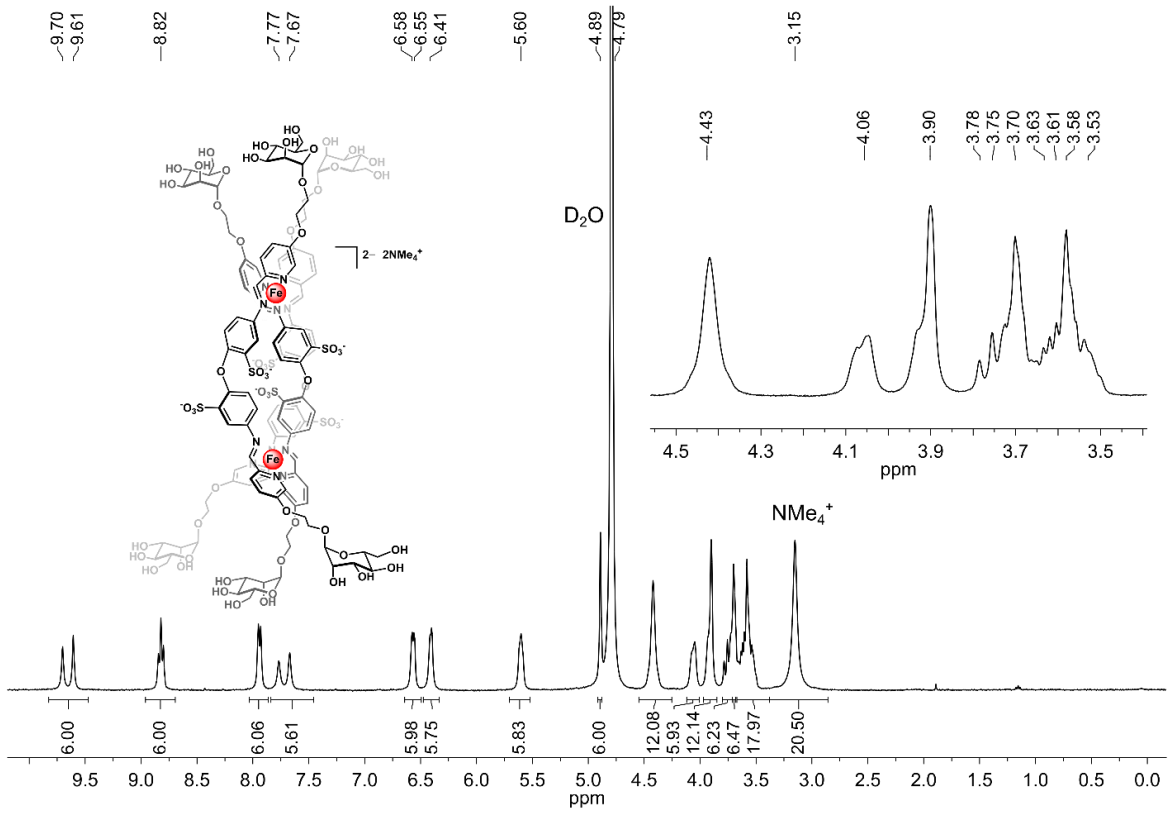

Figure S53. ^{1}H NMR spectrum of $[NMe_4]_2$[**2**-man] (D_2O, 400 MHz, 25 °C).

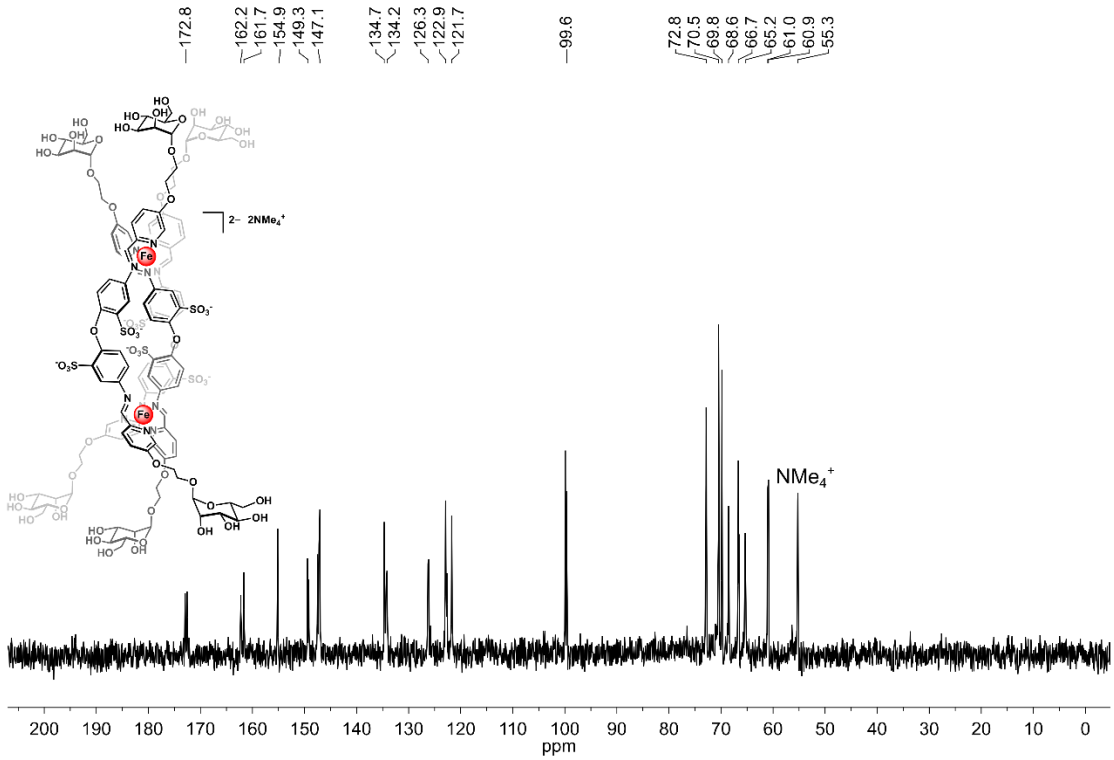

Figure S54. $^{13}C\{^{1}H\}$ NMR spectrum of $[NMe_4]_2$[**2**-man] (D_2O, 100 MHz, 25 °C).

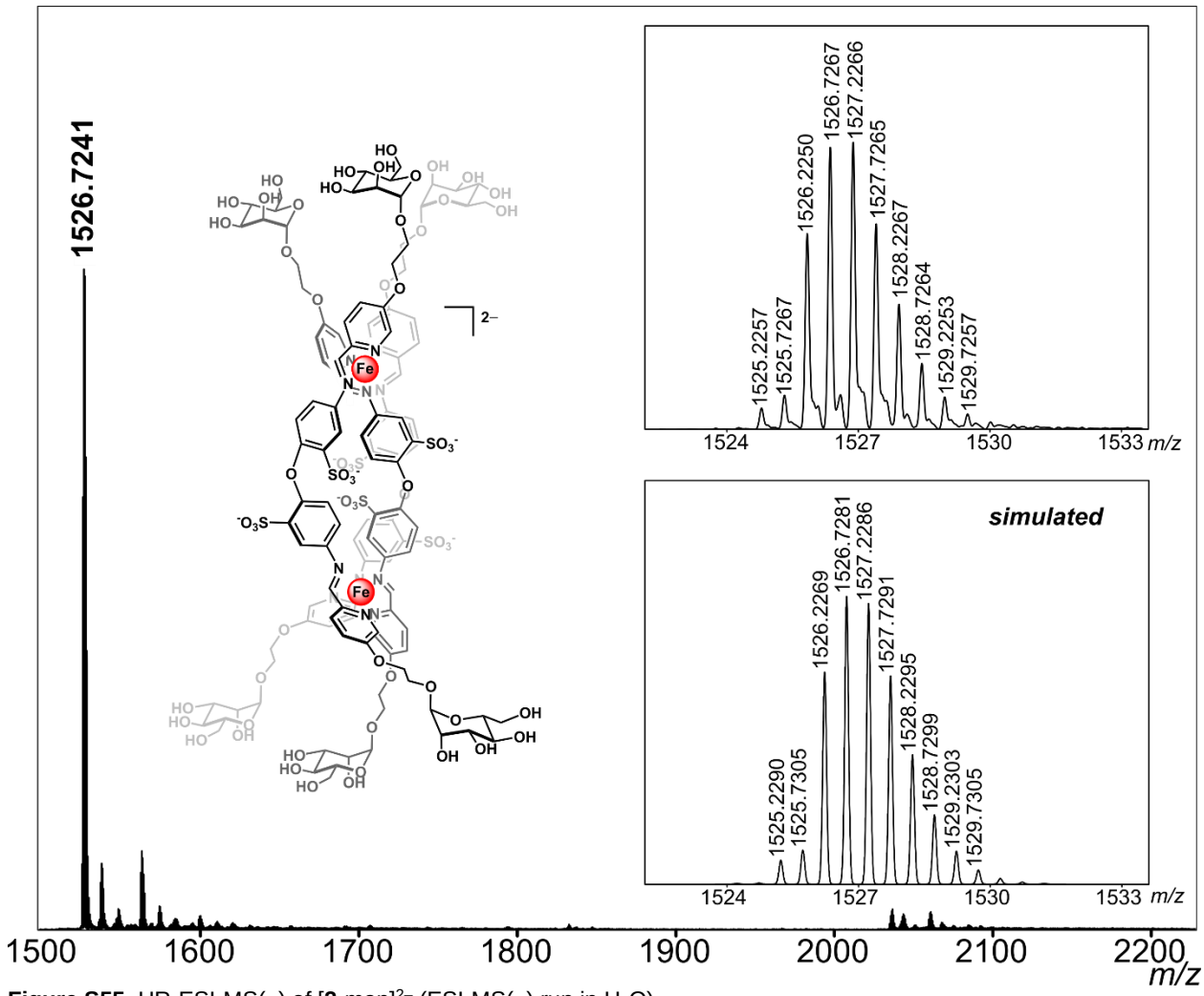

Figure S55. HR-ESI-MS(–) of [**2**-man]$^{2-}$ (ESI-MS(–) run in H_2O).

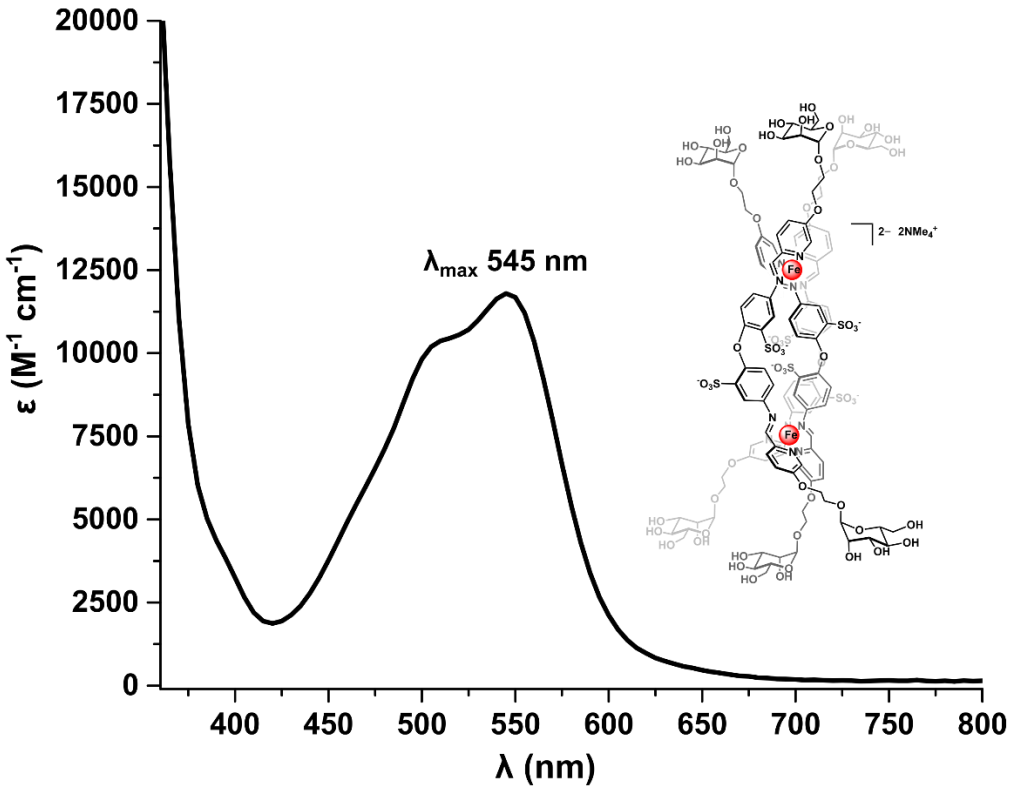

Figure S56. UV-vis spectrum of $[NMe_4]_2$[**2**-man] (H_2O, 50 μM).

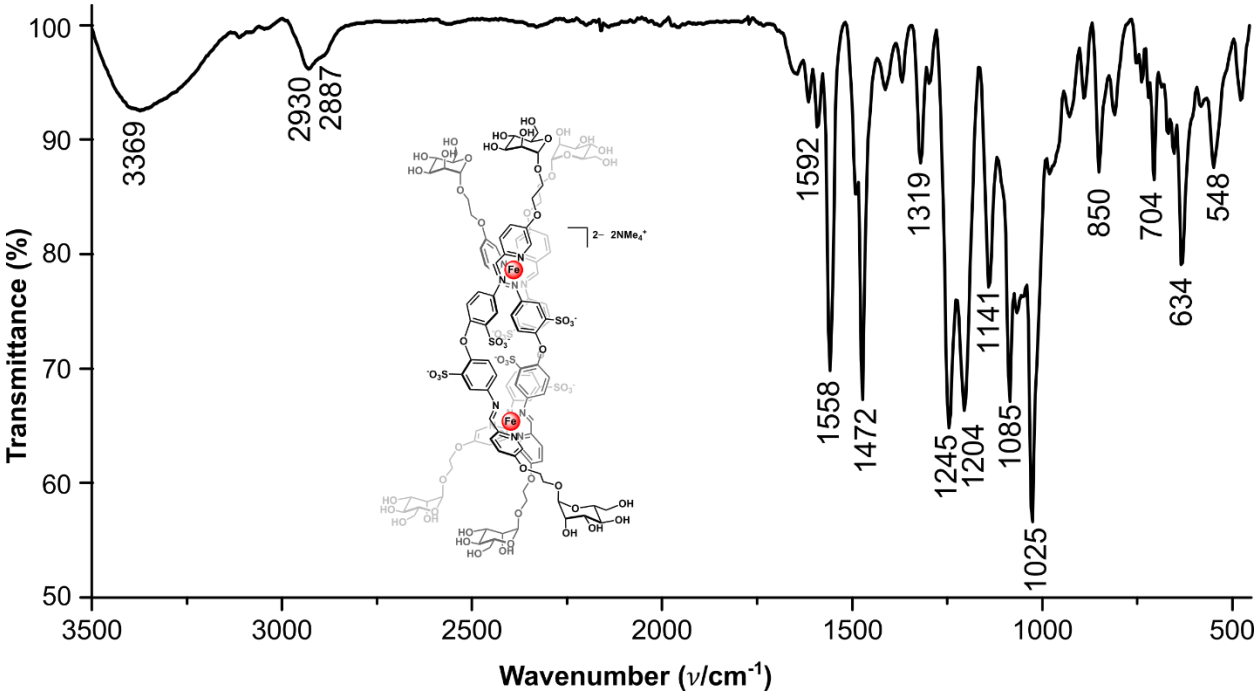

Figure S57. ATR-IR spectrum of $[NMe_4]_2$[**2**-man].

S2.3.8. [3-man][SO_4]

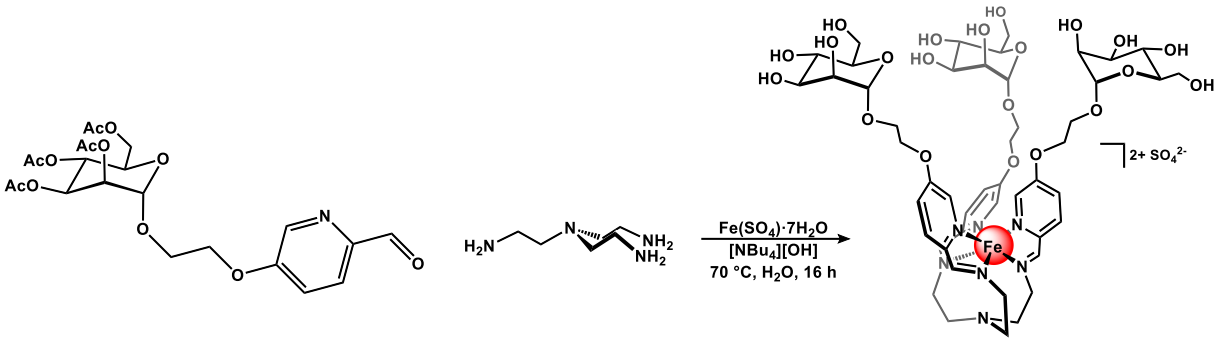

To an 8 mL reaction tube was added 5-((OAc)$_4$-α-D-mannoseEtO)-2-picolinaldehyde (51 mg, 0.10 mmol, 3.0 equiv), and [NBu_4][OH] (aq, 55%, 0.19 mL, 0.41 mmol, 12 equiv) followed by degassed H_2O (0.8 mL). The solution was allowed to stir under N_2 at 70 °C for 45 min, at which point tris(2-aminoethyl)amine (5 µL, 0.03 mmol, 1 equiv) and $Fe(SO_4)_2$•7H_2O (9 mg, 0.03 mmol, 1 equiv) were added. The dark pink solution was then sparged with N_2 for an additional 15 min. The reaction mixture was allowed to stir at 70 °C for 16 h, at which point the solution was allowed to cool to ambient temperature and filtered through a piece of glass microfiber filter paper. To the filtrate was added ^{i}PrOH (20 mL), resulting in the precipitation of magenta solids. The mixture was centrifuged (1975 x g, 10 min), and the pale pink supernatant was discarded. The resulting solids were suspended in Et_2O (5 mL), isolated by filtration, washed with ^{i}PrOH (2 mL) and Et_2O (2 mL), and dried under reduced pressure to afford the product as a dark magenta powder (yield: 32 mg, 0.026 mmol, 75%). ^{1}H NMR (400 MHz, 25 °C, D_2O) δ: 9.05 (s, 3H, *H*C=N), 8.23 (dd, 3H, *J* = 8.8, 1.4 Hz, py-*H*-3), 7.73 (dt, 3H, *J* = 8.8, 2.5 Hz, py-*H*-4), 6.78 (d, 3H, *J* = 1.4 Hz, py-*H*-6), 4.85 (d, 3H, *J* = 1.3 Hz, man-*H*-1), 4.25 (m, 6H, –CH_2–), 4.06 (m, 6H, man-*H*-6$_a$), 3.93 (m, 6H, man-*H*-6$_b$, man-*H*-2 signals overlapping), 3.85 (m, 6H, man-*H*-6$_b$), 3.71–3.50 (m, 18H, man-*H*-3, man-*H*-4, man-*H*-5, –CH_2–, tren –CH_2– signals overlapping), 3.39 (d, 3H, *J* = 12.3 Hz, tren –CH_2–), 3.16 (m, 3H, tren –CH_2–), 3.06 (m, 3H, tren –CH_2–) ppm. ^{13}C {^{1}H} NMR (100 MHz, 25 °C, D_2O) δ: 169.7 (*C*=N), 157.9, 150.5, 143.9, 129.1, 121.0, 99.9, 72.8, 70.5, 69.8, 67.9, 66.6, 65.5, 60.8, 58.3, 53.6 ppm. ESI-MS(+) observed for [M]$^{2+}$: 567.6944 (calc'd, 567.6944) *m/z*. UV-vis [ε] (H_2O, 50 µM): λ_{max} 375 [5,600 $M^{-1}cm^{-1}$], 495 [5,600 $M^{-1}cm^{-1}$], 540 [7,400 $M^{-1}cm^{-1}$] nm. ATR-IR (v): 3264 (OH), 2925, 1595 (C=N), 1562 (C=N), 1451, 1386, 1312, 1234, 1059, 816, 613 cm^{-1}.

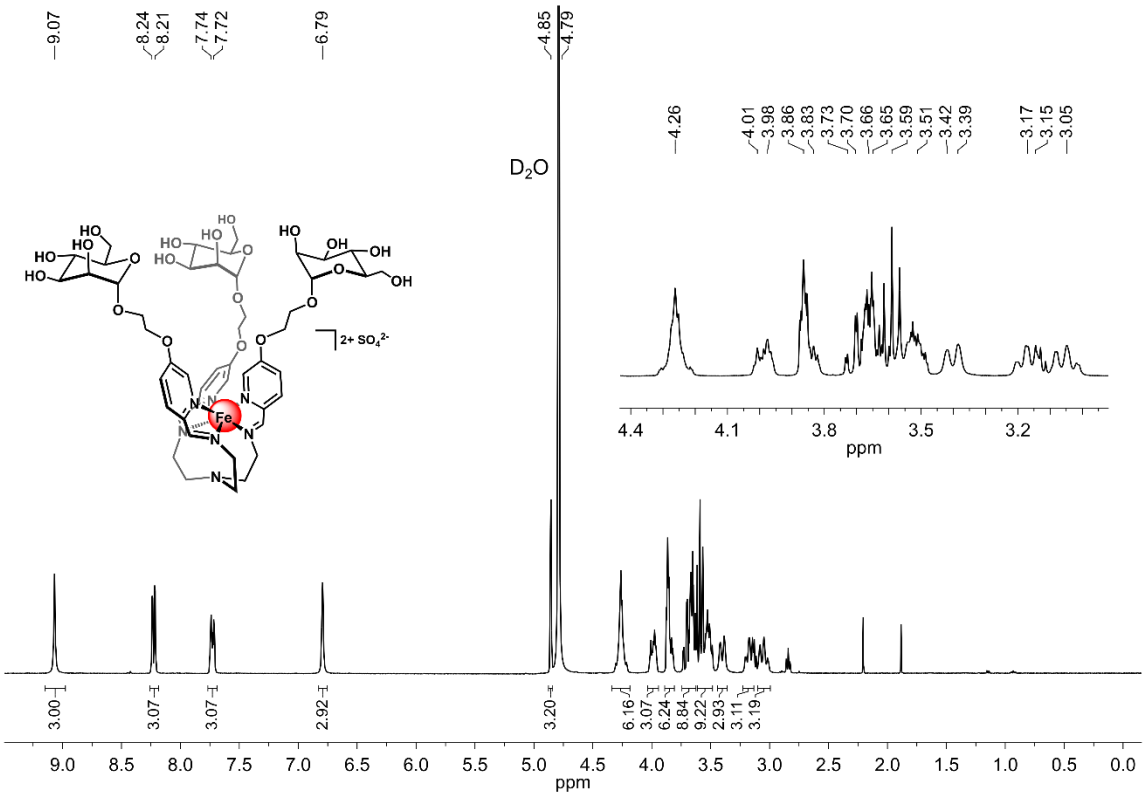

Figure S58. ^{1}H NMR spectrum of [**3**-man][SO_4] (D_2O, 400 MHz, 25 °C).

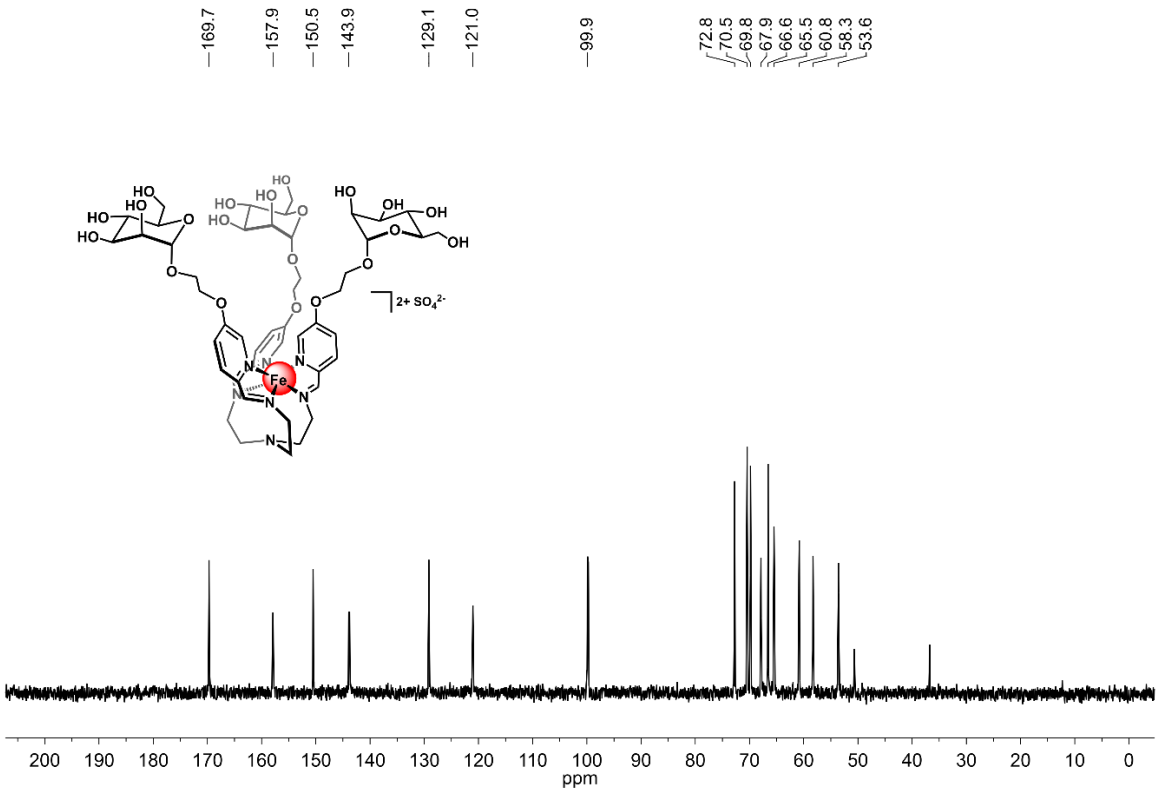

Figure S59. $^{13}C\{^{1}H\}$ NMR spectrum of [**3**-man][SO_4] (D_2O, 100 MHz, 25 °C).

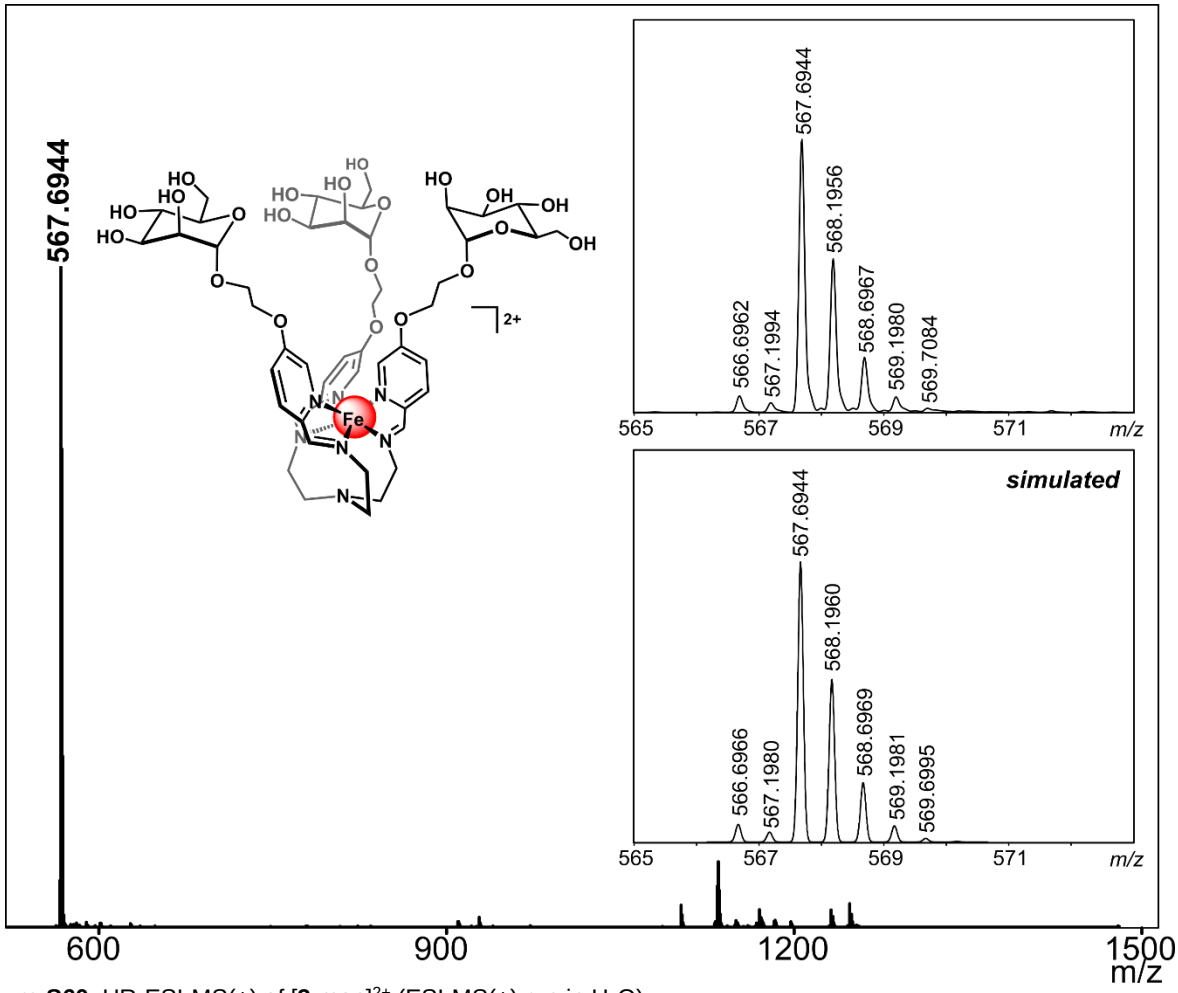

Figure S60. HR-ESI-MS(+) of [**3**-man]$^{2+}$ (ESI-MS(+) run in H_2O).

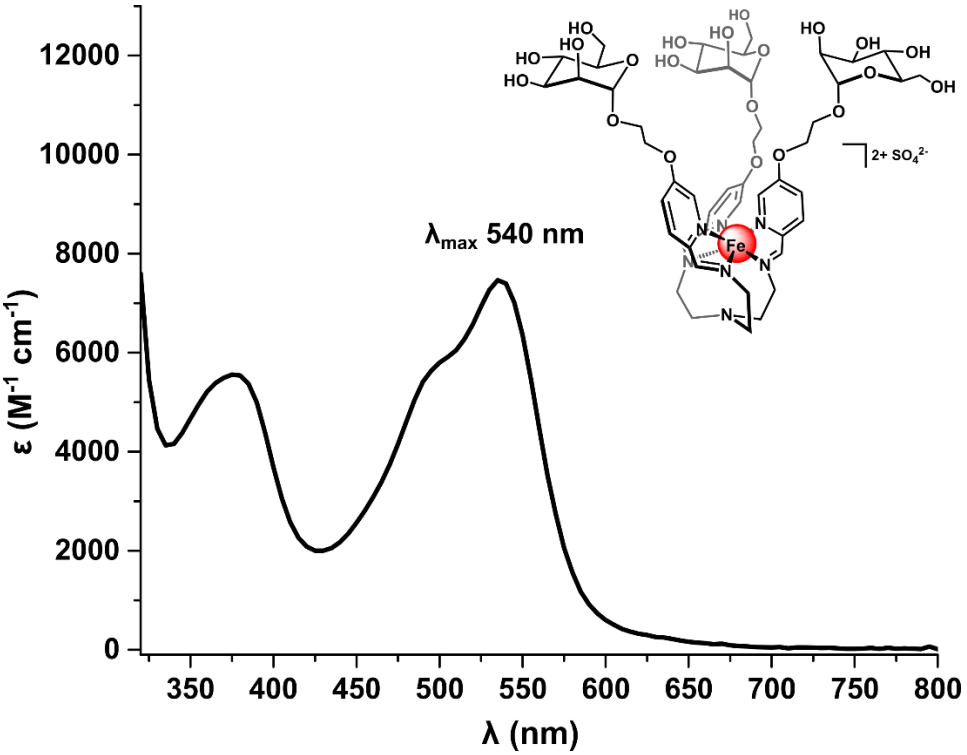

Figure S61. UV-vis spectrum of [**3**-man][SO_4] (H_2O, 50 μM).

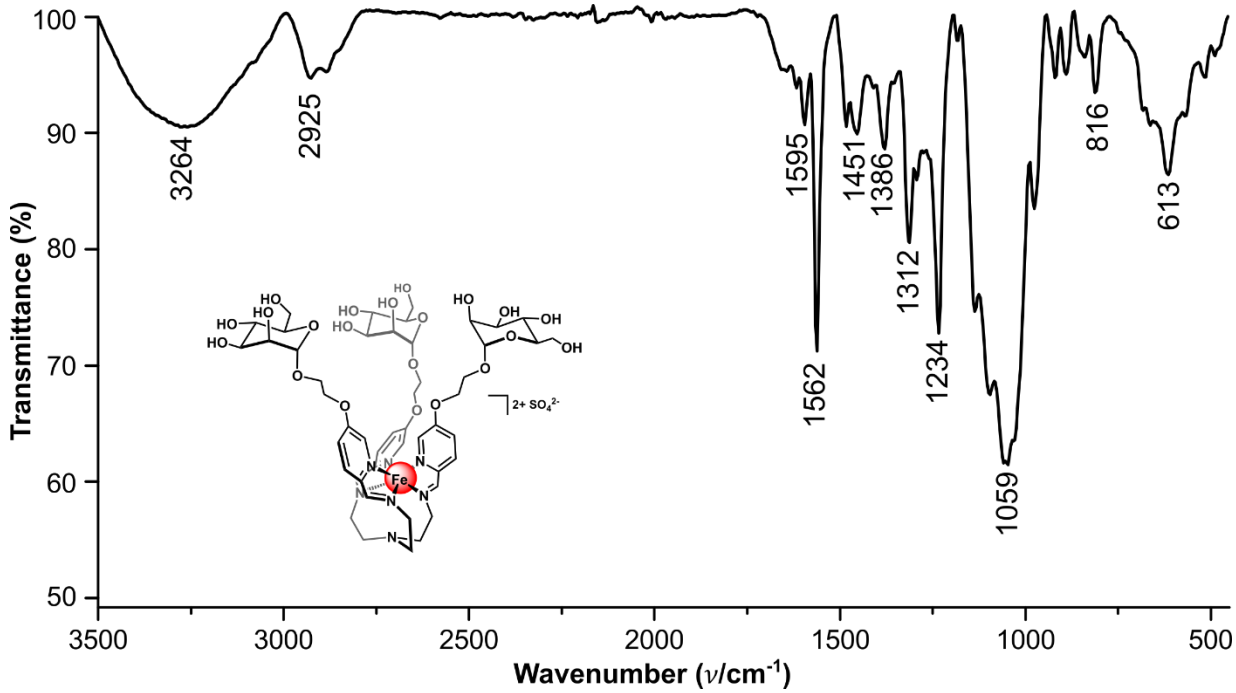

Figure S62. ATR-IR spectrum of [**3**-man][SO_4].

S2.3.9. [NMe_4]$_4$[1-gal]

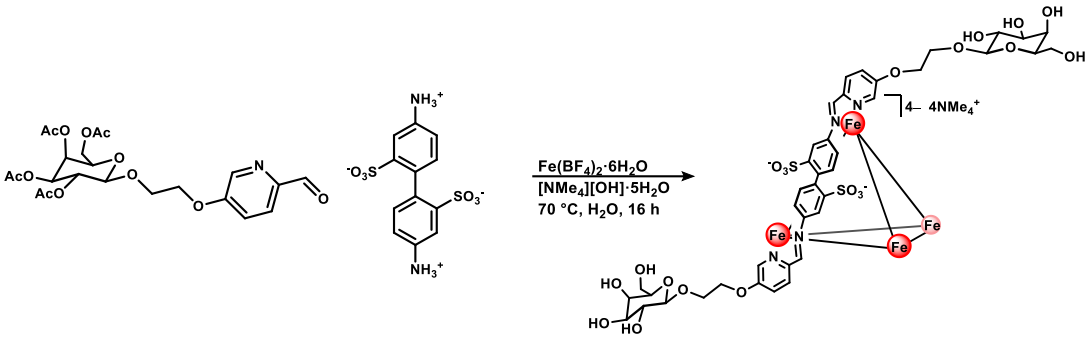

To an 8 mL reaction tube was added 5-((OAc)$_4$-β-D-galactoseEtO)-2-picolinaldehyde (68 mg, 0.14 mmol, 4.8 equiv) and [NMe_4][OH]•5H_2O (112 mg, 0.618 mmol, 22.0 equiv) as solids. Degassed H_2O (2 mL) was added, and the mixture was allowed to stir under an atmosphere of N_2 for 45 min at 70 °C, during which time it became homogeneous. To the solution was added 2,2'-benzidinedisulfonic acid (70 wt% balance H_2O, 14 mg, 0.028 mmol, 1.0 equiv) and $Fe(BF_4)_2$•6H_2O (15 mg, 0.044 mmol, 1.8 equiv) as solids, which resulted in an immediate color change to dark magenta. The reaction mixture was sparged with N_2 for 15 min and then allowed to stir at 70 °C for 16 h. The mixture was then allowed to cool to ambient temperature and the magenta solution was filtered through a piece of glass microfiber filter paper. To the filtrate was added ^{i}PrOH (20 mL), resulting in the precipitation of magenta solids. The suspension was centrifuged (1975 x g, 10 min), and the colorless supernatant was discarded. The resulting solids were suspended in Et_2O (5 mL), isolated by filtration, and dried under reduced pressure to afford the product as a dark magenta powder. The crude solids were dissolved in H_2O (4 mL) and filtered through a piece of glass microfiber filter paper into the sample reservoir of a Pall Microsep® (3K Omega membrane) centrifuge device. The device was centrifuged at 7500 x g for 75 min, at which point the filtrate in the collection tube was removed and fresh H_2O (4 mL) was added to the sample reservoir. The device was centrifuged again at 7500 x g for 75 min, and this process was repeated for a total of three centrifuge cycles. After the third cycle, the solution in the sample reservoir was removed and lyophilized overnight to afford the pure product, [NMe_4]$_4$[**1**-gal], as a magenta powder (yield: 20 mg, 3.2 μmol, 68% based on theoretical yield of 4.7 μmol with 2,2'-benzidinedisulfonic acid as the limiting reagent (4:12:6 ratio of Fe:py:benzidine)). ^{1}H NMR (400 MHz, 25 °C, D_2O) δ: 9.11 (s, 12H, *H*C=N), 8.59 (d, 12H, *J* = 7.6 Hz, py-*H*-3), 7.88 (d, 12H, *J* = 7.6 Hz, py-*H*-4), 7.16 (br s, 12H, py-*H*-6), 7.05 (br s, 12H, Ar-*H* 6,6'-benzidine), 6.43 (s, 12H, Ar-*H* 3,3'-benzidine), 5.77 (br s, 12H, Ar-*H* 5,5'-benzidine), 4.42–4.37 (m, 36H, gal-*H*-1, –CH_2– signals overlapping), 4.20 (m, 12H, gal-*H*-6$_a$), 4.02 (m, 12H, gal-*H*-6$_b$), 3.85 (m, 12H, gal-*H*-4), 3.69–3.56 (m, 48H, gal-*H*-5, gal-*H*-3, –CH_2– signals overlapping), 3.44 (dd, 12H, *J* = 9.8, 8.4 Hz, gal-*H*-2), 3.13 (s, 48H, N(CH_3)$_4$) ppm. ^{13}C{^{1}H} NMR (100 MHz, 25 °C, D_2O) δ: 174.1 (*C*=N), 159.2, 150.5, 150.1, 146.5, 142.7, 135.8, 132.8, 131.9, 121.9, 121.6, 121.0, 103.0, 75.2, 72.7, 70.6, 68.6, 68.4, 67.9, 61.0, 55.2 (N(*C*H_3)$_4$) ppm. ESI-MS(–) observed for [M]$^{4–}$: 1502.2317 (calc'd, 1502.2363) *m/z*. UV-vis [ε] (H_2O, 50 μM): λ_{max} 505 [20,000 $M^{-1}cm^{-1}$], 545 [24,000 $M^{-1}cm^{-1}$] nm. ATR-IR (ν): 3373 (OH), 2896, 1558 (C=N), 1469, 1319, 1234, 1085, 1044, 727, 626, 555 cm^{-1}.

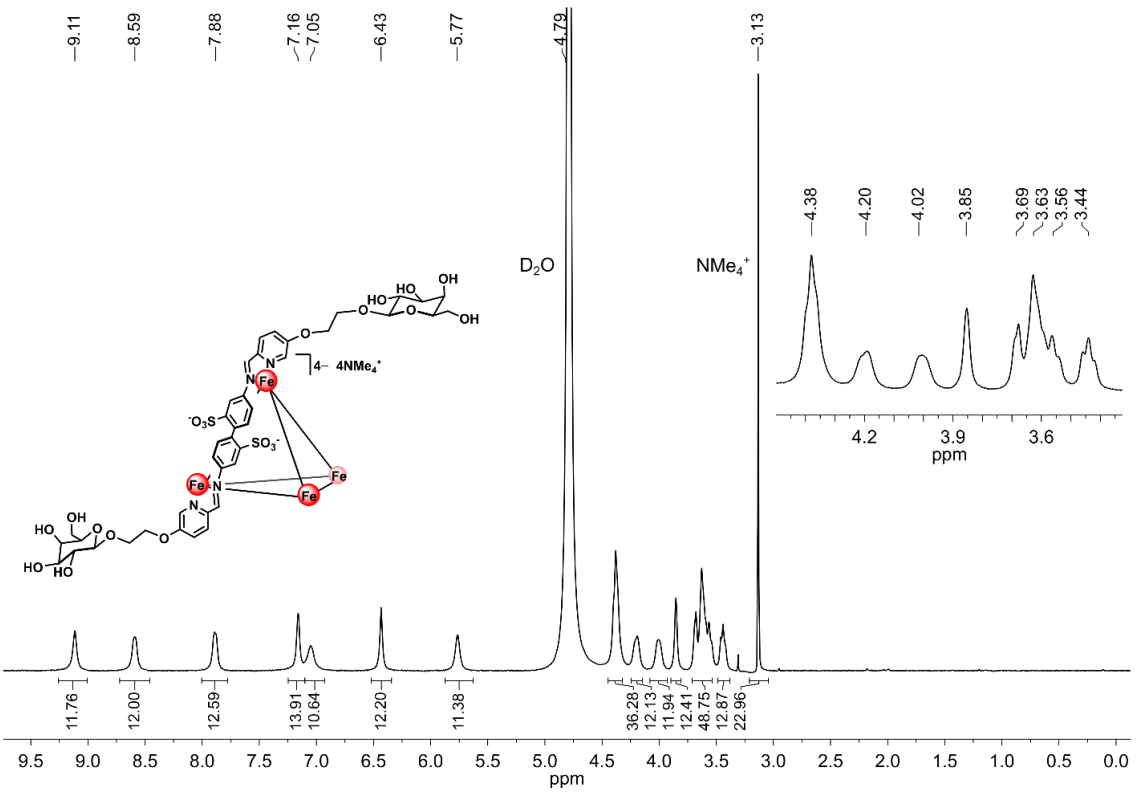

Figure S63. ^{1}H NMR spectrum of $[NMe_4]_4$[**1**-gal] (D_2O, 400 MHz, 25 °C).

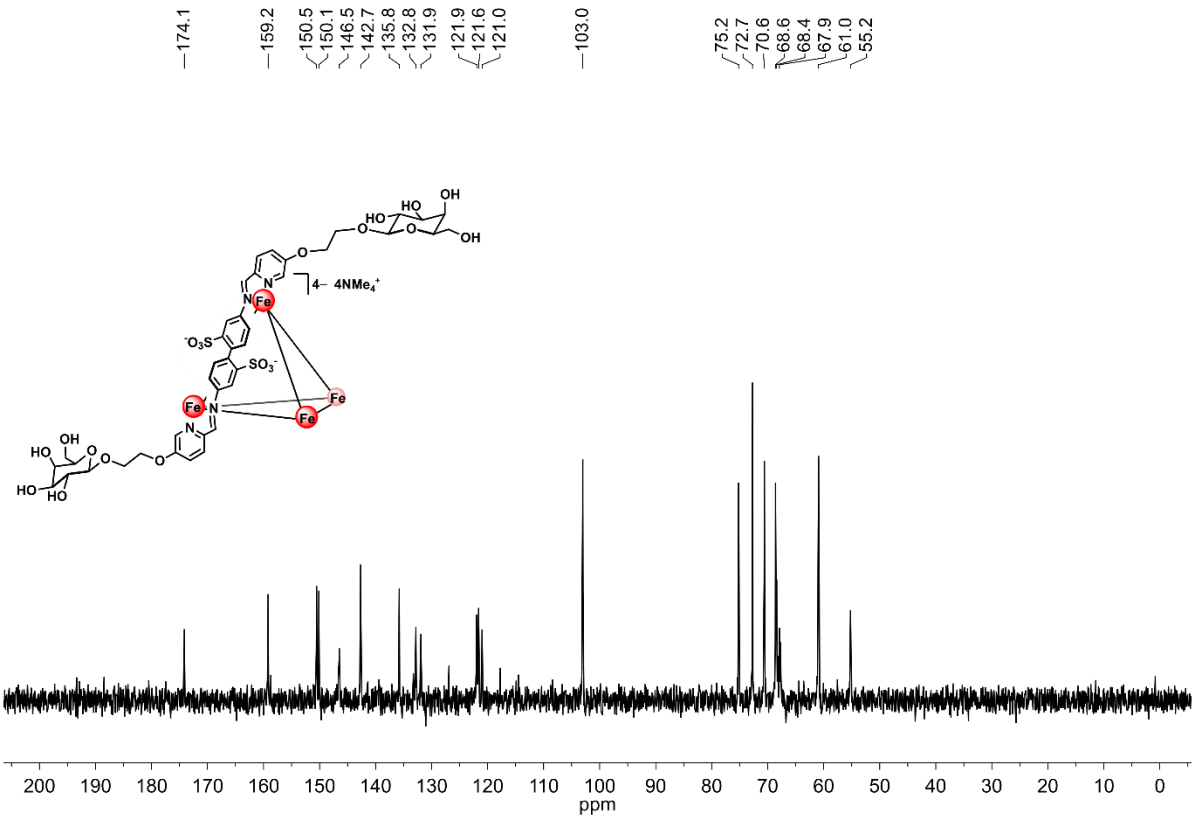

Figure S64. ^{13}C{^{1}H} NMR spectrum of $[NMe_4]_4$[**1**-gal] (D_2O, 100 MHz, 25 °C).

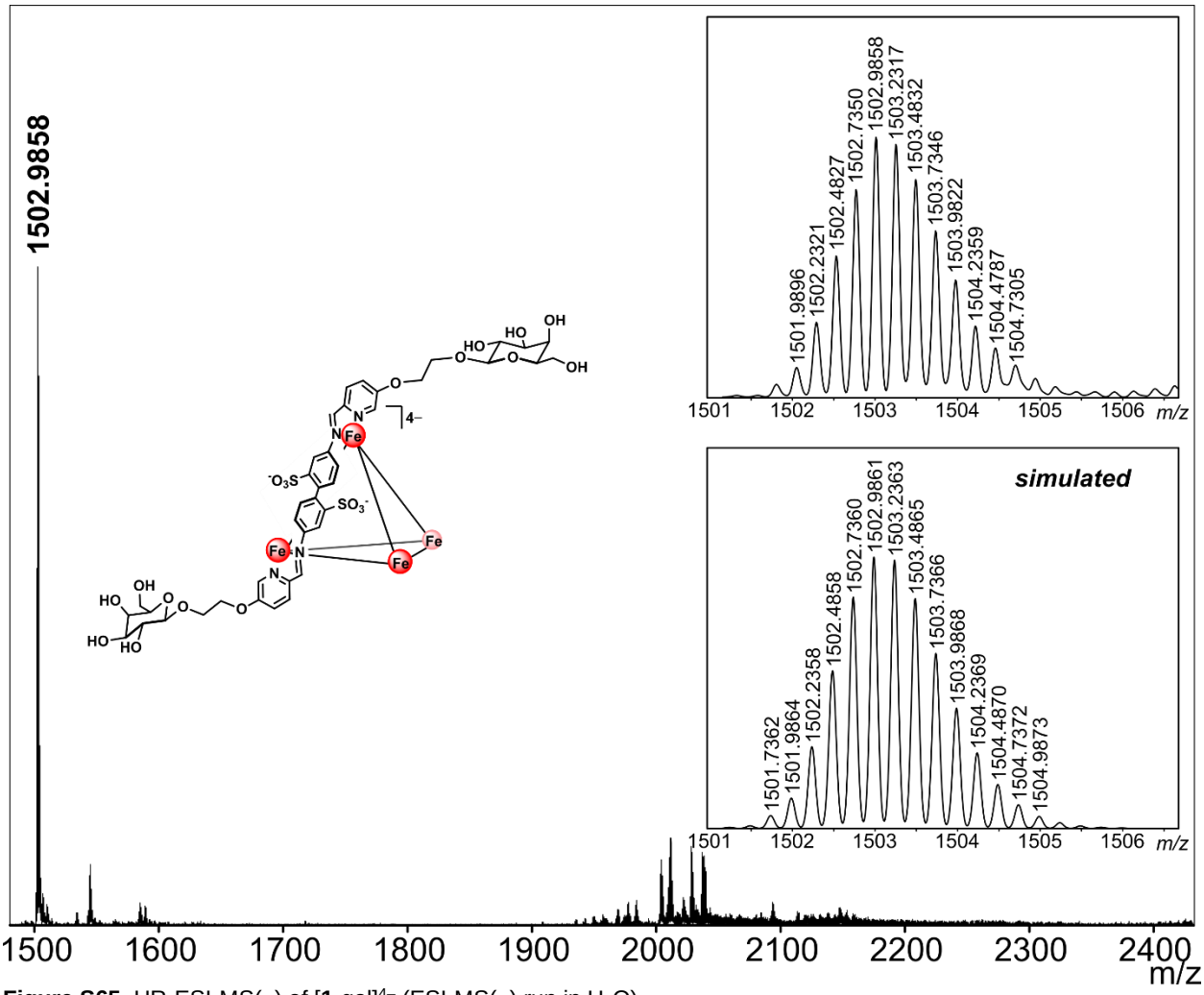

Figure S65. HR-ESI-MS(–) of [**1**-gal]$^{4-}$ (ESI-MS(–) run in H_2O).

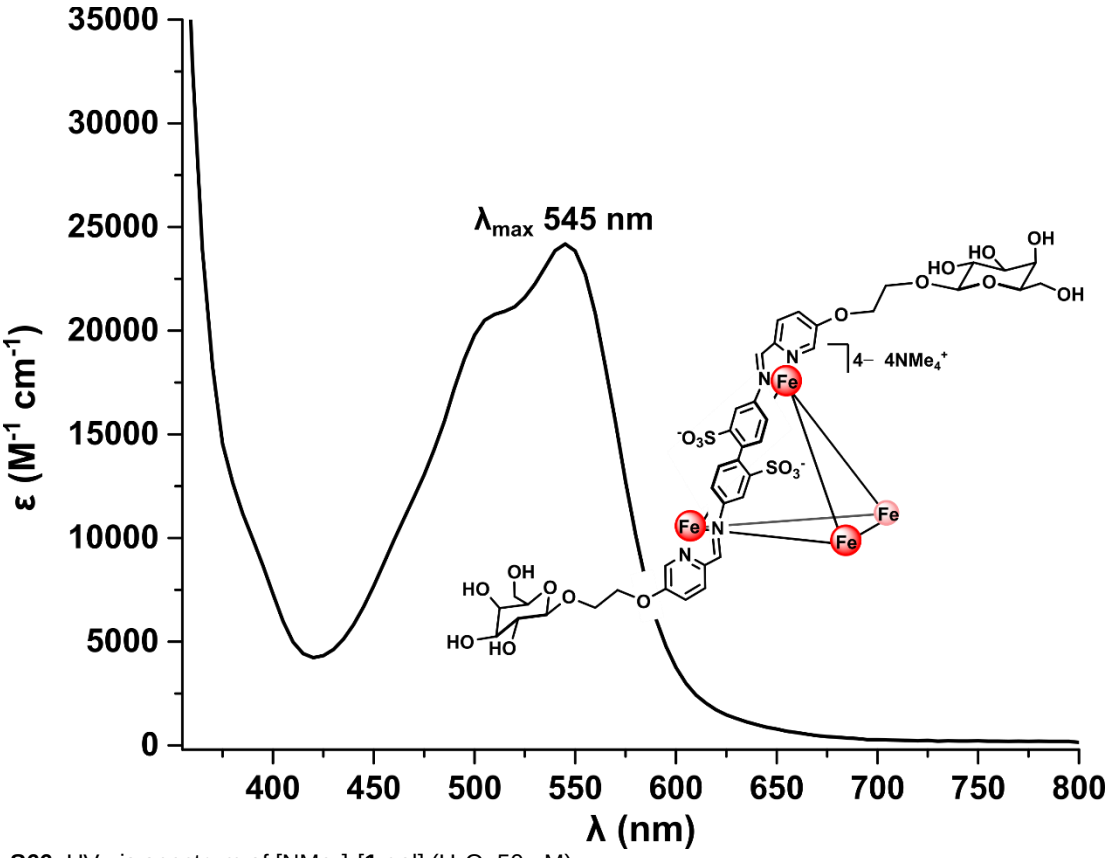

Figure S66. UV-vis spectrum of $[NMe_4]_4$[**1**-gal] (H_2O, 50 μM).

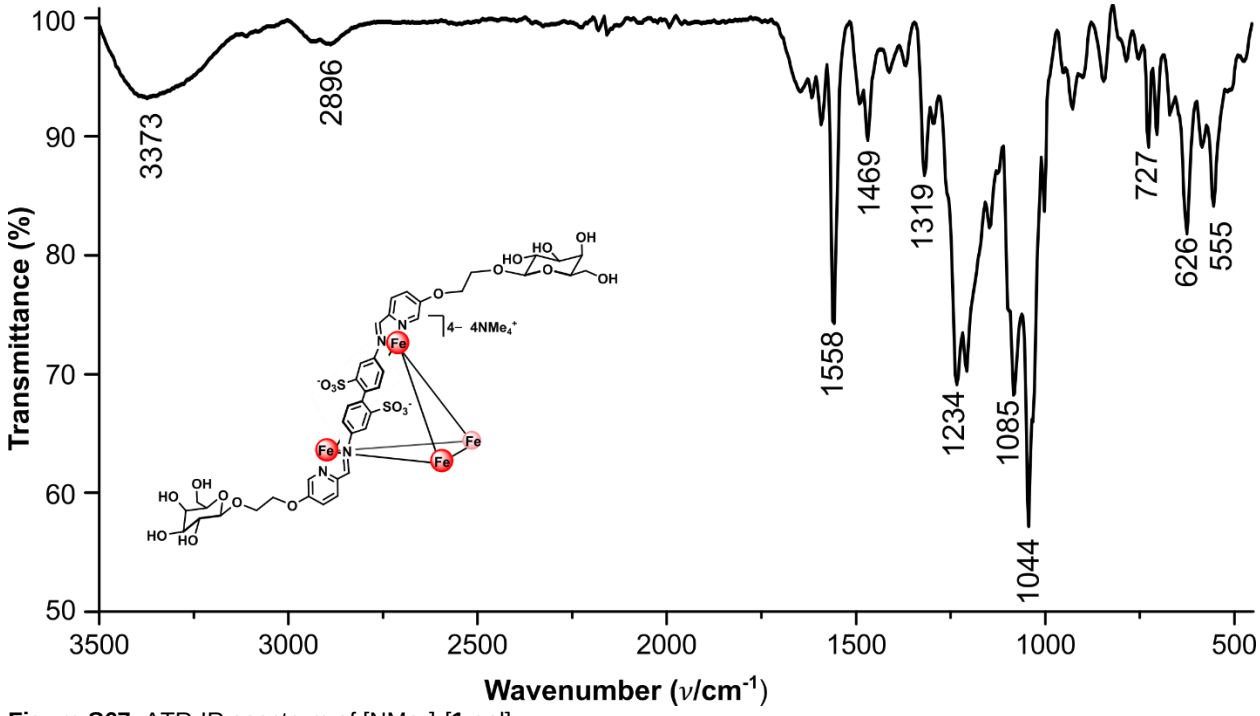

Figure S67. ATR-IR spectrum of $[NMe_4]_4$[**1**-gal].

S2.3.10. $[NMe_4]_2$[2-gal]

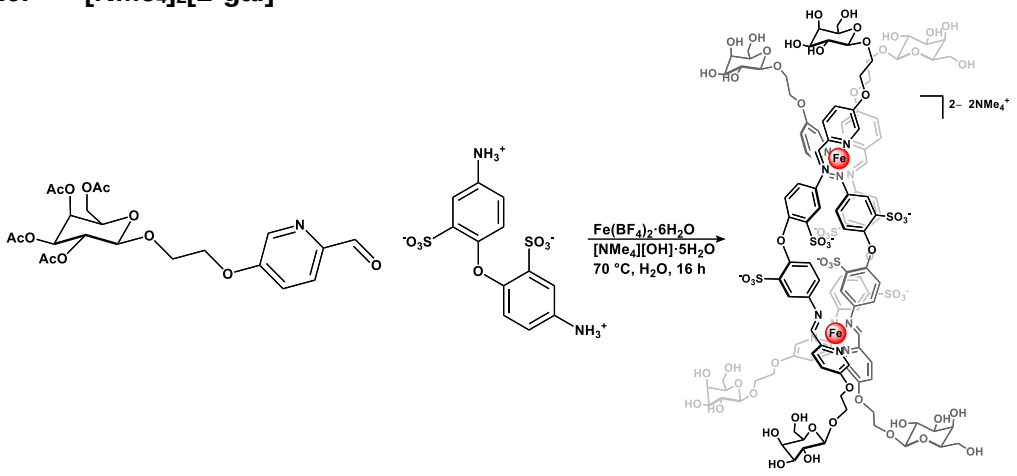

To an 8 mL reaction tube was added 5-((OAc)$_4$-β-D-galactoseEtO)-2-picolinaldehyde (60 mg, 0.12 mmol, 3.6 equiv), and $[NMe_4][OH]•5H_2O$ (111 mg, 0.612 mmol, 18.0 equiv) as solids. Degassed H_2O (2 mL) was added, and the mixture was stirred under a flow of N_2 at 70 °C for 45 min. To the tube was added 4,4′-diaminodiphenyl ether-2,2′-disulfonic acid (80 wt% balance H_2O, 15 mg, 0.033 mmol, 1.0 equiv), and $Fe(BF_4)_2•6H_2O$ (18 mg, 0.053 mmol, 1.6 equiv) as solids, which resulted in an immediate color change to dark pink. The reaction mixture was sparged with N_2 for 15 min and then allowed to stir at 70 °C for 16 h. The reaction was then allowed to cool to ambient temperature and the magenta solution was filtered through a piece of glass microfiber filter paper. To the filtrate was added ^{i}PrOH (20 mL), resulting in the precipitation of magenta solids. The suspension was centrifuged (1975 x g, 10 min), and the colorless supernatant was discarded. The resulting solids were suspended in Et_2O (5 mL), isolated by filtration, and dried under reduced pressure to afford the product as a dark magenta powder. The crude solids were dissolved in H_2O (4 mL) and filtered through a piece of glass microfiber filter paper into the sample reservoir of a Pall Microsep® (1K Omega membrane) centrifuge device. The device was centrifuged at 7500 x g for 75 min, at which point the filtrate in the collection tube was removed and fresh H_2O (4 mL) was added to the sample reservoir. The device was centrifuged again at 7500 x g for 75 min, and this process was repeated for a total of three centrifuge cycles. After the third cycle, the solution in the sample reservoir was removed and lyophilized overnight to afford the pure product, $[NMe_4]_2$[**2**-gal], as a magenta powder (yield: 17 mg, 5.3 μmol, 48% based on theoretical yield of 11 μmol with 4,4′-diaminodiphenyl ether-2,2′-disulfonic acid as the limiting reagent (2:6:3 ratio of Fe:py:benzidine)). ^{1}H NMR (400 MHz, 25 °C, D_2O) δ: ^{1}H NMR (400 MHz, 25 °C, D_2O) δ: 9.48, 9.46 (two singlets, 6H, *H*C=N, ΔΔ, ΛΛ, and ΔΛ configurations), 8.74 (two doublets overlapping, 6H, *J* = 8.6 Hz, py-*H*-3, ΔΔ, ΛΛ, and ΔΛ configurations), 7.92 (d, 6H, *J* = 8.6 Hz, py-*H*-4), 7.56, 7.53 (two singlets, 6H, py-*H*-6, ΔΔ, ΛΛ, and ΔΛ configurations), 6.56 (d, 6H, *J* = 8.6 Hz, Ar-*H* 6,6'-benzidine), 6.44 (s, 6H, Ar-*H* 3,3'-benzidine, ΔΔ, ΛΛ, and ΔΛ configurations), 5.63 (d, 6H, *J* = 8.6 Hz, Ar-*H* 5,5'-benzidine), 4.41–4.37 (m, 18H, gal-*H*-1, –C*H*$_2$– signals overlapping), 4.23 (m, 6H, gal-*H*-6$_a$), 4.03 (m, 6H, gal-*H*-6$_b$), 3.87 (m, 6H, gal-*H*-4), 3.71 (m, 6H, gal-*H*-5), 3.71–3.54 (m, 18H, gal-*H*-3, –C*H*$_2$– signals overlapping), 3.49–3.43 (m, 6H, gal-*H*-2), 3.13 (s, 24H, N(C*H*$_3$)$_4$) ppm. ^{13}C{^{1}H} NMR (100 MHz, 25 °C, D_2O) δ: 173.2 (*C*=N), 161.0, 155.0 (two signals overlapping), 149.5, 147.1, 134.7, 133.8, 126.0, 122.9, 122.6, 121.7, 103.0, 75.2, 72.7, 70.6, 68.6, 67.9, 67.7, 60.9, 55.2 (N(*C*H$_3$)$_4$) ppm. ESI-MS(–) observed for $[M]^{2-}$: 1526.7241 (calc'd, 1526.7282) *m/z*. UV-vis [ε] (H_2O, 50 μM): λ_{max} 505 [11,000 $M^{-1}cm^{-1}$], 545 [13,000 $M^{-1}cm^{-1}$] nm. ATR-IR (ν): 3369 (OH), 2938, 1592 (C=N), 1558 (C=N), 1472, 1319, 1245, 1204, 1085, 1029, 928, 850, 704, 634, 548 cm^{-1}.

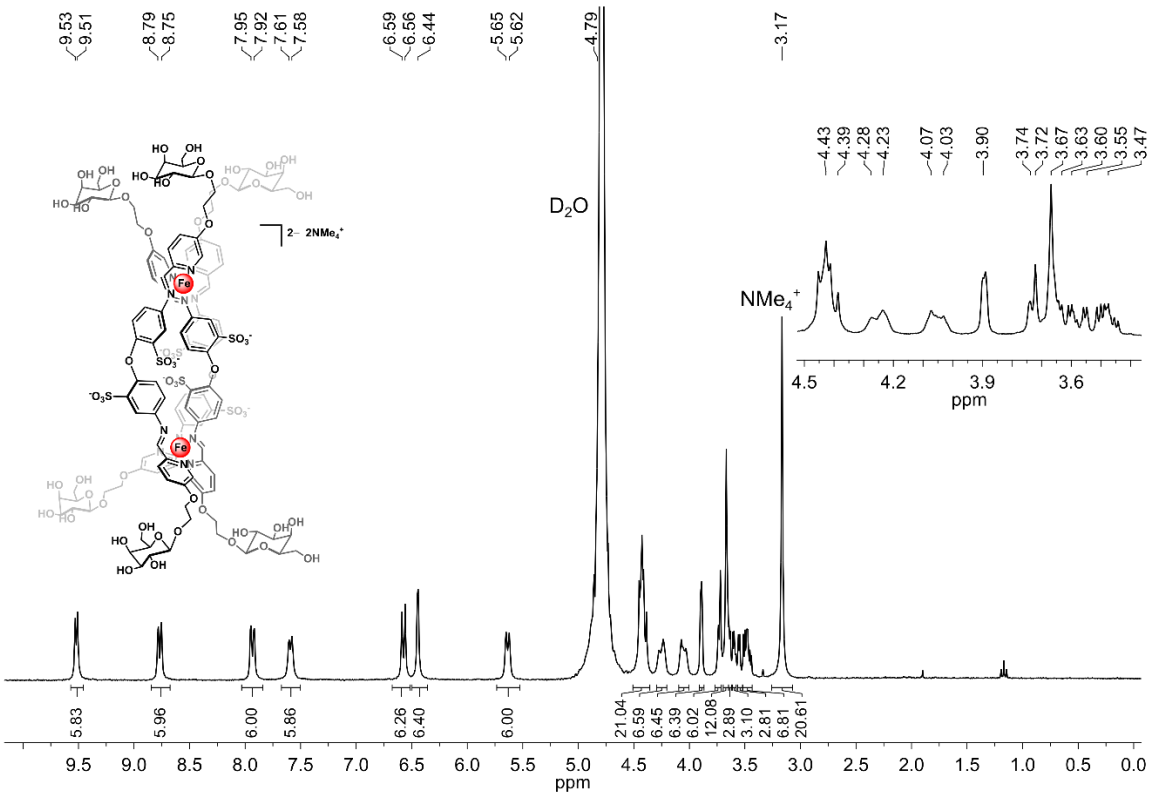

Figure S68. ^{1}H NMR spectrum of $[NMe_4]_2$[**2**-gal] (D_2O, 400 MHz, 25 °C).

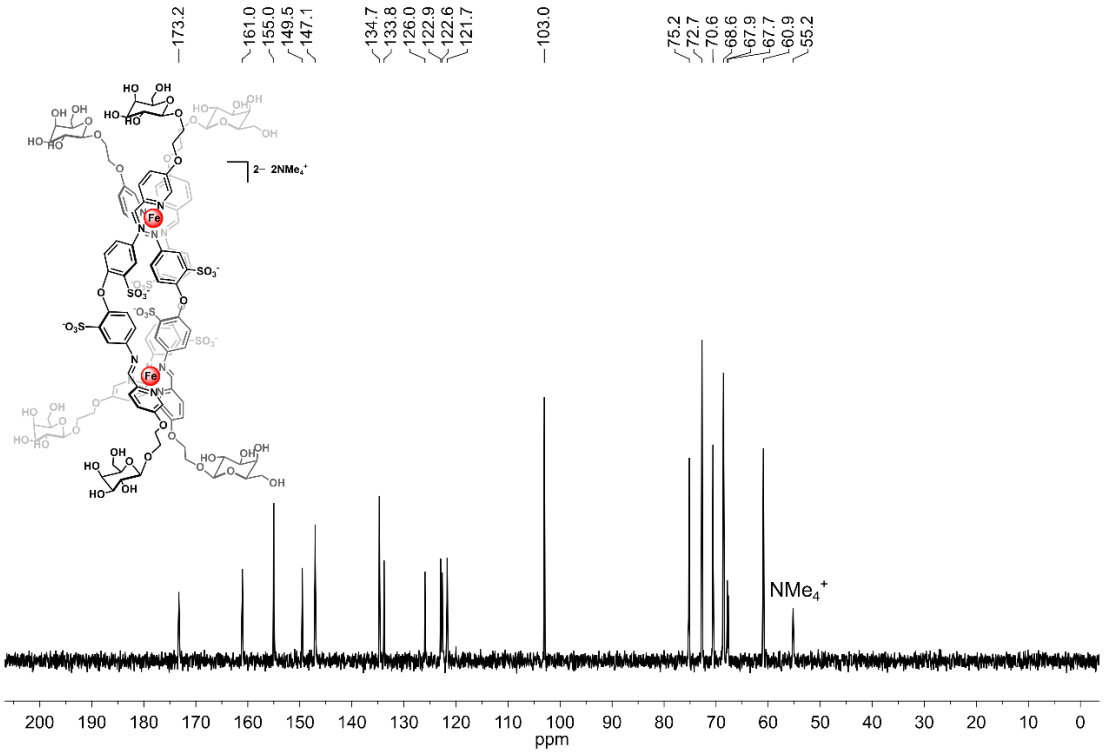

Figure S69. $^{13}C\{^{1}H\}$ NMR spectrum of $[NMe_4]_2$[**2**-gal] (D_2O, 100 MHz, 25 °C).

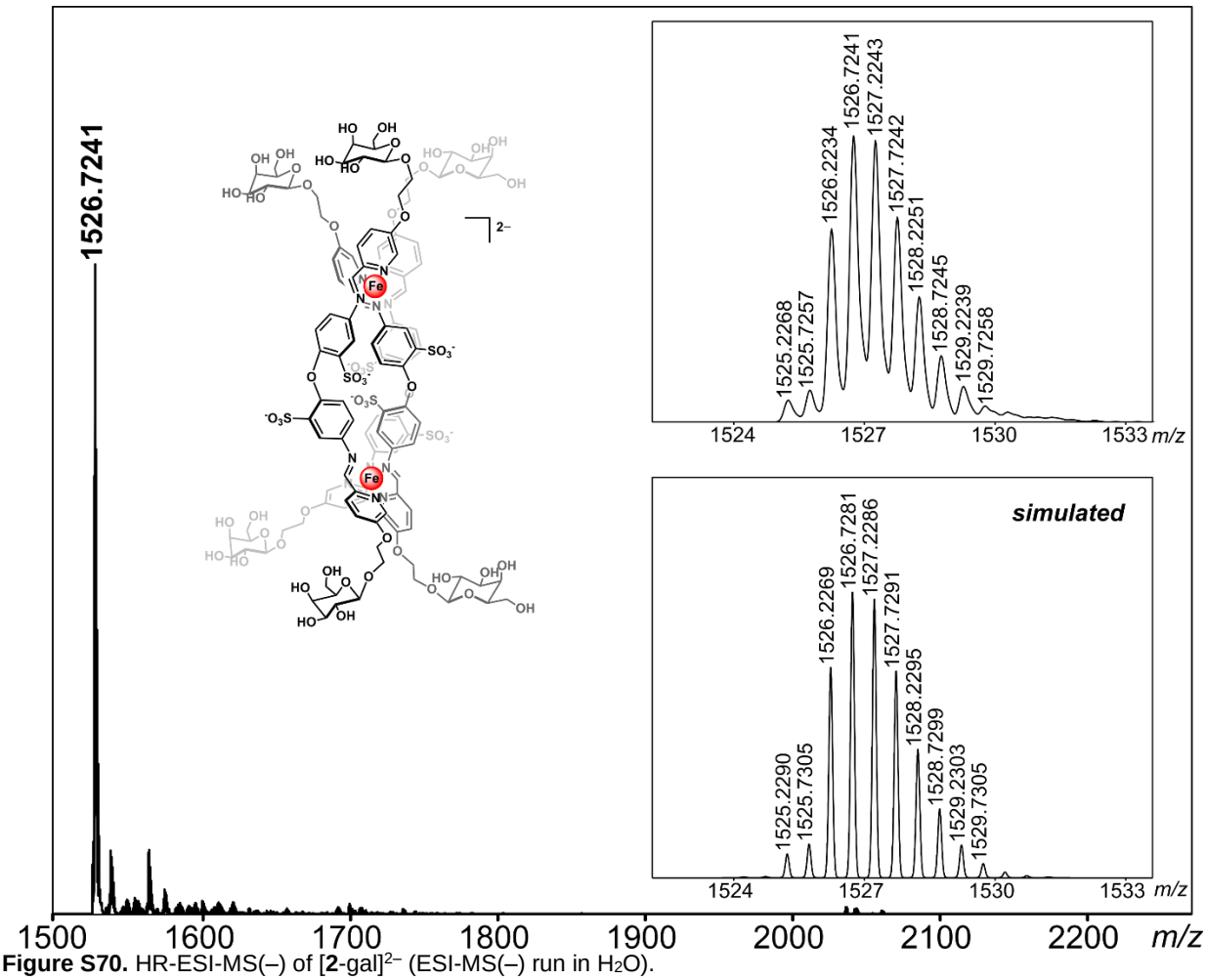

Figure S70. HR-ESI-MS(–) of [**2**-gal]$^{2-}$ (ESI-MS(–) run in H_2O).

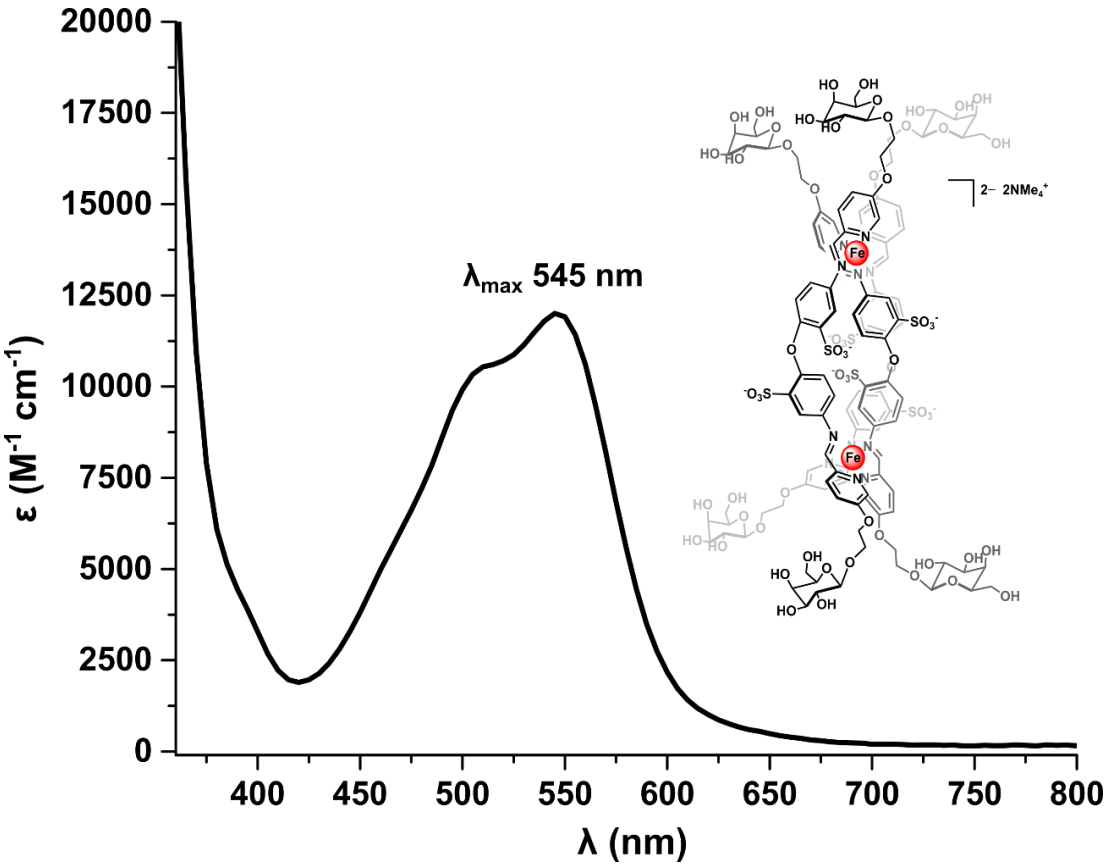

Figure S71. UV-vis spectrum of $[NMe_4]_2$[**2**-gal] (H_2O, 50 μM).

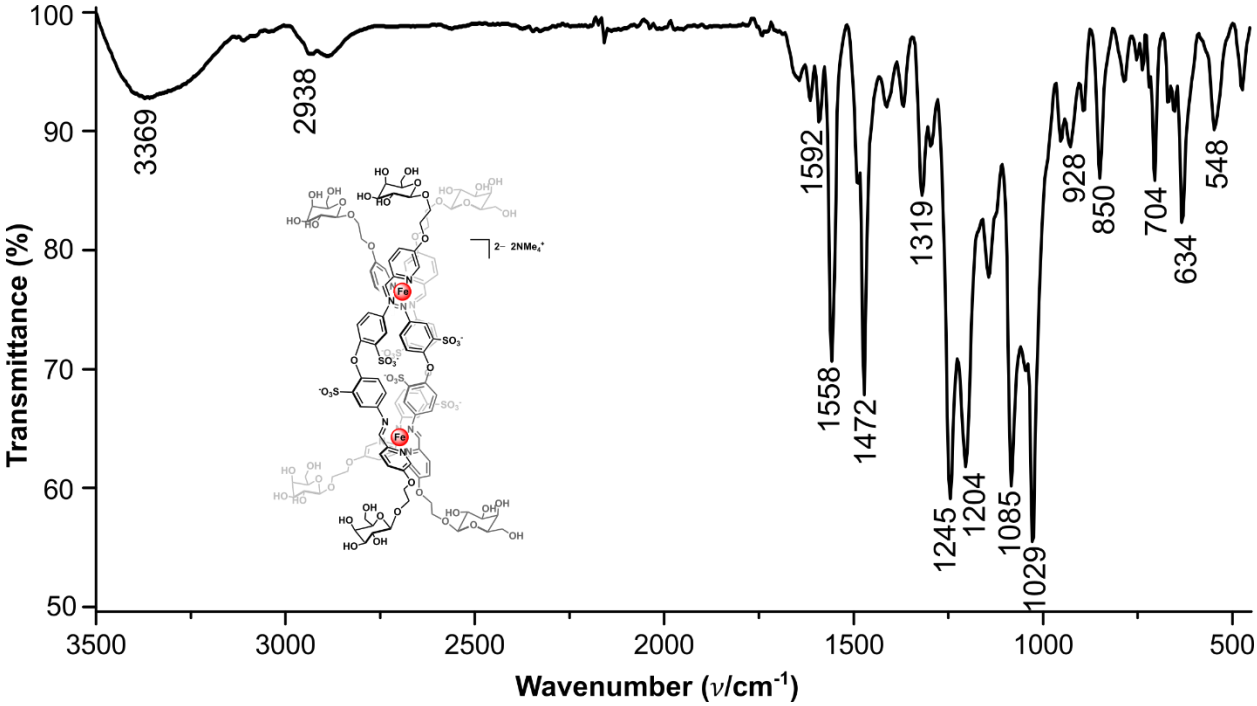

Figure S72. ATR-IR spectrum of $[NMe_4]_2$[**2**-gal].

S2.3.11. [3-gal][SO_4]

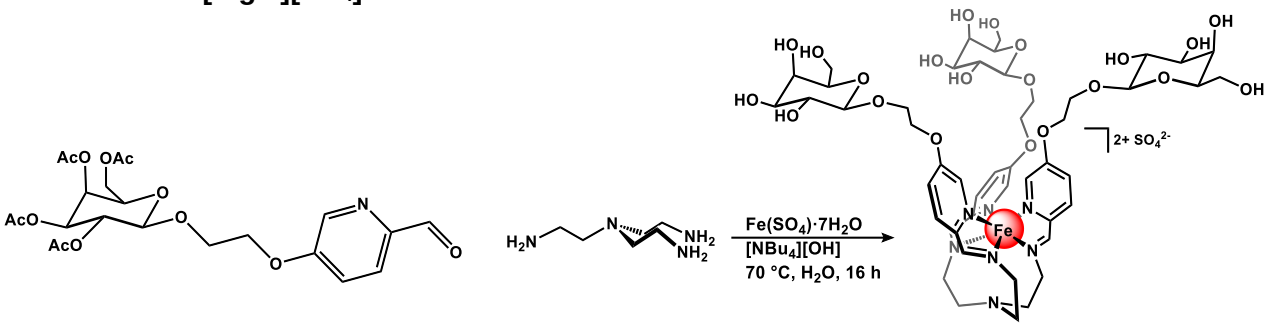

To an 8 mL reaction tube was added 5-((OAc)$_4$-β-D-galactoseEtO)-2-picolinaldehyde (51 mg, 0.10 mmol, 3.0 equiv), and [NBu_4][OH] (aq, 55%, 0.19 mL, 0.41 mmol, 12 equiv) followed by degassed H_2O (0.8 mL). The solution was allowed to stir under N_2 at 70 °C for 45 min, at which point tris(2-aminoethyl)amine (5 µL, 0.03 mmol, 1 equiv) and $Fe(SO_4)_2$•$7H_2O$ (9 mg, 0.03 mmol, 1 equiv) were added. The dark red solution was then sparged with N_2 for an additional 15 min. The reaction mixture was allowed to stir at 70 °C for 16 h, at which point the solution was allowed to cool to ambient temperature and filtered through a piece of glass microfiber filter paper. To the filtrate was added ^{i}PrOH (20 mL), resulting in the precipitation of magenta solids. The mixture was centrifuged (1975 x g, 10 min), and the pale pink supernatant was discarded. The resulting dark pink solids were suspended in Et_2O (5 mL), isolated by filtration, washed with ^{i}PrOH (2 mL) and Et_2O (2 mL), and dried under reduced pressure to afford the product as a dark magenta powder (yield: 30 mg, 0.024 mmol, 72%). ^{1}H NMR (400 MHz, 25 °C, D_2O) δ: 9.02 (s, 3H, *H*C=N), 8.19 (d, 3H, *J* = 8.7 Hz, py-*H*-3), 7.69 (d, 3H, *J* = 8.7 Hz, py-*H*-4), 6.76 (s, 3H, py-*H*-6), 4.39 (d, 3H, gal-*H*-1), 4.23 (m, 6H, –C*H*$_2$–), 4.17 (m, 3H, gal-*H*-6$_a$), 3.96 (m, 3H, gal-*H*-6$_b$), 3.88 (m, 3H, gal-*H*-4), 3.70–3.57 (m, 12H, gal-*H*-5, gal-*H*-3, –C*H*$_2$– signals overlapping), 3.53 (d, 3H, *J* = 10.3 Hz, tren –C*H*$_2$–), 3.43 (dd, 3H, *J* = 9.7, 8.1 Hz, gal-*H*-2), 3.37 (d, 3H, *J* = 13.1 Hz, tren –C*H*$_2$–), 3.17 (t, 3H, *J* = 10.9 Hz, tren –C*H*$_2$–), 3.03 (t, 3H, *J* = 10.3 Hz, tren –C*H*$_2$–) ppm. ^{13}C{^{1}H} NMR (100 MHz, 25 °C, D_2O) δ: 169.7 (*C*=N), 157.8, 150.5, 144.0, 129.1, 121.0, 102.9, 75.2, 72.7, 70.6, 68.5, 68.1, 67.8, 61.0, 58.3, 53.6 ppm. ESI-MS(+) observed for [M]$^{2+}$: 567.6950 (calc'd, 567.6944) *m/z*. UV-vis [ε] (H_2O, 50 µM): λ_{max} 375 [6,100 $M^{-1}cm^{-1}$], 495 [6,300 $M^{-1}cm^{-1}$], 540 [8,100 $M^{-1}cm^{-1}$] nm. ATR-IR (v): 3264 (OH), 2925, 2874, 1595 (C=N), 1562 (C=N), 1450, 1379, 1312, 1234, 1047, 921, 613 cm^{-1}.

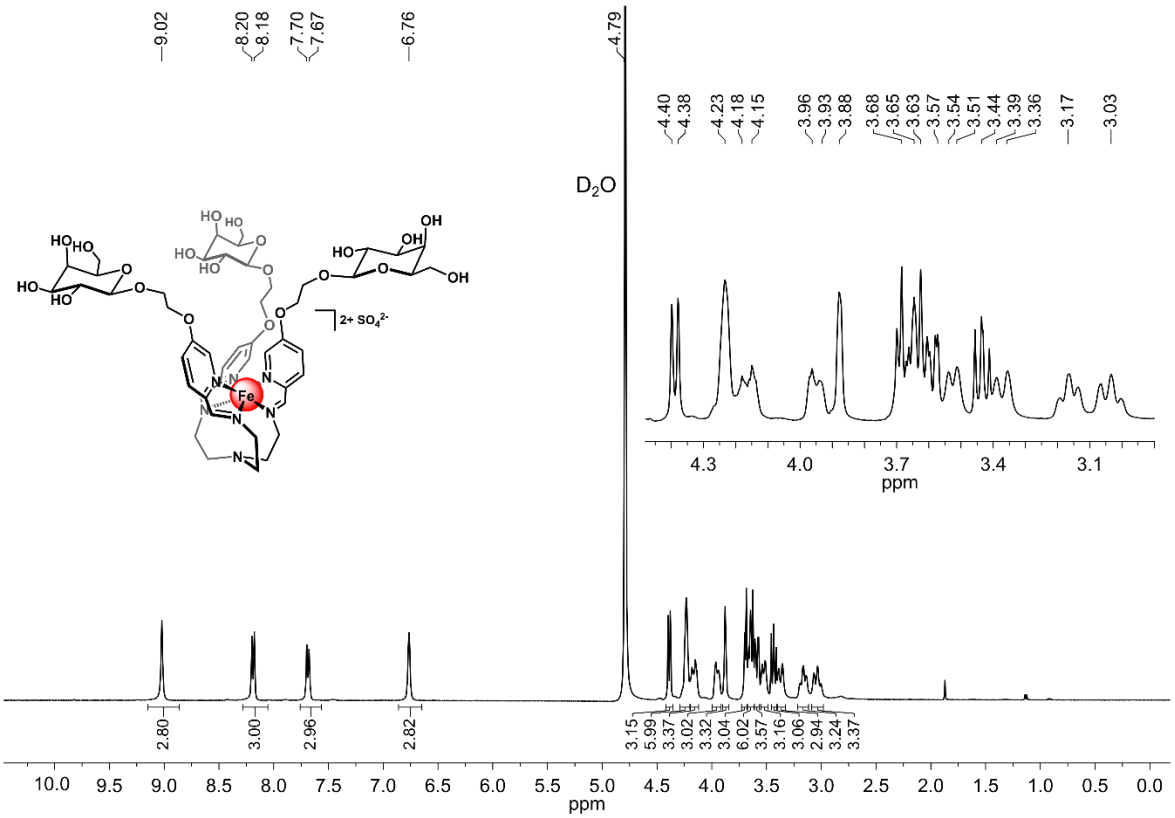

Figure S73. ^{1}H NMR spectrum of [**3**-gal][SO_4] (D_2O, 400 MHz, 25 °C).

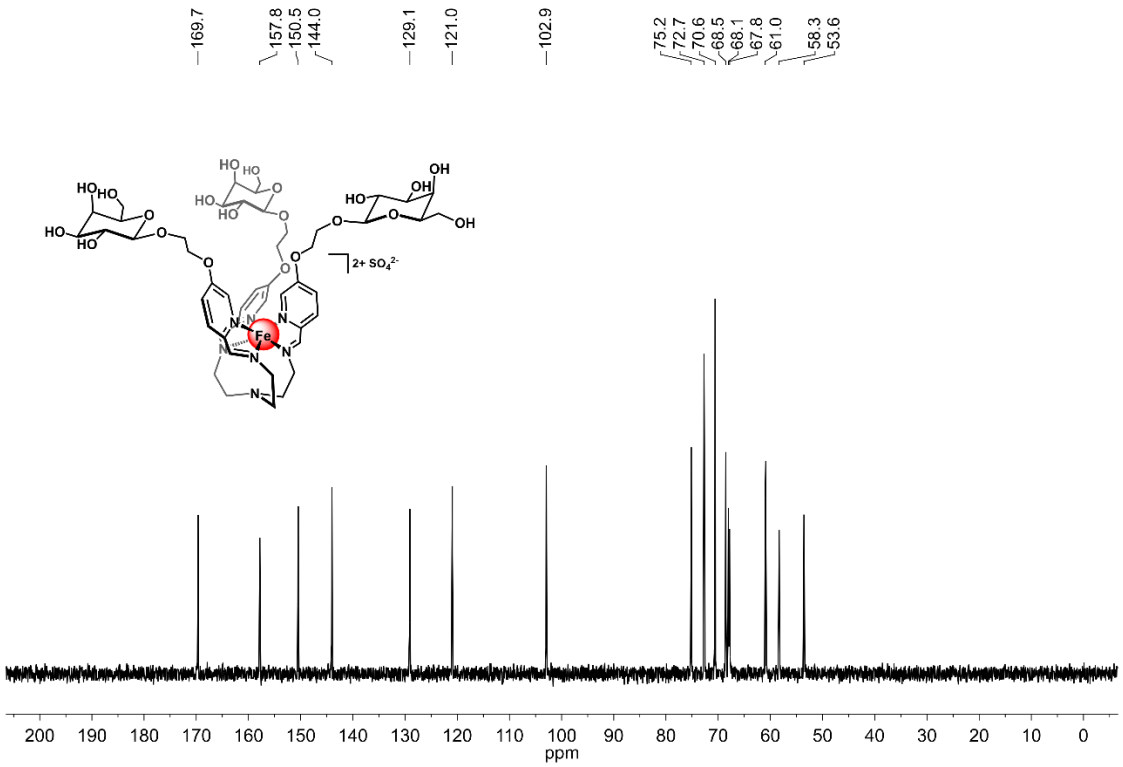

Figure S74. $^{13}C\{^{1}H\}$ NMR spectrum of [**3**-gal][SO_4] (D_2O, 100 MHz, 25 °C).

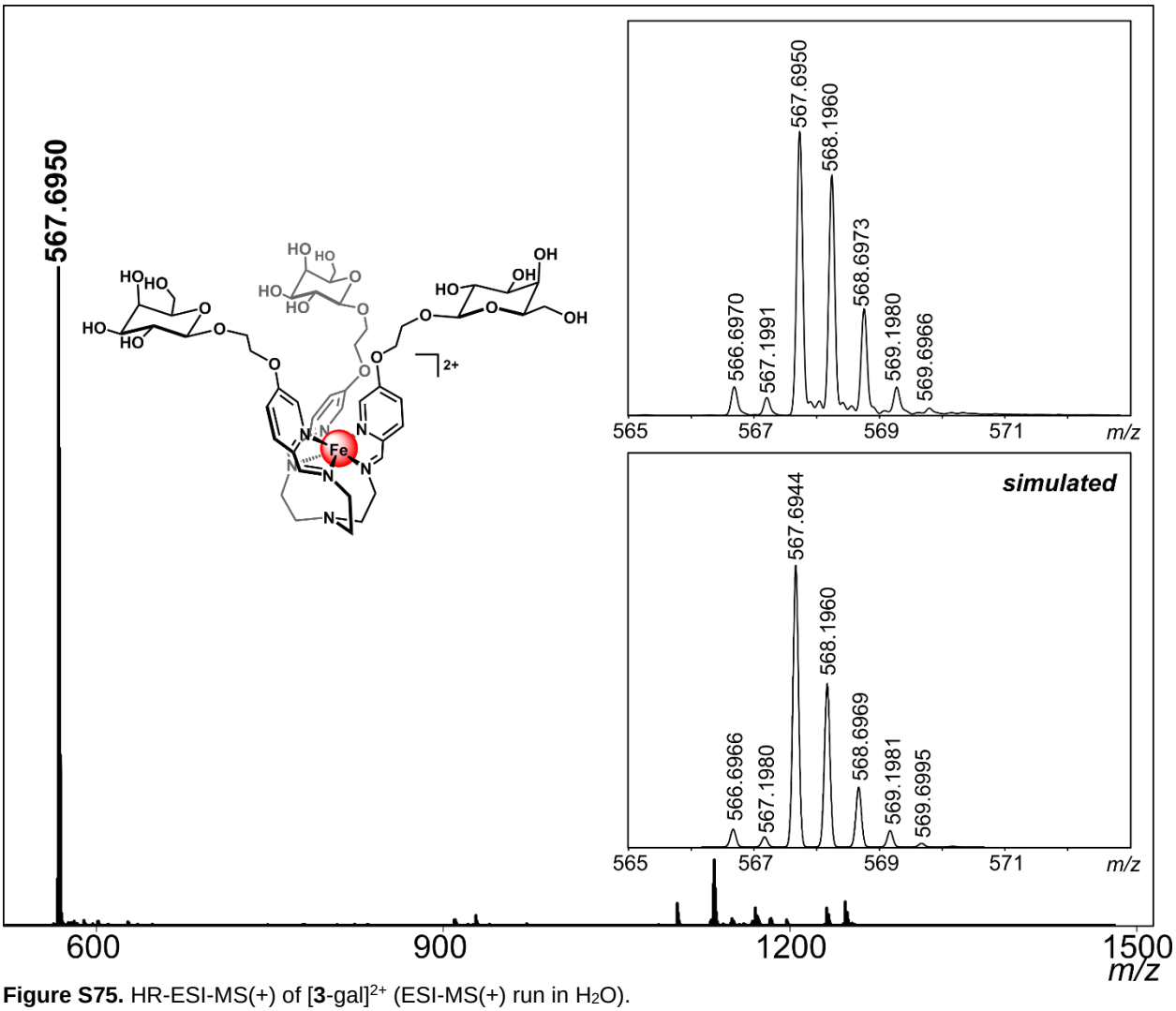

Figure S75. HR-ESI-MS(+) of [**3**-gal]$^{2+}$ (ESI-MS(+) run in H_2O).

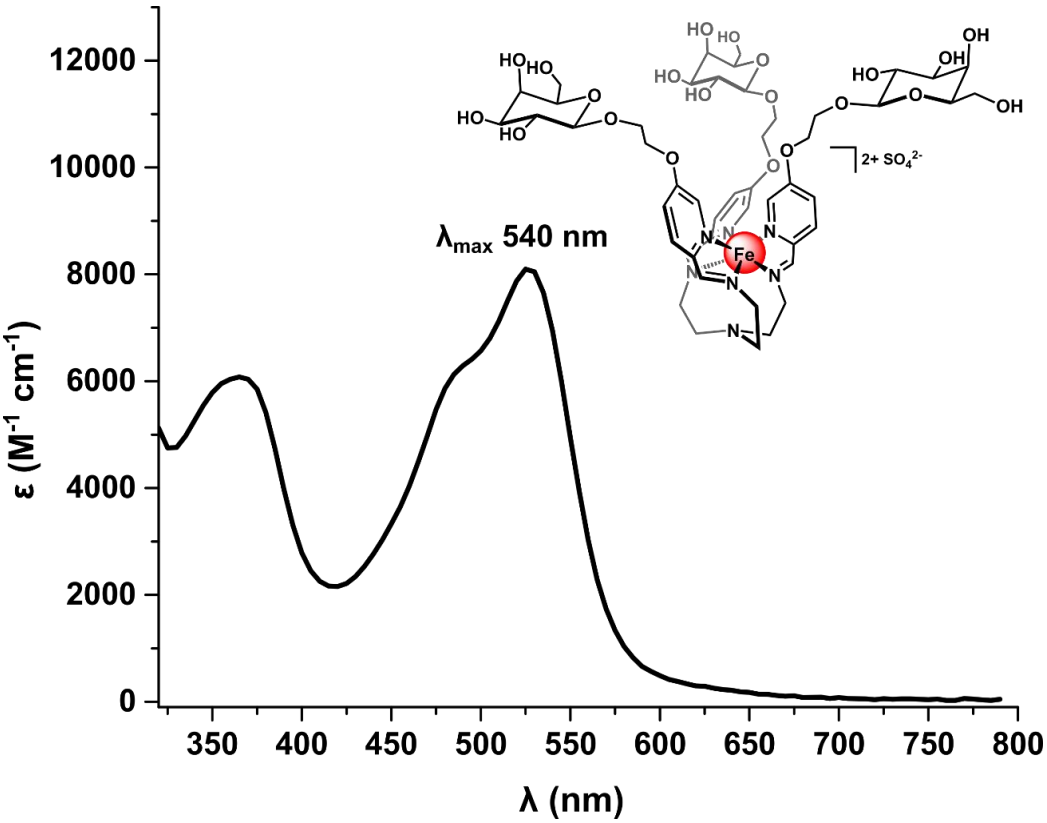

Figure S76. UV-vis spectrum of [**3**-gal][SO_4] (H_2O, 50 μM).

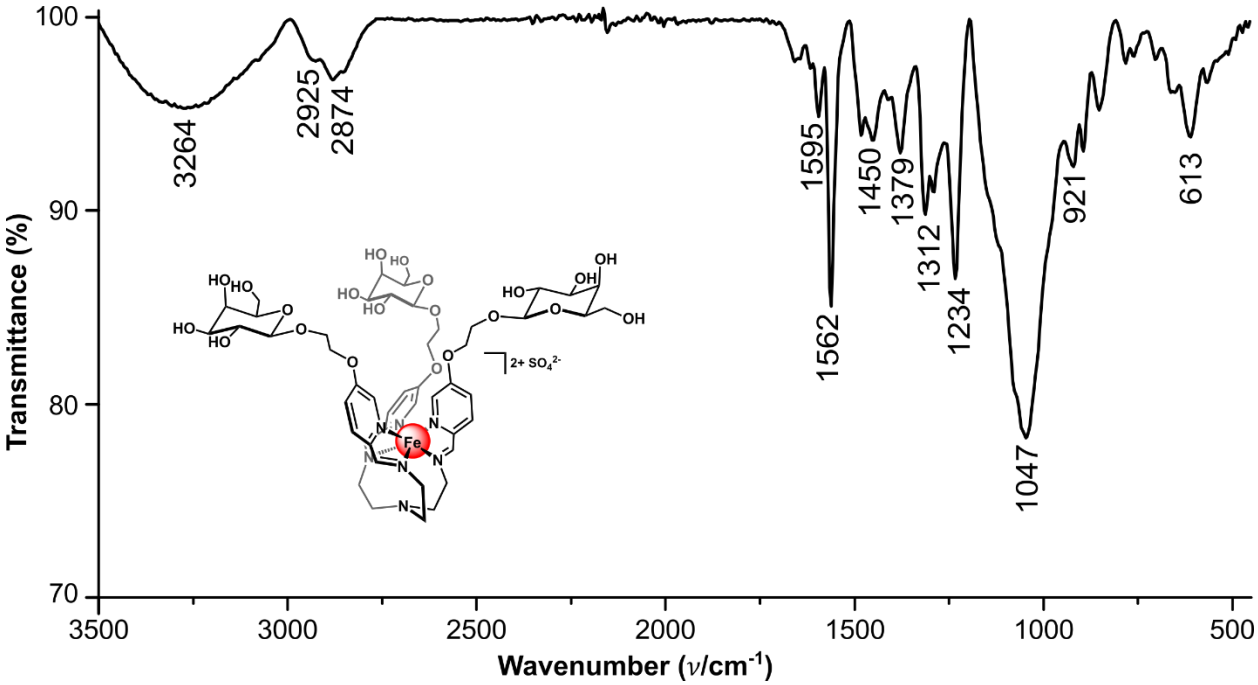

Figure S77. ATR-IR spectrum of [**3**-gal][SO_4].

S2.3.12. [NMe_4]$_4$[1-mal]

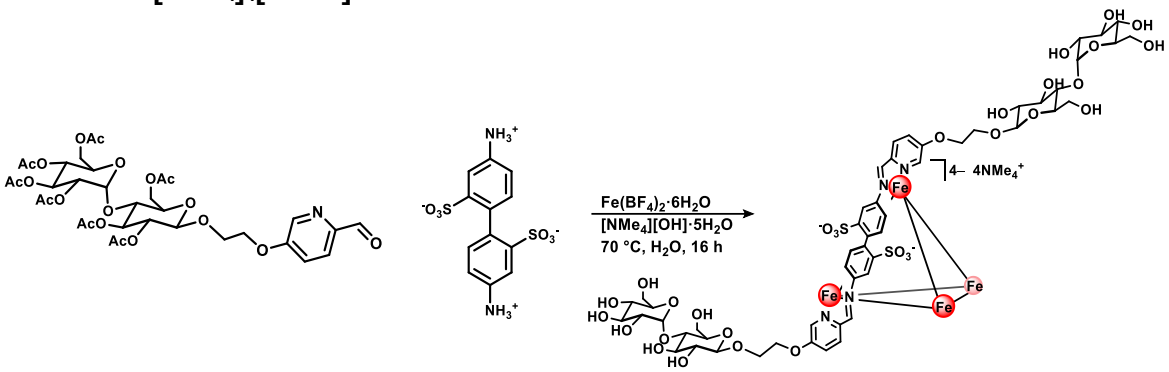

To an 8 mL reaction tube was added 5-((OAc)$_7$-β-D-maltoseEtO)-2-picolinaldehyde (66 mg, 0.084 mmol, 3.6 equiv) and [NMe_4][OH]•5H_2O (114 mg, 0.629 mmol, 26.0 equiv) as solids. Degassed H_2O (2 mL) was added, and the mixture was allowed to stir under an atmosphere of N_2 for 45 min at 70 °C, during which time it became homogeneous. To the solution was added 2,2'-benzidinedisulfonic acid (70 wt% balance H_2O, 12 mg, 0.024 mmol, 1.0 equiv) and $Fe(BF_4)_2$•6H_2O (8 mg, 0.02 mmol, 1 equiv) as solids, which resulted in an immediate color change to dark magenta. The reaction mixture was sparged with N_2 for 15 min and then allowed to stir at 70 °C for 16 h. The mixture was then allowed to cool to ambient temperature and the magenta solution was filtered through a piece of glass microfiber filter paper. To the filtrate was added ^{i}PrOH (15 mL), resulting in the precipitation of magenta solids. The mixture was centrifuged (1975 x g, 10 min), and the colorless supernatant was discarded. The resulting dark pink solids were suspended in Et_2O (5 mL) and isolated by filtration. The solids were washed with Et_2O (10 mL) and dried under reduced pressure to afford the product as a dark magenta powder. The crude solids were dissolved in H_2O (4 mL) and filtered through a piece of glass microfiber filter paper into the sample reservoir of a Pall Microsep® (3K Omega membrane) centrifuge device. The device was centrifuged at 7500 x g for 75 min, at which point the filtrate in the collection tube was removed and fresh H_2O (4 mL) was added to the sample reservoir. The device was centrifuged again at 7500 x g for 75 min, and this process was repeated for a total of three centrifuge cycles. After the third cycle, the solution in the sample reservoir was removed and lyophilized overnight to afford the pure product as a magenta powder (yield: 21 mg, 2.6 μmol, 64% based on theoretical yield of 4.0 μmol with 2,2'-benzidinedisulfonic acid as the limiting reagent (4:12:6 ratio of Fe:py:benzidine)). ^{1}H NMR (400 MHz, 25 °C, D_2O) δ: 9.06 (s, 12H, *H*C=N), 8.57 (d, 12H, *J* = 7.1 Hz, py-*H*-3), 7.86 (d, 12H, *J* = 7.5 Hz, py-*H*-4), 7.13 (s, 12H, py-*H*-6), 7.03 (br s, 12H, Ar-*H* 6,6'-benzidine), 6.42 (s, 12H, Ar-*H* 3,3'-benzidine), 5.74 (br s, 12H, Ar-*H* 5,5'-benzidine), 5.35 (br s, 12H, *J* = 9.6, 3.0 Hz, mal-*H*-1'), 4.46 (d, 12H, *J* = 6.6 Hz, mal-*H*-1), 4.35 (m, 24H, –CH_2–), 4.18 (m, 12H, mal-*H*-6$_a$), 3.98 (m, 12H, mal-*H*-6$_b$), 3.86–3.78 (m, 36H, mal-*H*-6$_{a',b'}$, mal-*H*-3 signals overlapping), 3.71–3.60 (m, 48H, mal-*H*-3', mal-*H*-5', –CH_2– signals overlapping), 3.58–3.50 (m, 36H, mal-*H*-5, mal-*H*-4', mal-*H*-2', signals overlapping), 3.35 (t, 12H, *J* = 7.3 Hz, mal-*H*-4), 3.23 (t, 6H, *J* = 8.2 Hz, mal-*H*-2), 3.11 (s, 48H, N(CH_3)$_4$) ppm. ^{13}C{^{1}H} NMR (100 MHz, 25 °C, D_2O) δ: 174.2 (*C*=N), 159.1, 150.5, 146.5, 142.8, 135.7, 132.9, 131.8, 121.9, 121.0, 102.2, 99.4, 76.6, 76.4, 76.1, 74.6, 72.8, 72.7, 71.6, 69.3, 68.3, 67.8, 60.7, 60.5, 55.2 (N(*C*H$_3$)$_4$) ppm. ESI-MS(–) observed for [M]$^{4–}$: 1989.3989 (calc'd, 1989.3952) *m/z*. UV-vis [ε] (H_2O, 50 μM): λ_{max} 505 [23,000 M^{-1}cm^{-1}], 545 [26,000 M^{-1}cm^{-1}] nm. ATR-IR (ν): 3329 (OH), 2932, 1562 (C=N), 1469, 1316, 1234, 1148, 1029, 924, 626, 555 cm^{-1}.

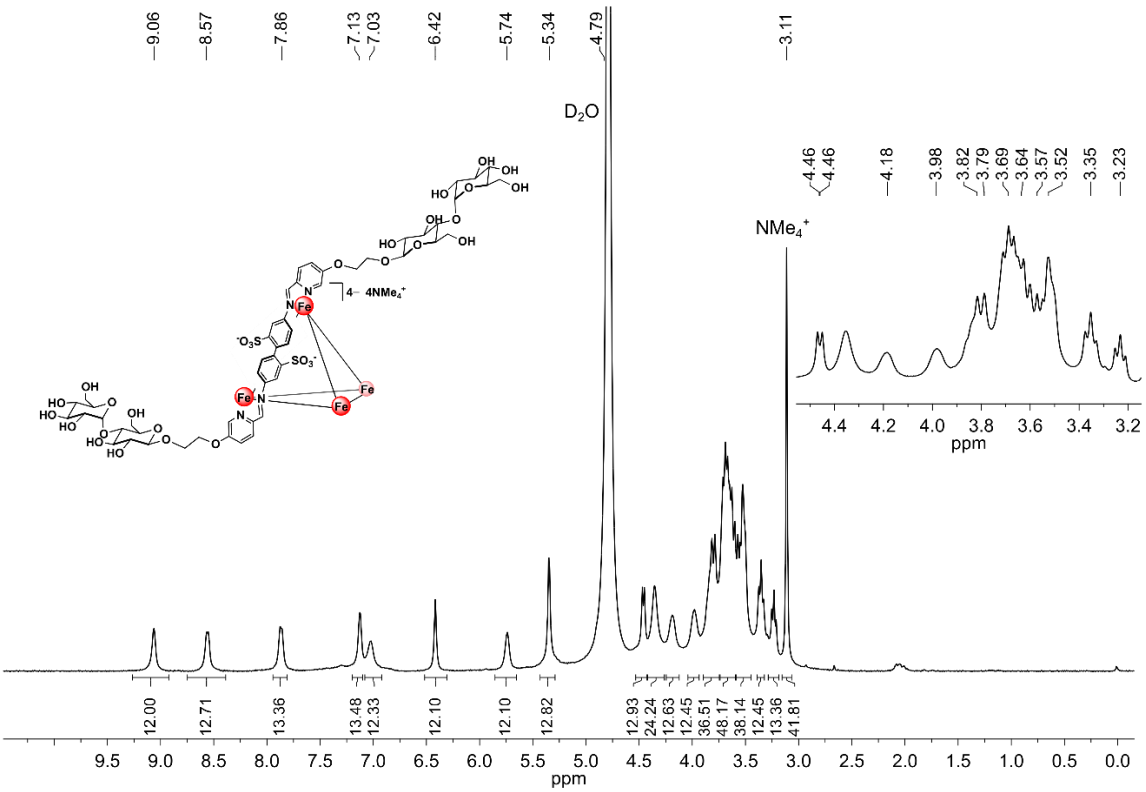

Figure S78. ^{1}H NMR spectrum of $[NMe_4]_4$[**1**-mal] (D_2O, 400 MHz, 25 °C).

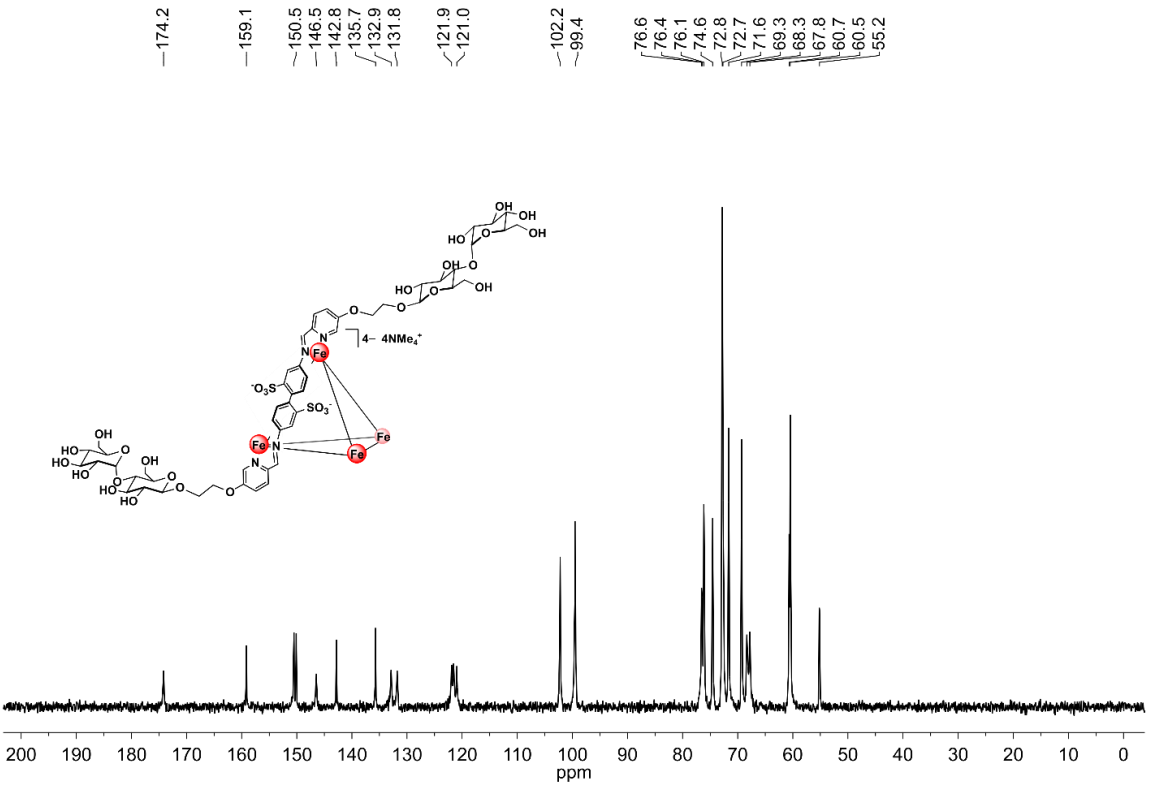

Figure S79. ^{13}C{^{1}H} NMR spectrum of $[NMe_4]_4$[**1**-mal] (D_2O, 100 MHz, 25 °C).

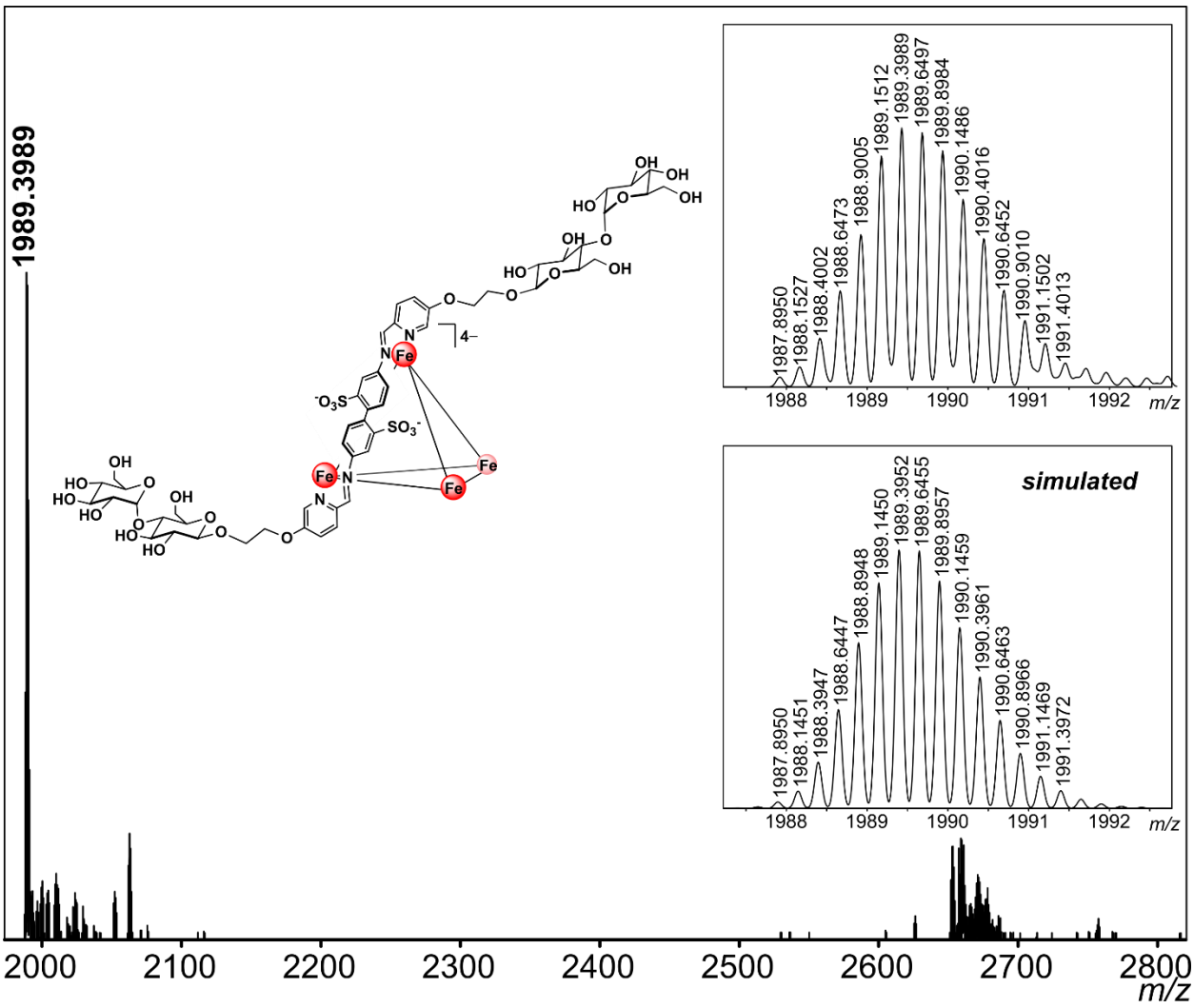

Figure S80. HR-ESI-MS(–) of [**1**-mal]$^{4-}$ (ESI-MS(–) run in H_2O).

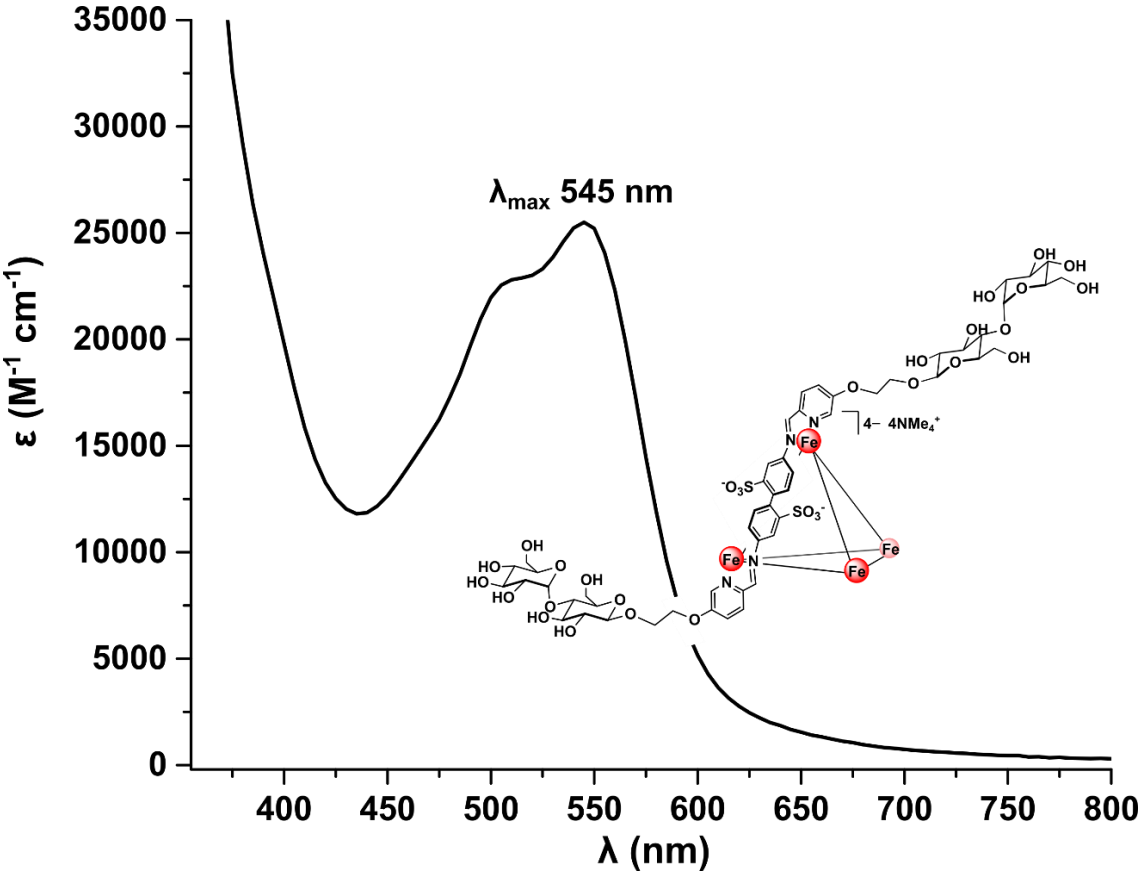

Figure S81. UV-vis spectrum of $[NMe_4]_4$[**1**-mal] (H_2O, 50 μM).

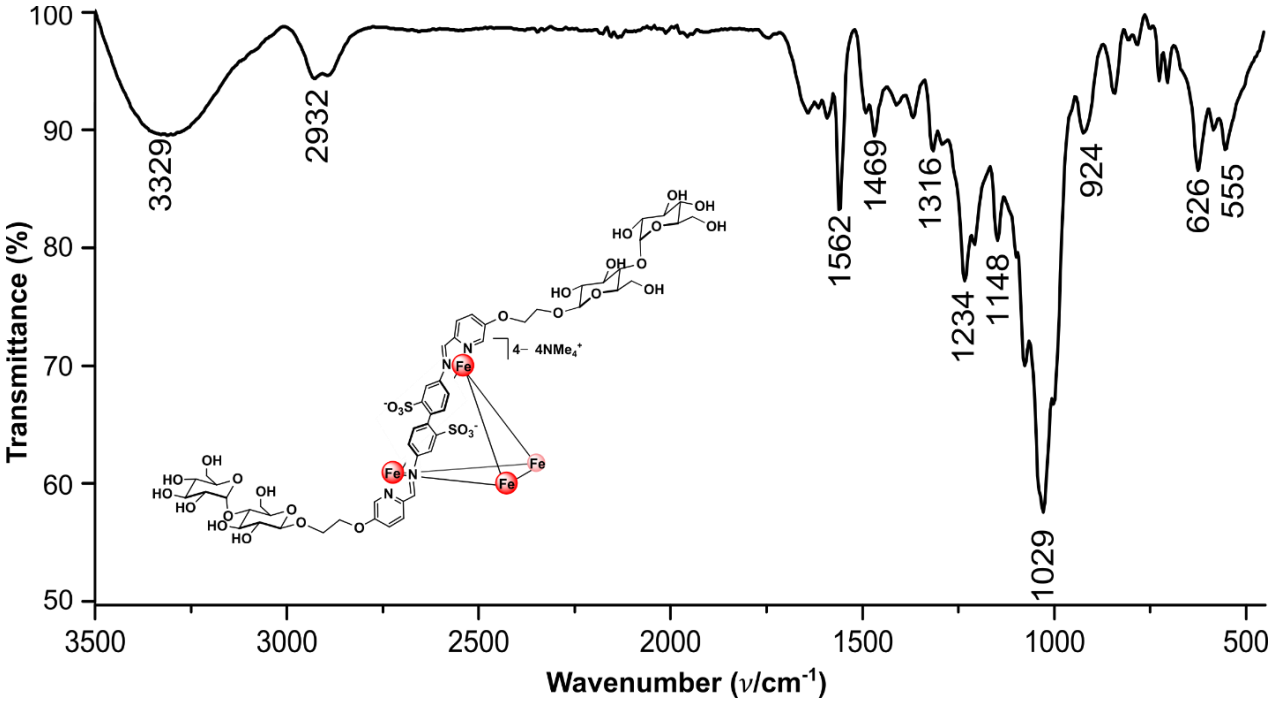

Figure S82. ATR-IR spectrum of $[NMe_4]_4$[**1**-mal].

S2.3.13. $[NMe_4]_2$[2-mal]

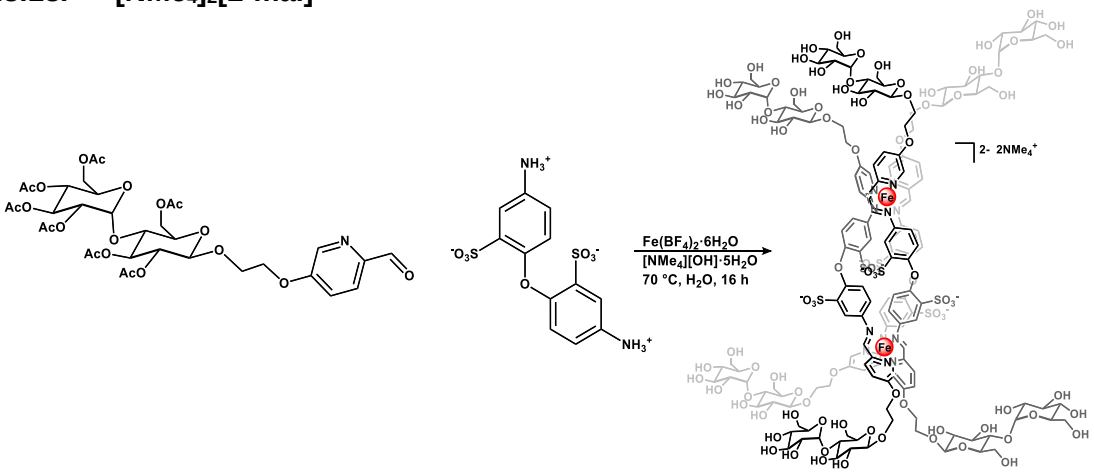

To an 8 mL reaction tube was added 5-((OAc)$_7$-β-D-maltoseEtO)-2-picolinaldehyde (68 mg, 0.057 mmol, 3.0 equiv), and [NMe$_4$][OH]•5H$_2$O (115 mg, 0.638 mmol, 22.0 equiv) as solids. Degassed H$_2$O (2 mL) was added, and the mixture was allowed to stir under an atmosphere of N$_2$ for 45 min at 70 °C, during which time it became homogeneous. To the reaction tube was added 4,4′-diaminodiphenyl ether-2,2′-disulfonic acid (80 wt% balance H$_2$O, 13 mg, 0.029 mmol, 1.0 equiv) and Fe(BF$_4$)$_2$•6H$_2$O (15 mg, 0.044 mmol, 1.6 equiv) as solids, which resulted in an immediate color change to dark pink. The solution was sparged with N$_2$ for 15 min and then allowed to stir at 70 °C for 16 h, at which point the solution was allowed to cool to ambient temperature. The dark pink solution was filtered through a piece of glass microfiber filter paper, and to the filtrate was added ^{i}PrOH (15 mL), resulting in the precipitation of magenta solids. The suspension was centrifuged (1975 x g, 10 min), and the pale pink supernatant was discarded. The resulting solids were suspended in Et$_2$O (5 mL), isolated by filtration, washed with Et$_2$O (10 mL) and dried under reduced pressure to afford the crude product as a magenta powder. The solids were dissolved in H$_2$O (4 mL) and filtered through a piece of glass microfiber filter paper into the sample reservoir of a Pall Microsep® (3K Omega membrane) centrifuge device. The device was centrifuged at 7500 x g for 75 min, at which point the filtrate in the collection tube was removed and fresh H$_2$O (4 mL) was added to the sample reservoir. The device was centrifuged again at 7500 x g for 75 min, and this process was repeated for a total of three centrifuge cycles. After the third cycle, the solution in the sample reservoir was removed and lyophilized overnight to afford the pure product as a magenta powder (yield: 18 mg, 4.3 μmol, 44% based on theoretical yield of 9.7 μmol with 4,4′-diaminodiphenyl ether-2,2′-disulfonic acid as the limiting reagent (2:6:3 ratio of Fe:py:benzidine)). ^{1}H NMR (400 MHz, 25 °C, D$_2$O) δ: 9.48 (s, 6H, *H*C=N), 8.74 (d, 6H, *J* = 7.8 Hz, py-*H*-3), 7.91 (d, 6H, *J* = 7.8 Hz, py-*H*-4), 7.57 (s, 6H, py-*H*-6), 6.55 (d, 6H, *J* = 6.6 Hz, 6,6'-benzidine), 6.42 (s, 6H, 3,3'-benzidine), 5.61 (d, 6H, *J* = 6.6 Hz, 5,5'-benzidine), 5.35 (dd, 6H, *J* = 9.6, 3.0 Hz, mal-*H*-1'), 4.48 (t, 6H, *J* = 8.2 Hz, mal-*H*-1), 4.40 (m, 12H, –C*H*$_2$–), 4.21 (m, 6H, mal-*H*-6$_a$), 4.04 (m, 6H, mal-*H*-6$_b$), 3.83 (t, 6H, *J* = 10.9 Hz, mal-*H*-6$_a$'), 3.73–3.53 (m, 18H, mal-*H*-6$_b$', mal-*H*-3, mal-*H*-3' signals overlapping), 3.65–3.61 (m, 18H, mal-*H*-5', –C*H*$_2$– signals overlapping), 3.57–3.53 (m, 18H, mal-*H*-5, mal-*H*-4', mal-*H*-2', signals overlapping), 3.38 (t, 6H, *J* = 9.0 Hz, mal-*H*-4), 3.25 (t, 6H, *J* = 8.7 Hz, mal-*H*-2), 3.13 (s, 24H, N(C*H*$_3$)$_4$) ppm. ^{13}C{^{1}H} NMR (100 MHz, 25 °C, D$_2$O) δ: 173.1 (*C*=N), 161.2, 155.1, 149.5, 147.1, 134.7, 133.9, 126.0, 122.8, 121.6, 102.2, 99.7, 76.7, 76.1, 74.6, 72.8, 72.6, 71.6, 69.2, 68.6, 67.8, 60.7, 60.5, 60.3, 55.2 (N(*C*H$_3$)$_4$) ppm. ESI-MS(–) observed for [M]$^{2-}$: 2013.3865 (calc'd, 2013.3876) *m/z*. UV-vis [ε] (H$_2$O, 50 μM): λ$_{max}$ 505 [9,000 M^{-1}cm^{-1}], 545 [11,000 M^{-1}cm^{-1}] nm. ATR-IR (ν): 3351 (OH), 2923, 2895, 1558 (C=N), 1472, 1319, 1245, 1204, 1144, 1081, 1025, 928, 850, 704, 630, 548 cm^{-1}.

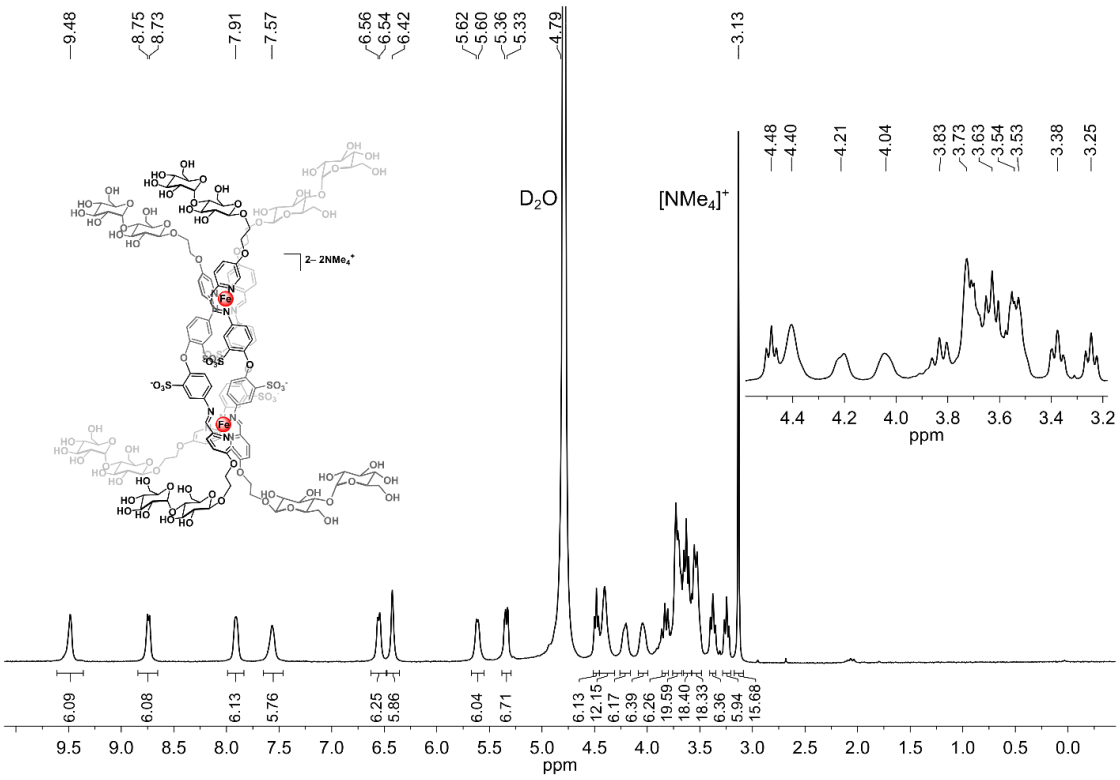

Figure S83. ^{1}H NMR spectrum of $[NMe_4]_2$[**2**-mal] (D_2O, 400 MHz, 25 °C).

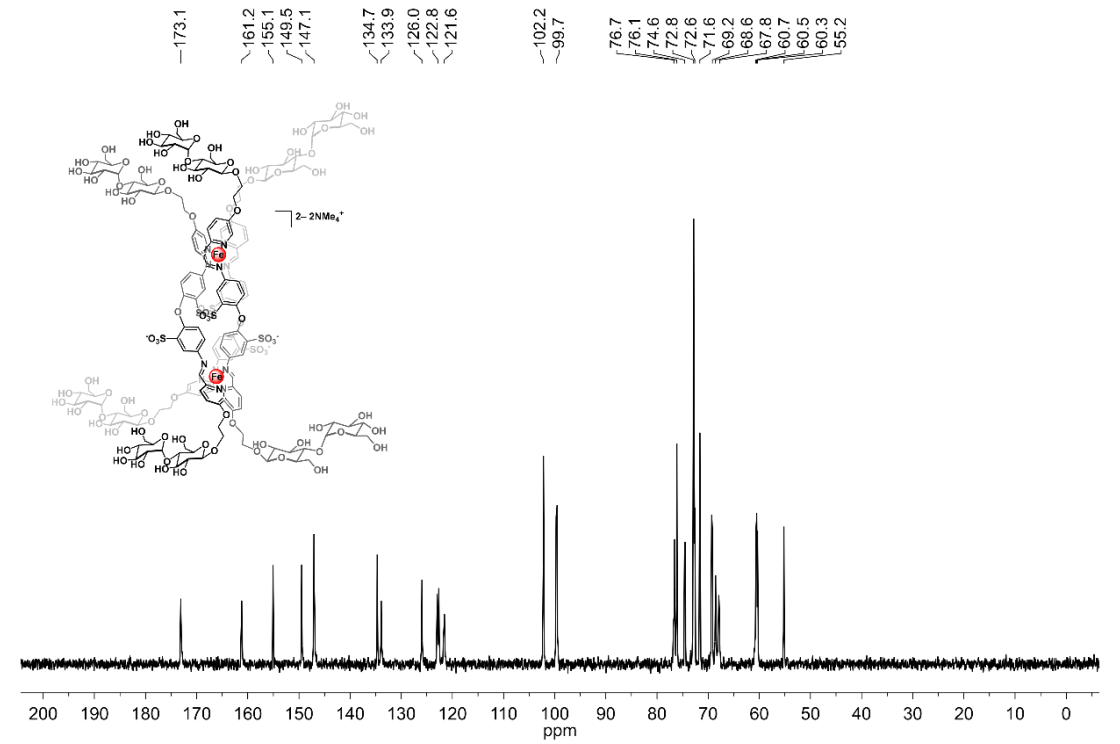

Figure S84. ^{13}C{^{1}H} NMR spectrum of $[NMe_4]_2$[**2**-mal] (D_2O, 100 MHz, 25 °C).

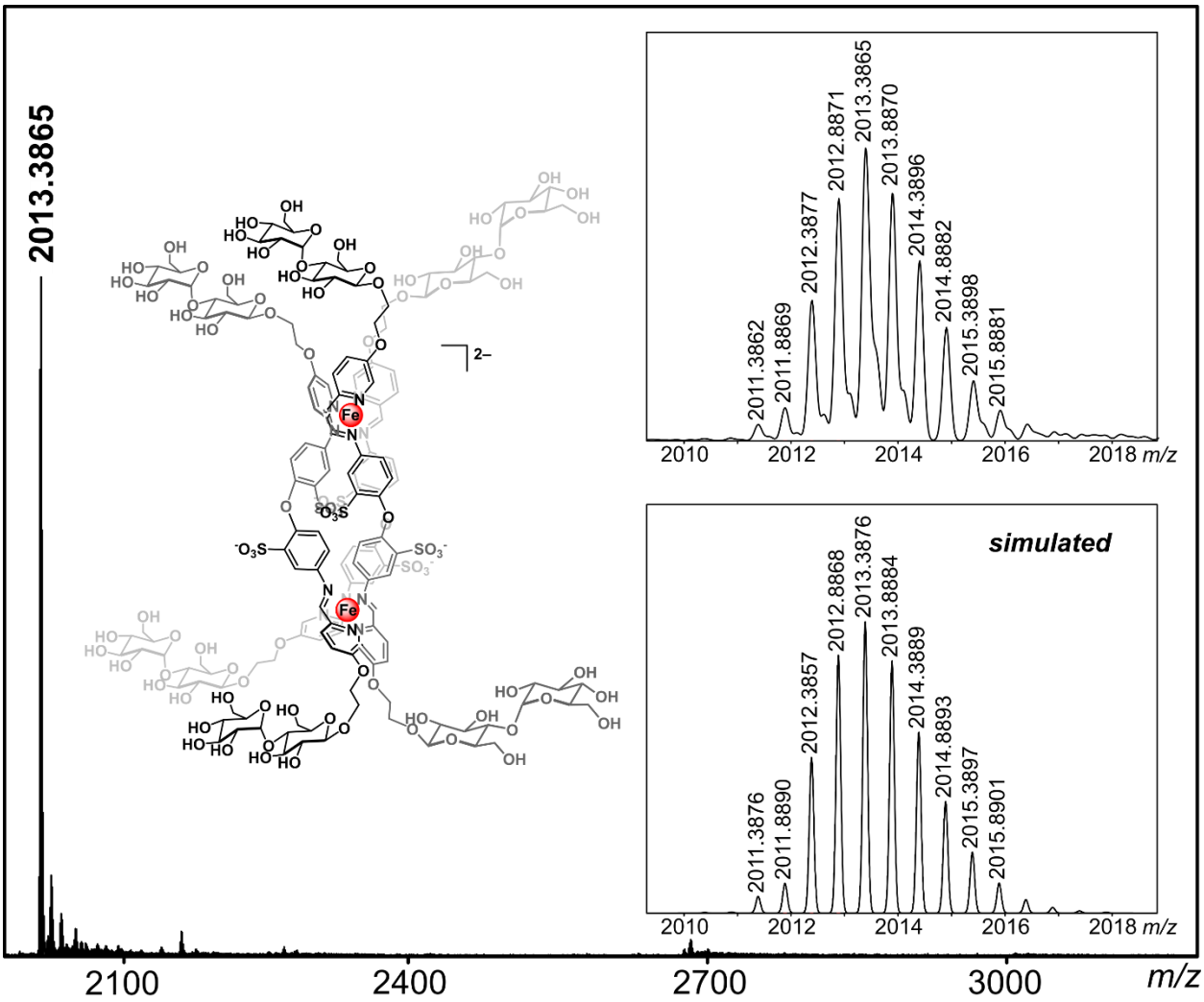

Figure S85. HR-ESI-MS(–) of [**2**-mal]$^{2-}$ (ESI-MS(–) run in H_2O).

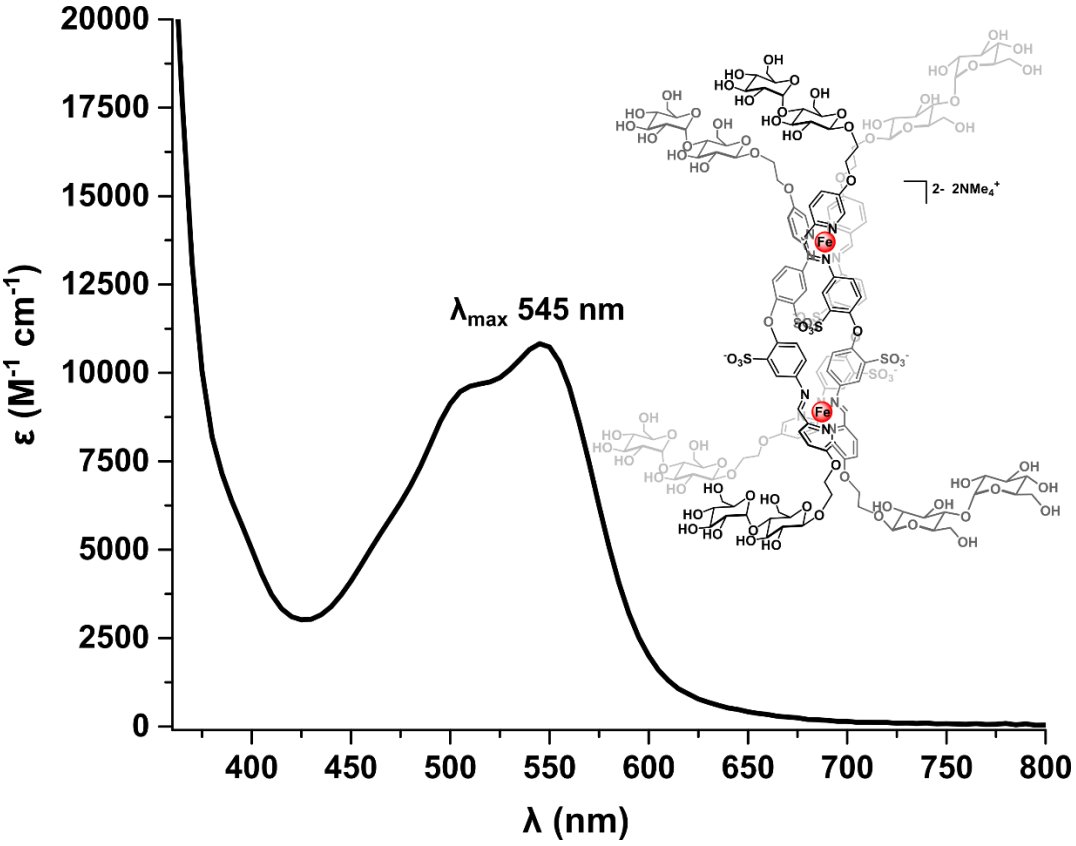

Figure S86. UV-vis spectrum of $[NMe_4]_2$[**2**-mal] (H_2O, 50 μM).

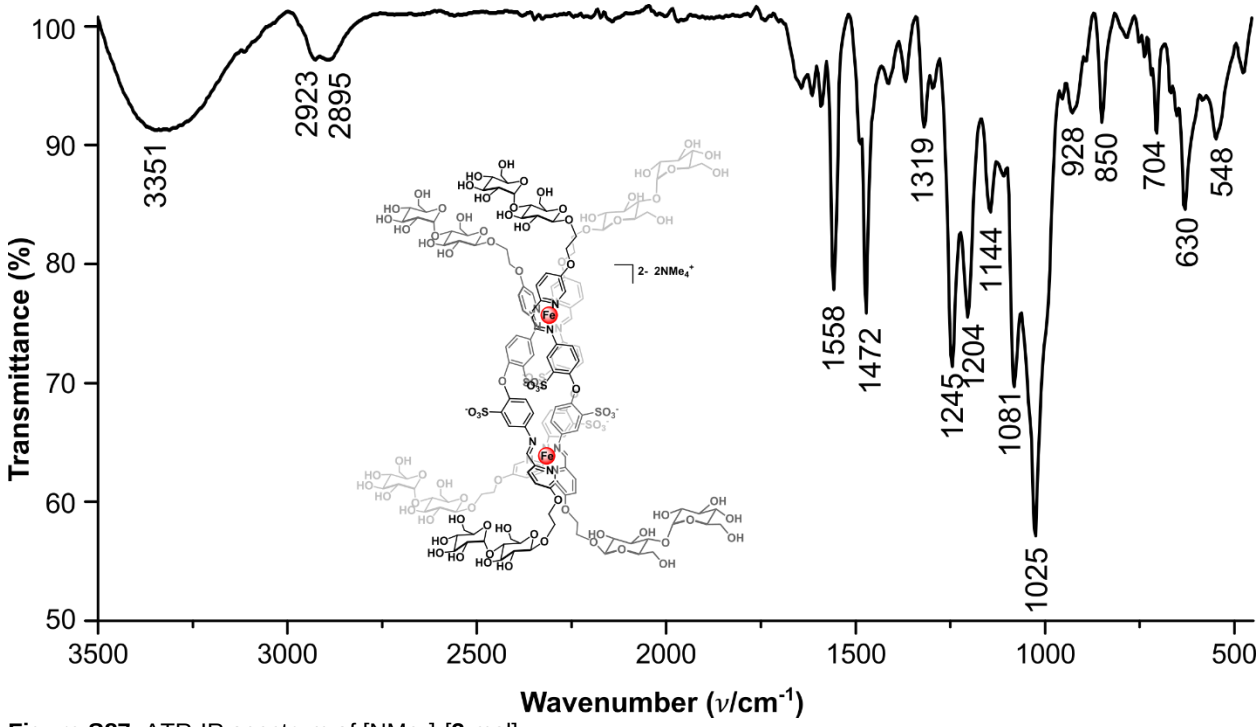

Figure S87. ATR-IR spectrum of $[NMe_4]_2$[**2**-mal].

S2.3.14. [3-mal][SO_4]

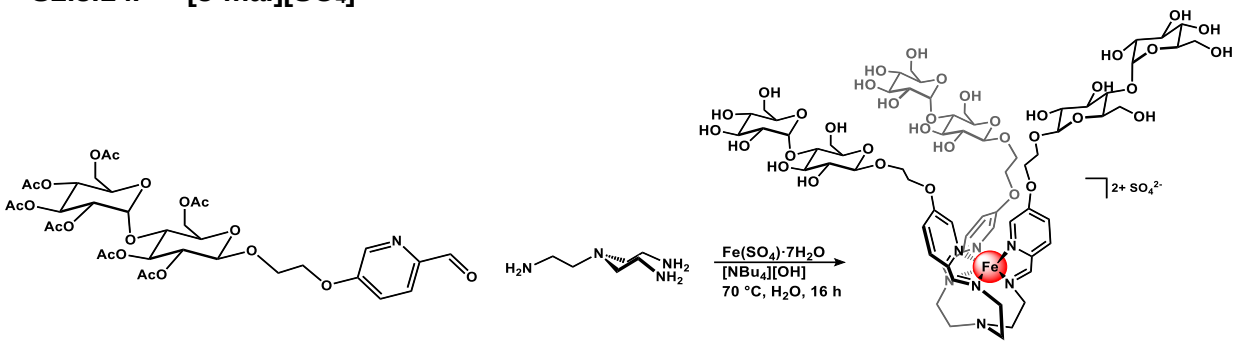

To an 8 mL reaction tube was added 5-((OAc)$_7$-β-D-maltoseEtO)-2-picolinaldehyde (64 mg, 0.081 mmol, 3.0 equiv), and [NBu_4][OH] (aq, 55%, 0.27 mL, 0.57 mmol, 21 equiv) followed by degassed H_2O (0.8 mL). The solution was allowed to stir under N_2 at 70 °C for 45 min, at which point tris(2-aminoethyl)amine (4 µL, 0.03 mmol, 1 equiv) and $Fe(SO_4)_2$•$7H_2O$ (8 mg, 0.03 mmol, 1 equiv) were added. The dark pink solution was then sparged with N_2 for an additional 15 min. The reaction mixture was allowed to stir at 70 °C for 16 h, at which point the solution was allowed to cool to ambient temperature and filtered through a piece of glass microfiber filter paper. To the filtrate was added ^{i}PrOH (20 mL), resulting in the precipitation of magenta solids. The mixture was centrifuged (1975 x g, 10 min), and the pale pink supernatant was discarded. The resulting dark pink solids were suspended in Et_2O (5 mL), isolated by filtration, washed with ^{i}PrOH (2 mL) and Et_2O (2 mL), and dried under reduced pressure to afford the product as a dark magenta powder (yield: 32 mg, 0.026 mmol, 75%). ^{1}H NMR (400 MHz, 25 °C, D_2O) δ: 8.93 (s, 3H, *H*C=N), 8.17 (d, 3H, *J* = 7.8 Hz, py-*H*-3), 7.67 (d, 3H, *J* = 7.8 Hz, py-*H*-4), 6.74 (s, 3H, py-*H*-6), 5.35 (3H, d, *J* = 4.2 Hz, mal-*H*-1'), 4.45 (dd, 3H, *J* = 7.7, 3.8 Hz, mal-*H*-1), 4.22 (m, 6H, –C*H*$_2$–), 4.13 (m, 3H, mal-*H*-6$_a$), 3.94 (m, 3H, mal-*H*-6$_b$), 3.83–3.80 (m, 6H, mal-*H*-6$_{a,b}$'), 3.73–3.59 (m, 15H, mal-*H*-3, mal-*H*-3', mal-*H*-5', –C*H*$_2$– signals overlapping), 3.57–3.49 (m, 12H, mal-*H*-5, mal-*H*-4', mal-*H*-2', mal-*H*-4 signals overlapping), 3.37 (t, 6H, *J* = 9.4 Hz, tren –C*H*$_2$–), 3.21 (t, 3H, *J* = 7.2 Hz, mal-*H*-2), 3.15 (t, 3H, *J* = 12.6 Hz, tren –C*H*$_2$–), 3.02 (t, 3H, *J* = 12.6 Hz, tren –C*H*$_2$–) ppm. ^{13}C{^{1}H} NMR (100 MHz, 25 °C, D_2O) δ: 169.6 (*C*=N), 157.8, 150.4, 144.0, 129.0, 120.8, 102.2, 99.6, 76.6, 76.1, 74.6, 74.5, 72.8, 72.7, 71.6, 69.3, 68.0, 67.8, 60.6, 60.5, 58.3, 53.6 ppm. ESI-MS(+) observed for $[M]^{2+}$: 810.7722 (calc'd, 810.7737) *m/z*. UV-vis [ε] (H_2O, 50 µM): λ_{max} 375 [6,000 $M^{-1}cm^{-1}$], 495 [6,200 $M^{-1}cm^{-1}$], 540 [7,900 $M^{-1}cm^{-1}$] nm. ATR-IR (v): 3258 (OH), 2925, 2881, 1603 (C=N), 1565 (C=N), 1451, 1379, 1316, 1234, 1029, 917, 615 cm^{-1}.

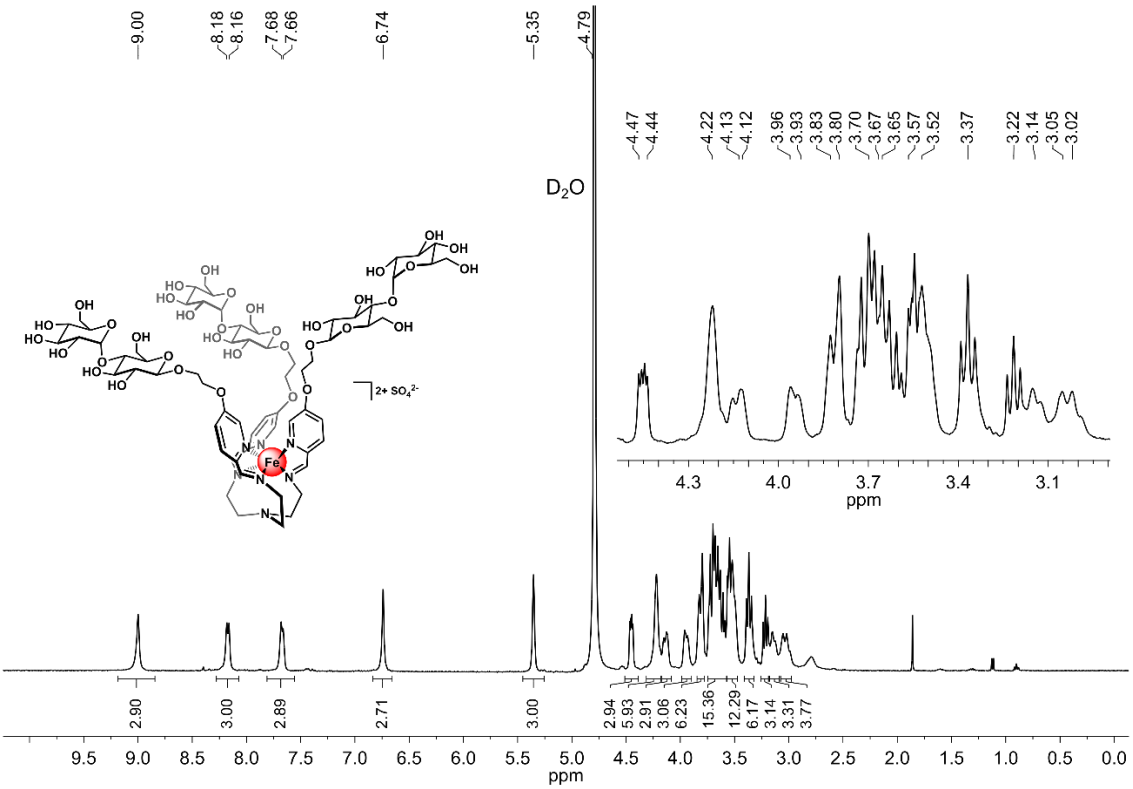

Figure S88. ^{1}H NMR spectrum of [**3**-mal][SO_4] (D_2O, 400 MHz, 25 °C).

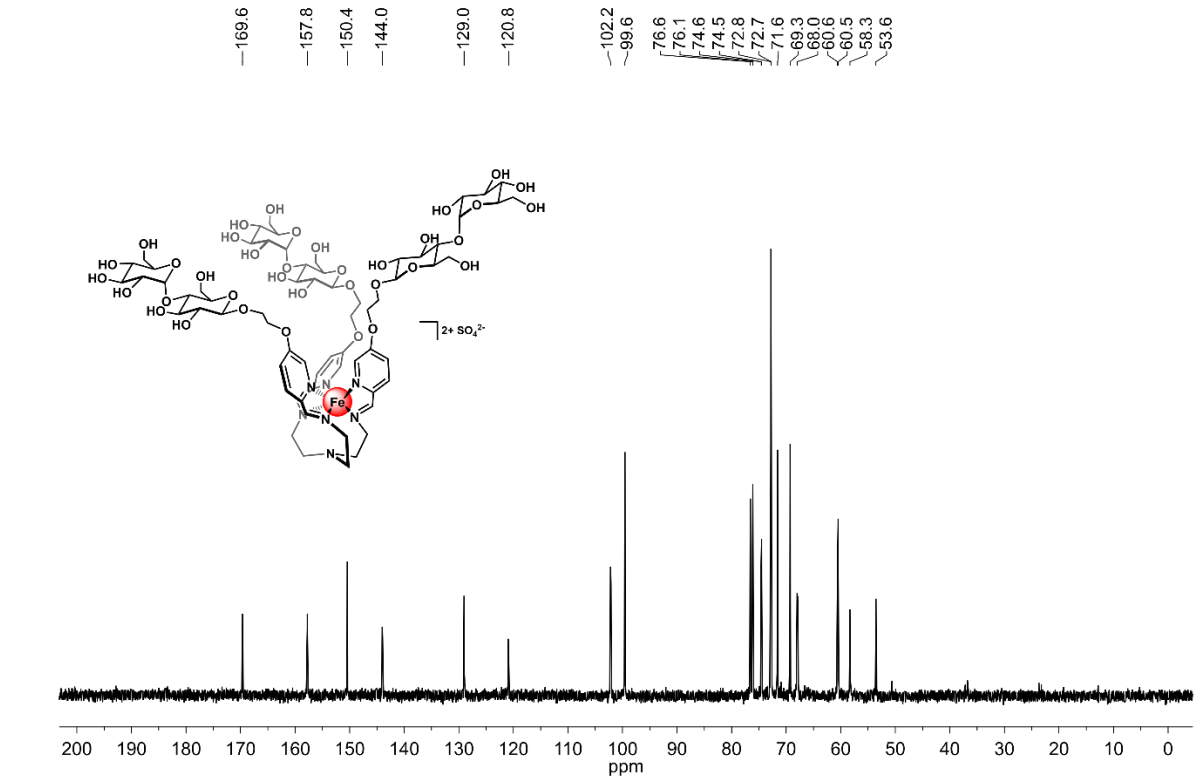

Figure S89. $^{13}C\{^{1}H\}$ NMR spectrum of [**3**-mal][SO_4] (D_2O, 100 MHz, 25 °C).

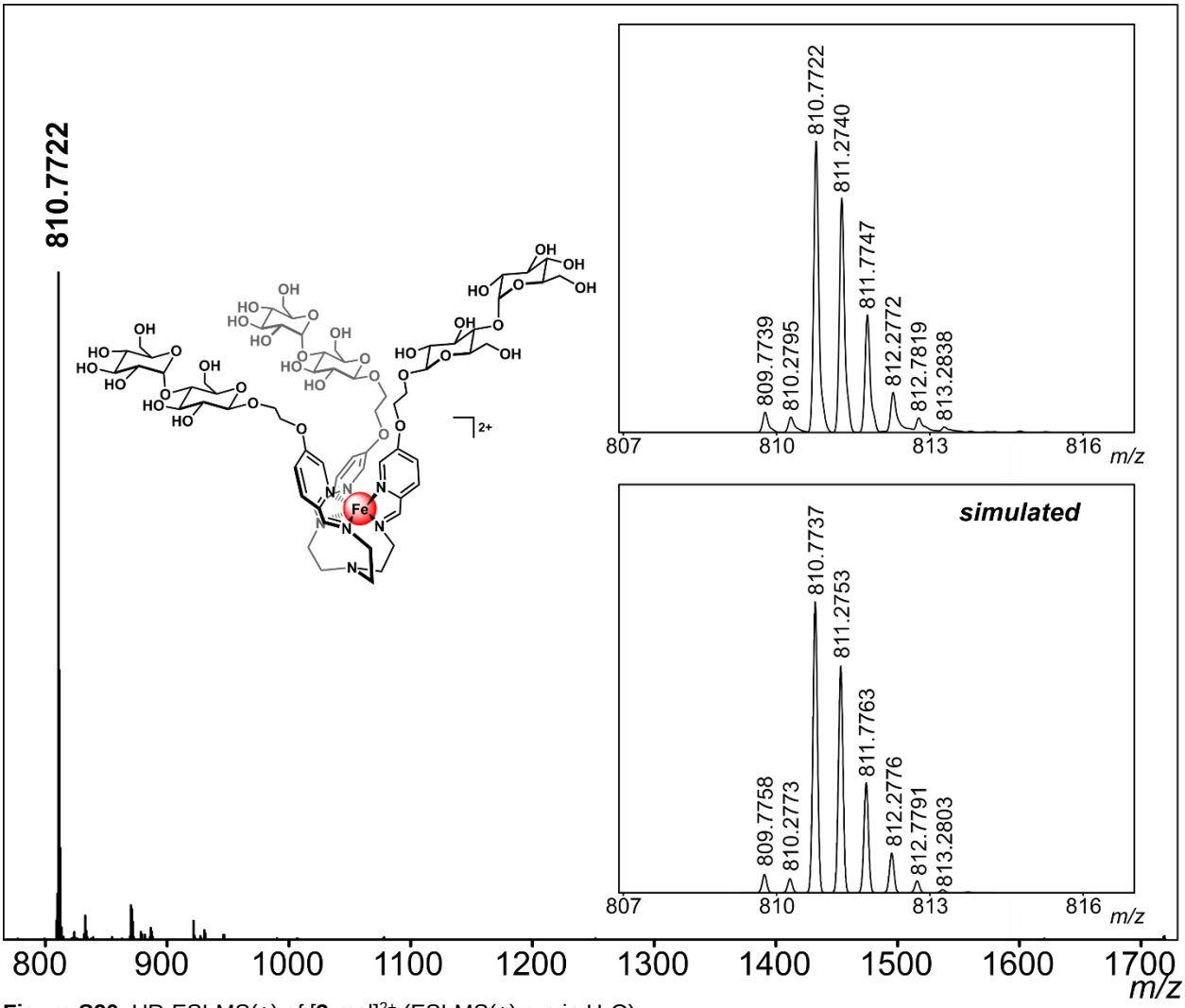

Figure S90. HR-ESI-MS(+) of [**3**-mal]$^{2+}$ (ESI-MS(+) run in H_2O).

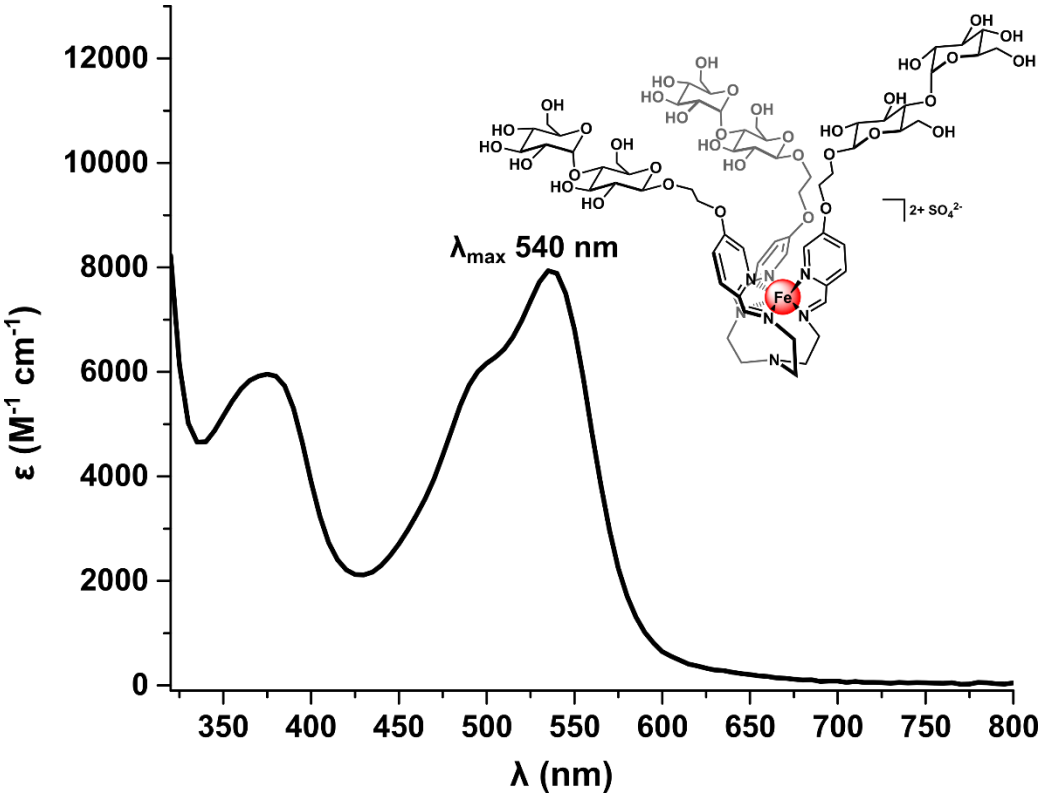

Figure S91. UV-vis spectrum of [**3**-mal][SO_4] (H_2O, 50 μM).

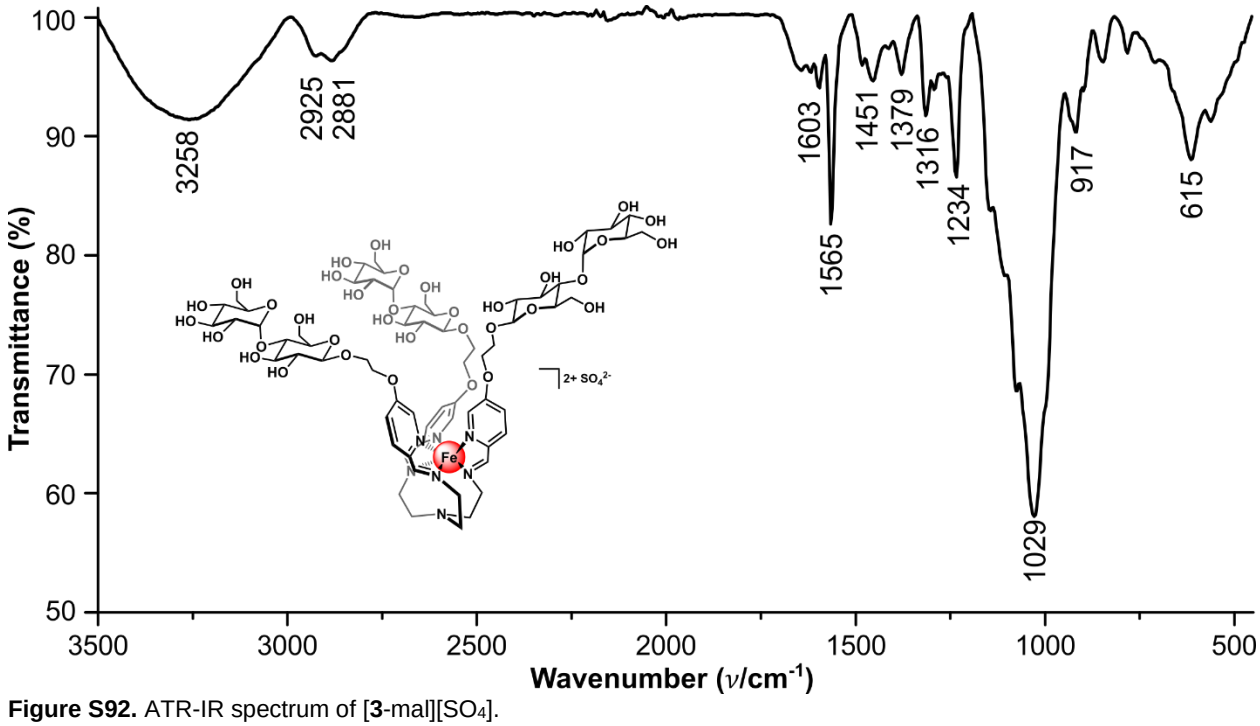

Figure S92. ATR-IR spectrum of [**3**-mal][SO_4].

S2.3.15. Unfunctionalized $[NMe_4]_4[Fe_4L_6]$

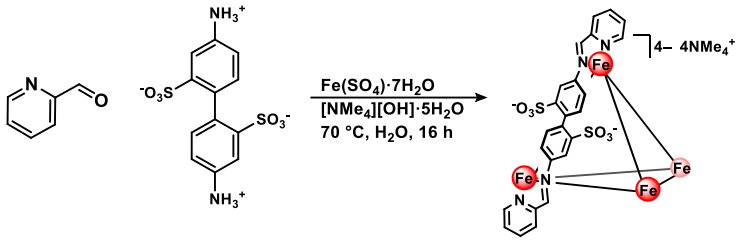

The unfunctionalized $[NMe_4]_4[FeL_6]$ complex was prepared according to the literature reported procedure.[18]

To an 8 mL reaction tube was added 4,4'-diaminobiphenyl-2,2'-disulfonic acid (70 wt% balance H_2O, 100 mg, 0.203 mmol, 5.80 equiv), 2-formylpyridine (39 µL, 0.41 mmol, 12 equiv), $[NMe_4][OH]•5H_2O$ (74 mg, 0.41 mmol, 12 equiv), and $Fe(SO_4)•7H_2O$ (38 mg, 0.14 mmol, 4.0 equiv) as solids. To this tube was added degassed H_2O (2.5 mL). The reaction mixture was then sparged with N_2 for 15 min, at which point the tube was placed in a preheated oil bath set to 70 °C. The purple reaction mixture was allowed to stir at 70 °C for 20 h, at which point it was filtered through a piece of glass microfiber filter paper, and the product was allowed to crystallize by vapor diffusion of acetone into the aqueous solution of the crude reaction mixture. ^{1}H NMR spectroscopic data of the purified product (Figure S93) match the literature report.[18]

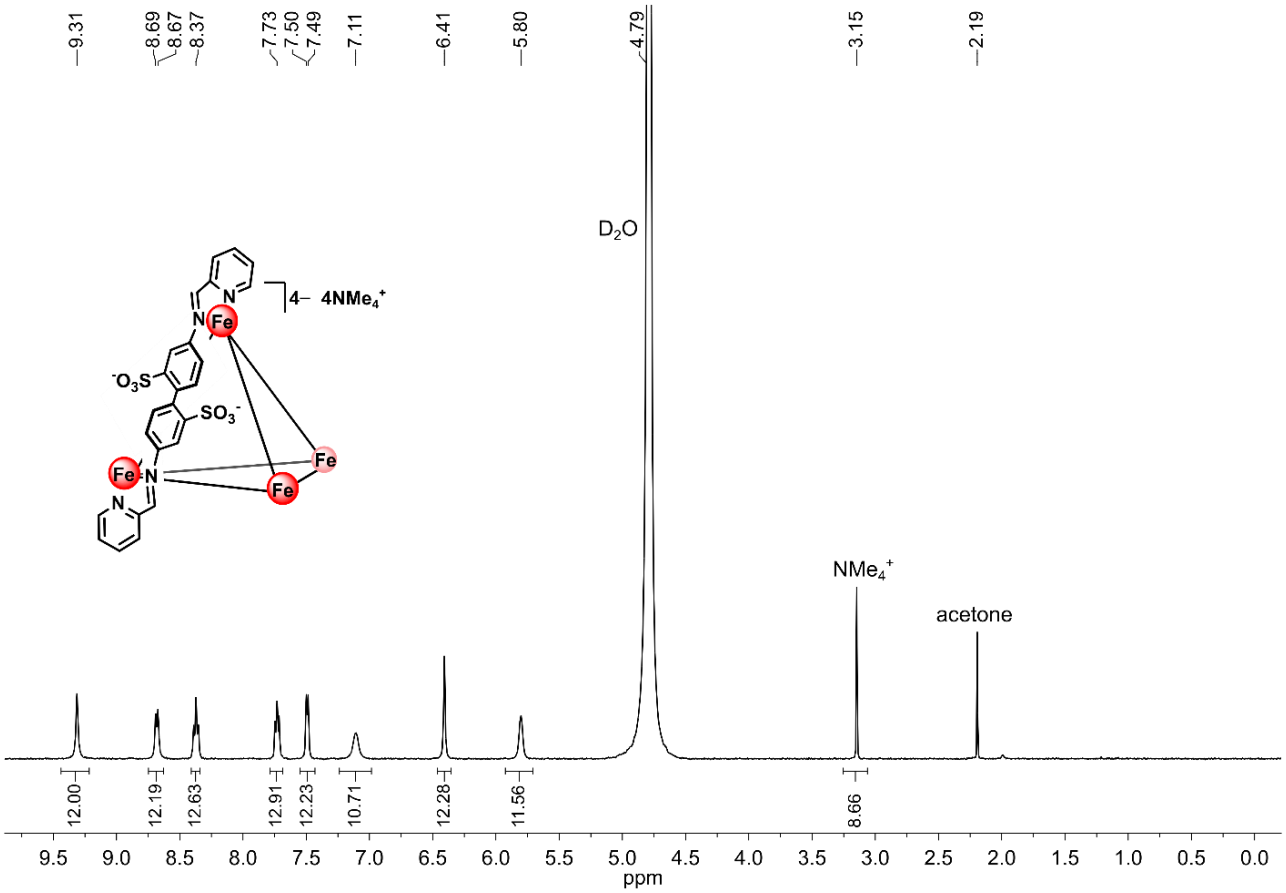

Figure S93. ^{1}H NMR spectrum of $[NMe_4]_4[Fe_4L_6]$ (D_2O, 400 MHz, 25 °C).

S3. Solubility determination of $[NMe_4]_4$[1-glc] in H_2O

A 100 µM solution of $[NMe_4]_4$[**1**-glc] in H_2O (750 µL) was prepared, and a UV-vis spectrum was collected. The solution was then diluted in 0.2 mL increments until a final volume of 1.950 mL was reached. Absorbances of the seven solutions were measured at λ = 545 nm and used to prepare a calibration curve of absorbance as a function of concentration.
Equation of regression line: $y = 0.0211x + 0.122$

Solubility determination: To a solid sample of $[NMe_4]_4$[**1**-glc] (17 mg) was added a minimal amount of H_2O (70 µL) until complete dissolution was achieved. Next, a 2 µL aliquot was removed and diluted to 1.000 mL with H_2O, and a UV-vis spectrum of the solution was collected. Four more 2 µL aliquots were removed, diluted to 1.000 mL, and analyzed by UV-vis spectroscopy.

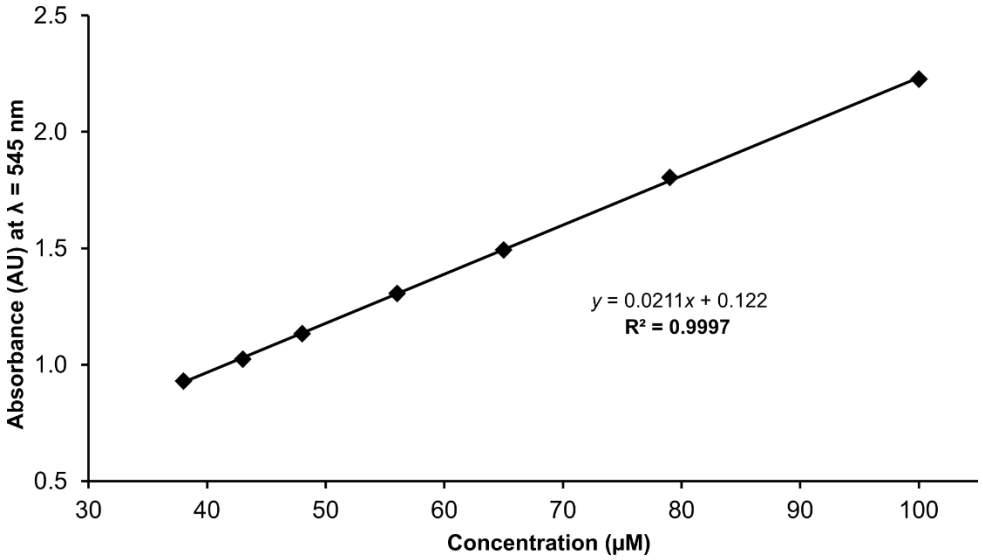

Figure S94. Calibration curve of absorption as a function of concentration of $[NMe_4]_4$[**1**-glc] at λ = 545 nm measured in H_2O at 25 °C. *Equation of regression line: y = 0.0211x + 0.122.*

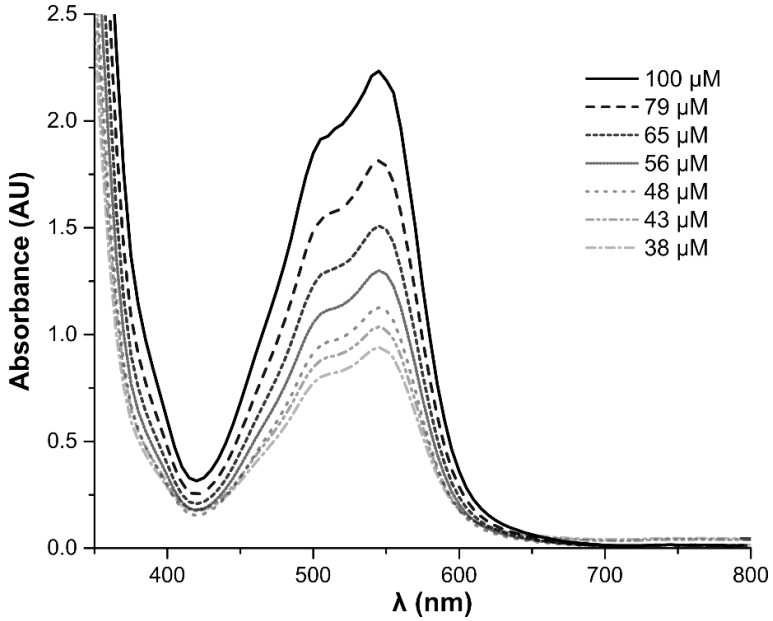

Figure S95. UV-vis spectra of $[NMe_4]_4$[**1**-glc] at various concentrations (H_2O, 25 °C).

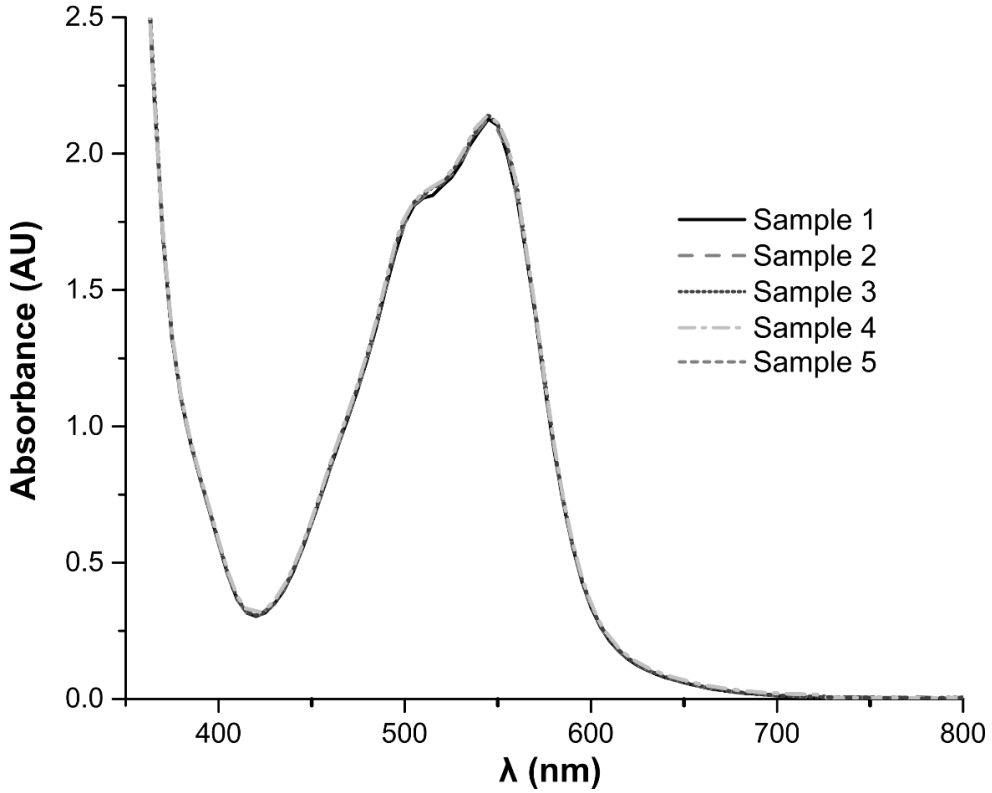

Figure S96. UV-vis spectra of 5 samples of $[NMe_4]_4$[**1**-glc] (H_2O, 25 °C).

Sample number	Absorbance (AU)	Concentration of diluted sample (mM)	Concentration of saturated sample (mM)
1	2.13	0.0950	47.6
2	2.13	0.0950	47.6
3	2.14	0.0957	47.9
4	2.13	0.0952	47.7
5	2.19	0.0979	49.0

Average concentration of saturated solution: **47.9 ± 0.6 mM** (302 ± 4 g L^{-1}).

S4. Stability studies of glycosylated complexes to various conditions, buffers, and pH environments

S4.1. Water stability of $[NMe_4]_4$[1-glc] as analyzed by ^{1}H NMR spectroscopy

The $[NMe_4]_4$[**1**-glc] complex was prepared as described in Section S2.3.1. A ^{1}H NMR spectrum of the complex was initially collected (5 mM, D_2O, 400 MHz), and then the solution was allowed to stand at ambient temperature for 24 h, at which point a ^{1}H NMR spectrum of the sample was collected again. ^{1}H NMR spectra of the same sample were collected every 24 h for a total of 7 days, and then every month for a total of 9 months. The ^{1}H NMR data indicated no observable signs of degradation throughout this timeframe.

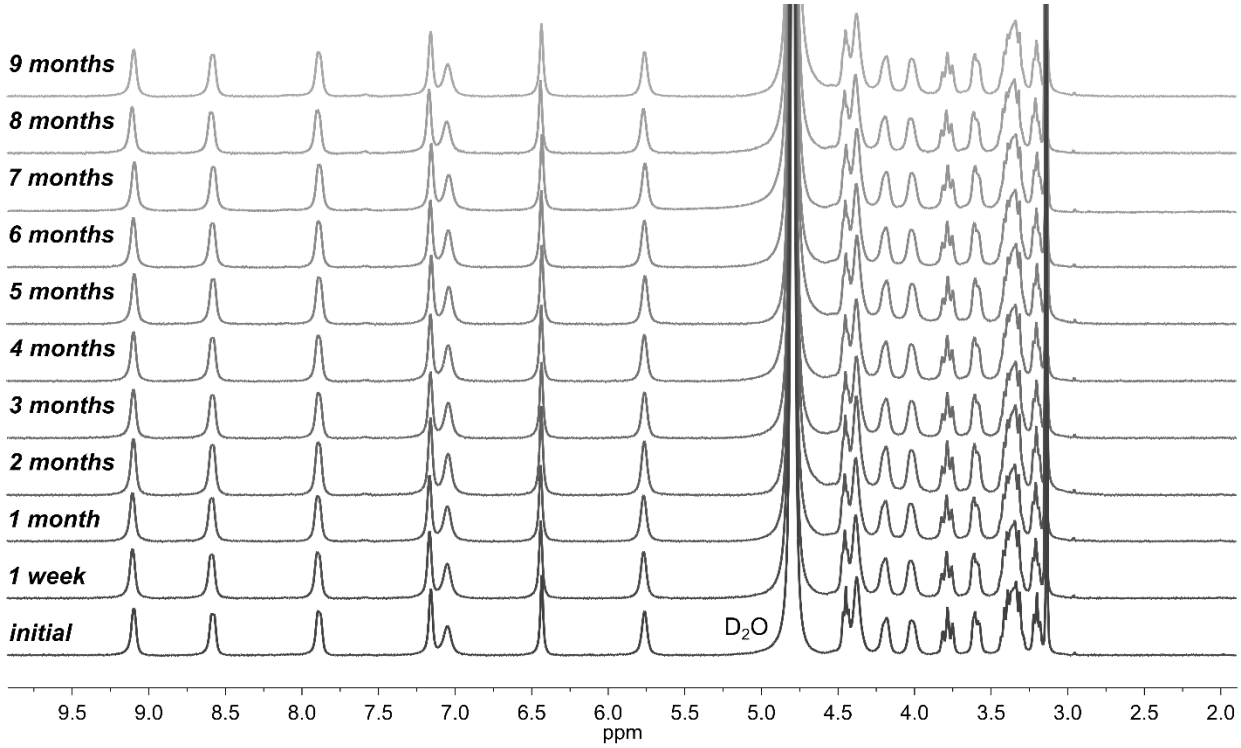

Figure S97. ^{1}H NMR spectra of $[NMe_4]_4$[**1**-glc] collected over the course of 9 months (D_2O, 400 MHz, 25 °C).

S4.2. Stability of $[NMe_4]_4$[1-glc] to solutions of various pH, common buffers, and biologically-relevant conditions as analyzed by UV-vis spectroscopy

A stock solution of $[NMe_4]_4$[**1**-glc] (10 mM) was prepared in H_2O. An aliquot was diluted in the following solutions to 50 μM concentration unless otherwise indicated, and an initial UV-vis spectrum was collected. The solutions were allowed to stand at 25 °C for up to 72 h, and UV-vis spectra were collected at the indicated time-points.

S4.2.1. Carbonate buffer (10 mM), pH 10.0

This experiment was carried out in carbonate buffer ($NaHCO_3/Na_2CO_3$, 10 mM) at pH 10.0.

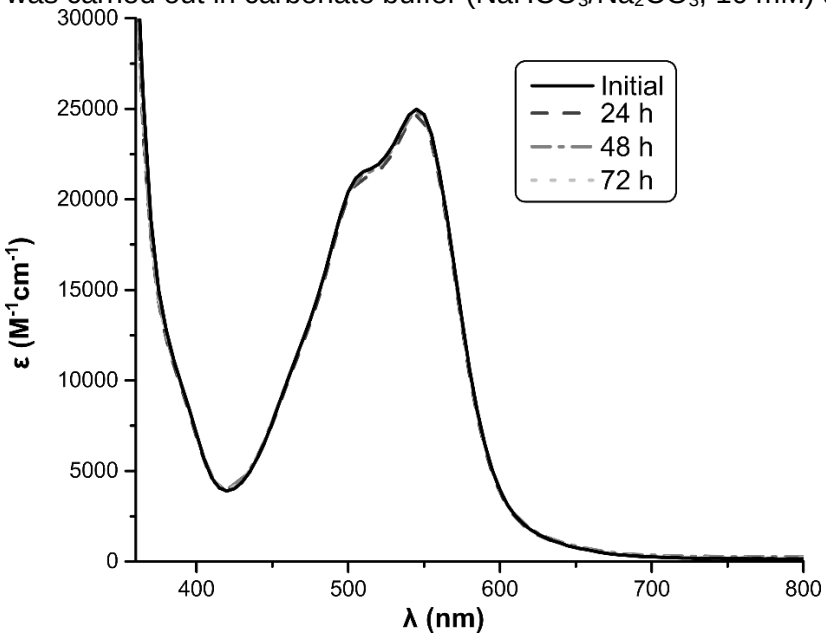

Figure S98. UV-vis spectra of $[NMe_4]_4$[**1**-glc] (50 μM) in carbonate buffer, pH 10.0 (10 mM) collected over the course of 72 h at 25 °C.

S4.2.2. Tris buffer (10 mM), pH 9.0

This experiment was carried out in Tris buffer (10 mM) at pH 9.0.

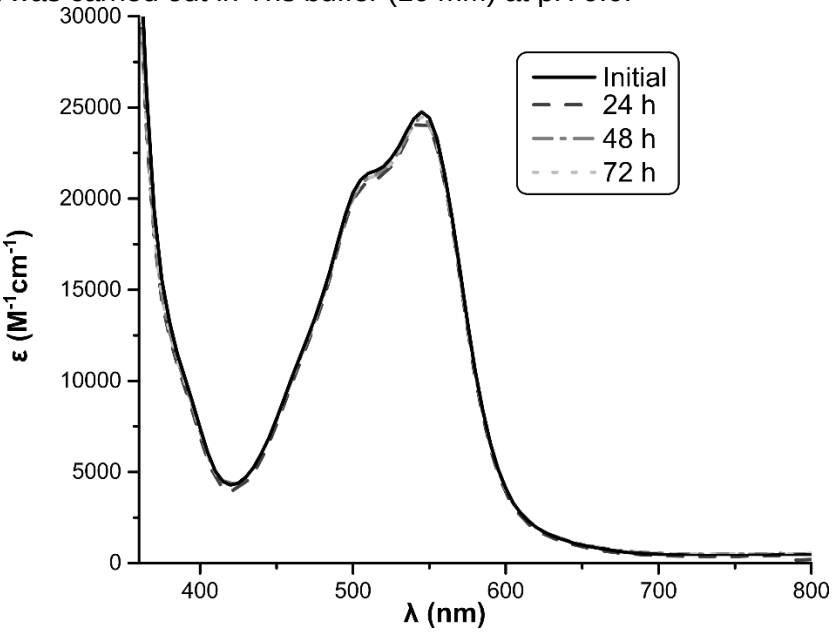

Figure S99. UV-vis spectra of $[NMe_4]_4$[**1**-glc] (50 μM) in Tris buffer, pH 9.0 (10 mM) collected over the course of 72 h at 25 °C.

S4.2.3. Tris buffer (10 mM), pH 7.4

This experiment was carried out in Tris buffer (10 mM) at pH 7.4.

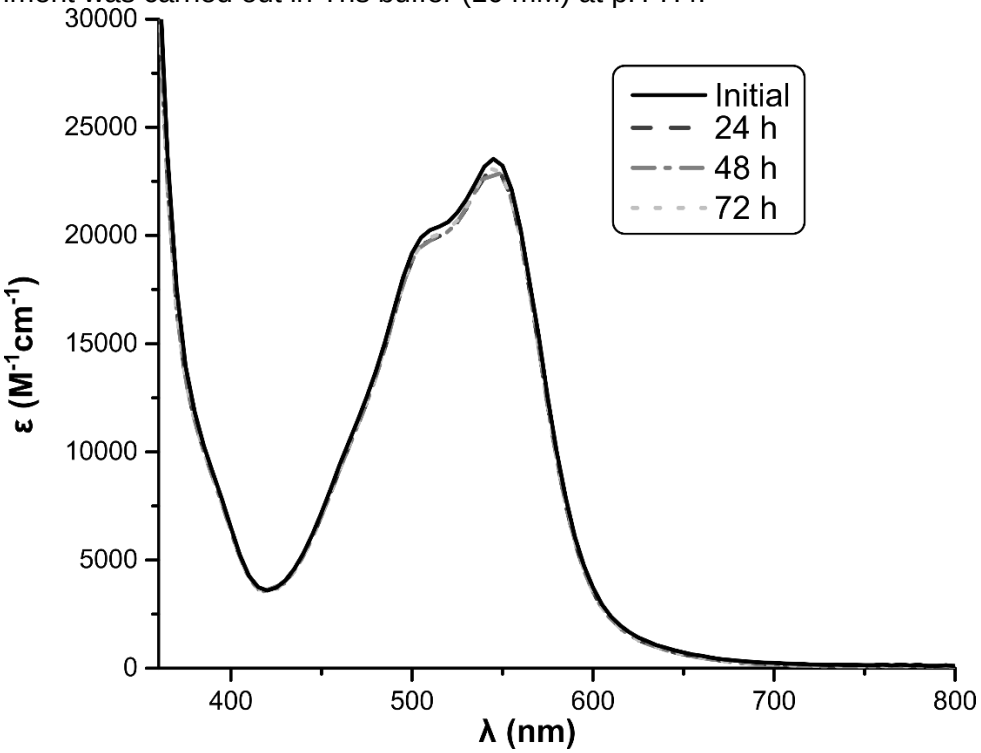

Figure S100. UV-vis spectra of $[NMe_4]_4$[**1**-glc] (50 μM) in Tris buffer, pH 7.4 (10 mM) collected over the course of 72 h at 25 °C.

S4.2.4. PBS buffer (10 mM), pH 7.4

This experiment was carried out in PBS buffer (10 mM) at pH 7.4.

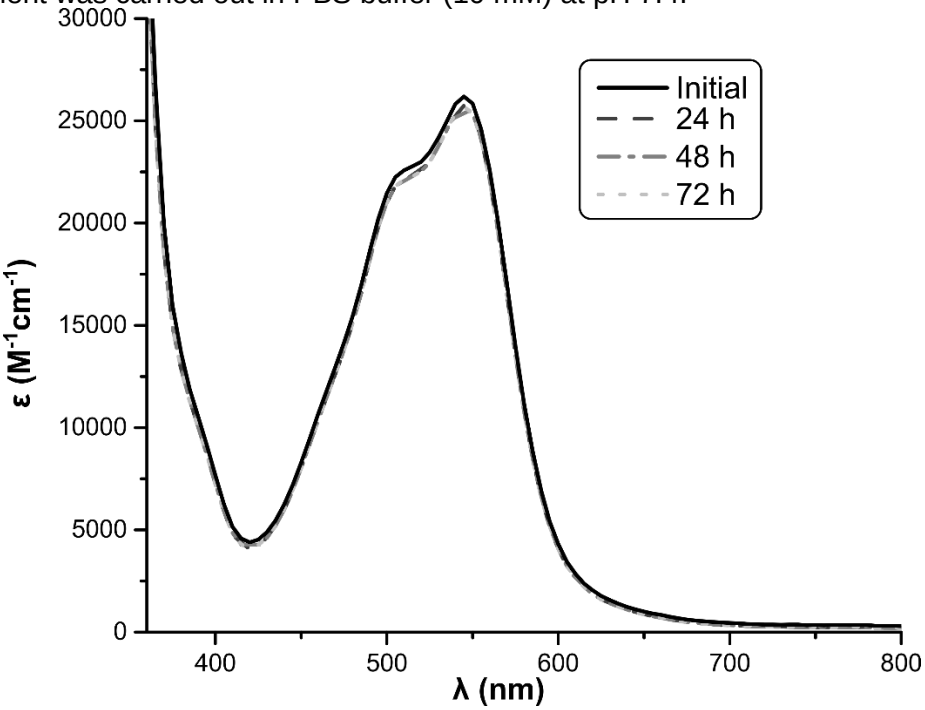

Figure S101. UV-vis spectra of $[NMe_4]_4$[**1**-glc] (50 μM) in PBS buffer, pH 7.4 (10 mM) collected over the course of 72 h at 25 °C.

S4.2.5. HEPES buffer (10 mM), pH 7.4

This study was carried out in HEPES buffer (10 mM) at pH 7.4.

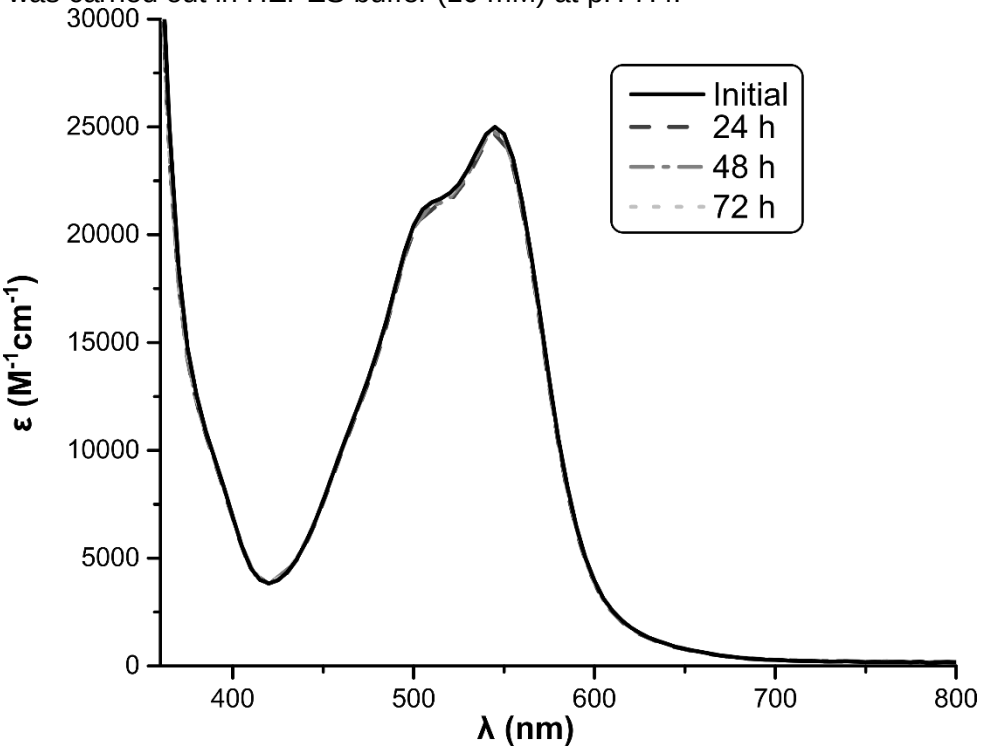

Figure S102. UV-vis spectra of $[NMe_4]_4$[**1**-glc] (50 μM) in HEPES buffer, pH 7.4 (10 mM) collected over the course of 72 h at 25 °C.

S4.2.6. Acetate buffer (10 mM), pH 5.0

This experiment was carried out in acetate buffer (10 mM) at pH 5.0.

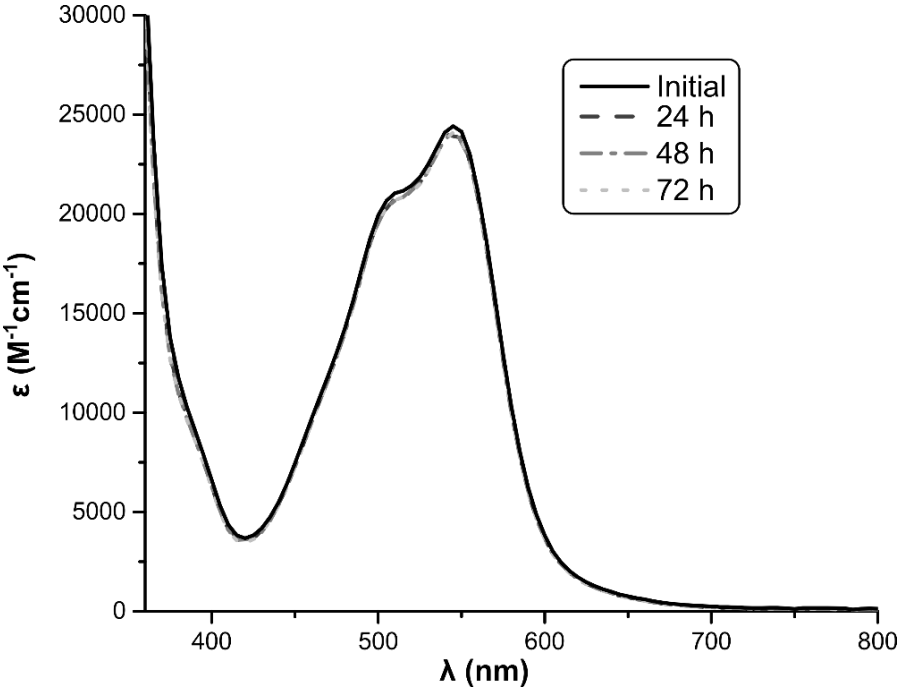

Figure S103. UV-vis spectra of $[NMe_4]_4$[**1**-glc] (50 μM) in acetate buffer, pH 5.5 (10 mM) collected over the course of 72 h at 25 °C.

S4.2.7. Acetate buffer (10 mM), pH 4.0

This experiment was carried out in acetate buffer (10 mM) at pH 4.0.

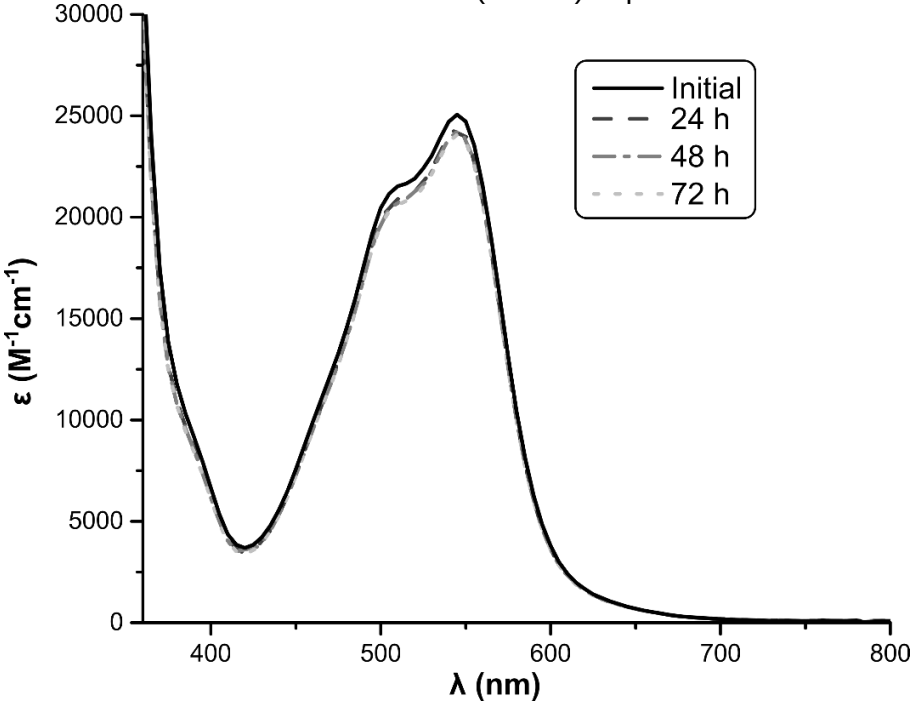

Figure S104. UV-vis spectra of $[NMe_4]_4$[**1**-glc] (50 μM) in acetate buffer, pH 4.0 (10 mM) collected over the course of 72 h at 25 °C.

S4.2.8. Glutathione (2 mM)

This experiment was carried out in a solution of glutathione (2 mM) in H_2O.

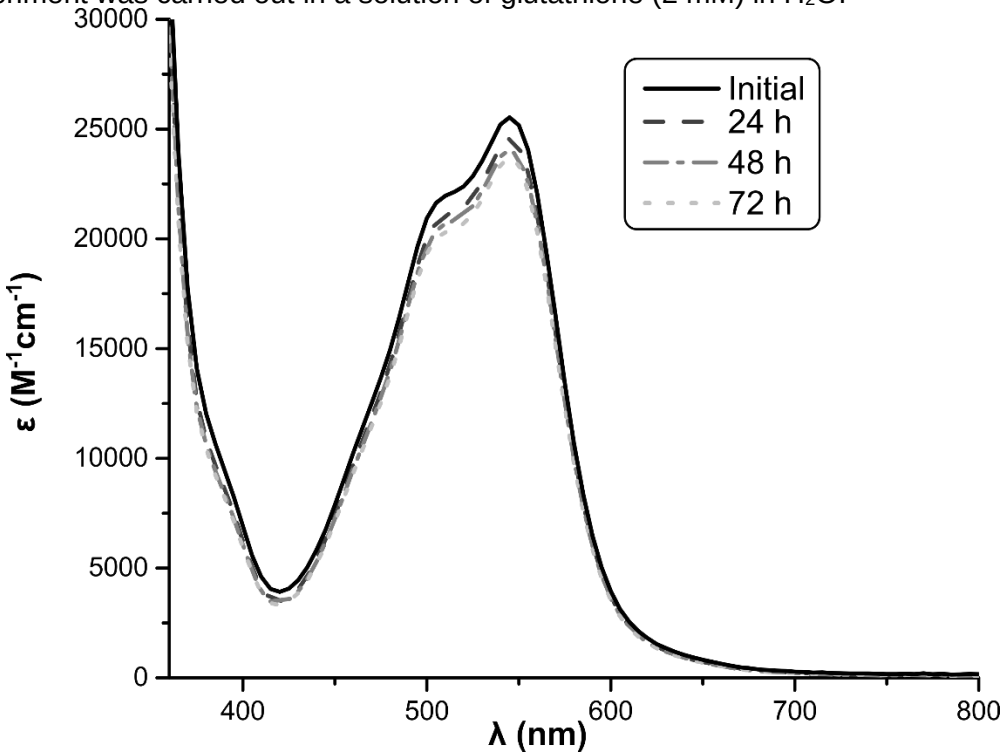

Figure S105. UV-vis spectra of $[NMe_4]_4$[**1**-glc] (50 μM) in a solution of glutathione (2 mM) collected over the course of 72 h at 25 °C.

S4.2.9. Fetal bovine serum cell culture media

A solution of $[NMe_4]_4$[**1**-glc] (100 µM) was prepared in fetal bovine serum RPMI 1640 cell media (gibco), and an initial UV-vis spectrum was collected. The solution was allowed to stand at ambient temperature and UV-vis were collected after 6 and 24 h. The same solution was then heated at 37 °C for 24 h, at which point a final UV-vis spectrum was collected.

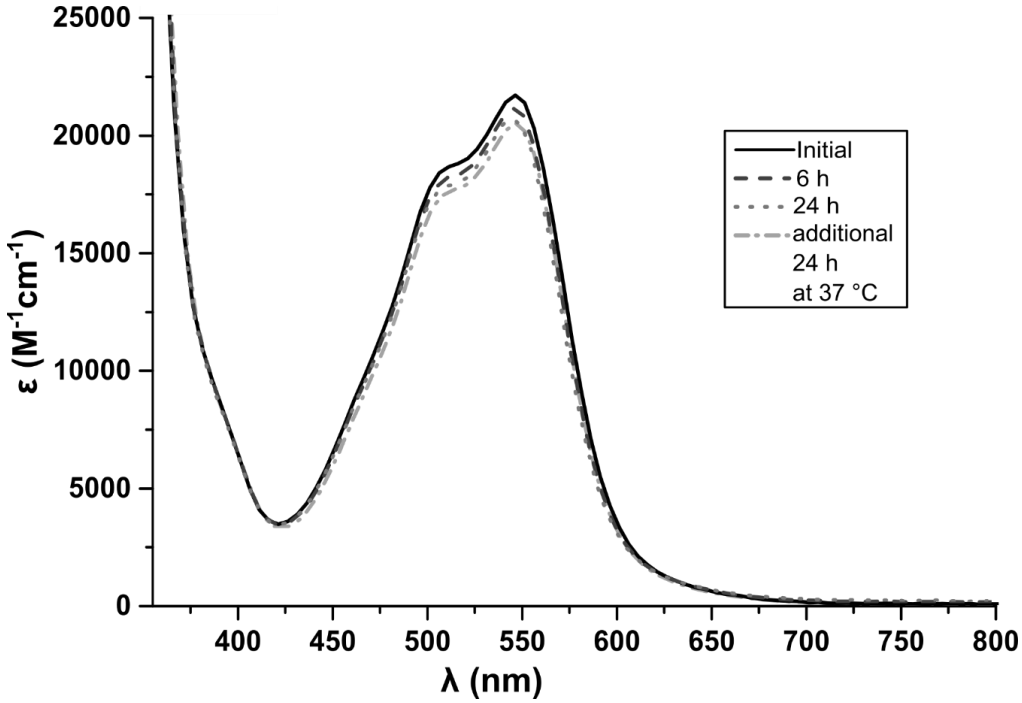

Figure S106. UV-vis spectra of $[NMe_4]_4$[**1**-glc] (100 µM) in fetal bovine serum cell media over the course of 24 h at 25 °C and then after an additional 24 h at 37 °C.

S4.3. Stability of mannosylated complexes under ITC experimental conditions as assayed by UV-vis spectroscopy

These studies were conducted to verify the stability of the glycosylated complexes to ITC experimental conditions using the mannose-substituted molecules as models. Each solution of complex was prepared at the indicated concentration in the indicated buffer and an initial UV-vis spectrum was collected. UV-vis spectra were recorded every 30 min for a total of 2 h, which provided conditions representative of the ITC binding experiments described in Section S6. Experiments were conducted at the indicated concentrations using a 0.1 cm path length quartz cuvette.

S4.3.1. $[NMe_4]_4$[1-man]

A solution of $[NMe_4]_4$[**1**-man] (180 μM) was prepared in acetate buffer (100 mM) adjusted to pH 4.8 containing $CaCl_2$ (0.1 mM), $MnCl_2$ (0.1 mM) and NaCl (10 mM). A UV-vis spectrum was collected initially, and then spectra were collected every 30 min for a total of 120 min.

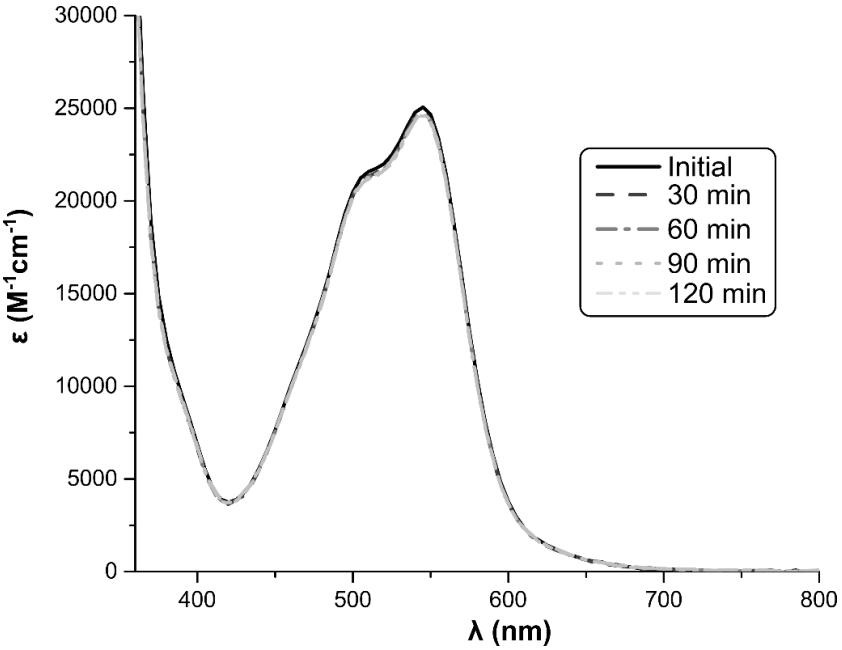

Figure S107. UV-vis spectra of $[NMe_4]_4$[**1**-man] (180 μM) in acetate buffer (100 mM) at pH 4.8 containing $CaCl_2$ (0.1 mM), $MnCl_2$ (0.1 mM), NaCl (10 mM) collected over the course of 120 min at 25 °C.

S4.3.2. $[NMe_4]_2$[2-man]

A solution of $[NMe_4]_2$[**2**-man] (210 μM) was prepared in acetate buffer (100 mM) adjusted to pH 4.8 containing $CaCl_2$ (0.1 mM), $MnCl_2$ (0.1 mM), and NaCl (10 mM). A UV-vis spectrum was collected initially, and then spectra were collected every 30 min for a total of 120 min.

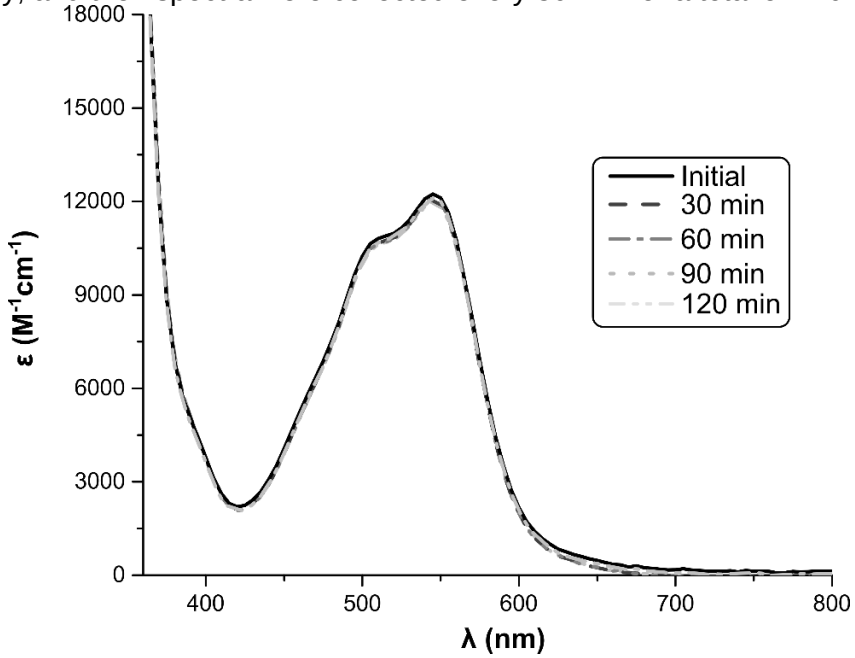

Figure S108. UV-vis spectra of $[NMe_4]_2$[**2**-man] (210 μM) in acetate buffer (100 mM) at pH 4.8 containing $CaCl_2$ (0.1 mM), $MnCl_2$ (0.1 mM), NaCl (10 mM) collected over the course of 120 min at 25 °C.

S4.3.3. [3-man][SO_4]

A solution of [**3**-man][SO_4] (660 μM) was prepared in acetate buffer (100 mM) adjusted to pH 4.8 containing $CaCl_2$ (1 mM), $MnCl_2$ (1 mM), and NaCl (50 mM). A UV-vis spectrum was collected initially, and then spectra were collected every 30 min for a total of 120 min.

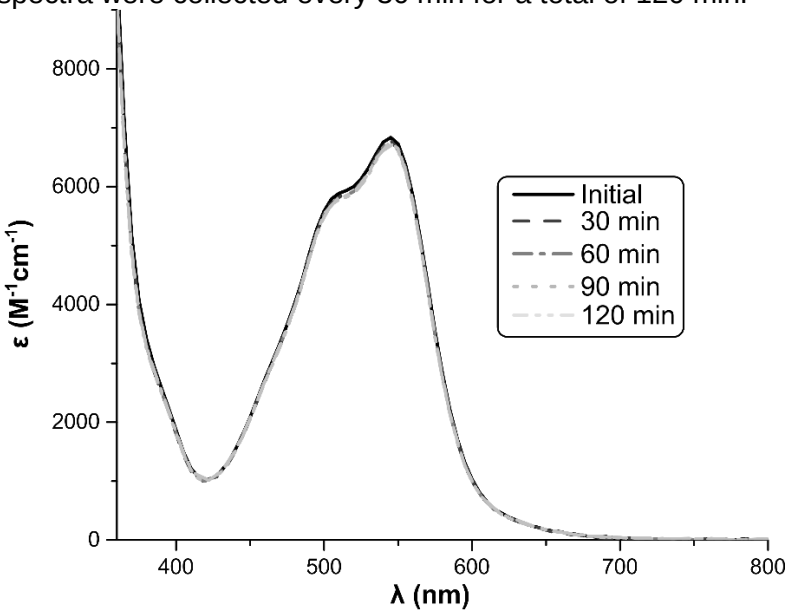

Figure S109. UV-vis spectra of [**3**-man][SO_4] (660 μM) in acetate buffer (100 mM) at pH 4.8 containing $CaCl_2$ (1 mM), $MnCl_2$ (1 mM), NaCl (50 mM) collected over the course of 120 min at 25 °C.

S5. Turbidimetry Assay

Turbidimetric experiments were carried out using a solution of tetrameric Con A (1 mL of a 10 μM solution, 10 nmol, ca. 1 mg/mL) in HEPES buffer (10 mM) containing NaCl (100 mM), $MnCl_2$ (1 mM), and $CaCl_2$(1 mM) at pH 7.0. The exact concentration of Con A was determined by absorption spectroscopy by measuring the absorbance at λ 280 nm [A_{280} = 1.37 x (mg/mL Con A)].[27] An initial UV-vis spectrum of each glycosylated complex (20 μM) in HEPES buffer was collected at 25 °C as a reference. For each experiment, the solution of Con A was transferred to a quartz cuvette, which was placed in the UV-vis spectrophotometer and an initial UV-vis spectrum was collected at 25 °C. To the solution was added an aqueous solution (2 μL of a 10 mM solution, 20 nmol) of the representative complex and the resulting solution was quickly mixed *via* pipette and a UV-vis spectrum was immediately collected. The solution was allowed to stand at 25 °C inside the spectrophotometer, and spectra were recorded every 15 sec for a total of 20 min and then every 3 min for an additional 160 min, at which point a solution of methyl-α-D-mannose (10 μL of a 1 M solution, 10 μmol, 1000 equiv) was added and the resulting solution was mixed quickly *via* pipette. UV-vis spectra were collected every 30 sec for a total of 5 min. The following plots show the change in absorbance at λ 545 nm as a function of time.

S5.1. $[NMe_4]_4$[1-man]

The concentration of Con A was determined to be 1.5 mg/mL based on A_{280}.

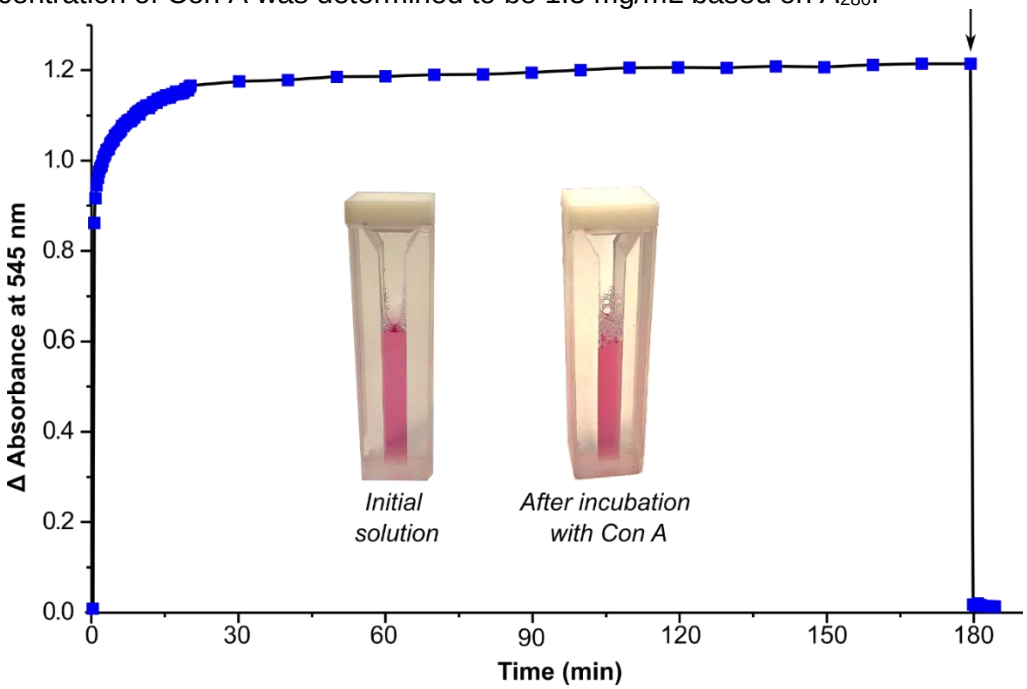

Figure S110. Time course of the absorbance (turbidity) changes at 25 °C for a solution of $[NMe_4]_4$[**1**-man] (20 μM) and Con A (10 μM) in HEPES buffer (10 mM, pH 7.0) monitored at A_{545}. The arrow indicates the addition of methyl-α-D-mannose (10 μL of a 1 M solution, 1000 equiv) at 180 min.

S5.2. $[NMe_4]_2$[2-man]

The concentration of Con A was determined to be 1.5 mg/mL based on A_{280}.

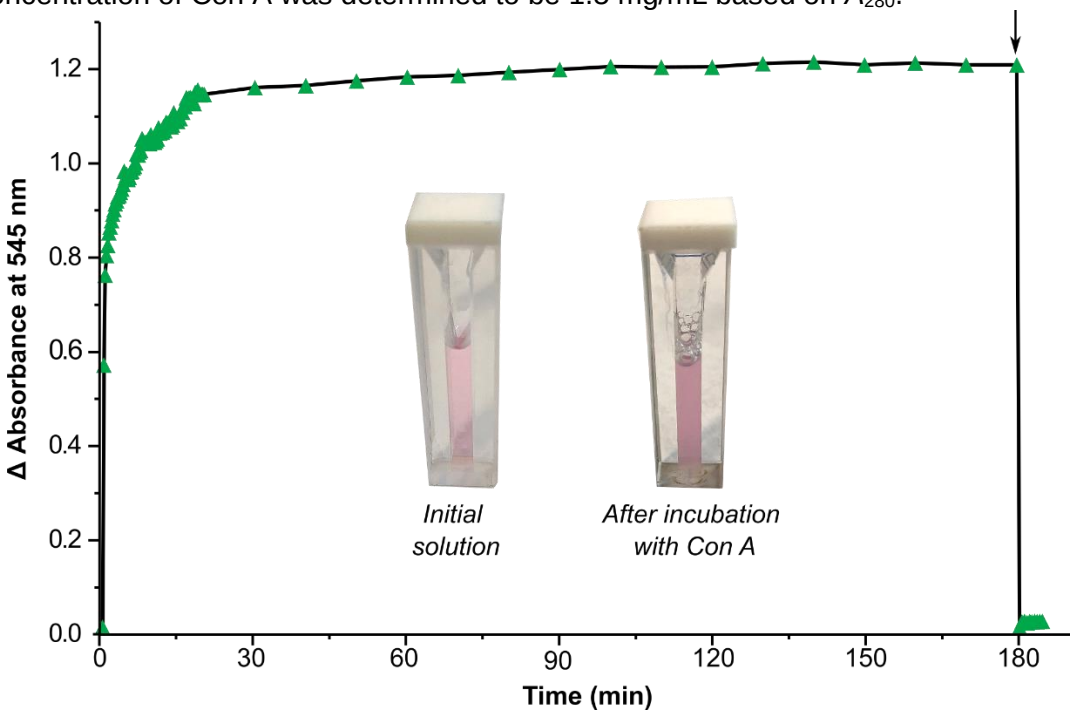

Figure S111. Time course of the absorbance (turbidity) changes at 25 °C for a solution of $[NMe_4]_2$[**2**-man] (20 μM) and Con A (10 μM) in HEPES buffer (10 mM, pH 7.0) monitored at A_{545}. The arrow indicates the addition of methyl-α-D-mannose (10 μL of a 1 M solution, 1000 equiv) at 180 min.

S5.3. [3-man][SO_4]

The concentration of Con A was determined to be 1.3 mg/mL based on A_{280}.

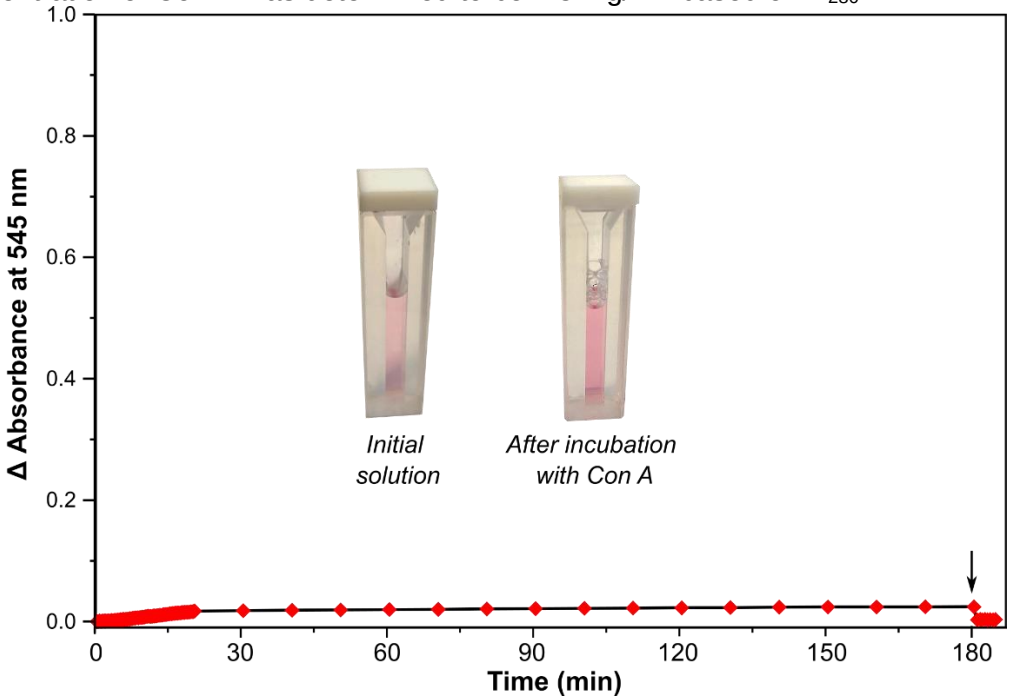

Figure S112. Time course of the absorbance (turbidity) changes at 25 °C for a solution of [**3**-man][SO_4] (20 μM) and Con A (10 μM) in HEPES buffer (10 mM, pH 7.0) monitored at A_{545}. The arrow indicates the addition of methyl-α-D-mannose (10 μL of a 1 M solution, 1000 equiv) at 180 min.

S5.4. $[NMe_4]_4$[1-mal]

The concentration of Con A was determined to be 1.5 mg/mL based on A_{280}.

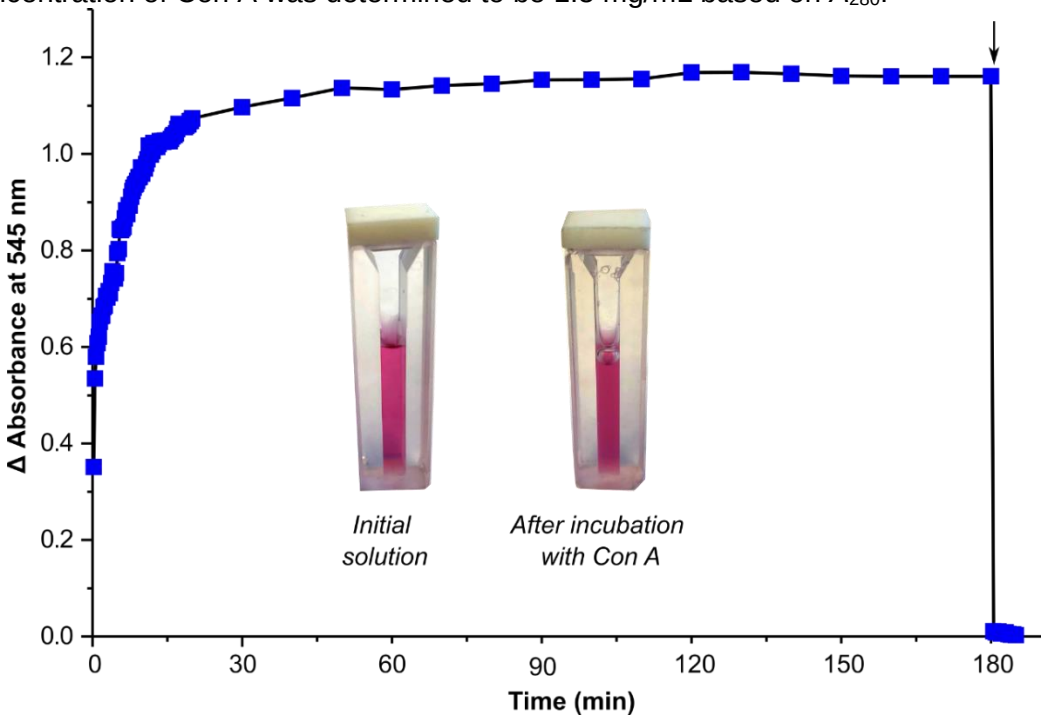

Figure S113. Time course of the absorbance (turbidity) changes at 25 °C for a solution of $[NMe_4]_4$[**1**-mal] (20 μM) and Con A (10 μM) in HEPES buffer (10 mM, pH 7.0) monitored at A_{545}. The arrow indicates the addition of α-methyl-mannose (10 μL of a 1 M solution, 1000 equiv) at 180 min.

S5.5. $[NMe_4]_2$[2-mal]

The concentration of Con A was determined to be 1.4 mg/mL based on A_{280}.

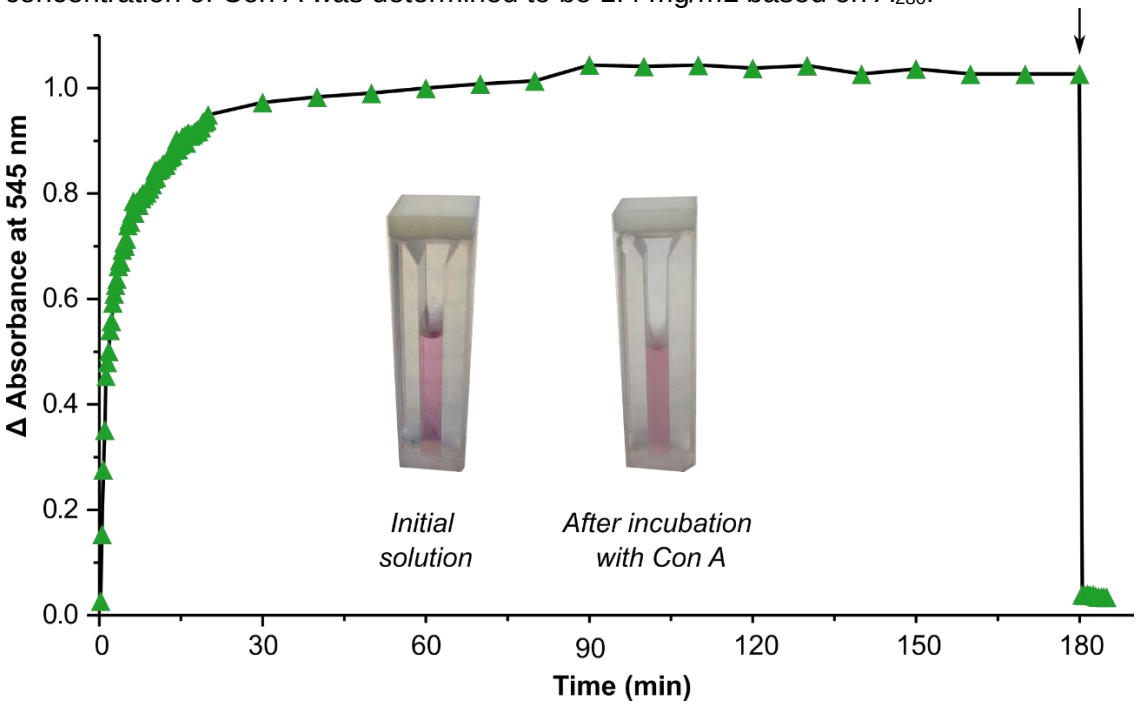

Figure S114. Time course of the absorbance (turbidity) changes at 25 °C for a solution of $[NMe_4]_2$[**2**-mal] (20 μM) and Con A (10 μM) in HEPES buffer (10 mM, pH 7.0) monitored at A_{545}. The arrow indicates the addition of α-methyl-mannose (10 μL of a 1 M solution, 1000 equiv) at 180 min.

S5.6. [3-mal][SO_4]

The concentration of Con A was determined to be 1.1 mg/mL based on A_{280}.

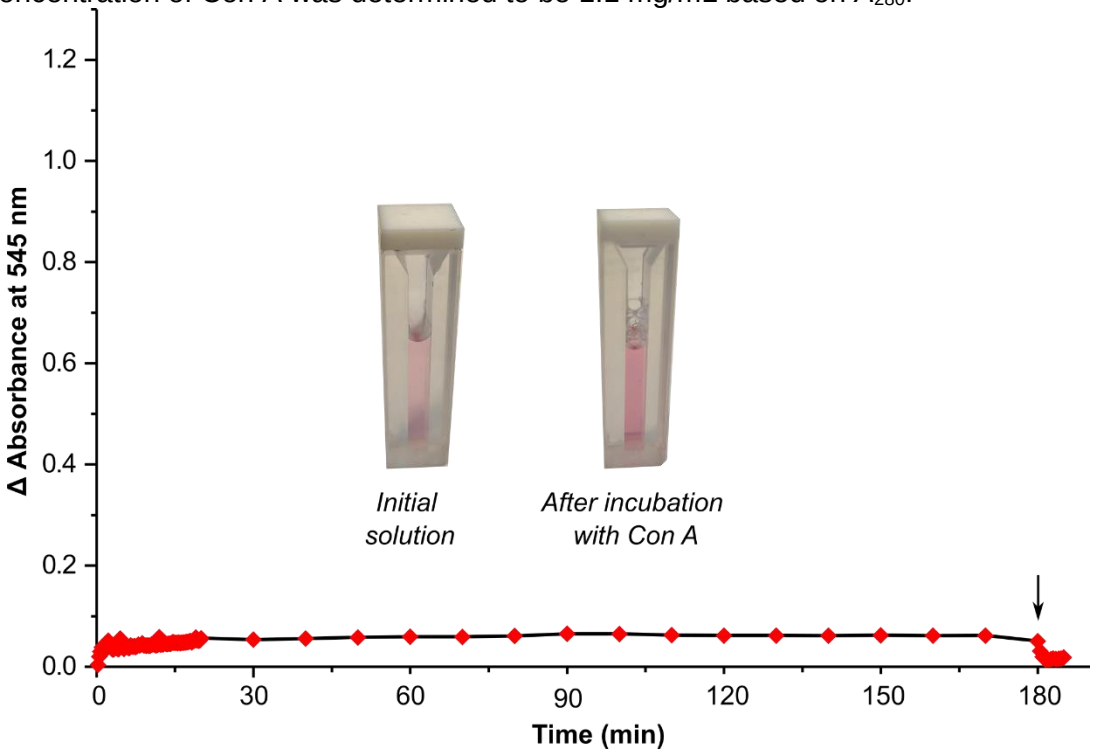

Figure S115. Time course of the absorbance (turbidity) changes at 25 °C for a solution of [**3**-mal][SO_4] (20 μM) and Con A (10 μM) in HEPES buffer (10 mM, pH 7.0) monitored at A_{545}. The arrow indicates the addition of α-methyl-mannose (10 μL of a 1 M solution, 1000 equiv) at 180 min.

S6. ITC binding studies

All ITC experiments were performed using an Affinity LV ITC (Waters/TA Instruments) instrument. Titrations were conducted in 100 mM acetate buffer at pH 4.8 to generate Con A in its dimeric form and in the presence of 0.1–1.0 mM $MnCl_2$, 0.1–1.0 mM $CaCl_2$, and 10–50 mM NaCl. The buffer solution was prepared in Milli-Q water and filtered through a Corning® 0.22 μm filter prior to use. Injections of solutions containing glycomolecules dissolved in buffer were added from a computer controlled 320 μL syringe at an interval of 245 sec into the sample solution of Con A (cell volume 350 μL) dissolved in the same buffer with a stirring rate of 125 rpm. Concentrations of Con A ranged from 40–110 μM and glycomolecule concentrations ranged from 0.18–1.05 mM. The exact concentration of Con A was determined by absorption spectroscopy by measuring the absorbance at λ 280 nm [$E_{1\mathrm{cm}}^{1\%}$ = 12.4].[28] The exact glycomolecule concentrations were obtained by absorption spectroscopy by measuring the absorbance at λ 545 nm (ε values reported for all complexes in Section S2.3). To eliminate any unspecific enthalpic contributions (heat of dilution), control experiments were performed by titration of the glycomolecule into the corresponding buffer solution in the absence of Con A. The data obtained for the glycomolecule dilution blank were subtracted from the data obtained for glycomolecule−protein titration experiments. The experimental data were fitted to a theoretical titration curve using NanoAnalyze 3.12.5 software, with Δ*H* (enthalpy change in KJ/mol), K_d (dissociation constant in M), and *n* (stoichiometry of binding with respect to Con A monomer) as adjustable parameters. Thermodynamic parameters were calculated according to the Gibbs−Helmholtz equation.

S6.1. Binding of mannose-functionalized complexes to Con A dimer

S6.1.1. $[NMe_4]_4$[1-man]

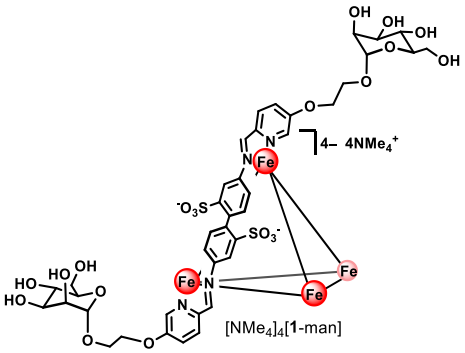

Measurements were conducted with solutions of dimeric Con A (40 μM) and $[NMe_4]_4$[**1**-man] (180 μM) in acetate buffer (100 mM) at pH 4.8 containing NaCl (10 mM), $MnCl_2$ (0.1 mM), and $CaCl_2$ (0.1 mM). The first of 26 injections was performed at 0.5 μL volume and was discarded from the data set. A total of 25 injections at 2.5 μL volume were subsequently performed at 245 sec intervals and the data for the described measurements were generated in triplicate (Figure S116).

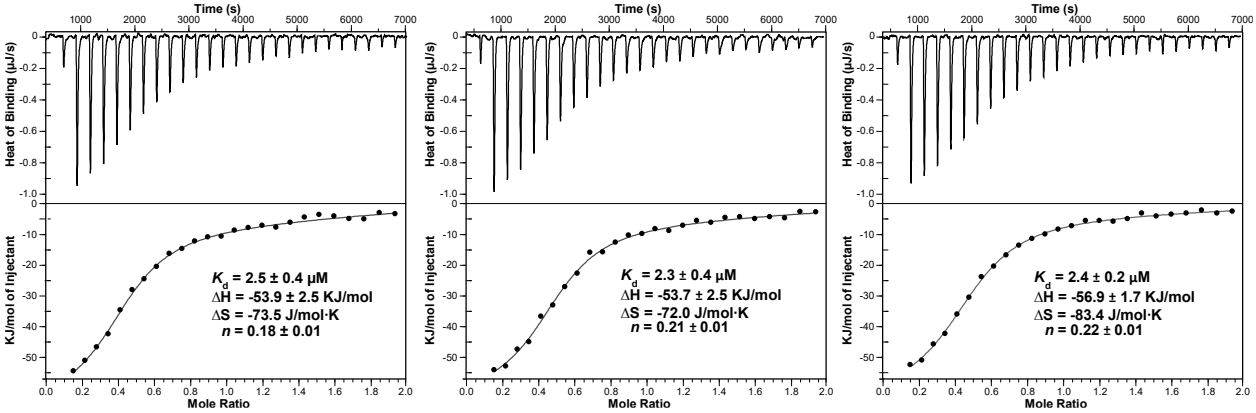

Figure S116. Isothermal titration calorimetry thermograms (top) and fitted binding isotherms (bottom) for the binding of $[NMe_4]_4$[**1**-man] to dimeric Con A for three independent runs. Values of *n* are reported with respect to the Con A monomer.

S6.1.2. $[NMe_4]_2$[2-man]

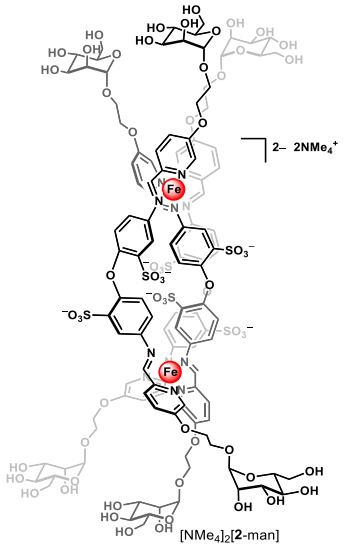

Measurements were conducted with solutions of dimeric Con A (40 μM) and $[NMe_4]_2$[**2**-man] (210 μM) in acetate buffer (100 mM) at pH 4.8 containing NaCl (10 mM), $MnCl_2$ (0.1 mM), and $CaCl_2$ (0.1 mM). The first of 26 injections was performed at 0.5 μL volume and was discarded from the data set. A total of 25 injections at 3.0 μL volume were subsequently performed at 245 sec intervals and the data for the described measurements were generated in triplicate (Figure S117).

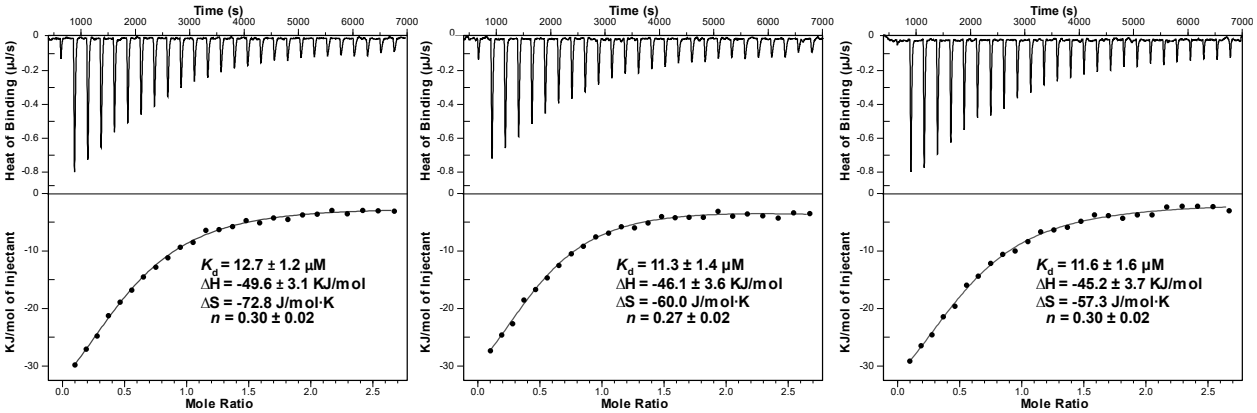

Figure S117. Isothermal titration calorimetry thermograms (top) and fitted binding isotherms (bottom) for the binding of $[NMe_4]_2$[**2**-man] to dimeric Con A for three independent runs. Values of *n* are reported with respect to the Con A monomer.

S6.1.3. [3-man][SO_4]

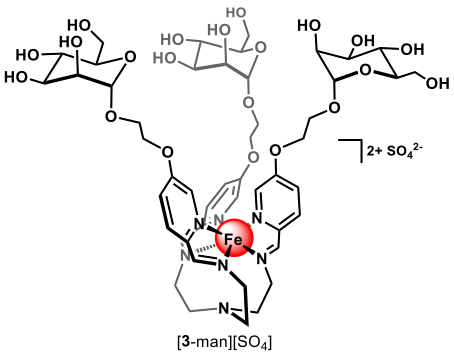

[**3**-man][SO_4]

Measurements were conducted with solutions of dimeric Con A (66 μM) and [**3**-man][SO_4] (660 μM) in acetate buffer (100 mM) at pH 4.8 containing NaCl (50 mM), $MnCl_2$ (1 mM), and $CaCl_2$ (1 mM). The first of 26 injections was performed at 1.0 μL volume and was discarded from the data set. A total of 25 injections at 4.0 μL volume were subsequently performed at 245 sec intervals and the data for the described measurements were generated in triplicate (Figure S118).

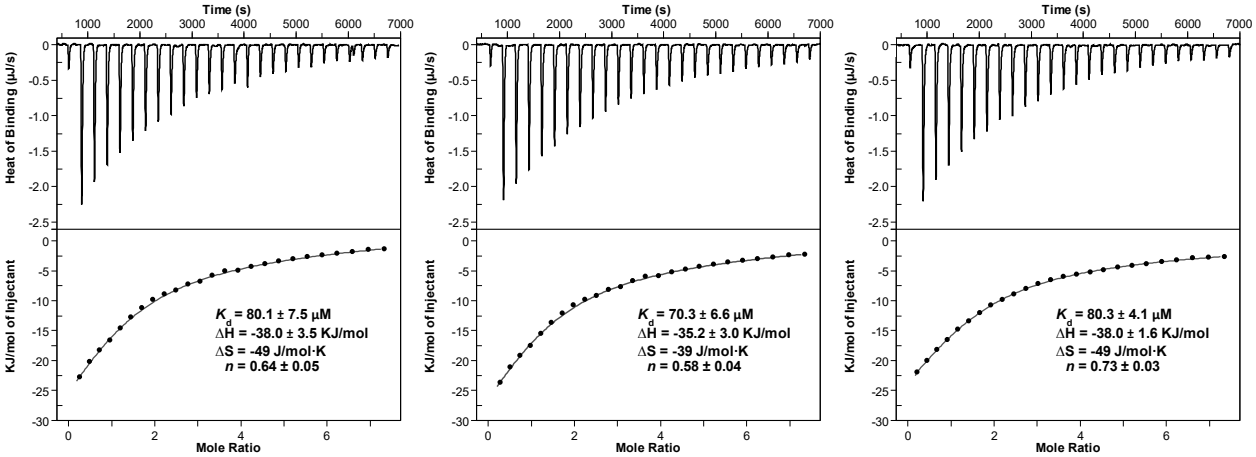

Figure S118. Isothermal titration calorimetry thermograms (top) and fitted binding isotherms (bottom) for the binding of [**3**-man][SO_4] to dimeric Con A for three independent runs. Values of *n* are reported with respect to the Con A monomer.

S6.2. Binding of maltose-functionalized complexes to Con A dimer

S6.2.1. $[NMe_4]_4$[1-mal]

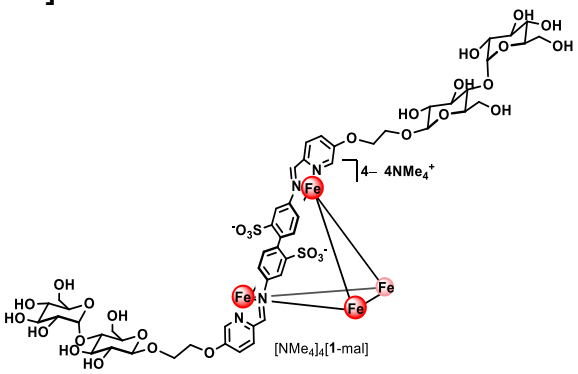

Measurements were conducted with solutions of dimeric Con A (88 μM) and $[NMe_4]_4$[**1**-mal] (244 μM) in acetate buffer (100 mM) at pH 4.8 containing NaCl (50 mM), $MnCl_2$ (1 mM), and $CaCl_2$ (1 mM). The first of 26 injections was performed at 0.5 μL volume and was discarded from the data set. A total of 25 injections at 2.5 μL volume were subsequently performed at 245 sec intervals and the data for the described measurements were generated in triplicate (Figure S119).

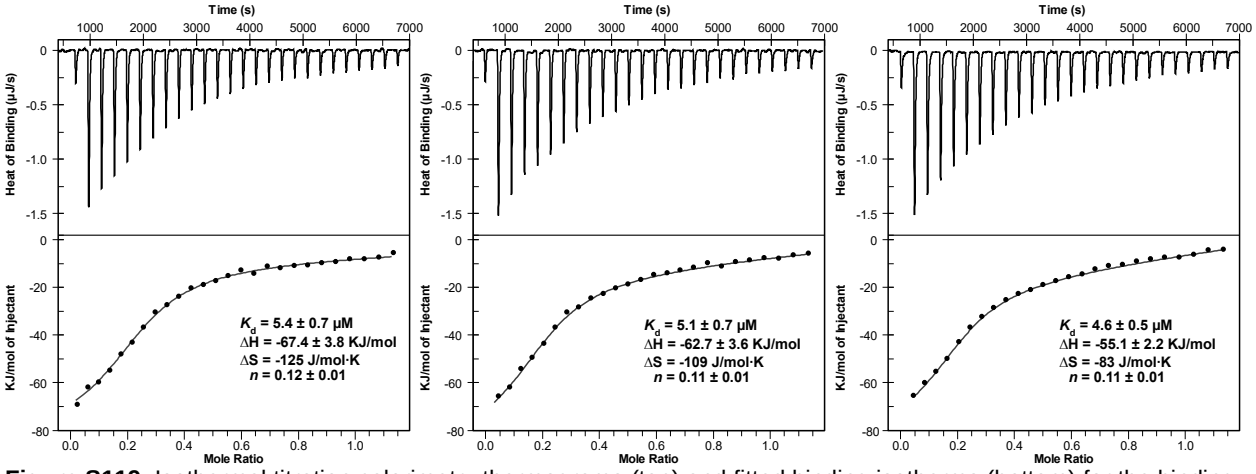

Figure S119. Isothermal titration calorimetry thermograms (top) and fitted binding isotherms (bottom) for the binding of $[NMe_4]_4$[**1**-mal] to dimeric Con A for three independent runs. Values of *n* are reported with respect to the Con A monomer.

S6.2.2. $[NMe_4]_2$[2-mal]

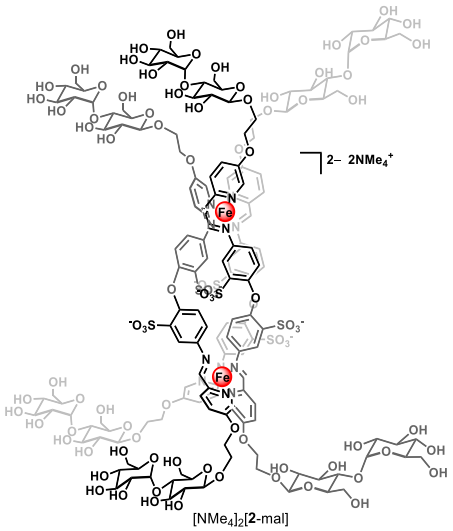

Measurements were conducted with solutions of dimeric Con A (60 μM) and $[NMe_4]_2$[**2**-mal] (400 μM) in acetate buffer (100 mM) at pH 4.8 containing NaCl (50 mM), $MnCl_2$ (1 mM), and $CaCl_2$ (1 mM). The first of 26 injections was performed at 0.5 μL volume and was discarded from the data set. A total of 25 injections at 3.0 μL volume were subsequently performed at 245 sec intervals and the data for the described measurements were generated in triplicate (Figure S120).

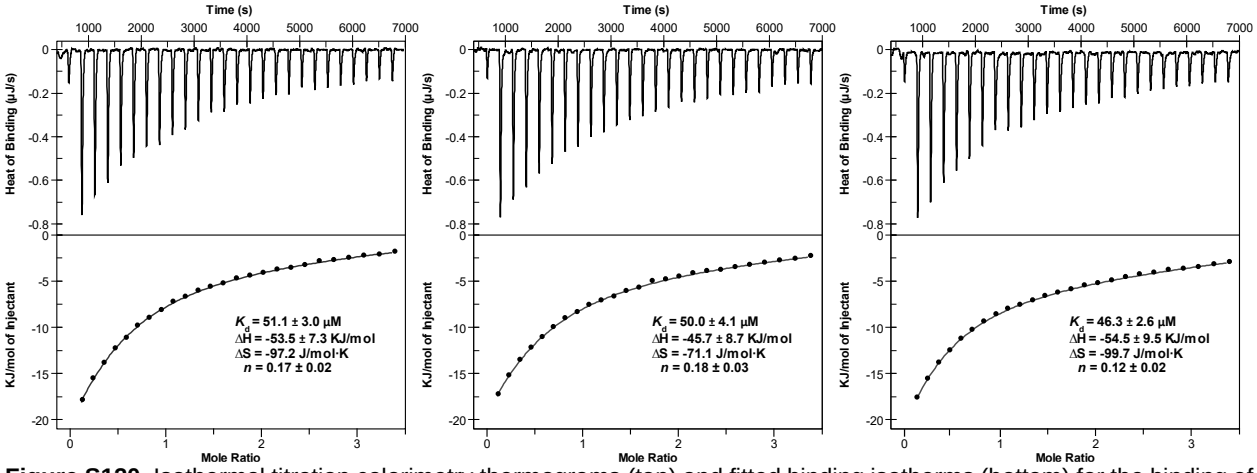

Figure S120. Isothermal titration calorimetry thermograms (top) and fitted binding isotherms (bottom) for the binding of $[NMe_4]_2$[**2**-mal] to dimeric Con A for three independent runs. Values of *n* are reported with respect to the Con A monomer.

S6.2.3. [3-mal][SO_4]

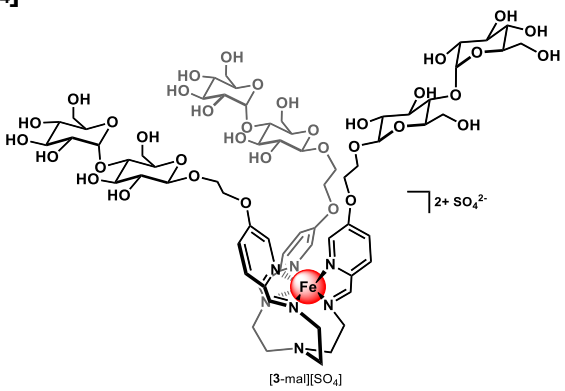

Measurements were conducted with solutions of dimeric Con A (110 μM) and [**3**-mal][SO_4] (1.05 mM) in acetate buffer (100 mM) at pH 4.8 containing NaCl (50 mM), $MnCl_2$ (1 mM), and $CaCl_2$ (1 mM). The first of 26 injections was performed at 1.0 μL volume and was discarded from the data set. A total of 25 injections at 4.0 μL volume were subsequently performed at 245 sec intervals and the data for the described measurements were generated in triplicate (Figure S121).

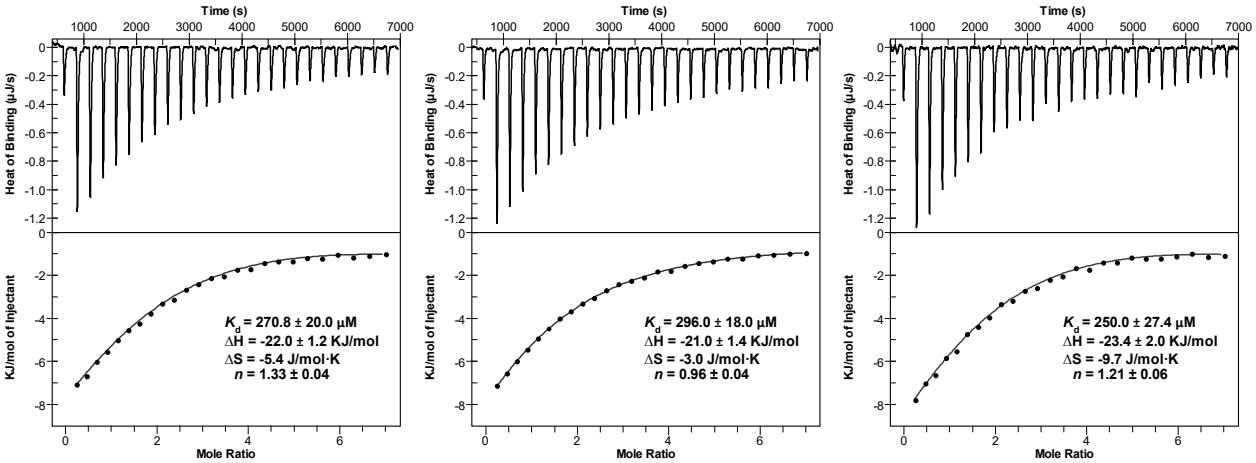

Figure S121. Isothermal titration calorimetry thermograms (top) and fitted binding isotherms (bottom) for the binding of [**3**-mal][SO_4] to dimeric Con A for three independent runs. Values of *n* are reported with respect to the Con A monomer.

S6.3. Binding of $[NMe_4]_4$[1-glc] to Con A dimer

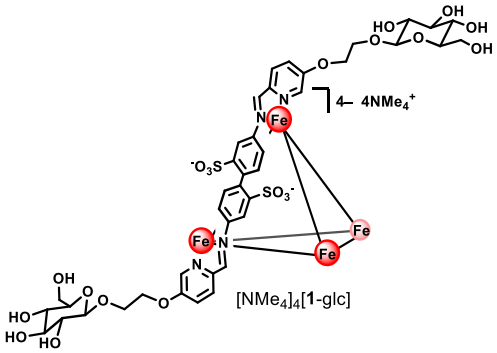

Measurements were conducted with solutions of dimeric Con A (80 μM) and $[NMe_4]_4$[**1**-glc] (1.02 mM) in acetate buffer (100 mM) at pH 4.8 containing NaCl (50 mM), $MnCl_2$ (1 mM), and $CaCl_2$ (1 mM). The first of 26 injections was performed at 0.5 μL volume and was discarded from the data set. A total of 25 injections at 3.0 μL volume were subsequently performed at 245 sec intervals and the data for the described measurements were generated in triplicate (Figure S122).

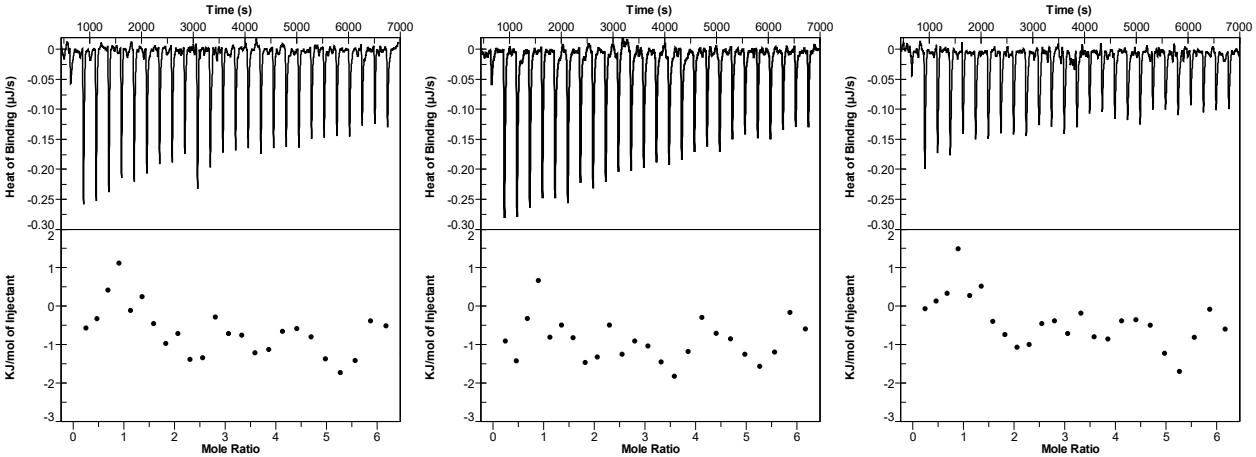

Figure S122. Isothermal titration calorimetry thermograms (top) and fitted binding isotherms (bottom) for the binding of $[NMe_4]_4$[**1**-glc] to dimeric Con A for three independent runs.

S6.4. Binding of $[NMe_4]_4$[1-gal] to Con A dimer

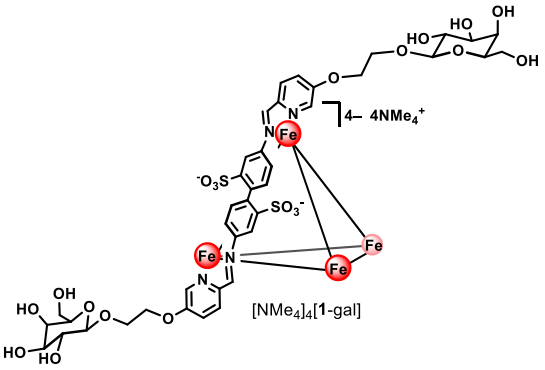

Measurements were conducted with solutions of dimeric Con A (80 μM) and $[NMe_4]_4$[**1**-gal] (1.02 mM) in acetate buffer (100 mM) at pH 4.8 containing NaCl (50 mM), $MnCl_2$ (1 mM), and $CaCl_2$ (1 mM). The first of 26 injections was performed at 0.5 μL volume and was discarded from the data set. A total of 25 injections at 3.0 μL volume were subsequently performed at 245 sec intervals and the data for the described measurements were generated in triplicate (Figure S123).

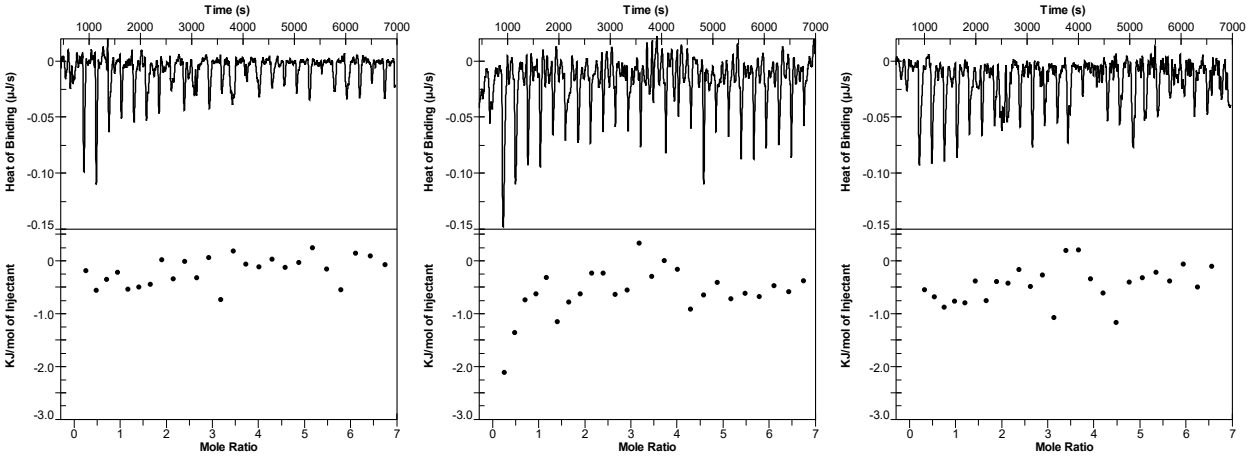

Figure S123. Isothermal titration calorimetry thermograms (top) and fitted binding isotherms (bottom) for the binding of $[NMe_4]_4$[**1**-gal] to dimeric Con A for three independent runs.

S6.5. Binding of unfunctionalized $[NMe_4]_4[Fe_4L_6]$ to Con A dimer – negative control

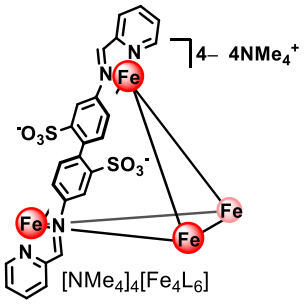

Measurements were conducted with solutions of dimeric Con A (80 μM) and $[NMe_4]_4[Fe_4L_6]$ (1.02 mM) in acetate buffer (100 mM) at pH 4.8 containing NaCl (50 mM), $MnCl_2$ (1 mM), and $CaCl_2$ (1 mM). The first of 26 injections was performed at 0.5 μL volume and was discarded from the data set. A total of 25 injections at 3.0 μL volume were subsequently performed at 245 sec intervals and the data for the described measurements were generated in triplicate (Figure S124).

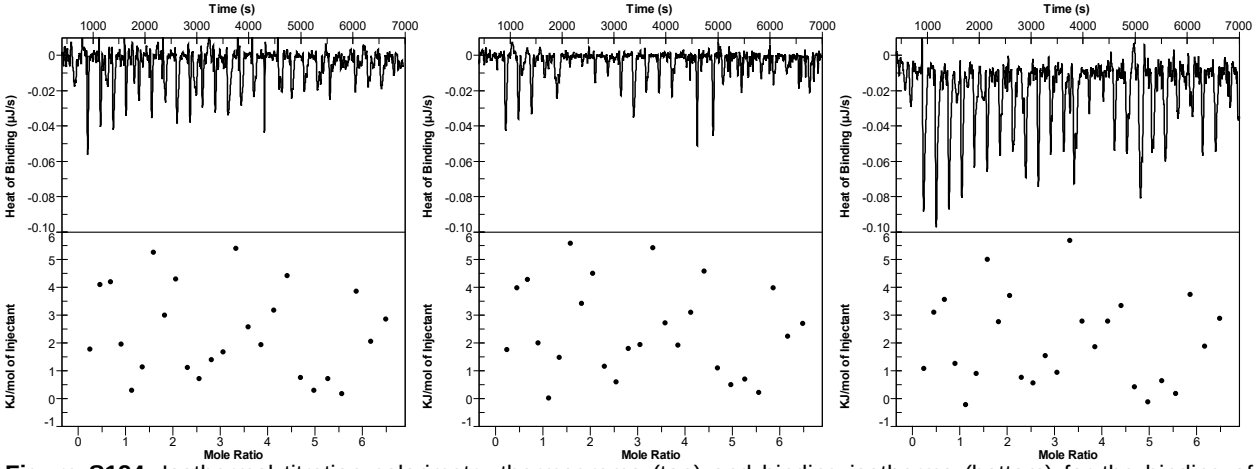

Figure S124. Isothermal titration calorimetry thermograms (top) and binding isotherms (bottom) for the binding of $[NMe_4]_4[Fe_4L_6]$ to dimeric Con A for three independent runs.

S6.6. Binding of methyl-α-D-mannose to Con A dimer

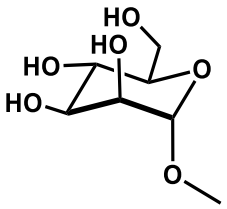

Measurements were conducted with solutions of dimeric Con A (362 μM) and methyl-α-D-mannose (6.2 mM) in acetate buffer (100 mM) at pH 5.2 containing NaCl (100 mM), $MnCl_2$ (5 mM), and $CaCl_2$ (5 mM). A total of 20 injections at 4.0 μL volume were performed at 225 sec intervals and the data for the described measurements were generated in triplicate.

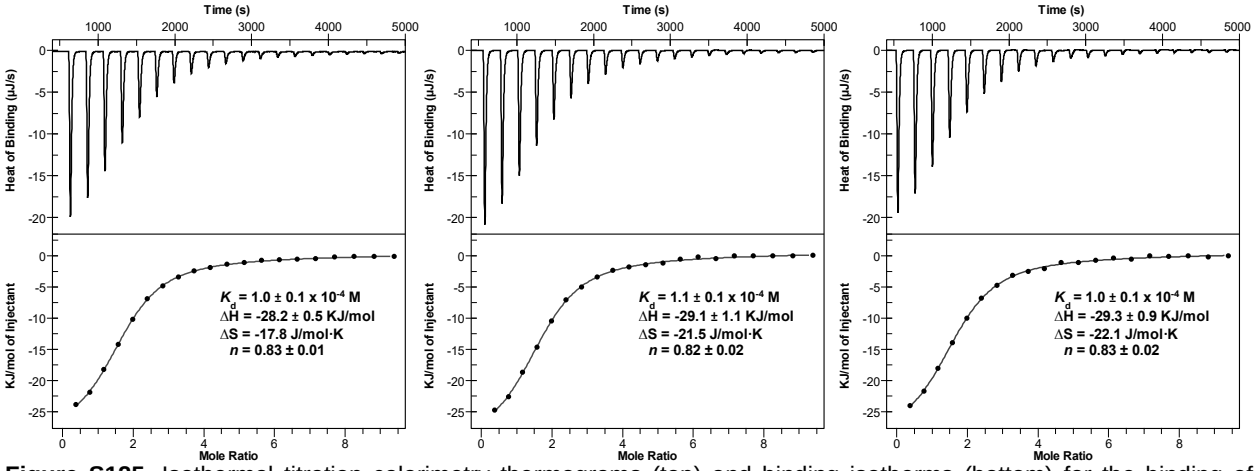

Figure S125. Isothermal titration calorimetry thermograms (top) and binding isotherms (bottom) for the binding of methyl-α-D-mannose to dimeric Con A for three independent runs. Values of *n* are reported with respect to the Con A monomer.

S6.7. Binding of D-(+)-mannose to Con A dimer

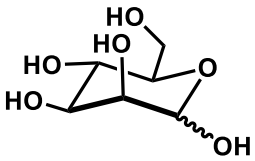

Measurements were conducted with solutions of dimeric Con A (63 μM) and D-(+)-mannose (4 mM) in acetate buffer (100 mM) at pH 4.8 containing NaCl (50 mM), $MnCl_2$ (1 mM), and $CaCl_2$ (1 mM). The first of 26 injections was performed at 0.5 μL volume and was discarded from the data set. A total of 25 injections at 3.0 μL volume were subsequently performed at 245 sec intervals and the data for the described measurements were generated in triplicate (Figure S126).

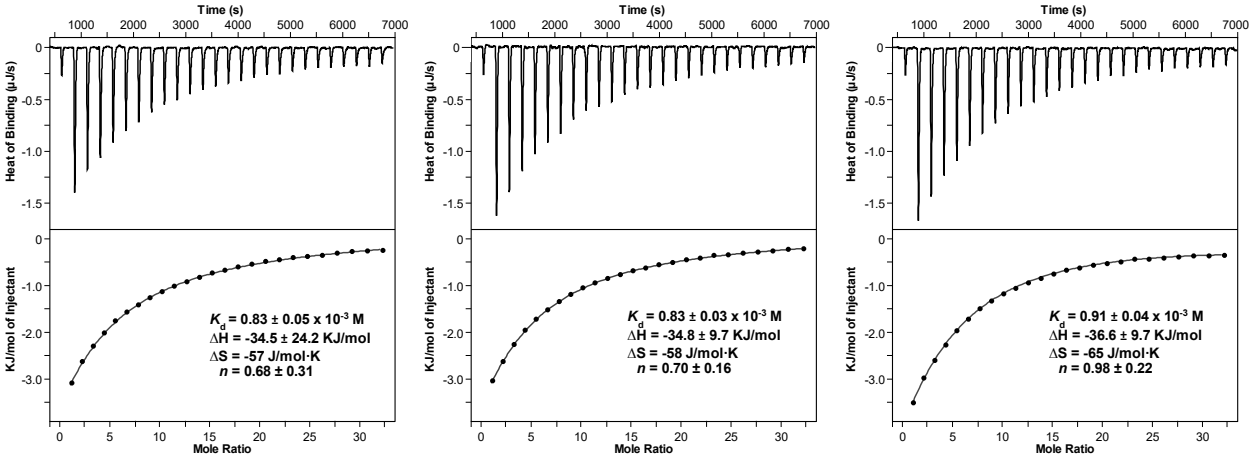

Figure S126. Isothermal titration calorimetry thermograms (top) and binding isotherms (bottom) for the binding of D-(+)-mannose to dimeric Con A for three independent runs. Values of *n* are reported with respect to the Con A monomer.

S7. X-Ray Crystallographic Details

Single crystal X-ray diffraction studies were carried out on a Bruker ApexII-Ultra CCD diffractometer equipped with Mo K_α radiation (λ = 0.7107 Å). Multiple datasets were collected on $[NMe_4]_2$[**2**-glc] crystals from different crystallization attempts and the best dataset was selected for publication.

A 0.21 x 0.2 x 0.2 mm piece of a pink crystal was mounted on a Cryoloop with Paratone oil. Data were collected in a nitrogen gas stream at 100(2) K using ϕ and ω scans. Crystal-to-detector distance was 60 mm and exposure time was 10 seconds per frame using a scan width of 0.70°. Data collection was 100% complete to 25.242° in θ. A total of 70965 reflections were collected covering the indices, -26 ≤ *h* ≤ 19, -22 ≤ *k* ≤ 26, -75 ≤ *l* ≤ 76. 22399 reflections were found to be symmetry independent, with a R_{int} of 0.0586. Indexing and unit cell refinement indicated a **Trigonal** lattice. The data were integrated using the Bruker SAINT Software[29] program and scaled using the SADABS[30] software program. The space group was found to be ***R*3**, which was selected over the better fitting ***R*−3** to account for the enantiopure β-D-glucose used during the synthesis of $[NMe_4]_2$[**2**-glc]. Solution by direct methods (SHELXT)[31] produced a complete phasing model consistent with the proposed structure.

The initial SHELXT solution yielded the core of $[NMe_4]_2$[**2**-glc] without the ether linkages and tethered β-D-glucose groups. There is some minor positional disordering on the Fe-coordinating core of $[NMe_4]_2$[**2**-glc]. The FLAT command was used to restrain the geometry of the aromatic rings. The asymmetric unit of the crystal structure contains 1/3 of two separate $[NMe_4]_2$[**2**-glc] complexes (one ΔΔ and one ΛΛ configuration). For both $[NMe_4]_2$[**2**-glc] complexes, the ethoxy linkages and sugar molecules are positionally disordered. The ether linkage could be reasonably modeled for one of the two $[NMe_4]_2$[**2**-glc] complexes. DFIX and DANG commands were used to restrain the bond distances and angles of the ether linkers. The exact positions of β-D-glucose could not be determined. The β-D-glucose groups were refined as a rigid body with a pivot point at the site of the ether group attachment. The bond distances and angles were taken from β-D-glucose published in the CCDC (1169302). The ether group was allowed to rotate; strong DFIX and DANG commands were used to restrain the bond distance and angles. Global RIGU was used to restrain the thermal ellipsoids of the $[NMe_4]_2$[**2**-glc] core. SQUEEZE, as implemented in PLATON,[32] was used to account for the disordered glucose groups, the $[NMe_4]^+$ counter ions, and any solvent that might have been present in the structure. This accounted for 483 electrons in the asymmetric unit.

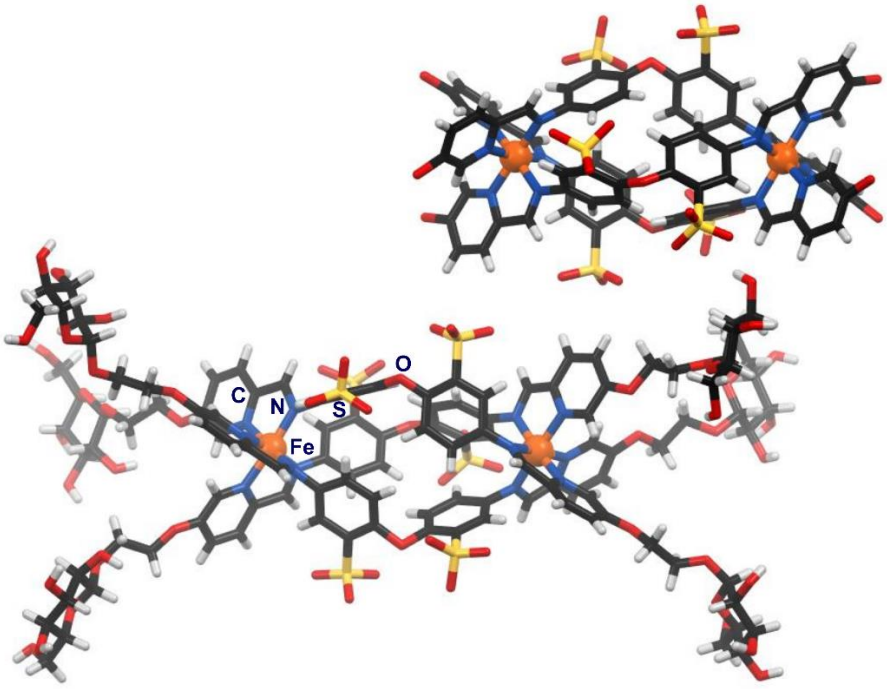

Figure S127. Solid-state molecular structures of the two independent [**2**-glc]$^{2-}$ complexes. The glucose groups were modeled for only one of the two complexes (see above). 1/3 of each complex is found in the asymmetric unit. Atom labels: Fe, orange; S, yellow; N, blue; C, grey; O, red; H, white.

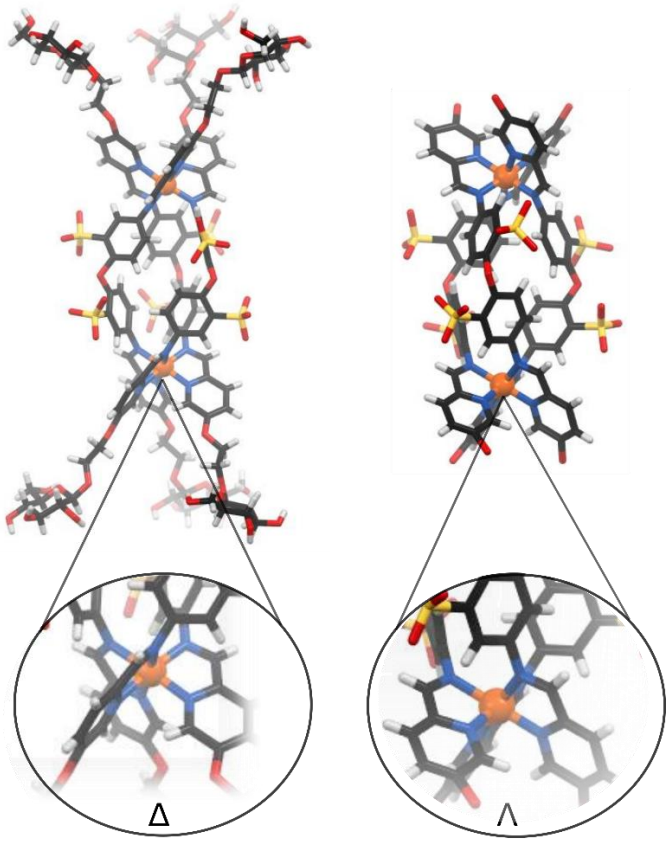

Figure S128. View of the two independent [**2**-glc]$^{2-}$ complexes showing both ΔΔ, and ΛΛ configurations.

Table S1. X-ray crystallographic and structure refinement data for $[NMe_4]_2$[**2**-glc]

CCDC Code	2190699	
Empirical formula	$C_{256}H_{432}Fe_4N_{28}O_{186}S_{12}$	
Formula weight	7486.39	
Temperature	100.00 K	
Wavelength	0.71073 Å	
Crystal system	Trigonal	
Space group	*R*3	
Unit cell dimensions	*a* = 22.1273(9) Å	*α* = 90°
	b = 22.1273(9) Å	*β* = 90°
	c = 62.674(4) Å	*γ* = 120°
Volume	26575(3) $Å^3$	
Z	3	
Density (calculated)	1.403 Mg/m^3	
Absorption coefficient	0.340 mm^{-1}	
F(000)	11844	
Crystal size	0.21 x 0.2 x 0.2 mm^3	
Theta range for data collection	1.679 to 25.680°	
Index ranges	$-26 \le h \le 19$, $-22 \le k \le 26$, $-75 \le l \le 76$	
Reflections collected	70965	
Independent reflections	22399 [*R*(int) = 0.0586]	
Completeness to theta = 25.242°	100.0%	
Absorption correction	Semi-empirical from equivalents	
Max. and min. transmission	0.4879 and 0.4461	
Refinement method	Full-matrix least-squares on F^2	
Data / restraints / parameters	22399 / 1053 / 913	
Goodness-of-fit on F^2	1.036	
Final *R* indices [$I > 2\sigma(I)$]	R_1 = 0.0858, wR_2 = 0.2421	
R indices (all data)	R_1 = 0.1235, wR_2 = 0.2881	
Absolute structure parameter	0.547(12)	
Largest diff. peak and hole	1.313 and -0.501 e.$Å^{-3}$	

S8. References

1 J. Fang, X. Guo, S. Harada, T. Watari, K. Tanaka, H. Kita and K. Okamoto, *Macromolecules*, 2002, **35**, 9022–9028.

2 C. Yang, F. Mehmood, T. L. Lam, S. L. F. Chan, Y. Wu, C. S. Yeung, X. Guan, K. Li, C. Y. S. Chung, C. Y. Zhou, T. Zou and C. M. Che, *Chem. Sci.*, 2016, **7**, 3123–3136.

3 P. Quagliotto, G. Viscardi, C. Barolo, D. D'Angelo, E. Barni, C. Compari, E. Duce and E. Fisicaro, *J. Org. Chem.*, 2005, **70**, 9857–9866.

4 H. Seto, T. Tono, A. Nagaoka, M. Yamamoto, Y. Hirohashi and H. Shinto, *Org. Biomol. Chem.*, 2021, **19**, 4474–4477.

5 M. Dowlut, D. G. Hall and O. Hindsgaul, *J. Org. Chem.*, 2005, **70**, 9809–9813.

6 M. K. Patel, B. Vijayakrishnan, J. R. Koeppe, J. M. Chalker, K. J. Doores and B. G. Davis, *Chem. Commun.*, 2010, **46**, 9119–9121.

7 E. Kaya, K. Gutsmiedl, M. Vrabel, M. Müller, P. Thumbs and T. Carell, *ChemBioChem*, 2009, **10**, 2858–2861.

8 W. Hayes, H. M. I. Osborn, S. D. Osborne, R. A. Rastall and B. Romagnoli, *Tetrahedron*, 2003, **59**, 7983–7996.

9 K. Neumann, A. Conde-González, M. Owens, A. Venturato, Y. Zhang, J. Geng and M. Bradley, *Macromolecules*, 2017, **50**, 6026–6031.

10 H. Tamiaki, A. Shinkai and Y. Kataoka, *J. Photochem. Photobiol. A Chem.*, 2009, **207**, 115–125.

11 Q. R. Yang, W. H. Qiao, S. M. Zhang and D. L. Liu, *Tenside, Surfactants, Deterg.*, 2010, **47**, 294–299.

12 H. O. Ham, S. H. Park, J. W. Kurutz, I. G. Szleifer and P. B. Messersmith, *J. Am. Chem. Soc.*, 2013, **135**, 13015–13022.

13 P. Mal and J. R. Nitschke, *Chem. Commun.*, 2010, **46**, 2417–2419.

14 A. Ferguson, R. W. Staniland, C. M. Fitchett, M. A. Squire, B. E. Williamson and P. E. Kruger, *Dalt. Trans.*, 2014, **43**, 14550–14553.

15 J. Mosquera, T. K. Ronson and J. R. Nitschke, *J. Am. Chem. Soc.*, 2016, **138**, 1812–1815.

16 D. Zhang, T. K. Ronson, J. Mosquera, A. Martinez, L. Guy and J. R. Nitschke, *J. Am. Chem. Soc.*, 2017, **139**, 6574–6577.

17 P. Mal, B. Breiner, K. Rissanen and J. R. Nitschke, *Science*, 2009, **324**, 1697–1700.

18 P. Mal, D. Schultz, K. Beyeh, K. Rissanen and J. R. Nitschke, *Angew. Chem. Int. Ed.*, 2008, **47**, 8297–8301.

19 T. K. Ronson, C. Giri, N. Kodiah Beyeh, A. Minkkinen, F. Topič, J. J. Holstein, K. Rissanen and J. R. Nitschke, *Chem. - A Eur. J.*, 2013, **19**, 3374–3382.

20 C. Giri, P. K. Sahoo, K. Rissanen and P. Mal, *Eur. J. Inorg. Chem.*, 2016, **2016**, 4964–4967.

21 J. Roukala, J. Zhu, C. Giri, K. Rissanen, P. Lantto and V. V. Telkki, *J. Am. Chem. Soc.*, 2015, **137**, 2464–2467.

22 K. Du, S. D. Zemerov, S. Hurtado Parra, J. M. Kikkawa and I. J. Dmochowski, *Inorg. Chem.*, 2020, **59**, 13831–13844.

23 I. A. Riddell, M. M. J. Smulders, J. K. Clegg and J. R. Nitschke, *Chem. Commun.*, 2011, **47**, 457–459.

24 S. Ma, M. M. J. Smulders, Y. R. Hristova, J. K. Clegg, T. K. Ronson, S. Zarra and J. R. Nitschke, *J. Am. Chem. Soc.*, 2013, **135**, 5678–5684.

25 R. L. Paul, Z. R. Bell, J. C. Jeffery, J. A. McCleverty and M. D. Ward, *Proc. Natl. Acad. Sci. U. S. A.*, 2002, **99**, 4883–4888.

26 S. Freye, J. Hey, A. Torras-Galán, D. Stalke, R. Herbst-Irmer, M. John and G. H. Clever, *Angew. Chem. Int. Ed.*, 2012, **51**, 2191–2194.

27 Y. Gou, J. Geng, S. J. Richards, J. Burns, C. Remzi Becer and D. M. Haddleton, *J. Polym. Sci. Part A Polym. Chem.*, 2013, **51**, 2588–2597.
28 J. Yariv, A. J. Kalb and A. Levitki, *BBA - Gen. Subj.*, 1968, **165**, 303–305.
29 Bruker. *SAINT*. Bruker AXS Inc.: Madison, Wisconsin, USA. 2012.
30 Bruker. *SADABS*. Bruker AXS Inc.: Madison, Wisconsin, USA 2001.
31 G. M. Sheldrick, *Acta Crystallogr. Sect. A Found. Crystallogr.*, 2015, **71**, 3–8.
32 A. L. Spek, *Acta Crystallogr. Sect. C Struct. Chem.*, 2015, **71**, 9–18.